A MECHANISTIC STUDY ON TRIVALENT METAL COMPLEXES AS MODEL PHARMACEUTICALS

KINA ANN VAN DER MERWE

2011

A MECHANISTIC STUDY ON TRIVALENT METAL COMPLEXES AS MODEL PHARMACEUTICALS

by

KINA ANN VAN DER MERWE

A dissertation submitted to meet the requirements for the degree of

MAGISTER SCIENTIAE

in the

DEPARTMENT OF CHEMISTRY

FACULTY OF NATURAL AND

AGRICULTURAL SCIENCES

at the

UNIVERSITY OF THE FREE STATE

SUPERVISOR: PROF. HENDRIK G. VISSER

CO-SUPERVISOR: DR. JOHAN A. VENTER

JUNE 2011

Acknowledgements

It is a pleasure to thank those that made this thesis possible.

First and foremost I would like to thank God for the many blessing that he has bestowed on me. For we are competent in ourselves to claim anything for ourselves, but our competence comes from God.

It is difficult to overstate my gratitude to my supervisor Prof. H.G. Visser, my co-supervisor Dr. J.A. Venter and finally to Prof. Andreas Roodt. I am truly privileged to have worked with such amazing men.

Thank you Prof. H.G. Visser for your patience, motivation, encouragement and advice during my thesis.

To Prof. Andreas Roodt thank you for your sound advice, for inspiring me, as well as your encouragement during my thesis.

Thank you Dr. J.A. Venter for your patience, kindness and your academic experience which have been invaluable to me.

To my mom, Tracy and my boyfriend, Mark who have helped me stay sane through these difficult years. Their support and care helped me overcome setbacks and stay focused. To my grandparents, Andy and Sonia, thank you for always being there for me, for your wisdom, love and kindness.

To Ceri, Kelvin, Larisse and Ricky, my closest friends, I am truly blessed to have friends like you and I deeply appreciate your love and belief in me. Thanks for your wonderful words of encouragement as well as your moral support.

The financial assistance from the University of the Free State and the National Research Foundation (NRF) towards this research is hereby gratefully acknowledged. Opinions expressed and conclusions arrived at, are those of the author and are not necessarily to be attributed to the NRF.

Table of contents

4 Dissociation Constants of Methylene Diphosphonate in an Aqueous Medium

5 Crystallographic Study of Cobalt(III) and Chromium(III) complexes

6 Crystallographic Study of Cobalt(II) complexes

Abbreviation	Meaning
APD	1-hydroxyl-3-aminopropilydenediphosphonic acid
ATR	Attenuated Total Reflectance
DTPA	diethylenetriaminepentaacetic acid
HEDP	1-hydroxyethylidene diphosphonate
HIDA	2,6-dimethylphenylcarbamoylmethyl iminodiacetic acid
HMPAO	3,6,6,9-tetramethyl-4,8-diazaundecane-2,10-dione dioxime
MDP	methylene diphosphonate
NTA	nitrilotriacetic acid
IR	Infrared Spectroscopy
NMR	Nuclear Magnetic Resonance
MRI	Magnetic Resonance Imaging
SPARC	SPARC Performs Automated Reasoning in Chemistry
SPECT	Single-photon Emission Computed Tomography
SMILE	Simplified Molecular Input Line Entry
Vis	Visible Spectroscopy
XPS	X-ray Photoelectron Spectroscopy

BFCA	bifunctional chelating agent
MOFs	Metal-organic frameworks
CFSE	crystal field stabilisation energy
CNS	central nervous system
LET	linear energy transfer
BE	binding energy
OX	oxidation state
α	alpha particles
β^+	positron
β^-	beta radiation/emission
γ	gamma
A	absorbance
Å	Ångström
δ	chemical shifts
°	degree
°C	degree Celsius
∆E	energy difference

E	energy state
ε	extinction coefficient
I_o	intensity
Z	number of molecules in a unit cell
l	path length
π	Pi
h	Plank's constant
σ	Sigma
σ*	Sigma anti-bonding
θ	Sigma
υ	stretching frequency on IR
3-D	three dimensional
ppm	unit of chemical shift in parts per million
λ	wavelength
cm	centimeter
J	coupling constants
eV	electron volt

keV	kilo electron volt
MeV	mega electron volt
g	grams
Hz	Hertz
kJ/mole	kilojoules per mole
µm	micrometer
mbar	millibar
mL	milliliter
M	concentration in $mol.dm^{-3}$
nm	nanometer
%	percentage

Abstract

Keywords: *Cobalt; Chromium; Methylene diphosphonate; bidentate ligand; bone imaging agent; radiopharmaceutical, polyprotic, protonation constants, pK_a.*

The aim of the study was to synthesize several novel Co(II)-, Co(III)- and Cr(III) complexes using an O,O-bidentate ligand, methylene diphosphonate, and to characterize these complexes by various means. Characterization of the complexes was done by elemental analysis, infrared spectroscopy, nuclear magnetic resonance spectroscopy (NMR), single X-ray crystallography and X-ray photoelectron spectroscopy (XPS).

The methylene diphosphonate ligand was selected as it is a ligand employed in a bone imaging agent in the radiopharmaceutical sector. Little is known about the structure and coordination chemistry of metal complexes with methylene diphosphonate.

Single crystal X-ray crystallographic structure determinations of six new structures were completed:

(1) Pyridinium diaquabis(methylenediphosphonato)chromate(III) tetrahydrate

(2) Potassium diaquabis(methylenediphosphonato)cobaltate(III)

(3) Potassium diaquadihydroxy(methylenediphosphonato)cobaltate(III)

(4) Diammonium diaquabis(methylenediphosphonato)cobaltate(II)

(5) Disodium diaquabis(methylenediphosphonato)cobaltate(II) dihydrate

(6) Dicesium diaquabis(methylenediphosphonato)cobaltate(II)

Each complex has a slightly distorted octahedral geometry. The cobalt or chromium ion in each complex is coordinated to four oxygen atoms derived from two methylene diphosphonate ligands, except for $K[Co(CH_4O_6P_2)(OH)_2(H_2O)_2]$ which has two oxygen atoms from one methylene diphosphonate ligand coordinated to it. In

addition each complex has two aqueous molecules which are coordinated to the metal center. Two phosphonate oxygen atoms from the ligand, methylene diphosphonate define the equatorial plane, whereas the water molecules reside in the axial positions.

Table 1: Selected crystallographic data for each complex.

Complex	Space Group	Z	O-M-O Angle (°)	P-C-P Angle (°)
$(C_5H_6N)[Cr(CH_4O_6P_2)_2(H_2O)_2]\cdot 4H_2O$	Triclinic, $P\bar{1}$	1	89.20(2)-91.66(2)	114.8(3)
$K[Co(CH_4O_6P_2)_2(H_2O)_2]$	Triclinic, $P\bar{1}$	2	88.66(1)-96.34(1)	115.2(2)
$K[Co(CH_4O_6P_2)(OH)_2(H_2O)_2]$	Orthorhombic, *Pnma*	4	87.44(2)-178.86(2)	116.11(1)
$(NH_4)_2[Co(CH_4O_6P_2)_2(H_2O)_2]$	Triclinic, $P\bar{1}$	1	87.49(9)-95.23(9)	116.9(2)
$Na_2[Co(CH_4O_6P_2)_2(H_2O)_2]\cdot 2H_2O$	Monoclinic, $P2_1/c$	2	86.62(5)-93.16(4)	114.36(8)
$Cs_2[Co(CH_4O_6P_2)_2(H_2O)_2]$	Triclinic, $P\bar{1}$	1	90.70(1)-94.52(1)	116.7(2)

These complexes correlate with other similar complexes but the occurrence of similar structures in literature is very limited, showing that this field is open to further study. We were unable to perform any meaningful studies on these complexes in solution due to its insolubility in water.

The stability constants for the polyprotic ligand MDP were established by means of volumetric titrations. Three methodologies namely, the geometric method, the first derivative method and the second derivative method in combination with the program SPARC were employed to determine the protonation constants as well as the equivalence points.

In order to investigate the effect of the ionic medium on the determination of the dissociation constants, it was decided to perform the volumetric titrations in an ionic medium of 0.1 M NaCl and compare these values with data obtained without any adjustments to the ionic medium, the temperature for all of the reactions was kept constant at 18.0 ºC. The K_{a1} value could not be determined using the Compact Titrator G20 as it is unable to perform titrations below pH 2. The K_{a2} value was 2.91(8) without and ionic medium and 2.95(1) with and ionic medium (0.1 M NaCl). The K_{a3} value was 7.22(5) without and ionic medium and 6.81(5) with and ionic medium (0.1 M NaCl). The K_{a4} value was 10.57(1) without and ionic medium and

10.41(2) with and ionic medium (0.1 M NaCl). These dissociation constants correlated to literature.

Opsomming

Sleutewoorde: *Kobalt; Chroom; Metileen difosfonaat; bidentate ligand; been beeldingsagent; radiofarmaseutiese, poliproties, protoneringskonstantes, pK_a.*

Die doel van die studie was die sintese van verskeie oorspronklike Co(II)-, Co(III)- en Cr(III) komplekse met die gebruik van `n O,O-bidentate ligand, metileen difosfonaat, en die karakterisering van hierdie komplekse deur verskillende tegnieke. Karakterisering van die komplekse is gedoen deur elementele analise, infrarooi spektroskopie, kernmagnetieseresonans (KMR) spektroskopie, enkelkristal X-straal kristallografie asook X-straal foto-elektron spektroskopie (XPS).

Die metileen difosfonaat ligand is gekies aangesien dit gebruik word as `n ligand in `n been beeldingsagent in die radiofarmaseutiese bedryf. Die struktuur en koördinasiechemie van metaalkomplekse met metileen difosfonaat is redelik onbekend.

Enkelkristal X-straal kristallografiese struktuurbepalings van ses nuwe strukture is voltooi:

(1) Piridinium diakwabis(metileendifosfonato)chromaat(III) tetrahidrate

(2) Kalium diakwabis(metileendifosfonato)kobaltaat(III)

(3) Kalium diakwadihidroksie(metileendifosfonato)kobaltaat(III)

(4) Diammonium diakwabis(metileendifosfonato)kobaltaat(II)

(5) Dinatrium diakwabis(metileendifosfonato)kobaltaat(II) dihidrate

(6) Disesium diakwabis(metileendifosfonato)kobaltaat(II)

Elke kompleks het `n effens verwronge oktahedriese geometrie. Die kobalt of chroom ioon in elke kompleks is aan vier suurstofatome gekoördineer; afkomstig van twee metileen difosfonaat ligande, behalwe vir $K[Co(CH_4O_6P_2)(OH)_2(H_2O)_2]$ wat twee suurstofatome van een metileen difosfonaat ligand daaraan gekoördineer het.

Benewens die bogenoemde het elke kompleks twee akwa molekule aan die metaalsenter gekoördineer. Twee fosfonaat suurstofatome van die ligand, metileen difosfonaat definieer die ekwatoriale vlak, terwyl water molekule die aksiale posisies betrek.

Tabel 1: Uitgesoekte kristallografiese data vir elke kompleks.

Kompleks	Ruimtegroep	Z	O-M-O Hoek (°)	P-C-P Hoek (°)
$(C_5H_6N)[Cr(CH_4O_6P_2)_2(H_2O)_2]\cdot 4H_2O$	Triklinies, $P\bar{1}$	1	89.20(2)-91.66(2)	114.8(3)
$K[Co(CH_4O_6P_2)_2(H_2O)_2]$	Triklinies, $P\bar{1}$	2	88.66(1)-96.34(1)	115.2(2)
$K[Co(CH_4O_6P_2)(OH)_2(H_2O)_2]$	Ortorombies, *Pnma*	4	87.44(2)-178.86(2)	116.11(1)
$(NH_4)_2[Co(CH_4O_6P_2)_2(H_2O)_2]$	Triklinies, $P\bar{1}$	1	87.49(9)-95.23(9)	116.9(2)
$Na_2[Co(CH_4O_6P_2)_2(H_2O)_2]\cdot 2H_2O$	Monoklinies, $P2_1/c$	2	86.62(5)-93.16(4)	114.36(8)
$Cs_2[Co(CH_4O_6P_2)_2(H_2O)_2]$	Triklinies, $P\bar{1}$	1	90.70(1)-94.52(1)	116.7(2)

Hierdie komplekse stem ooreen met ander soortgelyke komplekse maar die voorkoms van soortgelyke strukture in die literatuur is baie beperk, wat aantoon dat hierdie veld oop is vir verdere studiemoontlikhede. Geen betekenisvolle studies kon op hierdie komplekse in oplossing uit te voer nie as gevolg van hulle onoplosbaarheid in water.

Die stabiliteitskonstantes vir die poliprotiese ligand MDP is vasgestel deur middel van volumtriese titrasies. Drie metodes, naamlik die geometriese metode, eerste afgeleide metode en die tweede afgeleide metode in kombinasie met die program SPARC is gebruik om die protoneringskonstantes sowel as die ewewigspunte te bepaal.

Ten einde die effek van die ioniese medium op die bepaling van die dissosiasiekonstantes te ondersoek is daar besluit om die volumetriese titrasies in `n ioniese medium van 0.1 M NaCl uit te voer en hierdie waardes te vergelyk met data wat verkry is sonder enige aanpassing aan die ioniese medium; die temperatuur vir al die reaksies is konstant gehou by 18.0 ºC. Die K_{a1} waarde kon nie vasgestel word met die Compact Titrator G20 nie aangesien dit nie in staat is om titrasies laer as pH 2 uit te voer nie. Die K_{a2} waarde was 2.91(8) sonder `n ioniese medium en 2.95(1) met `n ioniese medium (0.1 M NaCl). Die K_{a3} waarde was 7.22(5) sonder `n ioniese

medium en 6.81(5) met `n ioniese medium (0.1 M NaCl). Die $K_{a4}$ waarde was 10.57(1) sonder `n ioniese medium en 10.41(2) met `n ioniese medium (0.1 M NaCl). Hierdie dissosiasiekonstantes stem ooreen met literatuur.

1 Introduction and Aim

1.1 The History of Cobalt

The origin of the word cobalt comes from the German word *kobold* which means "evil spirits or goblins".[1] Miners called it the "evil spirits" because it made them ill. This was probably due to the fact that the mineral contained arsenic.[2] It was also referred to as "goblins" as they believed that the malevolent goblins placed the cobalt in the silver ore.[3]

Early civilizations of Egypt and Mesopotamia valued minerals which comprised of cobalt as it was employed to colour glass deep blue.[2]

In 1733 the Swedish chemist Georg Brandt was the first person to declare cobalt as an element. He was attempting to illustrate that the blue colour of glass was a result of the cobalt and not the bismuth which is found to reside in the same locations as cobalt. In 1790 Bergmann confirmed that it was cobalt and in 1799 Tassaert confirmed Brandt's discovery.[2]

[1] D.R. Lide. *Chemical Rubber Company handbook of chemistry and physics*, 77th Edition, CRC Press, United States of America, **1996**.

[2] M.E. Weeks and H.M. Leicester. *Discovery of the Elements*, 7th Edition, Journal of Chemical Education,p 686-706, Easton, Pennsylvania, **1968**.

[3] Dictionary.com, "cobalt". Collins English Dictionary-Compete and Unabridged, 10th Edition, Harper Collins Publishers, http://dictionary.reference.com/browse/cobalt. Available: http://dictionary.reference.com. Accessed on the 3rd of January 2011.

1.2 Appearance and Applications of Cobalt

Cobalt is a hard transition metal with a bluish white appearance[4] and it resides between iron and nickel on the periodic table. It can have oxidation states of -1 to +4, but it occurs naturally in only two oxidation states namely Co^{+2} and Co^{+3}.[5] Cobalt is a metal employed in many diverse military, radiopharmaceutical and industrial applications.[4]

1.2.1 Applications of Cobalt

In industry cobalt is utilised in a vast amount of applications ranging from superalloys which are used for parts in gas turbines of aircraft engines, to corrosion- and wear-resistant alloys, magnets and magnetic recording media, catalysts predominantly for the chemical and petroleum industry, cemented carbides and diamond tools as well as for steel-belted radial tyres. Cobalt is also used for the preparation of drying agents (mainly paints, inks and varnishes), ground coats for porcelain enamels and pigments because of its brilliant blue colour.[4,6] It is a vital element required for modern rechargeable batteries and is also used for electroplating because it is hard and resistant to oxidation.[7]

^{60}Cobalt is employed in the industrial radiography sector in order to detect structural flaws in metal parts.[7] In the food industry it is used to disinfect food by a process

[4] S.S. Zumdahl. *Chemistry*, 3rd Edition, p 86, 936-1091, D.C. Heath and Company, United States of America, **1993**.

[5] M. Kobayashi and S. Shimizu. *European Journal of Biochemistry*, 1999, **261**, 1-9.

[6] R.S. Young. *Cobalt-Its Chemistry, Metallurgy, and Uses*, p 474, Reinhold Publishing Corporation, New York, **1960**.

[7] S. Watts. *The elements Cobalt*, p 1-32, Marshall Cavendish Benchmark, United States of America, **2007**.

known as cold pasteurisation. The gamma rays destroy bacteria and mould present in the food and thus extends the shelf-life of the food.[8]

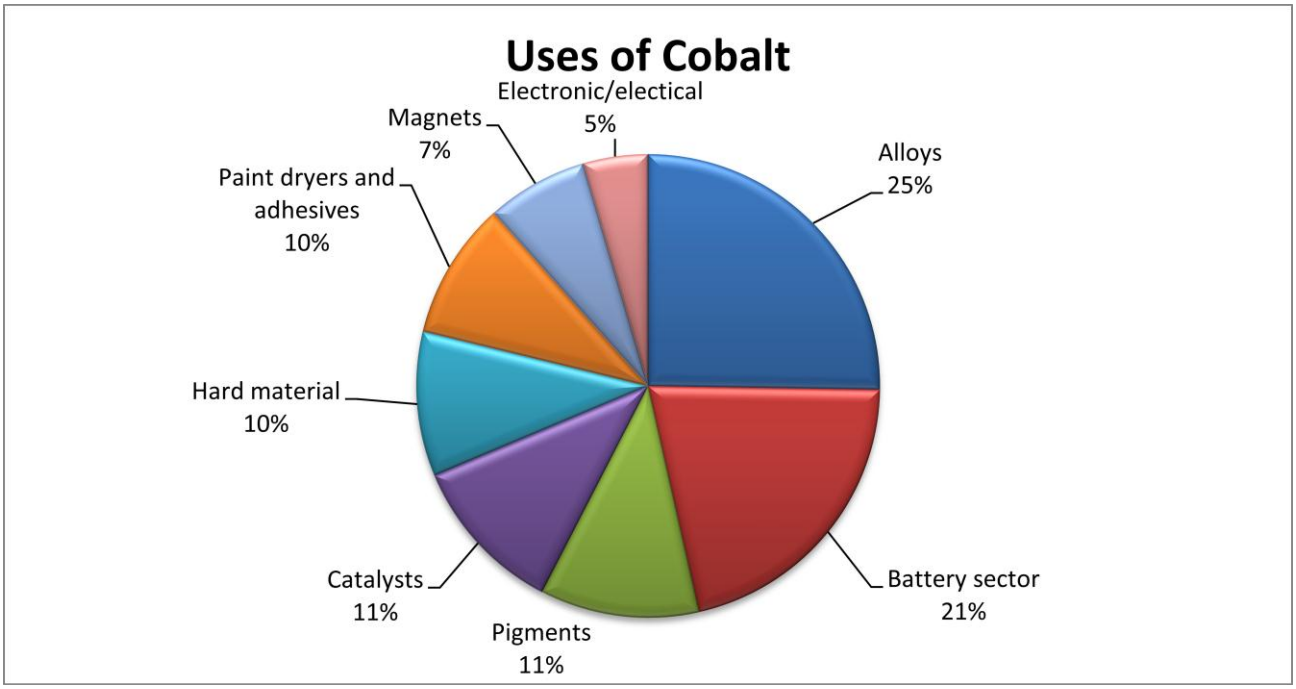

Figure 1.1: Graphical representation of the usage of cobalt in the industrial sector in 2007.[7]

1.3 Biological role of Cobalt

Less than 0.05% of the human body mass is comprised of cobalt. This trace element is an essential component of vitamin B_{12}, which is mainly used by the body to metabolise carbohydrates, proteins and fats. Vitamin B_{12} also known as cobalamin (**Figure 1.2**) assists in the development of red blood cells. The body is unable to generate vitamin B_{12} so it has to be obtained from our diet.[4]

[8] D.D. Ebbing and S.D. Gammon. *General Chemistry*, 8th Edition, p 271, 977, Houghton Mifflin Company, United States of America, **2005**.

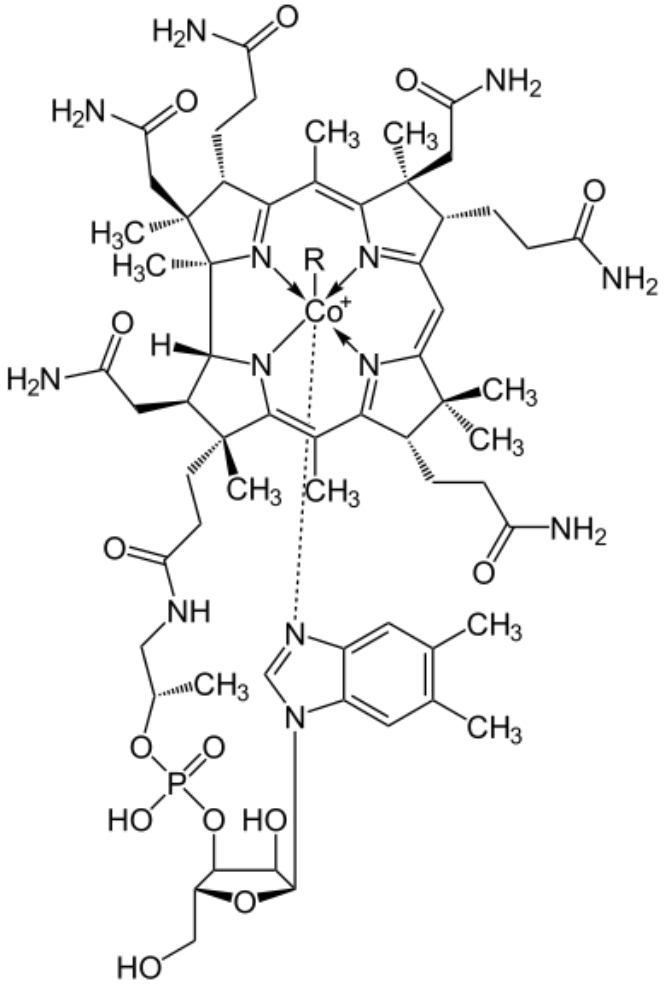

Figure 1.2: The structure of cobalamin.[4]

1.4 The History of Chromium

The origin of the word chromium is derived from the Greek word *chroma* which means “colour” because chromium is present in numerous coloured compounds like emerald and ruby gemstones.[9] Chromium was unfamiliar to ancient people as there are no records of its utilization. The reason for this could be that its appearance was not appealing or because not a lot of minerals contain chromium.[9]

In 1761 a German mineralogist named Johann Gottlob Lehmann discovered an orange-red mineral in the Ural Mountains. He assumed that the mineral was a compound which was comprised of lead, iron and selenium so he named it Siberian

[9] G. Roza. *Chromium*, 1st Edition, p 4-8, The Rosen Publishing Group, New York, **2008**.

red lead. It was actually lead chromate which is known as crocoite today.[9] In 1797 a French chemist named Louis Nicolas Vauquelin succeeded to extract chromium oxide from the crocoite. In 1798 he isolated the pure metal which he named chromium.[10]

1.5 Appearance and Applications of Chromium

Chromium is a hard, crystalline transition metal with a silvery white appearance and it is positioned between vanadium and manganese on the periodic table. It does not exist as a pure metal but is always attached to other elements like iron or oxygen.[11] It exhibits numerous oxidation states namely +2, +3 and +6 but the most common oxidation state is +3.[8] Chromium has an extensive range of applications because of its hardness, magnetic properties and resistance towards corrosion.

1.5.1 Applications of Chromium

As chromium is resistant to corrosion even at elevated temperatures, it is used in steel alloys and it is a vital alloying material in the manufacturing of stainless steel. Another application where chromium is used is in the surface coating and plating which is performed by depositing a thin layer of chromium from acidic chromate or dichromate solutions onto metal surfaces by means of a process known as electroplating. Chromium is also used in casting moulds, furnace linings and even to tan leather. It is also used as an oxidising agent and is added to glass to give it an emerald green colouring, while chromium oxide is employed to give synthetic rubies their colour. Audio tapes and cassettes are comprised of chromium(IV) oxide due to their magnetic properties. Chromium(VI) salts have toxic properties which prevent wood from decaying or being damaged by termites, insects or fungi.[4,11]

[10] N. Lepora. *The elements Chromium*, p 7-10, Marshall Cavendish Benchmark, New York, **2006**.

[11] H.F. Holtzclaw, Jr., W.R. Robinson and D.J. Odom. *General Chemistry*, 9th Edition, p 881-882, D.C. Heath and Company, United States of America, **1991**.

1.6 Biological role of Chromium

Only minute quantities of trivalent chromium (Cr(III) or Cr+3) is required by the human body.[12] The function of the chromium is to facilitate sugar and lipid metabolism and to assist insulin transport of glucose to the cells.[13]

1.7 Aim of the Study

Cobalt(II), cobalt(III) and chromium(III) complexes with methylene diphosphonate (MDP) as a ligand have not been investigated until now. Kinetic studies on any of these metal-MDP complexes have not yet been published and there is a limited amount of structural studies that has been reported on other metal-MDP complexes.

Methylene diphosphonate is unique in that it exhibits diversified coordination capabilities with metal ions. This coordination capability is due to the single methyl group which separates the two phosphonate groups and allows for the combined coordination ability to act as a single $[CP_2O_6]$ unit rather than two $[CPO_3]$ units. This leads to the formation of new structural types such as one-dimensional, two-dimensional and three-dimensional structures.[14,15] Diphosphonates also strongly inhibit bone resorption, and some act as inhibitors of the matrix metalloproteases, thus additionally blocking the initiating step in the bone resorption process.[16] They are also widely used for bone imaging purposes in the radiopharmaceutical industry.[17]

[12] M. Walter. *Journal of Nutrition*, 1993, **123**, 626-636.

[13] M.M. Manore, N.L. Meyer and J. Thompson. *Sport Nutrition for Health and Performance*, 2nd Edition, p 343-345, Human Kinetics, United States of America, **2009**.

[14] B.S. Zheng, L. Liu, Y. Wu and W. Feng. *Inorganic Chemistry*, 2003, **42**, 5037-5039.

[15] Q. Hu, X. Deng, Y. Sun and Z. Du. Acta Crystallographica, 2011, E67, m362-363.

[16] J. Xiang, M. Li, S. Wu, L. Yuan and J. Sun. *Journal of Molecular Structure*, 2007, **826**, 143-149.

[17] E. Matczak-Jon, B. Kurzak, A. Kamecha and P. Kafarski. *Polyhedron*, 2002, **21**, 321-332.

Metal-organic frameworks are predominantly composed of carboxylate ligands. Very few frameworks have been synthesized utilising phosphonate ligands because metal phosphonate complexes are notorioiusly difficult to crystallise. The phosphonates tend to precipitate out as less ordered, insoluble phases.

Based on this discussion it is evident that there is a vast amount of uncertainty with regard to the synthesis, characterization and reactions of Cr(III)-, Co(II)- and Co(III)-MDP complexes. This initiated the investigation to synthesize new novel complexes utilising various cations.

The aim of the study was to:

1. Synthesize suitable Co(II)-, Co(III)- and Cr(III)-MDP complexes which can be employed as biological models in future studies.
2. Develop different methods to synthesize Co(II)-, Co(III)- and Cr(III)-MDP complexes.
3. Characterize the complexes utilizing IR, UV/VIS, X-ray photoelectron spectroscopy (XPS), elemental analysis, nuclear magnetic resonance spectroscopy (NMR) and single-crystal X-ray crystallography in order to obtain a possible starting material for kinetic studies.
4. Study the aqueous behaviours of MDP, especially since the available literature differs quite substantially on some of the acid dissociation constants of the pharmaceutical.

2 Literature Study

2.1 Cobalt and Chromium

Cobalt(III) and chromium(III) complexes are interesting as they undergo ligand exchange considerably slower in comparison to other transition metal ions. Ligand exchange in cobalt(II) complexes proceeds rapidly.[1]

The configuration of these octahedral complexes is determined by its spin orientation. A low spin d^6 complex with a general formula of MA_3B_3 will prefer to adopt the *fac* rather than the *mer* configuration.[2]

2.1.1 Alfred Werner Complexes

Alfred Werner altered the way we visualise coordination complexes. As a young scientist he postulated that in cobalt ammines the metal ion is enclosed by six ligands in an octahedral orientation as depicted in **Figure 2.1**.[3,4]

He was contradicting all the major leaders in this field who believed that the ligands were attached to each other in chains and that only the ends of the chains were bonded to the metal. Jørgensen was unable to accept that a trivalent metal like Co^{+3}

[1] K.V. Krishnamurty, G.M. Harris and V.S. Sastri. *Chemical Reviews*, 1970, **70**, 171.

[2] E. Valenzuela, A. Sousa-Pedrares, M.L. Duran-Carril, J.A. Garcia-Vazquez, J. Romero and A. Sousa. *Z. Anorg. Allg. Chem.*, 2007, **633**, 1853-1859.

[3] K. Bowman-James. *Accounts of Chemical Research*, 2005, **38**, 671-678.

[4] R.H. Crabtree. *The Organometallic Chemistry Of The Transition Metals*, 4th Edition, p 3-27, John Wiley and Sons, New Jersey & Canada, **2005**.

could coordinate to six groups, as there were never more than three bonds to Co according to the chain theory.

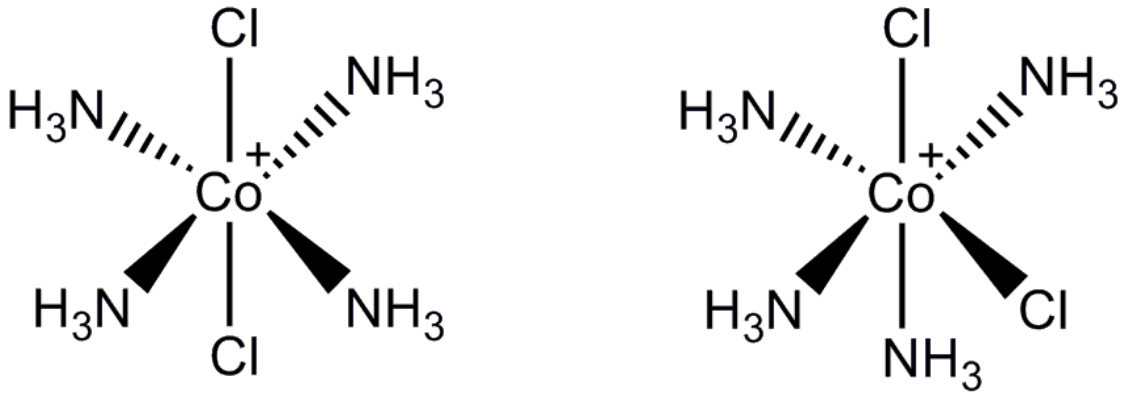

Figure 2.1 A schematic representation of the two types of orientations present for the cobalt ammines.

A Werner complex is one where the metal is bonded to a noncarbon ligand. The simplest metal-ligand bond is $L_nM\text{-}NH_3$, where ammonia is attached to the metal fragment. The metal is also able to be connected to other ligands which are represented by L_n. This type of chemical bond is one where the lone pair of electrons which are present on the free NH_3 are donated to the metal in order to form the complex. The metal is thus a polyvalent Lewis acid and it is able to accept lone pairs of numerous ligands, L, which acts as Lewis bases.

Werner proposed the concept of double valence for transition-metal ions like Co^{+3}, which will have a primary and secondary valence. The primary valence is the amount of negative ions that is required to fulfil the charge on the metal ion. Secondary valence is the amount of ions of molecules which coordinate to the metal ion. [3,4]

2.1.2 Stereochemistry

ML_6 is the most frequent type of complex and it has an octahedral type of coordination geometry as depicted in **Figure 2.2**. [4]

Octahedron

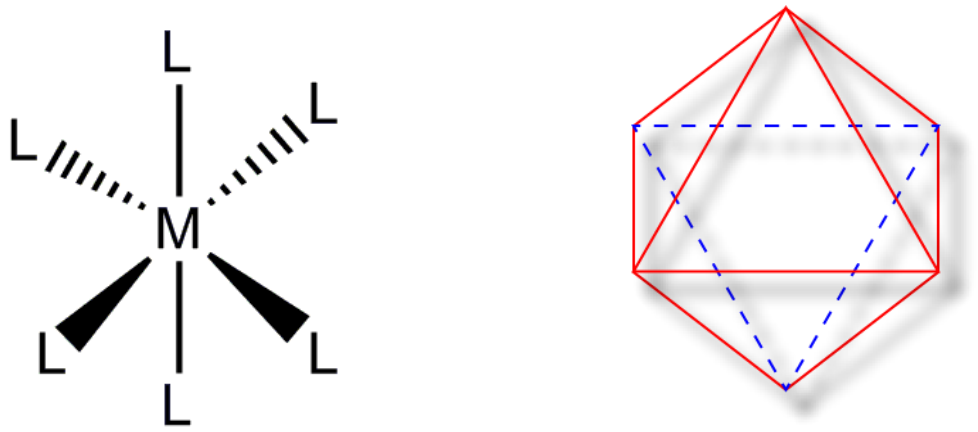

Figure 2.2 Octahedral coordination of a typical ML_6 complex.

The ligands occupy the six vertices of the octahedron and this allows them to reduce their M-L bonding distances while on the other hand maximizing their L···L nonbonding distances.

2.1.3 The Energy States of Cobalt and Chromium Complexes

Cobalt is in group 9 of the periodic table and it has the electron configuration [Ar] $4s^2 3d^7$ in the free atom with nine valence electrons.[4] The *d* orbitals become more stable once the atom forms a complex. This is because of metal-ligand bonding. The electron configuration for Co(III) is [Ar] $3d^6$ and this explains why Co^{+3} has a higher preference for the octahedral geometry. This d^6 configuration is composed of six electrons which fill the low-lying d_π orbitals of the crystal field diagram and the d_σ orbital is left vacant. In organometallic chemistry the low spin d^6 configuration is the most frequent type of metal complex. There is a trend to spin-pair the electrons in the d^6 configuration. If the ligand field splitting is small enough then periodically the electrons may rearrange in order to give the high-spin form $t_{2g4}e_{g2}$, where all the unpaired spins are aligned. The fact that fewer electrons are paired together in the same orbitals supports the formation of the high-spin form and as a result electron-electron repulsions are reduced as shown in **Figure 2.3**.

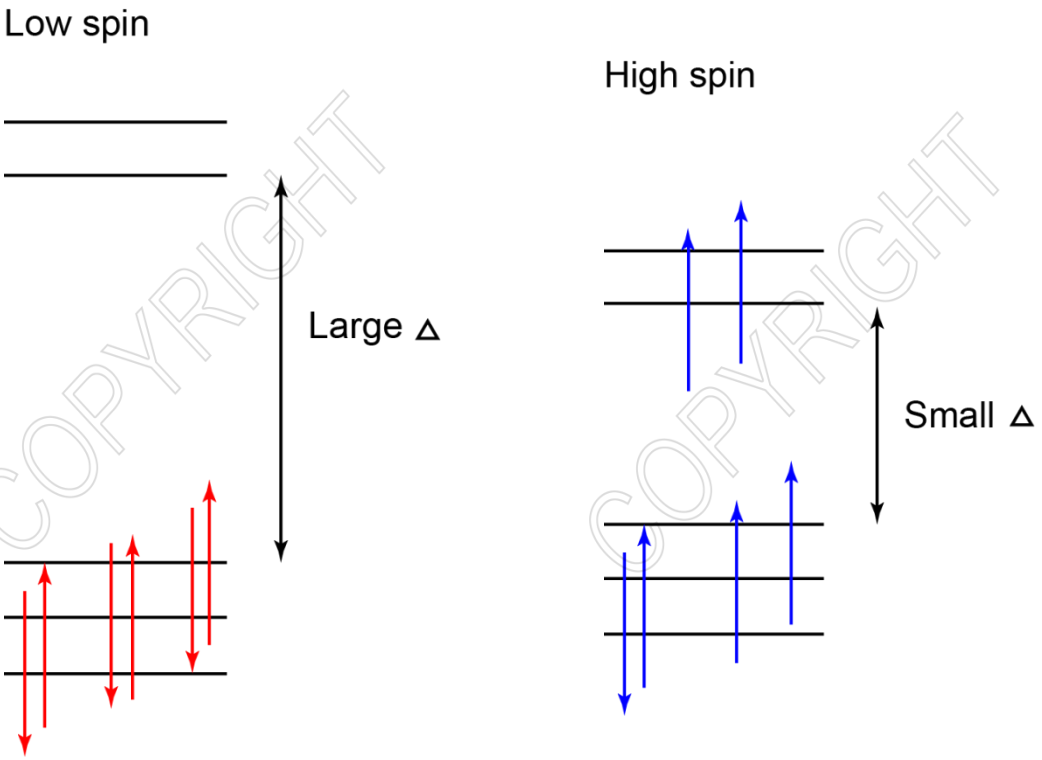

Figure 2.3 Both are d^6 metal ions; the Δ value will determine if it is a high or a low-spin complex. A high Δ leads to the low-spin form.

If Δ increases then the amount of energy gained by dropping from the e_g to the t_{2g} level will be adequate to force the electrons into pairing up.

If the magnetic moment of the complex is known, the spin state of the complex can be determined. This is accomplished by determining the weight of the sample of the complex in a magnetic field gradient.[4] Like Co(III) complexes a molecule is diamagnetic if it is weakly repelled by the field and the d^6 ion has a low-spin. On the other hand a molecule is paramagnetic like Co(II) and Cr(III) complexes if it has a high-spin form and attraction into the field occurs because of unpaired electrons. A vast number of organometallic complexes are diamagnetic as Δ is generally large in these complexes.

In an octahedral d^7 ion one electron is positioned in the higher-energy (less stable) d_σ level and is a paramagnetic complex with a $t_{2g6}e_{g1}$ configuration.[4] The crystal field stabilisation energy of such a system will be less than for a d^6 (low spin) complex,

where all the electrons are positioned into the more stable t_{2g} level. Co(II) is an octahedral d^7 ion which is more reactive in comparison to the d^6 analogs and is presented in **Figure 2.4**.

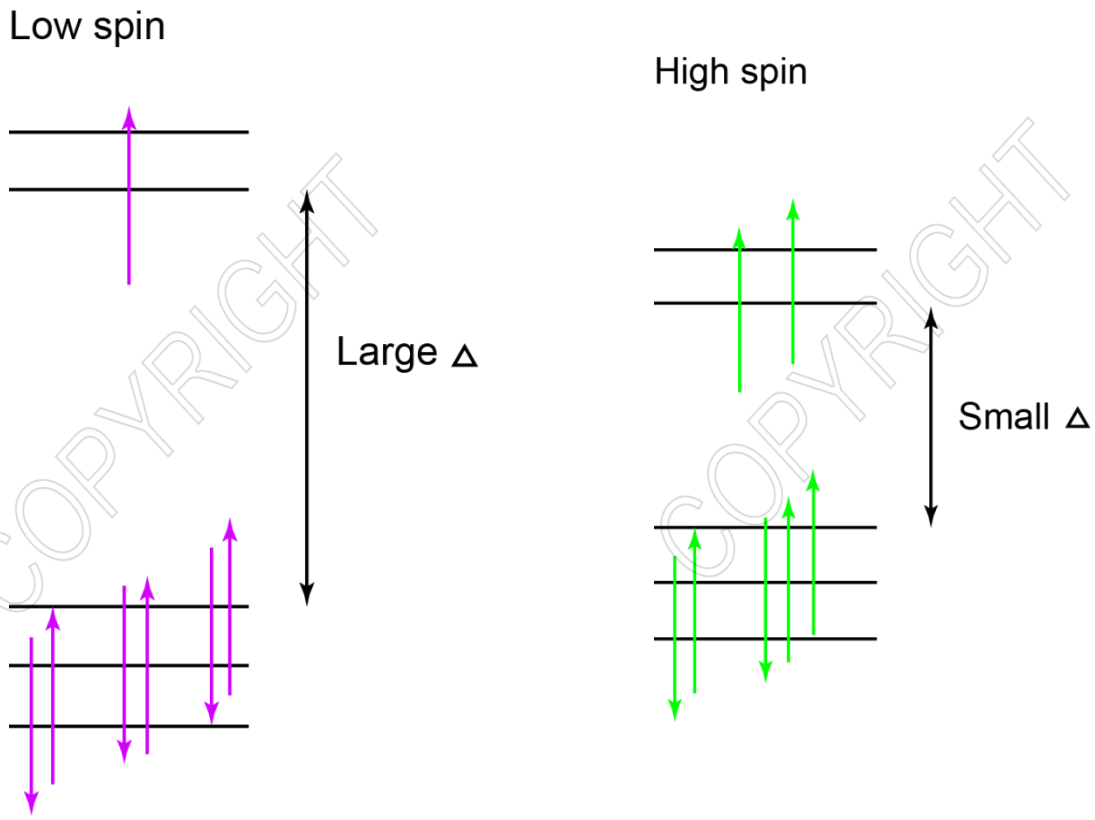

Figure 2.4 A d^7 octahedral ion is paramagnetic even in the low-spin form.

The reason for this is because the d_σ levels are M-L σ-antibonding in character.[4] Werner analysed Co(III) as the ligands are inclined to stay put and because low spin d^6 ions are often mentioned as being coordinatively inert. Cr(III) is a paramagnetic d^3 ion which has an inert coordination because the t_{2g} level is only half-filled. Co(II) is able to be coordinatively labile as it is not a d^6 or d^3 ion. The reason why second and third-row transition metals form more inert complexes is due to their higher Δ and CFSE (crystal field stabilisation energy).

2.1.4 Other Geometries

For any given geometry and ligand set, metal ions are inclined to have varying values for Δ.[4] Metals in low oxidation states and first-row metals are more likely to have low Δ values but second- and third-row metals as well as metals in higher oxidation states will most likely have higher Δ values.

2.2 Metal-Organic Frameworks

Metal-organic frameworks are a subdivision of two-dimensional or three-dimensional coordination polymers which are composed of metal ions or metal ion clusters and bridging organic ligands. These essential porous materials are important because of their unique functional and structural properties.

Metal-organic frameworks (MOFs) are a new form of crystalline porous material. The structure is composed of metal-oxide units which are connected to organic linkers through strong covalent bonds.[5,6] The choice of linker and metal will influence the structure as well as the properties of the metal-organic framework.[7] These compounds are generally comprised of inner "pores" which are used to house the guest molecule. The shape and size of the pores determines which atoms or molecules can be used.[5,6]

Metal-organic frameworks forms part of supramolecular chemistry, which is generally used to define the organization of molecules into larger structures by employing weak reversible interactions like hydrogen bonding, van der Waal forces and π stacking. Transition metals are mainly used in the construction of super molecules. Four-coordinate square planar or six-coordinate octahedral configurations of structures have been reported. Ligands with different types of coordination modes are employed and capping molecules are used in order to avoid

[5] H. Li, M. Eddaoudi, M. O'Keeffe and O.M. Yaghi. *Nature*, 1999, **402**, 276-279.

[6] J.L.C. Rowsell and O.M. Yaghi. *Microporous and Mesoporous Material*, 2004, **73**, 3-14.

[7] A.U. Czaja, N. Trukhan and U. Müller. *Chemical Society Review*, 2009, **38**, 1284-1293.

the formation of oligomers. Certain atoms like Ti(IV), Cr(III), Co(III) and Pt(II) can be compelled to form super molecules by influencing the reaction conditions so that thermodynamic equilibrium is reach. The overall construction of the species is controlled by the type of ligand as well as the oxidation state of the metal. For a solid which is crystalline to be termed a metal-organic framework it should have strong bonding which provides robustness, linking units which can be altered by organic synthesis and a structure which is geometrically well defined. **Figure 2.5** displays some building units which are found in metal carboxylates.[6]

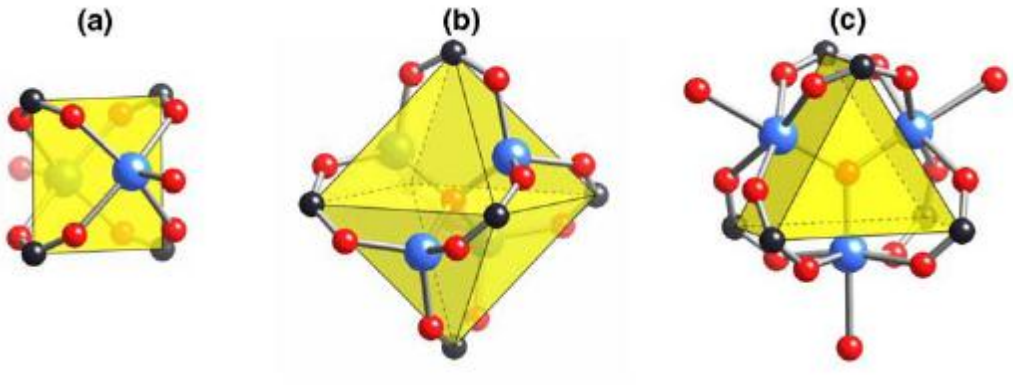

Figure 2.5 Illustration of inorganic secondary building units which generally occur in metal carboxylates (a) the square "paddlewheel" with two terminal ligand sites, (b) the octahedral "basic zinc acetate" cluster and (c) the trigonal prismatic oxo-centered trimer, with three terminal ligand sites.[6]

2.2.1 Phosphonate Frameworks

The utilisation of phosphonate ligands in the construction of framework structures is less abundant in comparison to the carboxylate ones. This could be due to several factors; (1) the ability to form basic phosphonate structures as compacted layered materials, (2) growing single crystals is more challenging because phosphonate phases tend to precipitate out more quickly as less ordered, insoluble phases and (3) the coordination chemistry of phosphonates is more complicated because of the different stages of deprotonation. Despite all of this phosphonate ligands are appealing as they form interesting compounds with different properties and structures. The structures of phosphonate frameworks are determined by numerous synthesis variables such as the type of metal, the type of phosphonate, the metal to

phosphonate ratio, the solvent, the concentration, the pH and finally the reaction temperature.[8] Shimizu and co-workers investigated the microporous behaviour present in a phosphonate, $[Cu_3(H_3L)(OH)(H_2O)_3]\cdot H_2O\cdot MeOH$ was synthesized where H_8L=1,3,5,7-tetrakis(4-phosphonatophenyl)adamantine. The structure as depicted in **Figure 2.6** is made up of $[Cu_3(\mu\text{-}OH)]$ trimer units and the phosphonate ligands which behave as tetrahedral nodes.[9]

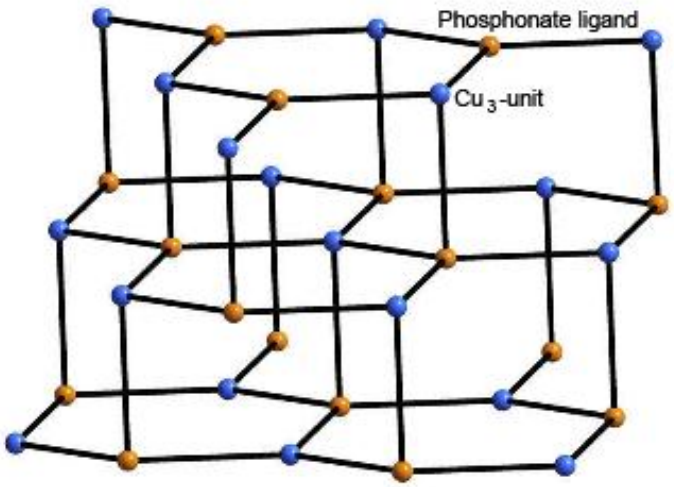

Figure 2.6 The connectivity between the $[Cu_3(\mu\text{-}OH)]$ trimer units and 1,3,5,7-tetrakis(4-phosphonatophenyl)adamantine forming the diamond structure.[9]

Bis(2,3-dimethylanilinium) diaquabis[dihydrogendiphosphato(2-)]cobaltate(II) as depicted in **Figure 2.7** was prepared by S. Ahmed and co-workers as part of a structural study on organic metal(II) diphosphonate systems.[10]

[8] S. Natarajan and P. Mahata. *Solid State and Material Science*, 2009, **13**, 46-53.

[9] G.K.H. Shimizu, R. Vaidhyanathan and J.M. Taylor. *Chemical Society Reviews*, 2009, **38**, 1430-1449.

[10] S. Ahmed, A. Samah and R. Mohamed. *Acta Crystallographica*, 2006, **E62**, m1796-m1798.

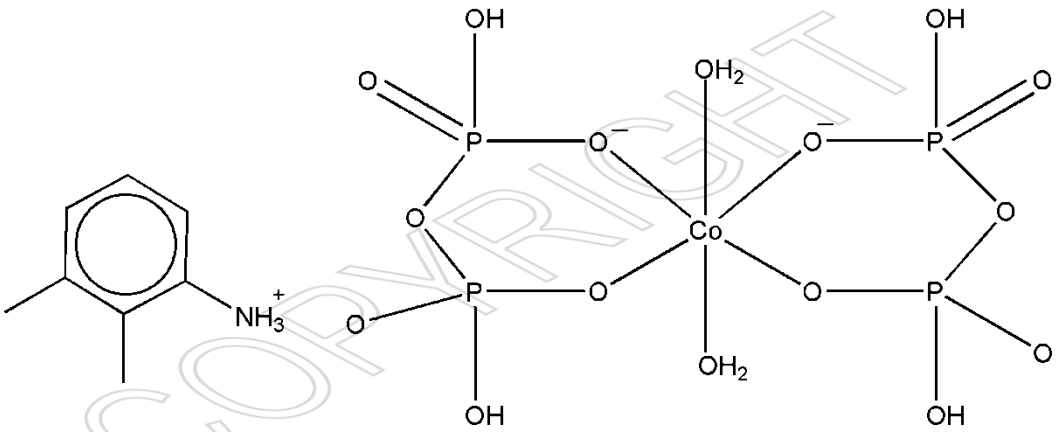

Figure 2.7 Structure of $(C_8H_{12}N)_2[Co(H_2P_2O_7)_2(H_2O)_2]$.[10]

2.3 Bis(phosphonate) Ligands

Geminal bis(phosphonate) ligands have been used extensively for the last 20 years and are characterised by having P-C-P bonds.[11] No known enzyme is able to cleave the P-C-P linkage. The CoPCP is stable to acid hydrolysis both at the enzyme-active site and in solution. This is due to the fact that the methylene carbon atom is saturated and therefore cannot be protonated any further.[12]

Methylenediphosphonates ($O_3PCH_2PO_3$) have a diversified coordination capability with metal ions, due to the single methyl group which divides the two phosphonate groups. The formation of a stable six-membered ring comprised of M-O-P-C-P-O is favoured.[13]

[11] V. Kubiček, J. Rudovskỳ, J. Kotek, P. Hermann, L. Vander Elst, R.N. Muller, Z.I. Kolar, H.T. Wolterbeek, J.A. Peters and I. Lukeš. *Journal of the American Chemical Society*, 2005, **127**, 16477-16485.

[12] T.P. Haromy, W.B. Knight, D. Dunaway-Mariano and M. Sundaralingam. *Inorganic Chemistry,* 1984, **23**, 2412-2415.

[13] S. Bao, L. Zheng, Y. Liu, W. Xu and S. Feng. *Inorganic Chemistry,* 2003, **42**, 5037-5039.

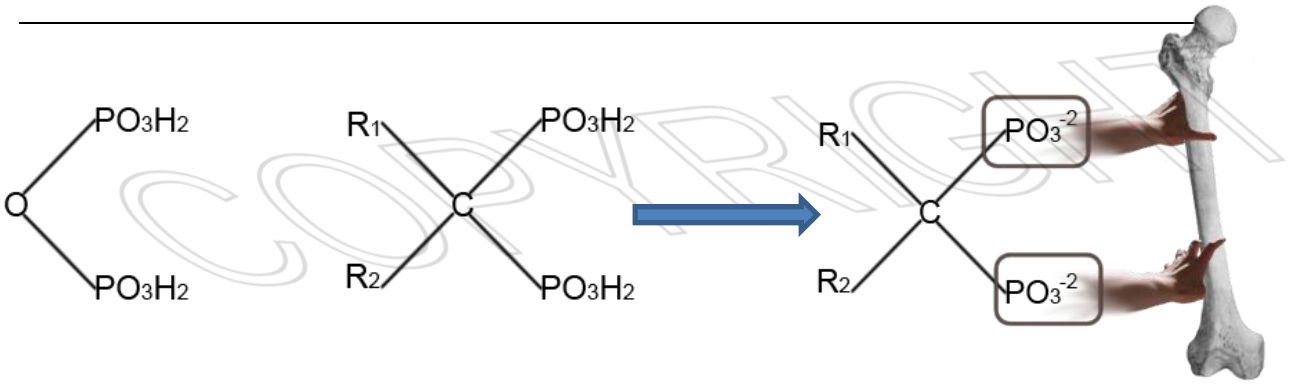

(a) Pyrophosphonate **(b) General structure of a bis(phosphonate)**

Figure 2.8 Schematic representation of (a) pyrophosphate and (b) bis(phosphonate).

The two other substituents (R1 and R2) of the bis(phosphonate) are coordinated to the central carbon atom as displayed in **Figure 2.8**. These substituents (R1 and R2) are responsible for the clinical effect of the drug as they have an effect on the cells which are responsible for the formation of bone and desorption.[11]

Diphosphonates are a class of ligands which are chemically similar and mimic the physiological behavior of phyrophosphate.[14]

Pyrophosphate and diphosphate are ligands which are chemically attracted to calcium(II) in a homogeneous solution at the surfaces of minerals and bone as depicted in **Figure 2.8(b).** Diphosphonates are better in comparison to pyrophosphate in that the P-CR(R')-P linkage is more resistant to hydrolysis when compared to the P-O-P linkage. Simple diphosphonate salts are therapeutically employed for the treatment of bone and calcium metabolic disorders.[14]

Bisphosphonates adhere strongly to hydroxyapatite crystals and constrain their formation and dissolution.[15] This physicochemical *in vivo* effect may result in the prevention of soft tissue calcification or even prevent normal calcification. The bis(phosphonic acid) has a high affinity for bone surfaces and it is also non-hydrolyzable.[16] They adhere to the active parts of the bone, where growth and

[14] S.S. Jurisson, J.J. Benedict, R.C. Elder, R. Whittle and E. Deutsch. *Inorganic Chemistry*, 1983, **22**, 1332-1338.

[15] H. Fleisch. *Drugs*, 1991, **42**, 919-944.

[16] H.L. Neville-Webbe, I. Holen and R.E. Coleman. *Cancer Treatment Reviews*, 2002, **28**, 305.

pathological changes take place. Bisphosphonates which contain a nitrogen atom like APD are more effective than MDP which doesn't contain a nitrogen atom. They also display anti-parasitic, anti-bacterial and herbicidal activity. Bisphosphonates seem to be the drug to use in order to slow down and prevent bone resorption and destruction.[17,18]

Bisphosphonates have been employed to manage numerous clinical conditions like ectopic bone formation, ectopic calcification, osteoporosis, Paget's disease and elevated osteolysis of malignant origin. There are three commercially available compounds currently being used for tumour induced bone diseases, namely etidronate, clodronate and pamidronate which are the most effective compounds.[15]

The cobalt diphosphonate complexes are unwavering over the pH range of 0-12 but in the pH range of 3-8 they are neutral and are also only slightly soluble in water.[19] Co(II) ions are linked to each other through O-P-O bridges and the weak antiferromagnetic interaction ought to be propagated through the O-P-O linkages.[20] Cobalt(III)-phosphine complexes with dimethylphosphino donor groups display a strong *trans* influence with substantial elongation of the *trans*-positioned Co(III)-ligand bond.[19]

2.4 Cobalt and Chromium Phosphonate Complexes

A literature search resulted in a few cobalt(II)- and cobalt(III) phosphonate complexes but no chromium phosphonate complexes were found.

T.P. Haromy and co-workers were investigating structurally similar analogues of adenosine triphosphate (ATP) by determining the differences present in structures

[17] K. Stahl, J. Oddershede, H. Preikschat, E. Fischer and J.S. Bennekou. *Acta. Cryst*., 2006, **C62**, m112-m115.

[18] J. Mao, S. Mukherjee, Y. Zhang, R. Cao, J.M. Sanders, Y. Song, Y. Zhang, G.A. Meints, Y.G. Gao, D. Mukkamala, M.P. Hudock and E. Oldfield. *Journal of the American Chemical Society*, 2006, **128**, 14485-14497.

[19] T. Suzuki, T. Imamura, S. Kaizaki and K. Kashiwabara. *Polyhedron*, 2002, **21**, 835-841.

[20] P. Yin, X. Wang, S. Gao and L. Zheng. *Journal of Solid State Chemistry*, 2005, **178**, 1049-1053.

with chelate rings formed from adenosine triphosphate and adenylyl methylene disphosphonate. They were able to successfully synthesis $CoH_2P_2O_6CH_2(NH_3)_4^+Cl^-$ (**Figure 2.9)**. This Co(III) complex has a methylene group in the bridge oxygen position. The P-C-P angle is 116.4(3)º and the Co-O distances are 1.942 Å and 1.949 Å. The P-C bonds (1.789(5) and 1.799(5) Å) are considerably longer than the bridge P-O bonds (1.601 Å and 1.627 Å).[12]

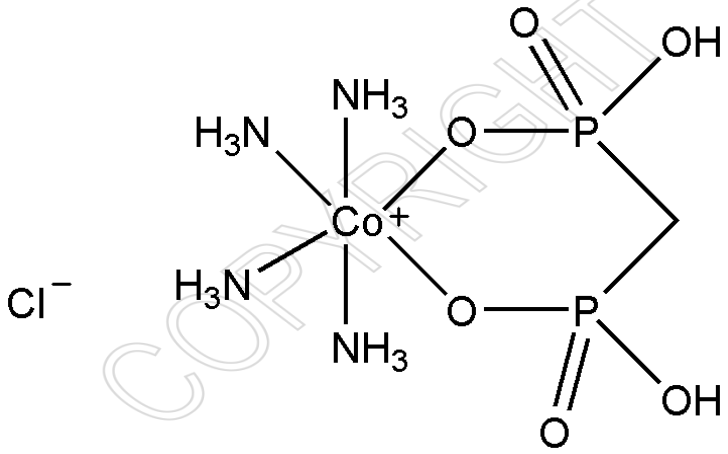

Figure 2.9 Structure of tetraammine(methylenediphosphonato)cobalt(III) hydrochloride.[12]

In a study investigating the calcium affinity of coordinated diphosphonate ligands and the implications thereof on the technetium-99m-diphosphonate skeletal imaging agents, S.S. Jurisson and co-workers were able to successfully synthesize $[(en)_2Co(O_2P(OH)CH_2P(OH)O_2)]ClO_4 \cdot H_2O$. The structure, is illustrated in **Figure 2.10**, was synthesized to be utilized as chemical probes to determine the extent of interaction present between the calcium(II) and the coordinated diphosphonate ligands. The P-C-P angle is 116.1(3)º and the Co-O distances are around 1.931(3) Å. The P-C bonds (1.793(3) Å and 1.799(4) Å) are considerably longer than the bridge P-O bonds which range from 1.491(2) Å to 1.562(2) Å.[14]

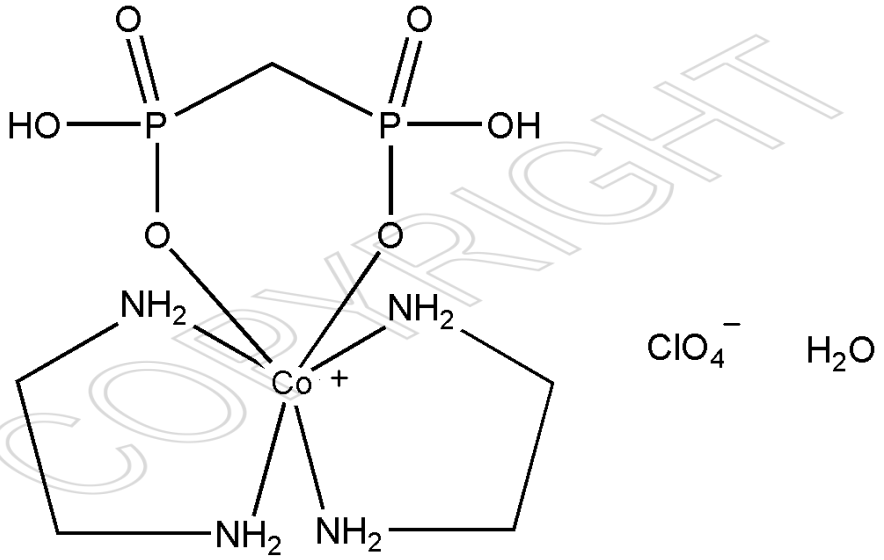

Figure 2.10 Structure of $[(en)_2Co(O_2P(OH)CH_2P(OH)O_2)]ClO_4 \cdot H_2O$.[14]

V.V. Bon and co-workers wanted to better understand the physiological activity of bisphosphonates so they synthesized $[Co(C_2H_8NO_6P_2)_2(H_2O)_2] \cdot 9H_2O$ (**Figure 2.11**) and studied the individual properties as well as the complex-forming driving factors of this complex. The P-C-P angle is 112.1(1)º and the Co-O distances range from 2.070(1) Å to 2.120(2) Å. The P-C bonds (1.843(2) and 1.844(2) Å) are considerably longer than the bridge P-O bonds which range from 1.500(2) Å to 1.560(2) Å.[21]

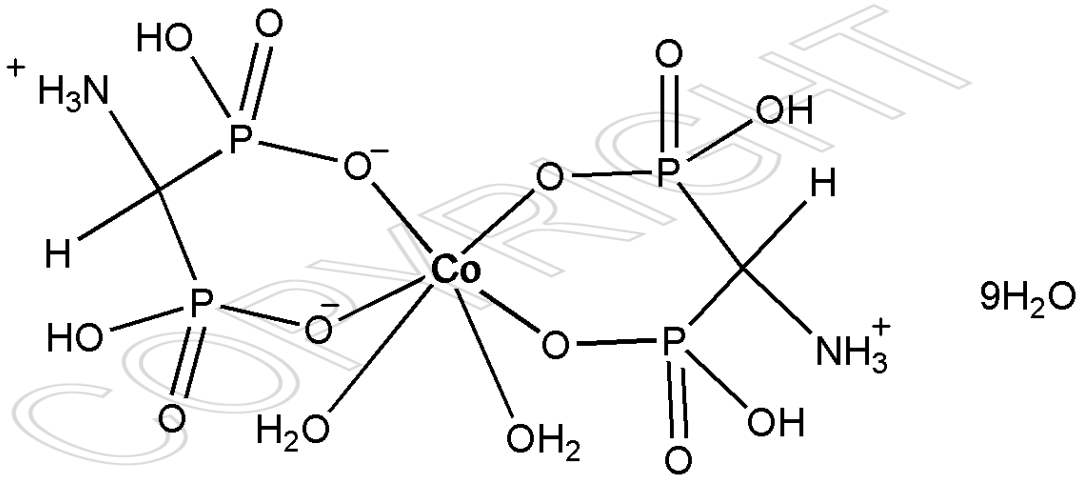

Figure 2.11 Structure of bis(1-ammonioethane-1,1-diyldiphosphonato)diaquacobalt(II) nonahydrate.[21]

[21] V.V. Bon, A.V. Dudko, A.N. Kozachkova, V.I. Pekhnyo and N.V. Tsaryk. *Acta Crystallographica*, 2010, **E66**, m537-m538.

2.5 Radiopharmaceuticals

2.5.1 Introduction

The definition of medicinal inorganic chemistry is the intentional or accidental "introduction" of a metal ion into a biological system. When the metal ion is intentionally placed into the biological system its purpose is either a therapeutic or a diagnostic one.[22] In imaging and radiotherapy the term radiopharmaceutical is applied when a drug contains a radionuclide with a suitable half-life, high purity and high specific activity.[23,24]

Radiopharmaceuticals are utilised primarily for medicinal diagnosis purposes. They are usually administered once and are comprised of a minute quantity of active substance which is coordinated to a radionuclide in order to obtain scintigraphic images or to measure biodistribution.[23,24]

Radiopharmaceuticals are continuously changing in composition as time passes and this is referred to as the radioactive decay.

2.6 The Significance of the Dissociation Constants in Radiopharmaceuticals

In medicinal chemistry acid-base titrations are used to determine the lipophilicity parameter, log P as well as the K_a values of a compound. If the protonation constants are known then the distribution plots can be determined, this displays the extent that a potential drug is ionized at the physiological pH (i.e., pH=7.40 in the blood). Specific properties like the solubility, lipophilicity and permeability through

[22] C. Orvig and M.J. Abrams. *Chemical Reviews*, 1999, **99**, 2201.

[23] S.S. Jurisson, D. Berning, W. Jai and D. Ma. *Chemical Reviews*, 1993, **93**, 1137.

[24] W. Jai, D. Mai, E.W. Volkert, A.R. Ketring, G.J. Ehrhardt and S.S. Jurisson. *Platinum Metals Review*, 2000, **44**, 50.

membranes are all pH dependent and must be optimised during the development of a new drug.[25]

2.7 The Use of Cobalt as a Radiopharmaceutical

The Co^{+3} ion is unstable in water and reduction to Co^{+2} can be prevented by coordinating it to a chelator or a ligand. Cobalt(III) complexes which are coordinated to N,O donor ligands are used as antibacterial and antiviral agents. Cobalt(II) complexes are also known to have antibacterial properties and are popular, primarily because of their aqueous stability, availability and because they are easily synthesised.[26] Cobalt has five essential isotopes as displayed in **Table 2.1**.[27]

Table 2.1: Selected cobalt isotopes

Nuclide	^{56}Co	^{57}Co	^{58}Co	^{59}Co	^{60}Co
Atomic Mass	55.940	56.936	57.936	58.933	59.934
Natural Abundance	≈0%	≈0%	≈0%	100%	≈0%
Half-life	77 days	270 days	71.3 days	Stable	5.26 years

^{60}Co is generated by the thermal neutron bombardment of ^{59}Co which is the natural isotope. ^{60}Co has a half-life of 5.3 years and decays to a non-radioactive nickel (^{60}Ni) by emitting β^- and γ rays. The gamma rays of ^{60}Co are used for food sterilization and cancer therapy.[28]

Radioactive cobalt, ^{60}Co, is employed to analyse defects present in the absorption of vitamin B_{12}. The metallic atom, cobalt is at the core of the B_{12} molecule. A patient is injected with vitamin B_{12} which has been labelled with the radioactive cobalt, the

[25] A. Kraft. *Journal of Chemical Education*, 2003, **80**, 554-559.

[26] E.L. Chang, C. Simmers and D.A. Knight. *Pharmaceuticals*, 2010, **3**, 1711-1728.

[27] L.C. Bate and G.W. Leddicotte. *The Radiochemistry of Cobalt*, p 1-7, United States Atomic Energy Commission, United States of America, **1961**.

[28] M. Kobayashi and S. Shimizu. *European Journal of Biochemistry*, 1999, **261**, 1-9.

physician is then able to analyse the course that the vitamin takes through the body and determine if there are any irregularities.[29,30,31]

2.8 The Use of Chromium as a Radiopharmaceutical

Chromium has four essential isotopes as displayed in **Table 2.2**.[32] Minute quantities of chromium(III) are vital as nutrients for humans and if one has a shortage of chromium it can lead to cardiovascular disease and diabetes. Chromium appears to play a vital role in helping the body metabolise sugar and lipids.[33] An excess of chromium(III) will result in skin rashes. Chromium(VI) on the other hand is harmful in large quantities and can even be carcinogenic.[34,35]

Table 2.2: Selected chromium isotopes

Nuclide	^{50}Cr	^{51}Cr	^{52}Cr	^{53}Cr	^{54}Cr
Atomic Mass	49.946	50.945	51.941	52.941	53.939
Natural Abundance	4.35%	≈0%	83.79%	9.50%	2.37%
Half-life	1.8 x 10^{17} years	27.7 days	Stable	Stable	Stable

Numerous chromium isotopes are being utilised for medical purposes.[36,37] ^{50}Cr is mainly used to generate the radioisotope ^{51}Cr which is predominantly used as a

[29] S.J. Baker and D.L. Mollin. *British Journal of Haematology*, 1955, **1**, 46-51.

[30] D.L. Mollin, C.C. Booth and S.J. Baker. *British Journal of Haematolo*gy, 1957, **3**, 412-428.

[31] J. Metz and D. Hart. *S.A. Medical Journal*, 1963, 404-406.

[32] J. Pijck. *Radiochemistry of Chromium*, p 3, United States Atomic Energy Commission, United States of America, **1964**.

[33] R.A. Anderson. *Regulatory Toxicology and Pharmacology*, 1997, **26**, 35-41.

[34] M.I. Greenberg. *Occupational, Industrial and Environmental Toxicology*, 2nd Edition, p 434, Elsevier Health Sciences, Philadelphia, Pennsylvania, **2003.**

[35] N.J. Peckenpaugh and C.M. Poleman. *Nutrition Essentials and Diet Therapy*, 9th Edition, p 120, Elsevier Health Sciences, United States of America, **2003**.

[36] A.V. Hoffbrand, P.A.H. Moss and J.E. Pettit. *Essential Haematology*, 5th Edition, p 27, Blackwell Publishing, United States of America, **2006**.

tracer which is injected into the patient. Once inside the blood, the isotope emits gamma radiation which can be detected by an external source. It is mainly used to determine the quantity of blood cells present in a patient as well as to quantify how long the blood cells will survive in the patient. ^{51}Cr is also used to diagnose spleen and gastrointestinal disorders.[38]

2.9 Therapeutic and Diagnostic Radiopharmaceuticals

2.9.1 Introduction

The utilisation of radioactive isotopes has had a profound effect on the practice of medicine. Radioisotopes were initially employed in medicine for the treatment of cancer. The treatment was founded on the bases that rapidly dividing cells, such as cancer cells, are affected more adversely by radiation from a radioactive substance than are the cells which divide slowly. A few years after the discovery of radioactivity, radium-226 and its decay product radon-222 were employed for cancer therapy. Today, cobalt-60 is more commonly used for gamma radiation.[39]

2.9.2 Selecting a Radioisotope

A radioisotope is the source of radiation which renders the therapeutic dose. The nuclear properties of a radioactive atom will determine whether the radiopharmaceutical will be used for therapeutic or diagnostic purposes. The desired therapeutic radioisotope should emit certain radiation: alpha emission, beta emission or Auger emission. Ideally there must be little to no gamma emission, but if there is it should have 5-20% abundance and be in the range of 100-200 keV in

[37] W.S. Beck. *Hematology*, 5th Edition, p 226, The Massachusetts Institute of Technology Press, United States of America, **1991**.

[38] J.J. Peterson, R.H. Pak and C.F. Meares. *Bioconjugate Chemistry*, 1999, **10**, 316-320.

[39] D.D. Ebbing and S.D. Gammon. *General Chemistry*, 8th Edition, p 880, Houghton Mifflin Company, United States of America, **2005**.

order to be utilized for *in vivo* tracking of the therapeutic dose, as well as for dosimetric calculations. The choice of which particle emitter to utilized will depend on the location and size of the tumour.[40]

2.9.3 Essential Factors to Consider when Designing a Radiopharmaceutical

1. Compatibility

   The nuclide that is chosen should be able to attach to a specific ligand. One can anticipate if this will work by looking at the chemical properties of the nuclide and the desired ligand.[41]

2. Stoichiometry

   During the preparation step the quantity of nuclide present must be known so that a precise amount of reducing agent can be added. The presence of too much reducing agent results in over reduction. Another crucial aspect is that enough chelating agent should be introduced in order to obtain maximum labelling.[41,42]

3. Charge of the molecule

   This ascertains the solubility of the compound in various solvents and also the site-specific biodistribution.[41,42]

4. Size of the molecule

   The size affects the rate of absorption and excretion, so cumbersome molecules (Mr > 60 000) are not filtered by the glomeruli of the kidneys. If the

[40] P.A. Schubiger, R. Alberto and A. Smith. *Bioconjugate Chemistry*, 1996, **7**, 165-179.

[41] G.B. Saha. *Fundamentals of Nuclear Pharmacy*, p 85, Springer-Verlag, New York, **1992**.

[42] Y. Lee. *The Open Nuclear Medicine Journal*, 2010, **2**, 178-185.

molecule is massive it gets blocked in the pulmonary tissue of the lungs and if it is too small it can get stuck in the liver.[41,42]

5. Protein binding

Most drugs attach to some degree to plasma proteins (albumin or globulin). This binding is determined by the charge of the molecule, the pH, the nature of the protein, the coordination sites which are accessible (i.e. O-, N-, S-donor atoms) and the concentration of anions in the plasma. When protein binding yields negative results it is because of the abnormal tissue distribution or slow plasma clearance of the radiopharmaceutical or because the uptake in the organs is inadequate.[41,43]

6. Solubility

Generally neutral drugs are insoluble in saline and first need to be protonated. A radiopharmaceutical that is to be injected must have a pH which is similar to that of the blood (which is roughly 7.4).[41,42]

7. Stability

A compound must be stable *in vivo* or *in vitro*.[41,44]

8. Biodistribution

This criterion is essential when assessing the usefulness and efficiency of the radiopharmaceutical and this includes the tissue distribution, plasma clearance, faecal excretion and urinary excretion.[41,44]

[43] K. Kawai, R. Nishii, N. Shikano, N. Makino, N. Kuga, M. Yoshimoto, S. Jinnouchi, S. Nagamachi, S. Tamura and N. Takamura. *Nuclear Medicine and Biology*, 2009, **36**, 99-106.

[44] G.P. Talwar and L.M. Srivastava. *Textbook of Biochemistry and Human Biology*, 3rd Edition, Prentice-Hall of India Private Limited, India, **2003**.

9. Redox properties

   A metal radionuclide can be oxidised by the oxygen found in the blood. Organic molecules and trace elements are able to reduce it. This results in poor or no uptake and must be considered when selecting a metal center. Certain oxidation states are more stable in *vivo* in comparison to others and this also applies to ligands which prefer certain oxidation states of the metal.[41]

10. Kinetic reactivity

    It is crucial to evaluate the reactivity of the metal towards the biological mimickers. Amino acids for instance, which are coordinating ligands react with the radiopharmaceutical by replacing the directing ligands and this might result in poor uptake in the desired organ.[41]

11. Mechanism of reaction

    The type of mechanism, be it associative, dissociative or interchange will have an effect on the uptake, washout rate and the design of the radiopharmaceutical.[41]

12. Radiation

    For therapeutic use the type of radiation used should be alpha, beta or Auger electron emission. For imaging only gamma and positron emissions are used. The strength and uptake of these emissions must be in the right ratios and localisation points in order to acquire usable results.[41]

2.10 Therapeutic Radiopharmaceuticals

Synthetic strategies[45] are employed to radiolabel a biomolecule as well as radionuclides,[46] which are crucial aspects to consider for the development of therapeutic radiopharmaceuticals. The intention is to deliver ionizing radiation to cancerous areas without affecting the healthy tissue. When treating bulk tumours, the desired approach is to use radionuclides which emit energetic alpha or beta particles.[45] Unlike external radiation beams these drugs are specifically designed to target certain organs and provide a vast amount of radiation. However, small tumour nests or small clusters of cancer cells are treated with radionuclides which distribute Auger electrons.[45] This approach is effective mainly because they have a high level of cytoxicity and a close range in which they are biologically effective.[47]

A crucial aspect to consider when developing an effective radiotherapeutic agent is to design and synthesize a bifunctional ligand which not only stabilises the metal center but also allows it to bind to a certain biomolecule.[48]

Table 2.3 Physical characteristics of therapeutic radioisotopes

Decay Mode	Particles	Energy Range	Penetrating depth
α	Helium nuclei	High (4 - 9 MeV)	50 - 100 μm
β^-	Electrons	Medium to high (0.5 - 2.3 MeV)	1 - 12 mm (100 times greater than an alpha particle)

[45] C.A. Hoefnagel. Annals of Nuclear Medicine, 1998, **12**, 61-70.

[46] S.R. Cherry, J.A. Sorenson and M.E. Phelps. *Physics in Nuclear Medicine*, 3rd Edition, 2003, Philadelphia, PA: Saunders.

[47] W.A. Volkert, W.F. Goeckeler, G.J. Ehrhardt and A.R. Ketring. *Journal of Nuclear Medicine*, 1991, **32**, 174-185.

[48] S. Liu and D.S. Edwards. *Bioconjugate Chemistry*, 2001, **12**, 7-34.

2.10.1 Alpha Particles

The reason why alpha decay takes place is because the nucleus has an excess of protons which causes too much repulsion and to reduce this repulsion a helium nucleus is expelled.[49] Alpha particles are positively charged and large in size. They are comprised of a high-energy helium nuclei which creates high densities of ionisation along linear tracks. It operates in a limited range which means that the "crossfire" effects are restricted as well as the mode of delivery. The linear energy transfer (LET) is substantially high, this implies that the alpha particle is highly destructive for small and homogenously distributed tumours. Some examples of alpha emitters are radium, radon, uranium and thorium.[50]

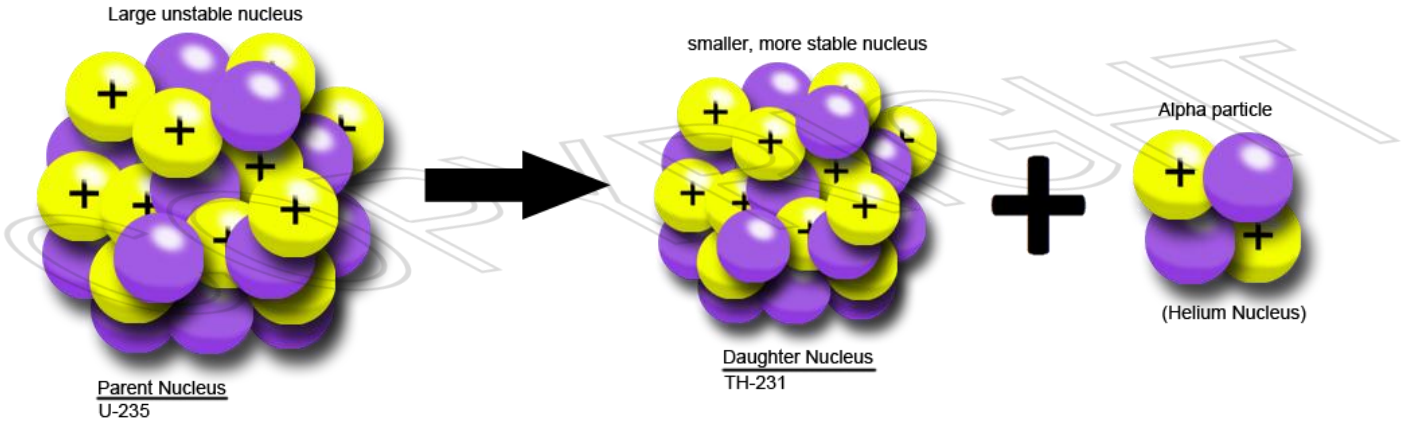

Figure 2.12 Schematic representation of alpha decay.

2.10.2 Beta Particles

They are negatively charged particles and are minute in size but have high energy electrons which are expelled from the nucleus.[49,50] The LET value is substantially lower than that of the alpha particle, thus to achieve effective cell destruction the concentration of the radioisotope within the tumour site must be high. These

[49] A. Jones. *Chemistry and Introduction for Medical and Health Sciences*, p 182-185, John Wiley and Sons Ltd, England, **2005**.

[50] W.A. Volkert and T.J. Hoffman. Chemical Reviews, 1999, **99**, 2269-2292.

particles are able to travel further into the tissue and this is advantageous in eradicating non-homogenously distributed tumours by producing a “crossfire” effect. Some examples of beta emitters are strontium-90, carbon-14, tritium and sulphur-35.

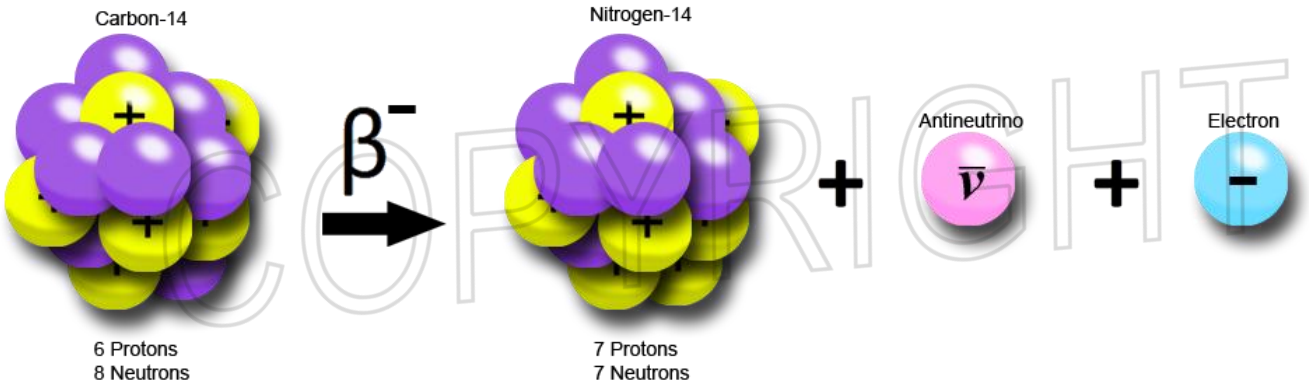

Figure 2.13 Schematic representation of beta decay.

2.10.3 Gamma Ray

Gamma decay occurs when the nucleus has too much energy, which causes the nucleus to drop to a lower energy state and emit a photon known as a gamma ray. It is comprised of a high-energy photon with a short wavelength and is similar to an X-ray but is more destructive and can penetrate even deeper into human tissue. It is just how X-rays and gamma rays are produced that makes them different.[49]

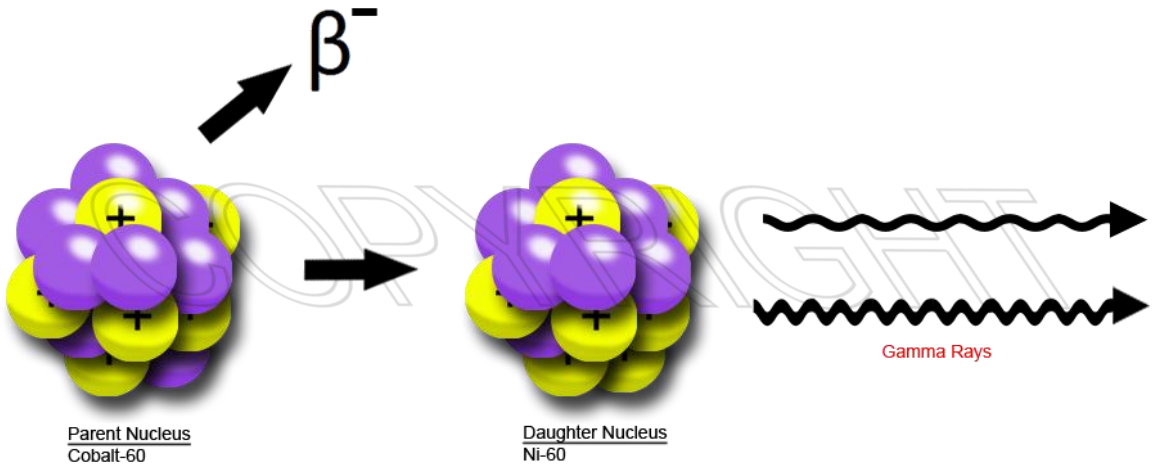

Figure 2.14 Schematic representation of gamma decay.

2.10.4 Properties of an Ideal Therapeutic Radiopharmaceutical

1. Beta decay

   Beta particle emitters have a large LET and are thus able to destroy tissue. With alpha emitting radionuclides the distribution in the tissue needs to be very specific in order to provide efficient therapy, whereas the beta particle emitters don't need the distribution in the tissue to be as optimal in order to administer the required therapy.[44,51,52]

2. High energy particles (> 1 MeV) is ideal

   The LET of the energy particles is large enough to cause satisfactory damage to the desired tissue.[44,51,52]

3. The half-life must be relatively long (5-20 days)

   After the radionuclide has been administered the therapeutic effects should follow.[51,52,53]

4. High target : nontarget ratio

   If the target : nontarget ratio is not high enough this will result in the treatment being ineffective with regards to the primary disease and possibly lead to the delivering of a fatal dose of radiation to the bone marrow or other radiosensitive tissue.[51,52]

5. Quantity of radiation administered should be small.[51.52,53]

[51] http://www.nucmedtutorials.com/dwradiopharm/rad3.html (cited on the 12th of February 2011).

[52] R.B. Gunderman. *Essential Radiology: Clinical Presentation, Pathophysiology, Imaging*, 2nd Edition, Thieme, United States of America, **2006**.

[53] C.L. Canon and C. Canon. McGraw-Hill Speciality Board Review Radiology, McGraw-Hill Professional, **2009**.

6. The diagnostic radiopharmaceutical must not be toxic.[44,51,53]

7. Able to produce large quantities of the radioisotope easily.[44,51,53]

2.10.5 Bifunctional Labelling Techniques of Biologically Active Molecules

Radiopharmaceuticals can be tiny inorganic/organic molecules or receptor-avid tracers like antibodies, hormones or peptides.[38,50,54,55,56,57] Recently there has been considerable interest in the use of small peptides in receptor-based targeted therapy mainly because vast quantities of tumours have high levels of cell surface receptors which adhere to peptides in comparison to normal tissue.[58] There are numerous ways to incorporate a radionuclide to a peptide, two of which are the direct labelling method and the bifunctional chelating agent (BFCA) method.[59]

❖ Direct labelling method

A radioisotope connects to a peptide via the side chain of a functional group or the peptide will assemble around the metal center.[48,60]

❖ Bifunctional chelating agent (BFCA) method

This method involves the attachment of the radioisotope to the peptide. The BFCA method is comprised of four parts: a targeting molecule, a ligand, a radionuclide and

[54] A. Buryak and K. Severin. *Angewandte Chemie*, International Edition, 2004, **43**, 4771-4774.

[55] A. Buryak and K. Severin. *Journal of the American Chemical Society*, 2005, **127**, 3700-3701.

[56] J.A. Katzenellenbogen. *Handbook of Radiopharmaceuticals*, p 715-750, John Wiley and Sons, United States of America, **2003.**

[57] M.J. Heeg and S.S. Jurisson. *Accounts of Chemical Research*, 1999, **32**, 1053-1060.

[58] K.T. Wheeler, L.M. Wang, C.A. Wallen, S.R. Childers, J.M. Cline, P.C. Keng and R.H. Mach. *British Journal of Cancer*, 2000, **82**, 1223-1232.

[59] J. Fichna and A. Janecka. *Bioconjugate Chemistry*, 2003, **14**, 3-17.

[60] M.F. Giblin, N. Wang, T.J. Hoffman and S.S. Jurisson. *Proceedings of the National Academy of Sciences of the United States of America,* 1998, **95**, 12814-12818.

a linker as depicted in **Figure 2.15**. When the linker is coordinated to the ligand before it is attached to the peptide, this ligand-linker combination is called the bifunctional chelating agent. It functions as the carrier and binding agent of the radioisotope while also being attached to the linker or in certain situations it is attached directly to the targeting molecule.[50]

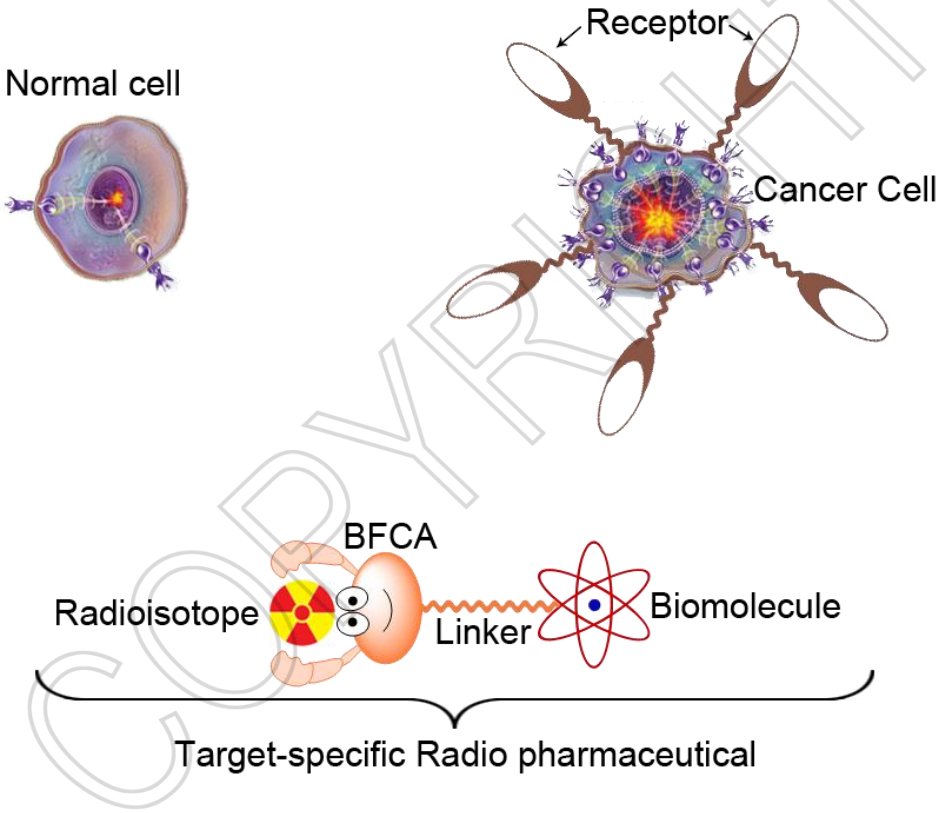

Figure 2.15 Schematic representation of a target-specific radiopharmaceutical.

The bifunctional chelate method is employed in two ways namely the pre-labelling or post-labelling method as explained in **Figure 2.16**.

- ✓ **Pre-labelling**

Step 1: Radioisotope coordinates to the chelate.

Step 2: The radioisotope chelate complex conjugates to the desired molecule.

- ✓ **Post-labelling**

Step 1: Involves the conjugation of the chelate and the target molecule.

Step 2: The radioisotope is bound to the conjugated complex.

Figure 2.16 A schematic explanation of the Pre- and Post-labelling methods

Post-labelling is the more desired approach mainly because of the time required to prepare the radiopharmaceutical and also because the radioisotope could have a short half-life. The pre-labelling approach is mainly used when extreme conditions are required for radiolabelling, such as high temperature or a low pH.

2.10.6 Several Factors to Consider when Developing an Ideal Bifunctional Chelating Agent (BFCA).

1. It is essential that the radioisotope-BFCA complex remain intact when delivered to the patient. A liberated radioisotope can potentially accumulate and deliver undesired radiation in organs.[57]

2. The BFCA must form a kinetically inert complex with the radioisotope, which determines the stability of the complex. This characteristic has an influence on the rate of dissociation of the radioisotope.[40,50]

3. The BFCA must be thermodynamically stable once it has coordinated to the radioisotope.[40,50]

4. Certain physical parameters play a role such as the lipophilicity and the bulkiness of the BFCA. If the BFCA is too lipophilic this results in the radiation concentrating in non-targeted organs like the fatty tissue or the liver. If the BFCA is too bulky the receptor's affinity is restricted.

2.11 Diagnostic Radiopharmaceuticals

Diagnostic medical imaging is a significant sector in the practice of modern medicine and is primarily used to assess the brain, kidney, liver, gall bladder, heart, lung and the bones. It involves the investigation, production and development as well as the use of radiopharmaceuticals, i.e. isotopes capable of emitting gamma-rays or positrons in certain chemical forms which are synthesized to gather in certain organs

of the body. A great deal of development has gone into use of radioactive isotopes in the diagnosis of diseases.[61] Radioactive isotopes are used for the diagnosis in two ways: firstly they are used to acquire images of internal organs in order to examine their functioning.[62] Secondly they are employed as tracers in the analysis of small amounts of substances like the growth hormone in the blood in order to determine the presence of possible disease conditions.[61]

The radionuclide which can be coordinated to a certain ligand is administered to the patient and accumulates in the diseased or cancerous tissue. It then emits photons like gamma (γ) rays or positrons (β^+) but not alpha (α) or beta (β^-) particles to the required area. The non-radioactive part of the drug is comprised of an organic molecule which could be a lipid, carbohydrate, nucleic acid, peptide, small protein or an antibody. A gamma-ray camera or PET which is located externally scans the organs and is able to provide diagnostic and prognostic data by displaying the images that the radioactive material emitted. This is a non-invasive technique.[61]

[61] S. Türker and A.Y. Özer. *FABAD Journal of Pharmaceutical Sciences*, 2004, **29**, 145-154.

[62] C.S. Cutler, J.S. Lewis and C.J. Anderson. *Advanced Drug Delivery Reviews*, 1999, **37**, 189-211.

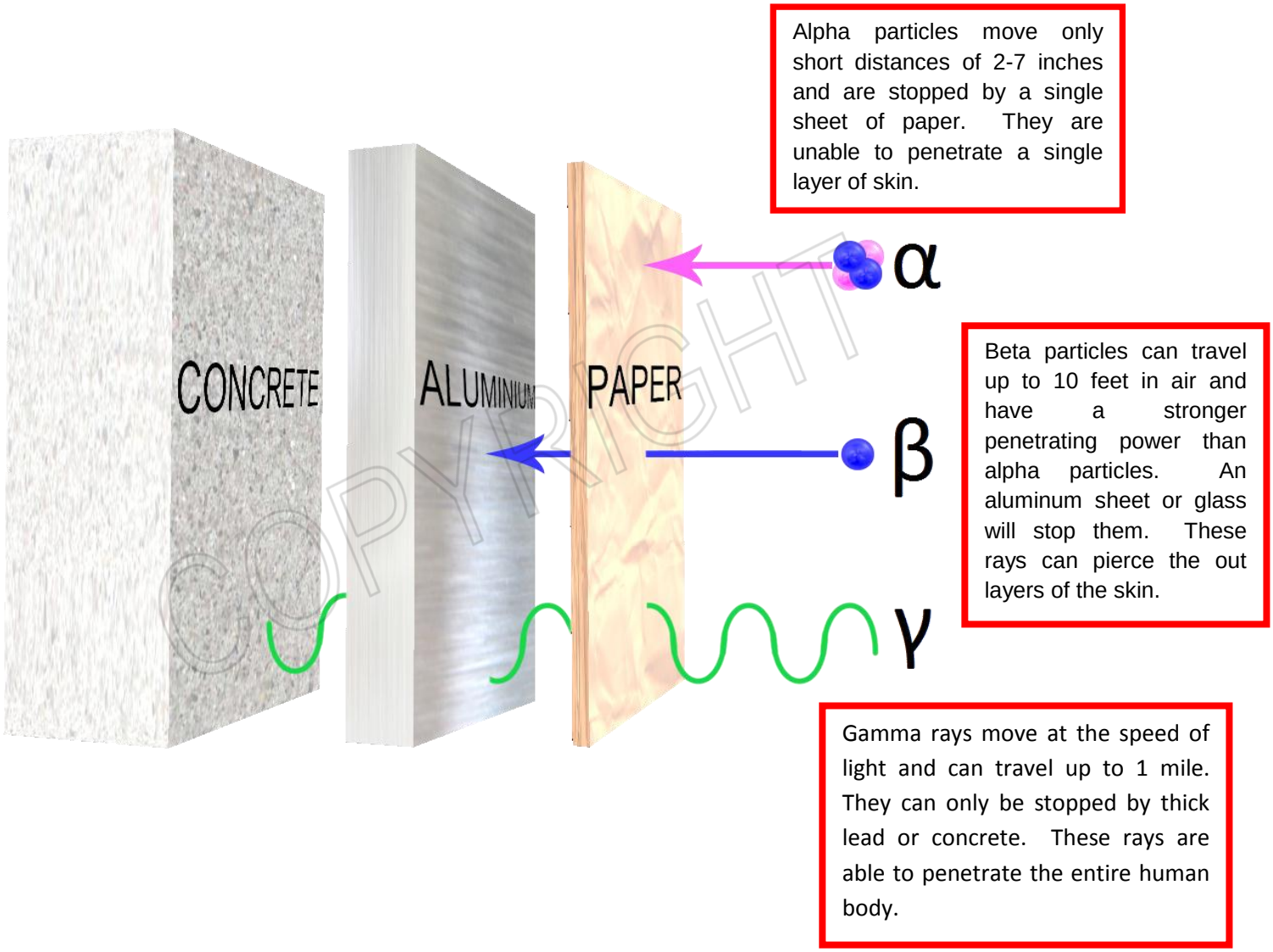

Figure 2.17 A schematic representation of the penetrating ability of an alpha, beta and a gamma particle.[63]

[63] B.T. Bennett. *Understanding, assessing, and responding to terrorism*, p 157, John Wiley and Sons, United States of America, **2007.**

2.11.1 Properties of an Ideal Diagnostic Radiopharmaceutical

1. It must only emit pure gamma rays

   A gamma ray is able to penetrate the body, enabling a gamma-ray camera to detect it. Gamma rays are unable to ionise cells so they can't damage them, but alpha and beta particles which have a high linear energy transfer (LET) can and if they ionise cells it would result in the formation of cancerous cells. The gamma emitter must decay by either isomeric transition or electron capture and examples of these types of radioisotopes are ^{201}TI and ^{133}Xe.[64,65,66]

2. An ideal imaging gamma energy range is between 100-250 keV.[64,66]

3. The half-life must be short

   The half-life is the time needed for a radioisotope to decay to 50% of its initial activity. Radionuclides normally have a short half-life and in order to compensate for this the final preparations are done just before the drug is administered to the patient. This results in the use of semi-manufactured products like precursors, radionuclide generators and kits.[64,65,66] Ideally the half-life should be 1.5 times the duration of the diagnostic procedure (a few hours), this guarantees that the radiation leaves the body rapidly and it doesn't accumulate in undesired areas.[67]

[64] http://www.nucmedtutorials.com/dwradiopharm/rad2.html (cited on the 12th of February 2011).

[65] A.W. Chao and W. Chou. *Reviews of Accelerator Science and Technology*, Volume 2, p 32, Mainland Press, Singapore, **2009**.

[66] R.B. Gunderman. *Essential Radiology: clinical presentation, pathophysiology, imaging*, 2nd Edition, p 20, Thieme Medical Publishers, United States of America, **2006**.

[67] S. Liu. *Chemical Society Reviews*, 2004, **33**, 445-461.

4. High target : nontarget ratio

   A minimum ratio of 5:1 is required for planar imaging and 2:1 for SPECT imaging, if the ratio is too small the result is a non-diagnostic scan which means that you can't differentiate between the pathology and the background.[64,65,66]

5. Quantity of radiation administered should be small.

   The patient is injected with a small amount in order to obtain good image quality.[64]

6. The diagnostic radiopharmaceutical must not be toxic.[64]

7. Chemical reactivity

   Target receptor sites present in tumours are limited thus a radiolabelled compound will have to be site-specific and have a high amount of activity. It must also be able to bind to numerous compounds.[64,65]

8. Able to produce large quantities of the radioisotope easily and at an affordable price.[64,66]

2.12 Technetium Radiopharmaceuticals

^{99m}Tc imaging agents were initially used in 1961. $^{99m}TcO_4^-$ was used to generate an image of the thyroid and was referred to as the technetium essential agent. The biodistribution was determined by the physical properties of the complex (essential aspects are the charge, lipophilicity and size, etc.) ^{99m}Tc complexes have been used to image various organs like the liver, kidney, heart, brain and bones.[68]

[68] U. Abram and R. Alberto. *Journal of the Brazilian Chemical Society*, 2006, **17**, 1486-1500.

2.12.1 Brain Imaging

Brain imaging agents are predominantly used for perfusion imaging and to label the central nervous system (CNS) receptor ligands. The function of these biological ligands is to target receptors located in the brain. These ligands are vital because of the influence they have on a vast range of mental disorders like Alzheimer's and Parkinson's diseases or schizophrenia.

An advantage of a radioactive tracer is its ability to pick up small structural changes or disruptions in brain-function. These agents must have certain biological and chemical properties in order to transverse the blood brain barrier. A vast amount of the complex must be extracted and be proportional to the blood flow. The complexes which are minute, lipophilic and neutral must be able to cross the blood brain barrier via passive diffusion.[69]

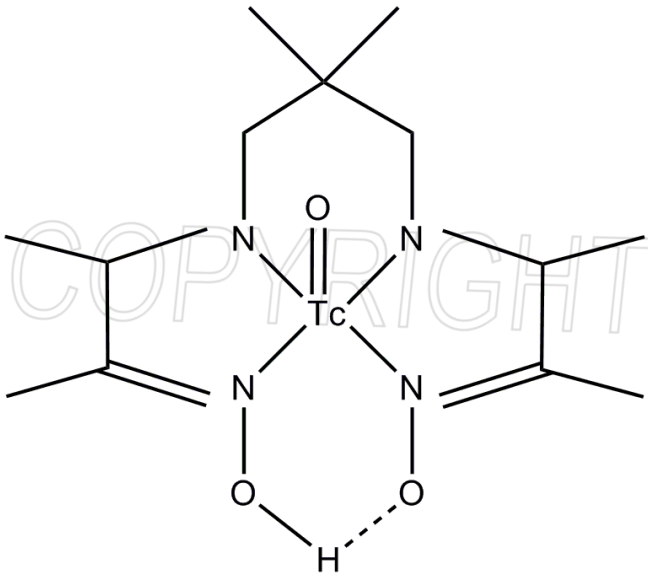

Figure 2.18 A graphical representation of ^{99m}Tc-HMPAO

An example of a brain imaging agent currently being used is ^{99m}Tc-HMPAO, it is lipophilic and is able to permeate the blood brain barrier and be extracted from the blood effectively.[70]

[69] B.B. Brodie and C.A.M. Hogben. Journal of Pharmacy and Pharmacology, 1957, **9**, 345-380.

[70] M.M. Khalil. *Basic Sciences of Nuclear Medicine*, p 43-48, Springer, United Kingdom, **2010**.

2.12.2 Cardiovascular Imaging

The advantage of using a technetium-labelled perfusion agent in comparison to using ^{201}TI which was originally used, is that the technetium imaging agents have a short half-life of 6 hours and emit (140 keV) photons, which results in better quality images. Two technetium-based agents which are currently in use are ^{99m}Tc-labelled sestamibi and ^{99m}Tc-labelled tetrofosmin.

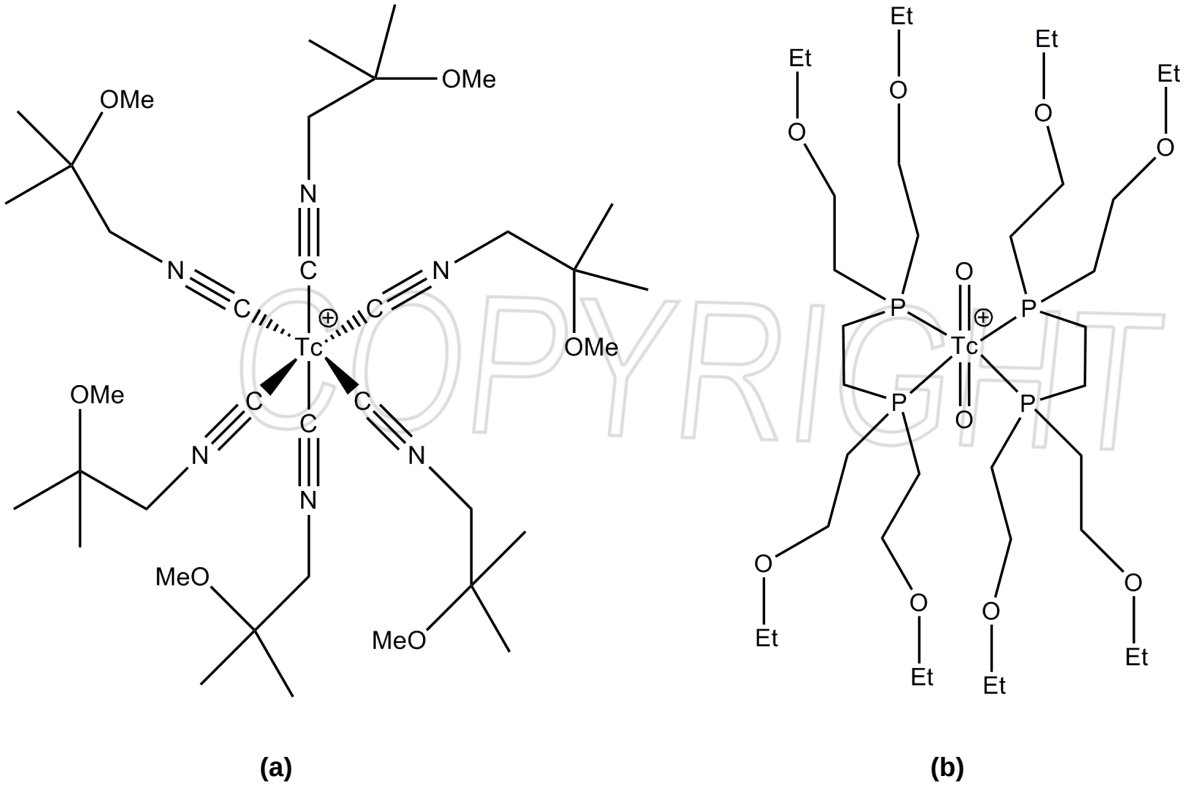

(a) **(b)**

Figure 2.19 The chemical structure of (a) ^{99m}Tc-sestamibi and (b) ^{99m}Tc- tetrofosmin.

They are distributed in the myocardium in relation to the myocardial blood flow. ^{99m}Tc-labelled sestamibi has a higher extraction fraction in comparison to ^{99m}Tc-labelled tetrofosmin but ^{99m}Tc-labelled tetrofosmin has a faster clearance from the liver and lungs compared to ^{99m}Tc-sestamibi. A major difference between the technetium-based perfusion tracers and thallium is that the technetium tracers show little redistribution within the first few hours after the tracer is administered via

injection. Thus the period between administering the isotope and acquiring the image is more flexible than that of thallium.[71]

2.12.3 Kidney Imaging

These imaging agents are employed to provide clinical information with regard to cortical structure, renal bloodflow and renal functioning in terms of both the glomerular filtration and the tubular secretion. Renal agents can be separated into three types: those which are filtered, those that are secreted and those which show mixed behaviour.[72] ^{99m}Tc radiopharmaceuticals used for renal imaging are hydrophilic complexes with a small molecular weight.[73]

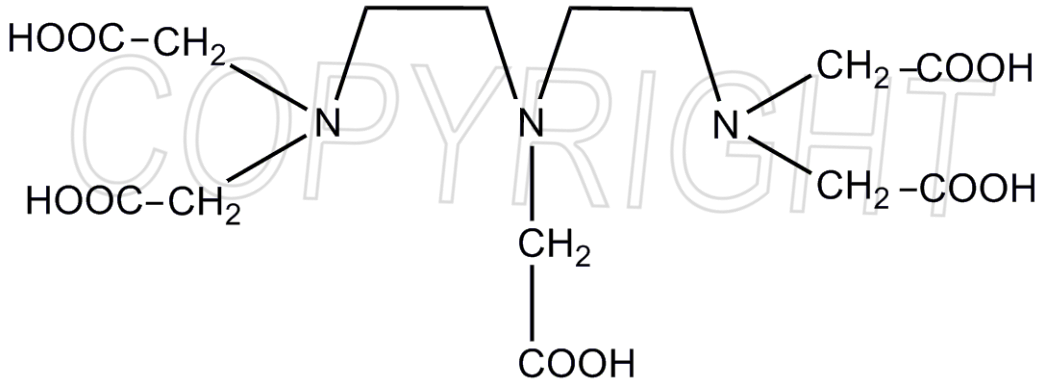

Figure 2.20 The schematic representation of the DTPA ligand

An example of a kidney imaging agent is ^{99m}Tc-DTPA which is hydrophilic in nature and has a negative charge. It is eradicated from the cells to the extracellular space where the kidneys remove it from circulation.[69]

[71] Y. Liu and F.J. Wackers. *Cardiovascular Imaging*, p 47, Manson Publishing, United Kingdom, **2010**.

[72] C.J. Jones and J. Thornback. *Medicinal applications of coordination chemistry*, p 156-160, Royal Society of Chemistry, United Kingdom, **2007**.

[73] J.T. Bushberg, J.A. Seibert, E.M. Leidholdt, Jr. and J.M. Boone. *The essential physics of medicinal imaging*, 2nd Edition, p 395, Lippincott Williams and Wilkins, United States of America, **2002**.

2.12.4 Liver Imaging

The liver uses the hepatocytes, Kupffer cells, endothelial cells, fat cells, blood vessels and the biliary epithelial cells to perform its complicated biological functions. The liver imaging agents are divided into two groups: the first group are those that identify pathology by detecting alterations in the liver morphology and the second group are the ones used to identify pathology by identifying modifications in the liver physiology. Numerous imaging agents are available to evaluate specific cell functions. Radiocolloids are the most frequently used agent for imaging morphology and ^{99m}Tc-HIDA complexes are mainly used to image the physiology.[74]

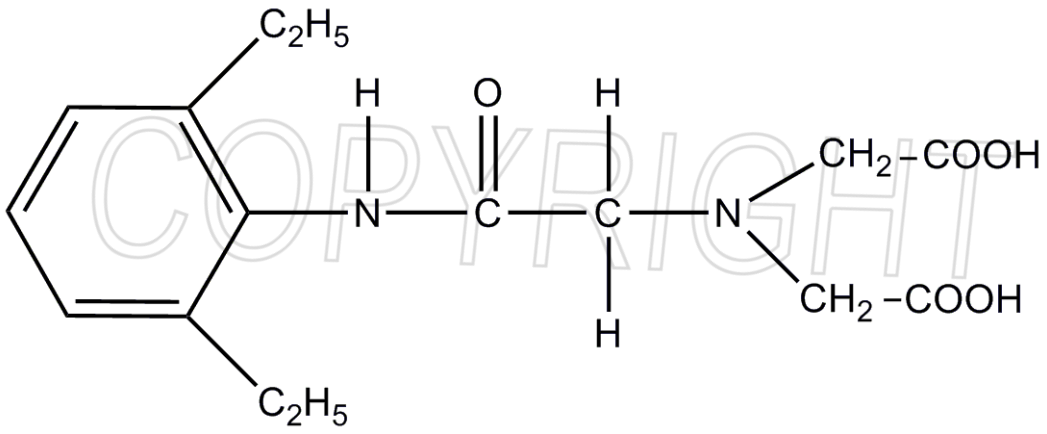

Figure 2.21 A graphical representation of the EHIDA ligand

2.12.5 Bone Imaging

Bone scintigraphy is a highly responsive but non-specific investigation. Elevated storage of radio-diagnostics is found in bone lesions with increased bone-turnover, like fractures, inflammatory diseases, bone tumors (in dogs) and skeletal metastases of malignant tumors which emanate from the bone tissue (in dogs). Bone

[74] G.T. Krishnamurthy and S. Krishnamurthy. *Nuclear Hepatology: A Textbook of Hepatobiliary Diseases*, 2nd Edition, p 49, Springer, New York, **2009**.

scintigraphy is found in patients with carcinoma whose tumours are expected to set skeletal metastases.[75]

The initial diphosphonate, employed clinically as a ^{99m}Tc bone scanning agent, was 1-hydroxyethylidene diphosphonate (HEDP) but this was later replaced with MDP in 1975. This was because it cleared the blood and soft tissue rapidly, provided better skeletal affinity and the cold kit was less expensive.[75,76] Today ^{99m}Tc-MDP is the most popular agent utilised for high-resolution clinical skeletal scintigraphy in patients suffering from bone disease and can identify lesions long before radiographs of the skeleton become abnormal.[77] Methylene diphosphonic acid is stable at elevated temperatures and has geometrical characteristics which correlate closely to other diphosphonate groups which are designed to bond in octahedral networks.[78]

The purpose of skeletal scintigraphy is that the uptake in the bone must be as wide spread as possible and it must be a rapid and complete elimination of the activity which is not bound to the bone. This is a function of the extent and speed of adsorption of the radio-diagnostic to the bone and the kinetics of the excretion from the extraosseus distribution space. Not only is the uptake in the bone essential but there must be an elevated uptake in bone lesions compared to normal bone in order to recognize these lesions.[75]

A patient diagnosed with prostate, lung or breast cancer has a 50% chance of developing skeletal metastases as the disease progresses.[62,79,80] The MDP bone scan is the most commonly requested diagnostic nuclear medical procedure. The bone scan operates by mapping certain physiological processes like the functional reaction of the bone to traumatic, neoplastic injury or inflammation.

---

[75] H. Schroth, F. Hausinger, H. Garth and E. Oberhausen. *European Journal of Nuclear Medicine*, 1984, **9**, 529-532.

[76] G. Subramanian, J.G. McAfee, R.J. Blair, F.A. Kallfelz and F.D. Thomas. *Journal of Nuclear Medicine*, 1975, **16**, 744-755.

[77] C.A. Murphy, L. Melendez-Alafort, C.E. Montoya-Molina and J. Sepulveda-Mendez. *Nuclear Medicine and Biology*, 1997, **24**, 27-33.

[78] K. Barthelet, M. Nogues, D. Riou and G. Férey. *Chemistry of Materials*, 2002, **14**, 4910-4918.

[79] V.J. Lewington, A.J. McEwan and D.M. Ackery. European Journal of Cancer, 1991, **27**, 954-958.

[80] A.J. McEwan. *Seminars in Nuclear Medicine*, 1997, **27**, 165-182.

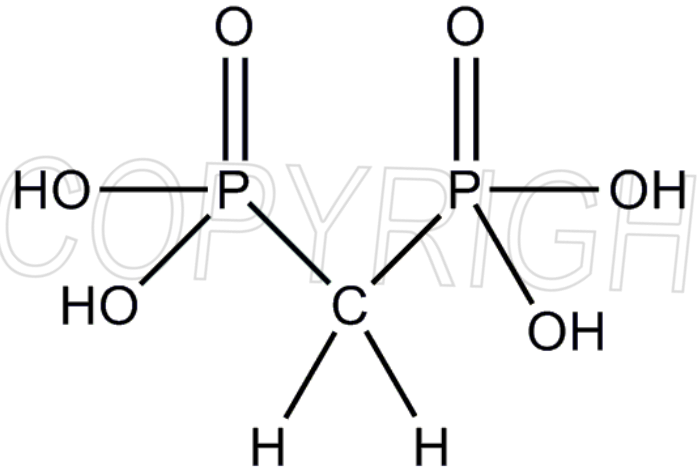

Figure 2.22 A schematic representation of the MDP ligand

Magnetic resonance imaging (MRI) or single-photon emission computed tomography (SPECT) scans utilise radionuclides to analyse bone injuries.[81] SPECT operates by generating images of radionuclides which concentrate in certain tissues. It also provides specific information concerning the anatomy and physiological state of the bone.[81,82] Bone SPECT has been employed to identify early osteonecrosis of the femoral head in renal transplant patients. It is also utilized to examine internal derangement and stress fractures of the knee and also to check bone metastasis in gastric, breast and prostate cancers.[83,84,85,86,87]

Radionuclide therapy is employed not only to treat thyroid cancer but also for bone pain palliation. It is able to provide cancer patients with a better quality of life. They

[81] V.R. Prasad. *Imaging Decisions MRI*, 2006, **10**, 8-13.

[82] Z.D. Kajan, S. Motevasseli, N.K. Nasab, H. Ghanepour and F. Abbaspur. *Aust. Orthod. Journal*, 2006, **22**, 127-130.

[83] J.S. Ryu, J.S. Kim, D.H. Moon, S.M. Kim, M.J. Shin, J.S. Chang, S.K. Park, D.J. Han and H.K. Lee. *Journal of Nuclear Medicine*, 2002, **43**, 1006-1011.

[84] M. Yildirim, R. Gursoy, E. Varoglu, Y. Oztasyonar and S. Cogalgil. *British Journal of Sports Medicine*, 2004, **38**, 15-18.

[85] C.W. Choi, D.S. Lee, J.K. Chung, M.C. Lee, N.K. Kim, K.W. Choi and C.S. Koh. *Clinical Nuclear Medicine*, 1995, **20**, 310-314.

[86] L. Chavdarova, E. Piperkova, A. Tsonevska, K. Timcheva and M. Dimitrova. *Journal of Buon*, 2006, **11**, 499-504.

[87] E. Even-Sapir, U. Metser, E. Mishani, G. Lievshitz, H. Lerman and I. Leibovitch. *Journal of Nuclear Medicine*, 2006, **47**, 287-297.

experience pain because of bone metastasis or joint pain because they have rheumatoid arthritis.[88]

- Normal bone remodelling process

This involves the continuous remodelling of bone at specific areas of the skeleton in order to preserve the tissue. The function of osteoclasts is to resorb the old bone and exchange it with a new osteoid which is secreted by the osteoblasts. Initially the osteoblasts are activated, followed by the resorption phase which generally takes 10 days. Macrophage cells then appear at the remodelling site in the intermediate or reversal phase. Then osteoblast precursors are introduced, which multiple and differentiate into mature osteoblasts, before the new bone matrix is secreted. **Figure 2.23** shows a graphical representation of the bone remodelling process. This whole process is dependent on the availability of sufficient quantities of vitamin D, calcium and phosphate.[88]

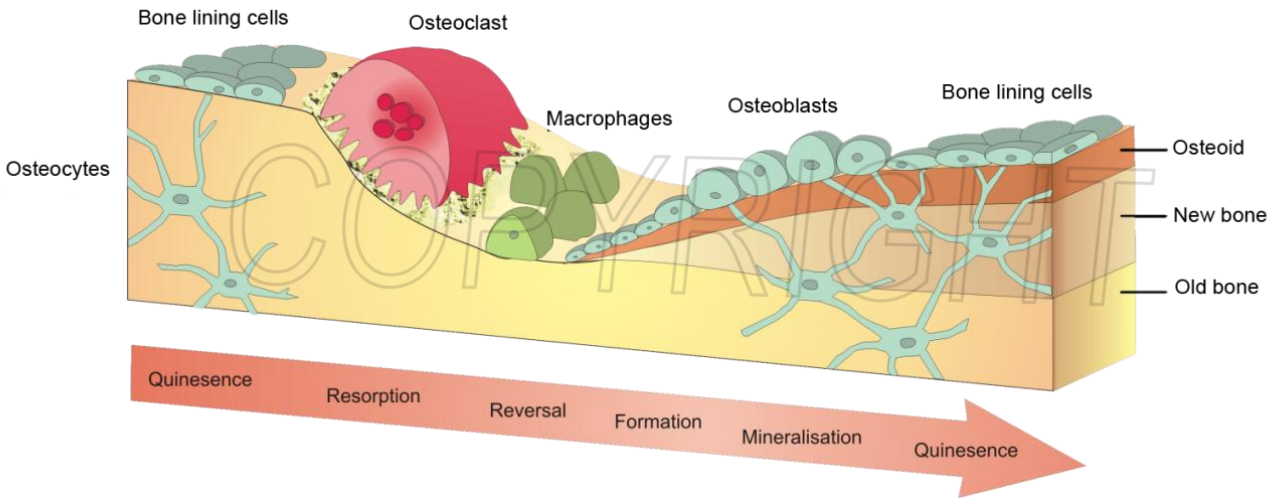

Figure 2.23 A graphical representation of the bone remodelling process.

[88] P. Abrahamsson. *European Urology Supplements*, 2004, **3**, 3-9.

When bone metabolism is elevated it causes a disruption in the normal bone remodelling process and is known as bone metastases. A vital step in the formation of bone metastases is the initiation of the osteoclast-mediated bone resorption. Bone metastases can be differentiated based on the radiographic appearance into osteolytic, osteoblastic or mixed lesions. Osteolytic lesions cause extensive bone resorption around tumour sites with a diminished amount of new bone formation and emerge as focal areas of profound osteopenia. Osteoblastic lesions are characterised by elevated bone formation and appear sclerotic.[88]

- Pathophysiology of bone metastates

Bone metastasis occurs due to interactions between the bone and tumour cells. Primary tumour cells infiltrate the basement membrane and elude the primary tumour site by invading the blood vessels or the lymphatic vessels. As a result of this the tumour cells spread and scatter to capillary beds found in the bone and finally leave the vasculature by extravasation.[88]

2.12.6 ^{99m}Tc-MDP

^{99m}Tc-MDP is a diagnostic radiopharmaceutical with a short radioactive half-life of 6 hours. It is distributed in freeze-dried kits which just need to be radiolabelled. In order to guarantee that the radiolabeling process acquires the highest radiochemical yield, a surplus of ligand is present in comparison to the quantity of $^{99m}TcO_4^-$. Physicochemical changes like the net charge and lipophilicity occur once the reduced $^{99m}TcO_4^-$ coordinates to the ligand (MDP) and these can influence the biological behaviour of the ^{99m}Tc-MDP. Therefore the ^{99m}Tc-MDP and the $^{99m}TcO_4^-$ must be characterized separately during the quality control procedure in order to

ensure that if radioactivity is retained or accumulated in an unrelated organ there is a reason for it.[89]

^{99m}Tc-MDP functions by accumulating on the bone via chemical adsorption and binds to the hydroxyapatite structure.[89] Bone scintigraphy can indicate slight alterations in the bone which cannot be observed by X-ray radiograms.[90] ^{99m}Tc-MDP is the most successful means of diagnosing early bone disease, by establishing the extent of the bone disease and identifying bone metastasis in malignant tumours, because it can be observed by using an external gamma camera. The image obtained from the camera displays the pattern of retention as well as the radioactive uptake. This image is then used to provide a diagnosis. It was developed in 1973 by Subramanian et al. It is the primary agent used for bone scintigraphy because it is more stable than conventional agents like polyphosphates or pyrophosphates in the human body.[89] The reason for this is that polyphosphates and pyrophosphates are comprised of a phosphate which is bound by P-O-P bonding compared to the MDP which is bound by P-C-P bonding and is not hydrolysed.[90]

2.12.7 ^{99m}Tc-MDP versus ^{188}Re-MDP

Technetium-99m is the most extensively utilised radioisotope in diagnostic nuclear medicine. Of the roughly 25 million diagnostic nuclear medical studies conducted every year it is estimated that 80% are done using Technetium-99m. It is used as an imaging nuclide because it emits pure gamma rays and has a half-life of six hours which is long enough for a diagnostic study but short enough to ensure that the patient doesn't need a large dose.

^{99m}Tc is an excellent diagnostic imaging radioisotope because it is able to coordinate to a variety of compounds easily

[89] D. Edwards, M. Battle, R. Lear, G. Farrar, D.J. Barnett, V. Godden, C. Coombes, A. Oliveira and H. Ahlström. *Drug Metabolism and Distribution*, 2006, **34**, 1128-1135.

[90] Y. Hiroshi and W. Hiromi. *Oral Radiol.*, 1996, **12**, 27-32.

Rhenium-186/188 is used for therapy mainly because of the two different isotopes which emit β^- emissions.

Rhenium-188 is similar to Technetium-99m in many respects as both are derived from an in-house generator which makes it suitable for clinical use.[91,92,93,94] They emit gamma and beta rays and both have a short half-life, which is essential as this eliminates problems regarding radioactive waste handling and storage.[95]

The main reason why Rhenium-188 is not used is because ^{188}Re-MDP is unable to concentrate in the skeletal system, but instead appears to gather in the soft tissue and liver. Technetium is also a superior oxidant compared to rhenium and when it comes to labelling of a diphosphonate, technetium undergoes labelling more easily. More $SnCl_2$ needs to be provided to the rhenium in order for the Rhenium-diphosphonate complex to occur.[94]

[91] F.F. Knapp Jr., A.L. Beets, S. Guhlke, P.O. Zamora, H. Bender, H. Palmedo and H.J. Biersack. *Anticancer Research*, 1997, **17**, 1783-1795.

[92] W.Y. Lin, C.P. Lin, S.J. Yeh, B.T. Hsieh, Z.T. Tsai, G. Ting, T.C. Yen, S.J. Wang, F.F. Knapp Jr. and M.G. Stabin, *European Journal of Nuclear Medicine*, 1997, **24**, 590-595.

[93] S.J. Wang, W.Y. Lin, M.N. Chen, B.T. Hsieh, L.H. Shen, Z.T. Tsai, G. Ting and F.F. Knapp Jr. *European Journal of Nuclear Medicine*, 1996, **23**, 13-17.

[94] S.J. Wang, W.Y. Lin, B.T. Hsieh, L.H. Shen, Z.T. Tsai, G. Ting and F.F. Knapp Jr. *European Journal of Nuclear Medicine*, 1995, **22**, 505-507.

[95] R.P. Spencer. *Nuclear Medicine and Biology*, 1987, **14**, 537-538.

3 Synthesis and Characterisation of Cobalt and Chromium Complexes

3.1 Introduction

The synthesis and characterisation of a range of Co(II), Co(III) and Cr(III) methylene diphosphonate complexes are discussed in this chapter. The complexes studied were characterized by spectroscopic techniques such as ultraviolet visible (UV Vis) spectroscopy, nuclear magnetic resonance (NMR), infrared spectroscopy (IR) and X-ray photoelectron spectroscopy (XPS).

Six novel complexes were fully characterized by means of X-ray diffractometry and will be discussed in detail in Chapter 5 and 6. The basic theory of the various techniques utilized in this study is briefly discussed in this chapter.

3.2 Infrared Spectroscopy

Infrared (IR) spectroscopy is a fast, relatively cheap and accurate analytical method used to identify a large range of complexes. Almost all inorganic and organic compounds which are comprised of covalent bonds, with the exception of a few homonuclear molecules such as N_2, H_2 and Cl_2, absorb infrared radiation. All molecular species in the crystalline state have a unique infrared spectrum, except for chiral molecules.

The infrared region in the electromagnetic spectrum is comprised of a wavelength range which extends from 100 μm to 100 nm. The near-infrared wavelength range is from 0.78 to 2.5 μm while the mid-infrared wavelength range is from 2.5 μm to

50 μm.[1] When a beam of electromagnetic radiation with an intensity of I_o is transmitted through a complex, the frequency of the light source, υ, as well as the molecule's structure will determine if it will be absorbed or transmitted. A molecule which absorbs radiation gains energy as it undergoes a quantum transition from one energy state ($E_{initial}$) to another (E_{final}).

The energy produced by IR radiation is able to excite vibrational as well as rotational transitions but it has inadequate energy to induce electronic transitions. If the rotational energy alters, this can cause the peak to split for each vibrational state. The rotation in liquid and solid state is often prevented or hindered, so the effects caused by the small energy differences are not observed. A typical IR spectrum comprises absorption peaks, which is formed by transitions that occur between the vibrational levels of a molecule in the electronic ground state.

With different types of energy absorption, molecules become excited when they absorb quantized infrared radiation and go to higher energy states. IR radiation is absorbed when there is a change in energy of 8-40 kJ/mole. Molecules will only absorb the energy produced by infrared radiation if it corresponds to the natural bending and stretching, vibrational frequencies of the molecule. The absorbed energy elevates the amplitude of the vibrational motions of the bonds which are present in the molecule.[2] Only bonds with a dipole moment, which alters as a function of time, are capable of absorbing infrared radiation. Symmetrical bonds such as N_2, H_2 and Cl_2 will not absorb infrared radiation because in the dipole moment they have, no net charge and stretching the bonds will not produce a charge in the dipole moment. In order for energy to be transferred, a bond must have an electrical dipole which alters at the same frequency as that of the entering radiation.

The natural frequency of vibration is unique to each type of bond and although two different compounds may have the same bond, these bonds will experience two different types of environments, therefore they cannot give the same infrared

[1] D.A. Skoog, D.M. West, F.J. Holler and S.R. Crouch. Fundamentals of Analytical Chemistry, 8th Edition, p710-777, Thomson Brooks/Cole, California, **2004**.

[2] K. Nakamoto. *Infrared Spectra of Inorganic and Coordination Compounds*, 2nd Edition, John Wiley and Sons, Inc., New York, **1970**.

absorption pattern. Hence different molecules will produce unique infrared spectrums which can be used to identify different compounds.

IR spectras are also employed to determine structural information regarding molecules. Different functional groups (N-H, C-O, C=O, O-H etc.) will absorb infrared radiation in certain sections of the vibrational infrared region and it is usually the stretching vibrations and not the bending vibrations which are used for analysis.[3]

3.3 Nuclear Magnetic Resonance Spectroscopy

Nuclear Magnetic Resonance Spectroscopy was developed in 1946 and over the years it has become a powerful and indispensible tool for chemists, physicists, biochemists and even in the medical sciences where it is utilized for diagnosis (magnetic resonance imaging, MRI). Unlike IR spectroscopy which displays the various functional groups present in a particular molecule, NMR provides information regarding the number of magnetically distinct atoms present in a structure. It is a non-destructive technique which provides excellent structural data in a relatively short period of time and very little sample is required (less than a milligram).

NMR makes use of the intrinsic magnetic character of the atomic nucleus. Nuclei which have an odd number of protons and neutrons possess an intrinsic angular momentum which is referred to as the *spin*. The *spin quantum number*, *I*, can have one of the following values:

$$I = 0, 1/2, 1, 3/2, 2\ldots$$

Quantum numbers larger than 4 are not that abundant.

Spin can be portrayed as a rotating motion of the nucleus about its own axis. If atomic nuclei have a charge then the spinning motion leads to the formation of a magnetic moment which is orientated in the direction of the spin axis. The type of nucleus will influence the strength of the magnetic moment.

[3] D.L. Pavia, G.M. Lampman, G.S. Kriz and J.R. Vyvyan. *Introduction to Spectroscopy*, 4th Edition, Brooks/Cole Cengage Learning, United States of America, **2009**.

In order to observe something utilizing NMR, the overall spin, *I*, for the nucleus must be bigger than zero. Generally the spin quantum number is $I = ½$ which is found in nuclides like ^{1}H, ^{13}C, ^{15}N, ^{19}F, ^{29}Si and ^{31}P. A broad NMR line is observed when the spin quantum number is larger than ½.[4] The overall spin is crucial and the following rules can be employed to determine *I*:

- If the number of neutrons and the number of protons within the nucleus are both even, then the nucleus has no spin.
- If the number of neutrons plus the number of protons is odd, then the nucleus has a half-integer spin (e.g. 1/2, 3/2, 5/2 etc.).
- If the number of neutrons and the number of protons are both odd then the nucleus has and integer spin (e.g. 1, 2, 3 etc.).

The absence of an external magnetic field results in nuclei having random orientations. A nucleus with a spin of *I*, will have $(2I + 1)$ possible orientations and these orientations are equal unless a magnetic field is applied. When a magnetic nucleus enters a magnetic field it can adopt a small number of possible orientations of different energy. A hydrogen nucleus is constrained to adopt one of two orientations with respect to the magnetic field: a clockwise spin (+1/2) when the magnetic moment is aligned with the magnetic field (parallel) or a counter clockwise spin (-1/2) where the magnetic moment or spins are directed in the opposite direction of the magnetic field (anti-parallel) as displayed in **Figure 3.1**.

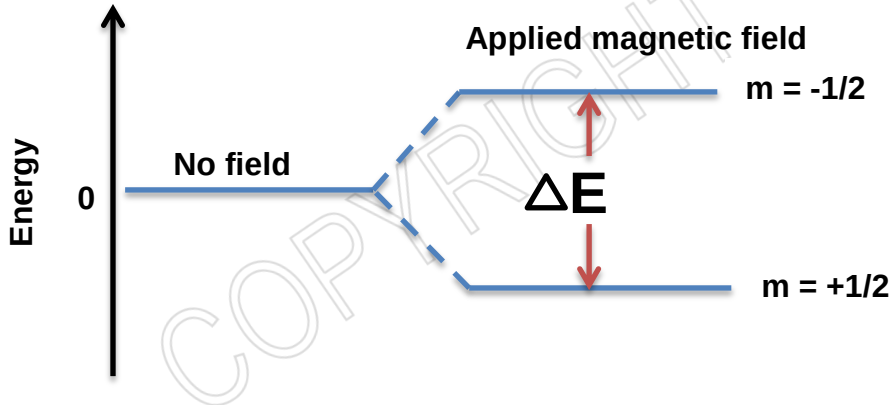

Figure 3.1 Energy levels of a hydrogen nucleus in a magnetic field.[4]

[4] P.J. Hore. *Nuclear Magnetic Resonance*, Oxford University Press, Inc., New York, **1995**.

The spin state with the lowest energy is that of +1/2 because it is aligned with the applied field and the other spin of -1/2 has the highest energy because it is orientated opposite to that of the applied field. The energy difference between the two states, ΔE, is influenced by the size of the nuclear magnetic moment as well as the strength of the magnetic field. ΔE can be determined by administering electromagnetic radiation with a frequency of υ, which leads to the nuclei flipping from a lower energy level to a higher level. In order for this to take place the resonance condition $\Delta E = h\upsilon$ must be fulfilled. The frequency of radiation which is required to excite a nuclei in a lower level to a higher energy level is dependent on the energy difference between the levels.[3]

The presence of a magnetic field leads to the nucleus revolving around its own axis in such a way as to be precessing around the magnetic field, (**Figure 3.2**) which has a frequency referred to as the Larmor frequency.

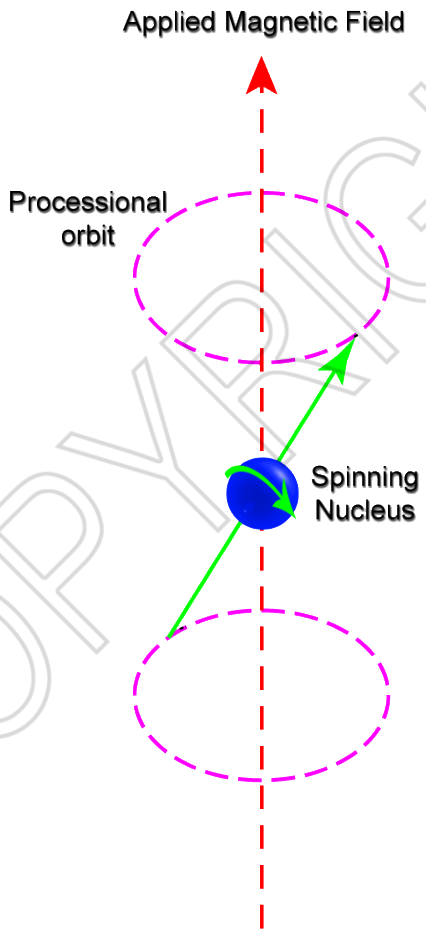

Figure 3.2 The axis of rotation precessing around the magnetic field.

The protons are shielded by the surrounding valence-shell electrons but this differs from proton to proton, and results in the formation of an effective magnetic field which is felt by the proton to be less than the applied magnetic field. Different resonance frequencies results in various signals which are known as chemical shifts (δ) or nuclear shielding. Many factors can influence the chemical shift by affecting the shielding of the proton, such as hydrogen bonding, polar functionality groups, stereochemistry and geometry.

Due to interactions between magnetic dipoles of nearby protons, which are two to four bonds removed, splitting of their resonant signals into more than one line occurs and this is determined by the amount of protons which are involved. This process is termed spin-spin coupling and happens because of interactions which are present between the magnetic moments of neighbouring protons. The multiplicity of spin-spin coupling is determined by the amount of neighbouring protons and the following concepts can be used when interpreting multiplicity:

- A proton which has *n* equivalent neighbouring protons will be divided into (*n*+1) lines.
- A proton which has *n* non-equivalent neighbouring protons will be divided into (2^n) lines.
- No splitting or spin-spin coupling is observed between equivalent protons therefore they don't interact with each other.

The coupling constant (J) which is measured in Hertz (Hz) is the interval which is present between the lines present on a NMR signal, made up of proton(s), which have been split due to spin-spin coupling.[3]

3.4 Ultraviolet-Visible Spectroscopy

Ultraviolet (UV) and visible (Vis) spectroscopy investigates the absorption of various substances between the wavelength limits of 190 nm to 800 nm. Visible spectroscopy is limited to the wavelength range of 400-800 nm and this is where electromagnetic radiation can be observed by the human eye. Ultraviolet spectroscopy operates at shorter wavelengths, 200-400 nm. UV-Vis spectroscopy is

based on the absorption of energy, which corresponds to the excitation of valence electrons (from atoms or molecules) and this leads to transitions from a low energy state (ground state) to a higher energy state (excited state). In UV-Vis there are certain types of electronic transitions e.g. transitions involving single *σ* bonding-, double or triple *π* bonding- and non-bonding (*n*, lone pair electrons) orbitals. If a molecule absorbs light, either in the form of visible or ultraviolet, the energy causes the electrons to become excited from a **highest occupied molecular orbital (HOMO)** to **the lowest unoccupied molecular orbital (LUMO)** as depicted in **Figure 3.3**.[5]

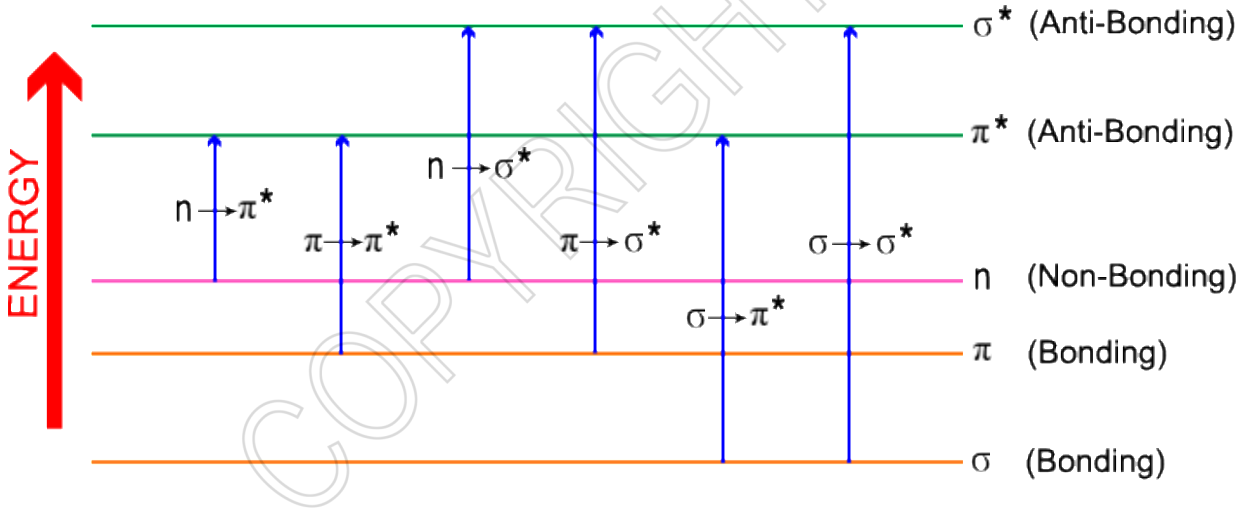

Figure 3.3 The different energy levels and the transition of *π, σ* and *n* electrons from HOMO to LUMO.[5]

Molecules absorb energy from the UV-Vis region because of interactions which are present between the photons and the electrons, which either engage directly in the bond formation or are localised about atoms like oxygen, halogens and sulphur. The wavelength at which the molecules absorb is determined by how strongly the valence electrons are bound to the atom. The valence electrons in double and triple bonds are not held together tightly and are thus easily excited by radiation and consequently they provide useful absorption peaks.

[5] D.L. Pavia, G.M. Lampman and G.S. Kriz. *Introduction to Spectroscopy*, 3rd Edition, Thompson Learning Inc., United States of America, **2001**.

Ultraviolet and visible spectroscopy has numerous applications but it is mainly used for quantitative analysis, such as the determination of a reaction mechanism by following the disappearance and formation of a coloured reaction mixture. UV-Vis spectroscopy is unable to provide important structural information because factors like the pH, temperature as well as the concentration of the compound influence the absorption spectra. Therefore other analytical techniques like IR spectroscopy, NMR spectroscopy and X-ray crystallography are needed in order to support the information obtained from the UV-Vis spectroscopy.[6]

The intention of kinetic investigations is to analyse the characteristics of a chemical reaction, the alteration of a system as it transforms from one state to another, the mechanism of chemical changes and the time required for these alterations to take place. Certain factors such as the temperature, pressure, concentration, how homogenous the solution is, sensitivity to air and light, etc. all influence the reaction mechanism as well as the rate at which the reaction is taking place.

Each compound has unique features which define it and this will influence how it absorbs ultraviolet or visible light. When a beam of monochromatic light (with an intensity of I_o) passes through a homogenous sample, some of the light will be absorbed by the sample, and the transmitted beam (I_{trs}) which is emitted from the sample will have a lower intensity in comparison to the incident beam. This is referred to as the Beer-Lambert law, which is used to determine the relationship between the concentration (c) of the single absorbing species, the intensity of the incident light (I_o) and the intensity of the transmitted light (I_{trs}).

$$\mathrm{Log}_{10}\frac{I_o}{I_{trs}} = \varepsilon c l = A \qquad \textbf{...Eq. 3.1}$$

[6] C.N.R. Rao. *Ultra-Violet and Visible Spectroscopy: Chemical Applications*, 2nd Edition, Butterworth and Co Publishers Ltd., England, **1967**.

Absorbance = A, path length = l and the molar absorption coefficient or extinction coefficient = ε. The total absorbance of a solution is determined by adding all the individual absorbance values for each species (**Equation 3.2**).[7]

$$A = \sum \varepsilon c l \qquad \textbf{…Eq. 3.2}$$

3.5 Theoretical Aspects of X-ray Crystallography

3.5.1 Introduction

X-ray crystallography is used to determine how atoms are arranged within a crystal. It generates a three-dimensional picture of the density of the electrons which are present within the crystal. The mean atomic positions, the chemical bonds, the disorders and other information can be determined by examining the three-dimensional sketch.

For a long time crystals were admired because of their symmetry and regularity but were only scientifically investigated in the 17th century. In 1611 Johannes Kepler hypothesized that a snowflake crystal had a hexagonal symmetry because of the regular packing of the water particles.[8] In 1669 Nicolas Steno was the first person to investigate the symmetry of a crystal experimentally, by displaying that the angles between the faces are identical in a particular type of crystal. Wilhelm Conrad Röntgen discovered X-rays in 1895 but the nature of the X-rays (particles or electromagnetic) was debated till 1912 when Max von Laue postulated that X-rays could be diffracted by crystals.[9]

[7] K. Wilson and J. Walker. *Principles and Techniques of Practical Biochemistry*, 5th Edition, p 460, Cambridge University Press, United Kingdom, **2000**.

[8] A. Dortmann. *Winter Facets: Traces and Tropes of the Cold*, p 67, Peter Lang AG., Germany, **2007**.

[9] J.P. Glusker and K.N. Trueblood. *Crystal Structure Analysis: A Primer*, 3rd Edition, p 9-10, Oxford University Press, United States of America, **2010**.

NMR and IR spectroscopy provide information regarding the structure of the molecule based on how it absorbs or emits radiation. X-ray crystallography utilises X-ray radiation to determine the shape of a molecule and the arrangement of atoms within a crystal. It measures the scattering of monochromatic radiation, which can be added de-constructively (out of phase) or constructively (in phase), and is dependent on the direction of the diffracted beam as well as the atomic position (each atom has the ability to scatter X-rays).[10] These intensity variations are due to the interference effects or diffraction and results in the formation of a complex scattering pattern which can be analysed. The positions of the atoms within the sample can be determined by performing measurements on the diffraction pattern.[11]

A crystal is made up of atoms which are distributed in an ordered manner. A single point is used to illustrate a molecule, this results in a simplified crystal structure. An array of identical points which are equivalent to each other due to translation symmetry are referred to as the *lattice* of the structure. The *unit cell* is the smallest possible unit that can be reproduced throughout the entire crystal and the lattice is comprised of multiple unit cells. The unit cell comprises three axis; *a*, *b* and *c,* at angles of α, β and γ. The crystal symmetry can generally be differentiated into seven *crystal systems* by placing certain limitations on the unit cell. There are 230 different *space groups* which arise when lattices are combined with a suitable point and translational symmetry elements. A description of each of the space groups is provided for in the *International Tables for Crystallography*.[12]

The *Miller index* (*hkl*) also referred to as the plane index describes a type of shorthand notation which is used to describe the direction as well as the planes present in a crystal lattice.

[10] M.F.C. Ladd and R.A. Palmer. *Structure Determination by X-ray Crystallography*, Plenum Press, New York, **1977**.

[11] W. Clegg. *Crystal Structure Determination*, Oxford University Press, United States of America, **1998**.

[12] *International Tables of Crystallography, Volume A*, 5th Edition, Kluwer Academic Publishers, Netherlands, **2002**.

Each atom present in a crystal scatters X-rays in order to provide an overall scattering pattern. It is crucial that the crystal be rotated in the X-ray beam in order for a complete pattern to be displayed. The diffraction pattern is made up of a pattern of spots with different intensity and also has three properties which correlate to the properties present in a crystal structure. These three properties are:

- The diffraction pattern has a distinct geometry which is related to the lattice and the unit cell geometry of the crystal structure.
- The symmetry of the diffraction pattern is linked to the symmetry present in the unit cell of the crystal structure.
- The diffraction pattern has different intensities, which reveal information regarding the orientation of the atoms within the unit cell.[11]

Max von Laue imagined that crystals were made up of a three-dimensional network consisting of rows of atoms and he based his analysis on the idea that a crystal behaved as a three-dimensional diffraction grating. In the crystal lattice a, b and c represents the primitive vectors.

$$\Delta k \cdot \mathrm{a} = h2\pi$$
$$\Delta k \cdot \mathrm{b} = k2\pi$$
$$\Delta k \cdot \mathrm{c} = l2\pi \qquad \textbf{…Eq. 3.3}$$

The conditions as displayed in **Equation 3.3** mean that the scattering vector must be positioned in a certain direction in relation to the primitive vectors of the crystal lattice. The *h*, *k* and *l* are any sets of integers which can be written in terms of angles.

$$\mathrm{a}(\cos\alpha - \cos\alpha_0) = h\lambda$$
$$\mathrm{b}(\cos\beta - \cos\beta_0) = k\lambda$$
$$\mathrm{c}(\cos\gamma - \cos\gamma_0) = l\lambda \qquad \textbf{…Eq. 3.4}$$

Equations 3.3 and **3.4** are referred to as the Laue equations. They are accurate but complicated to calculate. For constructive interference to take place all of the equations must be satisfied simultaneously. W.L. Bragg derived an easier equation known as the Bragg's Law.[13]

3.5.2 Bragg's Law

Interference is when waves interact with one another. Constructive interference is when the waves are in phase and this causes an increase in amplitude. Destructive interference is caused by waves which are out of phase with each other, therefore there is a decrease in amplitude. All X-rays which are reflected from a certain plane remain in-phase after reflection.

The quantity of electrons present in an atom will have an influence on its ability to scatter X-rays. Atoms in a crystal are ordered and lie in planes, with each plane being able to diffract X-rays. Bragg used a monochromatic X-ray beam which had a narrow wavelength range. This resulted in the X-rays being diffracted at specific angles which were determined by the wavelength as well as the interplanar spacing. Bragg's explanation was that X-rays impinge on a crystal with an angle of θ. The incident X-rays have a wavelength of λ, are reflected and result in the angle of incidence being equivalent to the angle of reflection.[14] At point **A,** a small portion of the beam is reflected from the surface atoms. Some of the beam will penetrate to the lower planes and be reflected.

In order for constructive interference to take place the difference in distances travelled by beams **F** and **F'** must be an integral number of wavelengths and the **EAF** path must be different to the **E'CF'** path by a number of wavelengths.

[13] A. Putnis. *Introduction to Mineral Science*, p 47-50, Cambridge University Press, United Kingdom, **1992**.

[14] K.J. Laidler, J.H. Meiser and B.C. Sanctuary. Physical Chemistry, 4th Edition, p 853, Houghton Mifflin Company, United States of America, **2003**.

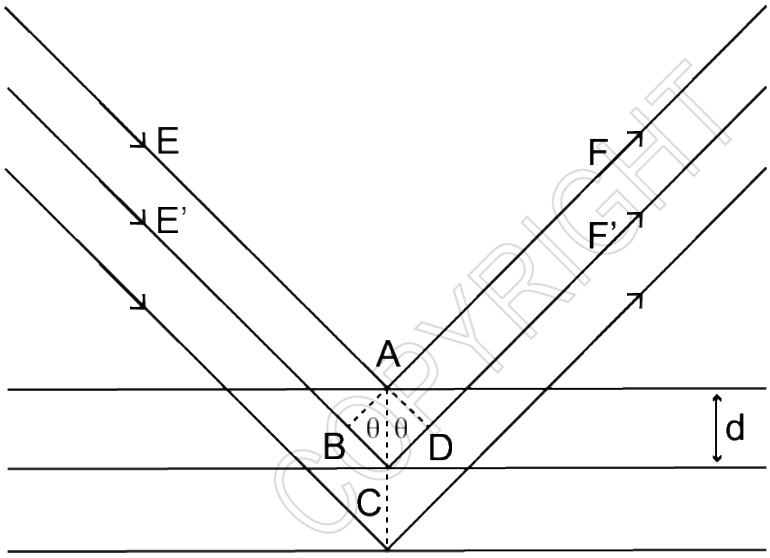

Figure 3.4 Diffraction of X-rays according to Bragg's law.

Bragg's law defined for rays which are reflected by two adjacent planes (constructive interference) is:

$$n\lambda = 2d_{\mathrm{hkl}} \sin\theta \qquad \textbf{...Eq. 3.5}$$

With n being the integer, λ the wavelength, d_{hkl} the distance between successive parallel planes and θ the angle of incidence and reflection.

$$n\lambda = \mathrm{BC} + \mathrm{CD}$$

This phenomenon is known as the Bragg's law and is employed to rectify the difference in phase that is present because of the X-rays which are reflected from different planes. Reflection will only take place if the incident beam has certain values which are determined by the wavelength as well as the lattice constants of the crystal.[14]

3.5.3 Structure Factor

Each reflection present in a crystal diffraction pattern is made up of two numerical values namely the *phase Øj* and the *amplitude* $|F(hkl)|$ of the diffracted wave. The *amplitude* $|F(hkl)|$ refers to the height of the wave and is determined by the number

of electrons which are present. The *phase Øj* is represented by the horizontal shift which corresponds to a specified origin. Every (*hkl*) reflection beam is the sum of all the beams reflected for all the atoms in a particular direction. The scattering for each atom within a unit cell must be added in order to obtain the resultant beam.

The structure factor F(*hkl*) displays the overall scattering of all the atoms (*j*) within the unit cell, compared to that of a single electron. The resultant wave for the unit cell is:[15]

$$F_{hkl} = \sum_{j=1}^{N} f_j \exp[i2\pi(\mathrm{h}x_j + \mathrm{k}y_j + \mathrm{l}z_j)] \qquad \textbf{...Eq. 3.6}$$

Where f_j = atomic scattering factor.

Equation 3.6 indicates that the magnitude of the structure factor is dependent on the relative disposition of the N atoms as well as their scattering factors. Each term expresses a wavelet with an amplitude f_j and a *phase Øj* = $2\pi(hx_j + ky_j + lz_j)$ which depicts the path length for each scattered wavelet. The structure factor F(*hkl*) is the effect of the wavelets which are scattered by the N atoms present in the unit cell.[15]
Equation 3.6 can be rewritten in the following form:

$$F_{hkl} = \sum_{j=1}^{N} f_j \left[\cos 2\pi\left(\mathrm{h}x_j + \mathrm{k}y_j + \mathrm{l}z_j\right) + \mathrm{i}\sin 2\pi\left(\mathrm{h}x_j + \mathrm{k}y_j + \mathrm{l}z_j\right)\right]$$

...Eq. 3.7

The intensities of the diffracted X-ray is proportional to F^2, because the energy associated with the cosine wave is proportional to the squaring of the amplitude of the wave. X-ray diffraction is displayed in terms of the strength of the scattered wave from the unit. The amplitude of the structure factor is $|F(hkl)|$ and the symbol $I_0(hkl)$ can be used to represent $|F(hkl)|^2$ (**Equation 3.8**), which is referred to as the ideal intensity.

[15] Y. Waseda, E. Matsubara and K. Shinoda. *X-Ray Diffraction Crystallography: Introduction, Examples and Solved Problems*, p 108-109, Springer, New York, **2011**.

$$I_0(hkl) \propto [F_0(hkl)]^2 \qquad \textbf{...Eq. 3.8}$$

Therefore **Equation 3.8** forms the basis of X-ray diffraction and enables the experimental quantities of $I_0(hkl)$ to be directly connected to the structure through $|F(hkl)|$.

An X-ray diffraction pattern or image is produced when electrons in a crystal scatter X-rays and this image can be utilised to determine the crystal structure. Atoms with elevated atomic numbers contribute a major concentration of electrons in comparison to atoms which have lower atomic numbers. The distribution and concentration of electrons around the atom is referred to as the electron density, ρ. Electron density is a function of position and can be represented as ρ (x, y, z). The electron density can be expressed in terms of the structure factor $|F(hkl)|$: [15]

$$F_{hkl} = \int \rho(x, y, z) \exp[i2\pi(\mathrm{h}x_n + \mathrm{k}y_n + \mathrm{l}z_n)]dV \qquad \textbf{...Eq. 3.9}$$

3.5.4 'Phase Problem'

The observed intensity data cannot be used directly to define the crystal structure. A major disadvantage in determining a structure by using X-ray diffraction is that it is unable to determine the complete vectorial structure factor. The modulus $|F(hkl)|$ can be acquired from the intensity data in **Equation 3.8** but the corresponding *phase Ø(hkl)* cannot be quantified directly. To determine the structure, both the phase and the amplitude must be known. This inability to ascertain the phase is regularly referred to as the 'phase problem' and can be easily resolved by utilising one of two methods known as the direct method or the Patterson function.[16]

[16] G. Rhodes. *Crystallography Made Crystal Clear: A Guide For Users Of Macromolecular Models*, 3rd Edition, p 101, Elsevier Inc., Canada, **2006**.

a. Direct Method

This method makes use of a mathematical formula referred to as the triple relations in order to determine the initial- and expanding phases from the measured X-ray intensities. This method yields the best results for structures which consist of only light atoms.[17]

b. Patterson Function

The Patterson Function is used for compounds which contain heavier atoms or when a significant part of the structure is already known. A major issue in single crystal analysis is the phase problem which precludes the direct interpretation of the intensity data from the diffraction experiment.

The Patterson Function or the Patterson Map resembles an electron density map constructed from an inverse Fourier transform with positive electron density peaks in numerous positions which can be defined by **Equation 3.10**:

$$\mathrm{P(u,v,w)} = \mathrm{V^{-1}} \sum_{h} \sum_{k} \sum_{l} (\mathrm{F_{hkl}})^2 \exp[-\mathrm{i}2\pi(\mathrm{hu} + \mathrm{kv} + \mathrm{lw})]$$

…Eq. 3.10

V represents the volume of the unit cell.

These are not the positions of the atoms in the structure but a function of vectors between pairs of atoms in the structure. The Patterson Function only provides information regarding the positions of the atoms relative to each other and not where they are relative to the unit cell. It will determine the orientation of one or two heavier

[17] C. Giacovazzo. *Direct Phasing in Crystallography: Fundamentals and Applications*, Oxford University Press, New York, **1998**.

atoms within the unit cell but the rest of the structure must be analysed using other techniques.[18]

3.5.5 Least-Squares Refinement

The least squares refinement is a method utilised to correlate the calculated diffraction pattern with the observed diffraction pattern to see what degree of similarity there is between them. The experimental structure factor (F_0) is compared to the calculated structure factor (F_c) and this comparison is described in terms of the *residual index* or *R-factor*.

$$R = \frac{\sum||F_0|-|F_c||}{\sum|F_0|} \qquad \textbf{…Eq. 3.11}$$

A *R-factor* of 0.02-0.07 signifies that a well-defined crystal structure was obtained. In order to acquire better refinement, a weighting factor, w, must be incorporated for each reflection. This gives rise to a new residual factor, which is extensively used for crystal structure determination (**Equation 3.12**).[19,20]

$$wR^2 = \frac{\sum w(F_0^2 - F_c^2)^2}{\sum w\,(F_0^2)^2} \qquad \textbf{…Eq. 3.12}$$

[18] P. Luger. *Modern X-Ray Analysis on Single Crystals*, Walter de Gruyter and Co., Germany, **1980**.

[19] J.P. Glusker, M. Lewis and M. Rossi. *Crystal Structure Analysis for Chemists and Biologists*, John Wiley and Sons, United States of America, **1994**.

[20] P. Müller, R. Herbst-Irmer, A.L. Spek, T.R. Schneider and M.R. Sawaya. *Crystal Structure Refinement: A Crystallographer's Guide to SHELXL,* Oxford University Press, New York, **2006**.

3.6 X-Ray Photoelectron Spectroscopy

The photoelectric effect, which was discovered by Hertz in 1887, is when a photon (X-ray in this instance) hits the surface of the material and this causes electrons to emerge from the surface with different energies. This technique is able to yield information regarding the chemical environment, the oxidation states and the concentration of the constituent atoms.[21] 1905 Albert Einstein defined the basic equation of XPS that linked the kinetic energy of the electrons to the binding energy of the electrons as well as the X-ray source energy.[22]

XPS (X-ray Photoelectron Spectroscopy) is a surface chemical analysis technique used to analyze the electronic state and composition of the surface region of most solids, insulators, conductors, powder or organics. A monochromatic soft X-ray beam irradiates a sample with energy which is in the range of 200- 2000 eV.[21] The X-ray photoelectron emits energy which is absorbed by the desired atom. This results in it becoming elevated to an excited state, where after it relaxes and emits a photoelectron.[23] The X-ray photons are only capable of penetrating a certain depth, which is determined by the angle of incidence, the photon energy and the material.

The photoelectron energies have a certain amount of kinetic energy which is a function of the binding energy as well as the chemical environments of the specific atom. XPS generally only affects the electrons which are orientated on the first few nanometers of the sample surface. An electron spectrometer is then able to observe electrons emerging from the sample due to the kinetic energy which is produced by the electrons. This technique is used to generate a spectrum comprised of peaks, which illustrates the flow of emitted electrons as a function of the binding energy. The areas underneath the peaks are employed to determine the concentrations of the elements which are present in the sample. Shifts in the elemental binding energies and the shape of the peaks provide information regarding the chemical state of the elements present on the surface.

[21] P.N. Prasad. *Nanophotonics*, p 192, John Wiley and Sons, Inc., United States of America, **2004**.

[22] R. Kohli and K.L. Mittal. *Developments in Surface Contamination and Cleaning: Fundamentals and Applied Aspects*, William Andrew, United States of America, **2008**.

[23] T.F. Yen. *Chemistry for Engineers*, p 177, Imperial College Press, Singapore, **2008**.

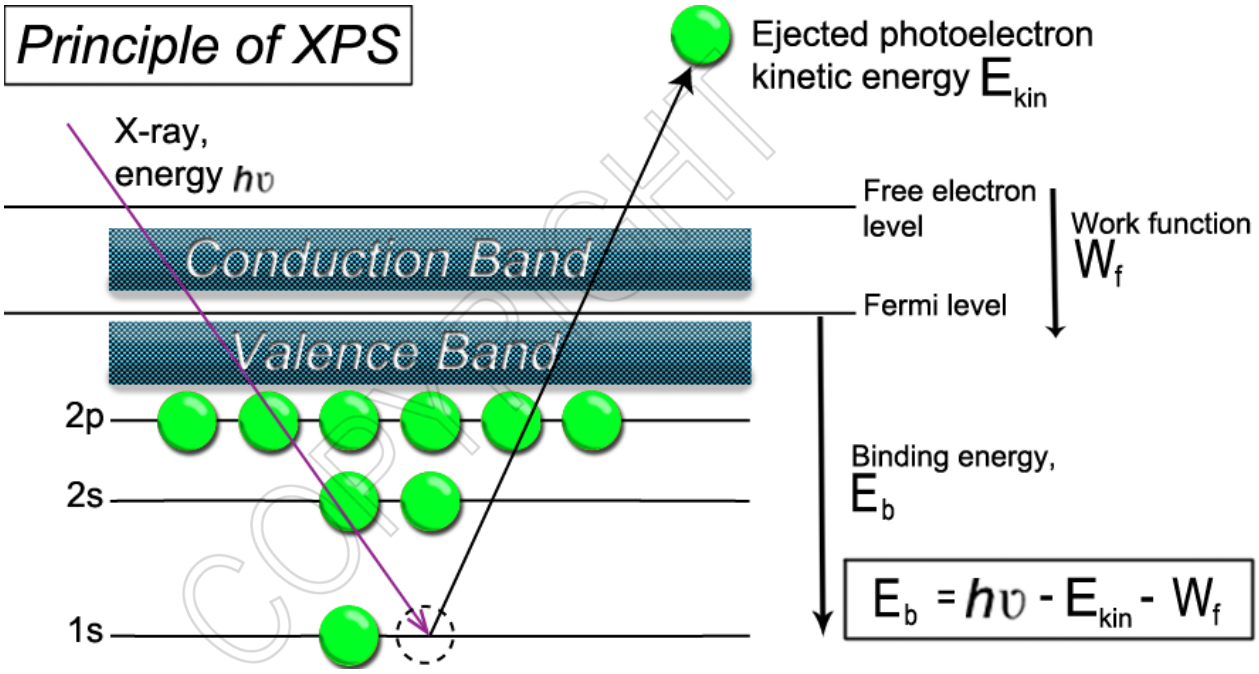

Figure 3.5 A graphical illustration displaying how X-ray Photoelectron Spectroscopy works.[24]

The splitting of the photoelectron lines on a XPS spectra are due to spin-orbit splitting. Electrons in the s-orbital have an orbital momentum of zero so that an electron which is emitted from an s-orbital will be displayed as a single peak on the XPS spectra. The rest of the orbitals (p, d and f) have orbital momentum values larger than zero which means that the spin can be either up (s = +½) or down (s = -½). Photoelectron lines generated from these orbitals display splitting into two peaks on the XPS spectra. The intensity of the ratios of the two peaks of a spin-orbit doublet is determined by its multiplicity ($2j + 1$). For p electrons ($p_{1/2}$ and $p_{3/2}$) where j is equal to 1/2 and 3/2, the relative intensity is 1:2, for the d electrons (the doublet pairs) which are in proportion, the ratio is 2:3 and for the f electrons the ratio is 3:4.[25] XPS is a technique which is able to provide information regarding the chemical bonding of the elements but cannot be used on light atoms like helium and hydrogen.[21]

[24] http://www.ifw-dresden.de/institutes/ikm/organisation/dep-31/methods/x-ray-photoelectron-spectroscopy-xps. Accessed on the 20th of March 2011.

[25] C.R. Brundle, C.A. Evans and S. Wilson. *Encyclopedia of Materials Characterisation: Surfaces, Interfaces, Thin Films*, p 287, Gulf Professional Publishing, United States of America, **1992**.

3.7 Synthesis and Spectroscopic Characterization

3.7.1 Chemicals and Instrumentation

The experimental procedures employed to synthesize the various complexes are reported in this section. All reagents and solvents utilized for the synthesis and characterisation of the complexes were of analytical grade and were purchased from Sigma-Aldrich, South Africa, unless otherwise stated. They were used as received, without further purification. All of the complexes were prepared aerobically using double distilled water. All pH measurements were done on a Hanna pH 213 meter using standard buffer solutions for calibration.

Infrared spectra were recorded on a Bruker Tensor 27 Standard System spectrophotometer equipped with a golden gate single reflection ATR which has a range of 370-4000 cm^{-1}. All samples were analysed as solid state species via ATR infrared spectrophotometry. The UV-Vis spectra was collected on a Varian Cary 50 Conc UV-Visible Spectrophotometer, equipped with a Julabo F12-mV temperature cell regulator (precise within 0.1 °C) in a 1.000 ± 0.001 cm quartz cuvette cell. All ^{1}H, ^{13}C and ^{31}P NMR spectra were acquired using D_2O as the deuterated solvent on a Bruker 600 MHz nuclear magnetic resonance spectrometer. The ^{1}H and ^{13}C NMR were calibrated relative to the residual D_2O peak (4.79 ppm) and the ^{31}P NMR spectrum was calibrated relative to 85% H_3PO_4 as the external standard in a capillary (0 ppm). XPS data were recorded on a PHI 5000 Versaprobe system with monochromatic aluminium K-alpha X-ray source. Spectra were obtained using the aluminium anode (Al Kα = 1486.6 eV) operating at 50µm, 12.5W and 15 kV energy (97 X-ray beam). The survey scans were recorded at constant pass energy of 187.85 eV and region scans at constant pass energy of 23.5 eV with the analyzer resolution ≤ 0.5 eV. The background pressure was 2 x 10^{-8} mbar. The XPS data were analysed utilizing Multipak version 8.2c computer software using Gaussian-Lorentz fits (the Gaussian/Lorentz ratios were always >95%).

3.7.2 Synthesis of Compounds

3.7.2.1 Synthesis of $(C_5H_6N)[Cr(CH_4O_6P_2)_2(H_2O)_2]\cdot 4H_2O$

Pyridinium diaquabis(methylenediphosphonato)chromate(III) tetrahydrate was prepared by dissolving chromium(III) chloride hexahydrate (0.0924 g, 0.347 mmol) in distilled water (40 mL) and adding ammonium hydroxide gradually in order to precipitate chromium(III) hydroxide. Methylene diphosphonate (0.3468 g, 2.00 mmol) was dissolved in distilled water (40 mL) and added to the chromium(III) hydroxide solution. The reaction solution was heated on an oil bath for 5 hours at 100 °C, after which pyridine (10 mL) was added to the solution. Boiling water (30 mL) was added and the solution was centrifuged. The product was allowed to stand in the open air to evaporate the solvent slowly, depositing green crystals.

Yield: 0.0023 g (1.12 %).
IR (ATR): υ (cm^{-1}) = 600 to 3700; (C-H) 2913.60 and 2965.40; (P=O) 1182.37; (P-C) 744.47; (N-H) 3081.68; coordinated water (O-H) 3000-3500.[3,26,27,28,29,30,31,33,34]
XPS data displaying the percentage of each element present (%): P, 12.1; Cr, 3.3; N, 3.5.
NMR: Not possible as the complex is paramagnetic.
Elemental analysis (%): Found- C, 14.21; H, 4.38; N, 2.29
Calculated- C, 14.28; H, 4.42; N, 2.38

[26] S.P. Man, M. Motevalli, S. Gardiner, A. Sullivan and J. Wilson. *Polyhedron*, 2006, **25**, 1017-1032.

[27] Y. Gong, W. Tang, W. Hou, Z. Zha and C. Hu. *Inorganic Chemistry*, 2006, **45**, 4987-4995.

[28] S.S. Jurisson, J.J. Benedict, R.C. Elder, R. Whittle and E. Deutsch. *Inorganic Chemistry*, 1983, **22**, 1332-1338.

[29] E. Valenzuela, A. Sousa-Pedrares, M.L. Durán-Carril, J.A. García-Vázquez, J. Romero and A. Sousa. *Zeitschrift für anorganische und allgemeine Chemie*, 2007, 1853-1859.

[30] E. Gerbert, A.H. Reis, Jr., M.E. Druyan, S.W. Peterson, G.W. Mason and D.F. Peppard. *The Journal of Physical Chemistry*, 1997, **81**, 471-475.

[31] G. Bonavia, R.C. Haushalter, C.J. O' Connor and J. Zubieta. *Inorganic Chemistry*, 1996, **35**, 5603-5612.

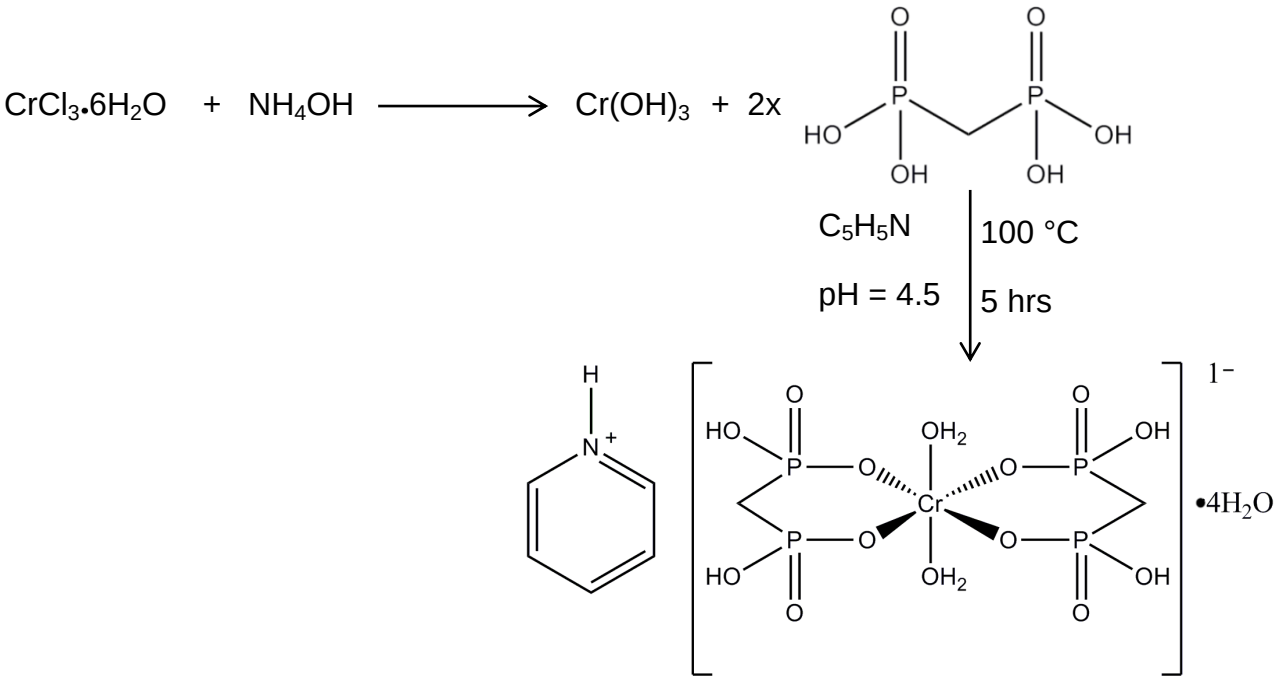

Figure 3.6 Reaction scheme of the formation of $(C_5H_6N)[Cr(CH_4O_6P_2)_2(H_2O)_2]\cdot 4H_2O$.

3.7.2.2 Synthesis of $K[Co(CH_4O_6P_2)_2(H_2O)_2]$

The $[Co(NTA)(\mu\text{-}OH)]_2^{-2}$ complex was synthesised based on the methodology described in literature.[32]

Yield: 2.6996 g (24.67 %).
IR (ATR): υ (cm^{-1}) = 600 to 3700; (COO-Co) 1608.08 and 1636.55.

The dimer, $[Co(NTA)(\mu\text{-}OH)]_2^{-2}$ (1 g, 1.87 mmol) was dissolved in hot water (7 mL) and the pH was raised to 2.01 using potassium bicarbonate (2 mL, 0.1 M). The solution was heated for 30 minutes at 30 °C. Methylene diphosphonate (0.6593 g, 3.75 mmol) was also dissolved in hot water (6 mL) giving a solution with a pH of 0.79, which was elevated to 1.88 using potassium bicarbonate. The two solutions were combined and the reaction mixture was heated for 3 hours at 80 °C. The solution was centrifuged and the product was allowed to stand in the open air to evaporate the solvent slowly, depositing purple crystals.

[32] H.G. Visser, W. Purcell, S.S. Basson and Q. Claassen. *Polyhedron*, 1997, **16**, 2851-2856.

Yield: 0.0755 g (8.38 %).

IR (ATR): υ (cm^{-1}) = 600 to 3700; (C-H) 2913.76 (P=O) 1174.99; (P-C) 741.54; coordinated water (O-H) 3000-3500.[3,26,27,28,29,30,31]

XPS data displaying the percentage of each element present (%): P, 11.2; Co, 3.5; K, 3.7.

NMR: Not possible as the complex had solubility issues.

Elemental analysis (%): Found- C, 5.25; H, 2.41

Calculated- C, 4.98; H, 4.18

UV/Vis: λ = 225 nm (ε = 101.25 $M^{-1}.cm^{-1}$)

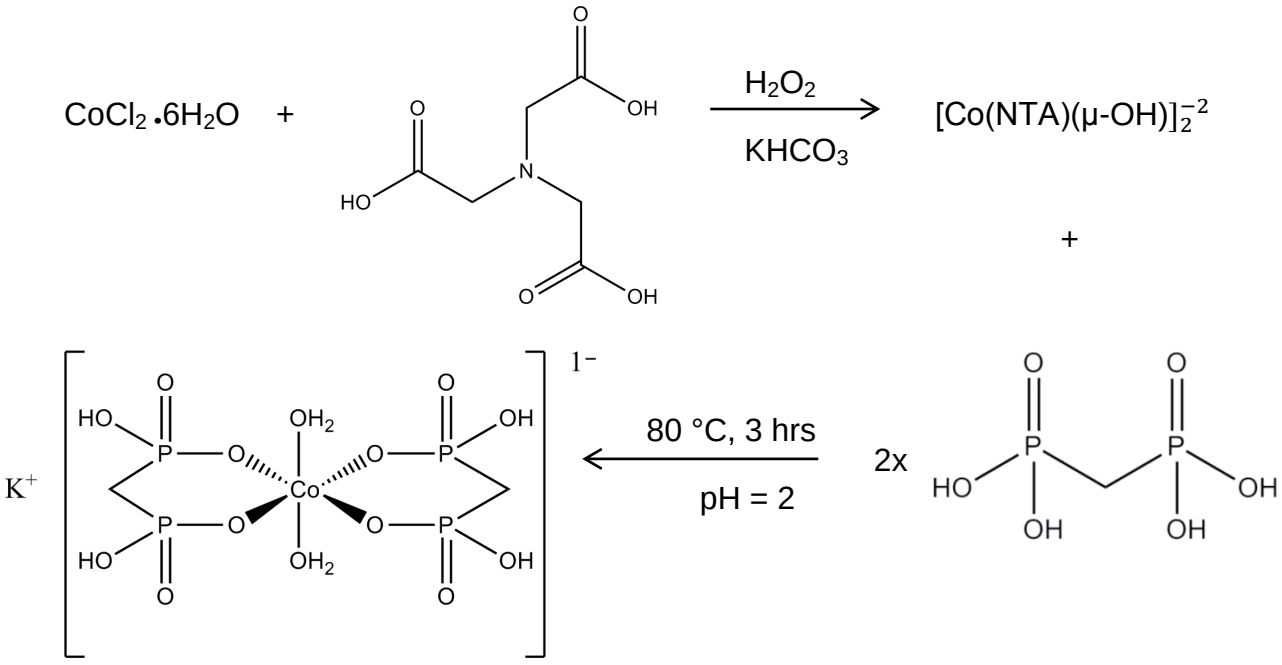

Figure 3.7 Reaction scheme of the formation of $K[Co(CH_4O_6P_2)_2(H_2O)_2]$.

3.7.2.3 Synthesis of $K[Co(CH_4O_6P_2)(OH)_2(H_2O)_2]$

Potassium diaquadihydroxy(methylenediphosphonato)cobaltate(III) was prepared by dissolving cobalt(II) chloride hexahydrate (6.0102 g, 25.30 mmol) and ammonium chloride (4.0168 g, 75.09 mmol) in distilled water (5 mL). The solution was stirred at room temperature till most of it had dissolved. Ammonium hydroxide (13 mL) was added to the reaction mixture and this resulted in the colour changing from purple to bright red. Activated carbon (0.13 g) was added and medical air was bubbled through the solution for 3 hours. The red solution was filtered and the filtrate was

added to distilled water (40 mL). It was then acidified using hydrochloric acid (1 mL) and filtered in order to remove the decolourizing carbon. Further heating to 60 °C and addition of more hydrochloric acid (10 mL) followed. The solution was cooled in an ice bath.

Yield: 4.153 g (61.37 %).
IR (ATR): υ (cm^{-1}) = 600 to 3700; (N-H) 1326.55 and 3270.[33,34]

Hexaammine cobalt (III) chloride (0.2016 g, 0.754 mmol) was dissolved in distilled water (7 mL) and the pH was lowered to 2.02 using hydrochloric acid (2 mL, 32%). The solution was heated for 30 minutes at 30 °C. Methylene diphosphonate (0.2958 g, 1.652 mmol) was dissolved in distilled water (5 mL) and the pH was elevated to 2.22 using potassium bicarbonate. The methylene diphosphonate solution and the hexaammine cobalt (III) chloride solution were combined and the reaction mixture was heated for 3 hours at 80 °C. The product was allowed to stand in the open air to evaporate the solvent slowly, depositing purple crystals.

Yield: 0.0816 g (32.49 %).
IR (ATR): υ (cm^{-1}) = 600 to 3700; (C-H) 2932.22; (P=O) 1205.06; (P-C) 737.73; coordinated water (O-H) 3148.52 and 3256.37.[3,26,27,28,29,30,31]
XPS data displaying the percentage of each element present (%): P, 12.4; Co, 4.3; K, 4.0
^{1}H NMR (D_2O): δ (ppm) 1.95 (t, 2H, OH), 2.25 (m, 2H, OH)
^{13}C NMR (D_2O): δ (ppm) 27.03 (t, CH_2, $^{1}J_{C-P}$ 129.83 Hz)
^{31}P NMR (D_2O): δ (ppm) 27.63 (s)
Elemental analysis (%): Found- C, 3.48; H, 4.96
Calculated- C, 3.60; H, 3.63
UV/Vis: λ = 385 nm (ε = 35.50 $M^{-1}.cm^{-}1$) and λ = 549 nm (ε = 41.42 $M^{-1}.cm^{-1}$)

[33] A.E. Ceniceros-Gómez, N. Barba-Behrens, S. Bernès, H. Nöth and S.E. Castillo-Blum. *Inorganica Chimica Acta,* 2000, **304**, 230-236.

[34] A.E. Ceniceros-Gómez, N. Barba-Behrens, M.E. Quiroz-Castro, S. Bernès, H. Nöth and S.E. Castillo-Blum. *Polyhedron*, 2000, **19**, 1821-1827.

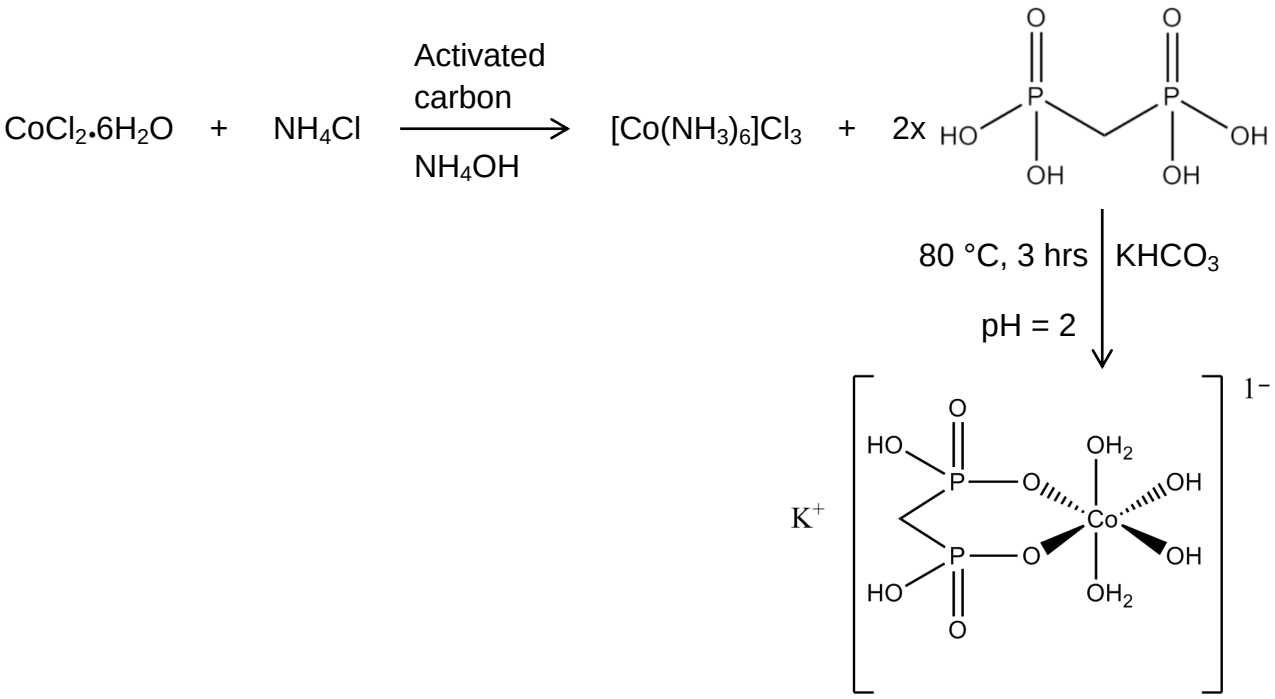

Figure 3.8 Reaction scheme of the formation of $K[Co(CH_4O_6P_2)(OH)_2(H_2O)_2]$.

3.7.2.4 Synthesis of $(NH_4)_2[Co(CH_4O_6P_2)_2(H_2O)_2]$

Diammonium diaquabis(methylenediphosphonato)cobaltate(II) was prepared by dissolving cobalt(II) chloride hexahydrate (0.1696 g, 0.71 mmol) in distilled water (7 mL) and heating it to 70 °C. Initially the pH was 4.89 but it rose to 5.61 after the addition of ammonium bicarbonate. The solution was rapidly cooled down by placing it in an ice bath, after which hydrogen peroxide (2 mL, 30 %) was added. The methylene diphosphonate (0.250 g, 1.42 mmol), which was dissolved in distilled water (5 mL), was then added dropwise to the solution and heated for 2 hours at 70 °C. The pH of the solution plummeted to 0.84 so additional ammonium bicarbonate was added in order to elevate the pH to 1.42. The product was allowed to stand in the open air to evaporate the solvent slowly, depositing pink crystals.

Yield: 0,0767 g (22.55 %).

IR (ATR): υ (cm^{-1}) = 600 to 3700; (C-H) 2912.82 and 2959.66; (P=O) 1182.50; (P-C) 736.86; (N-H) 3055.28; coordinated water (O-H) 3209.35-3500.[3,26,27,28,29,30,31,33,34]

NMR: The complex is paramagnetic so NMR was not possible.

XPS data displaying the percentage of each element present (%): P, 16.2; Co, 5.2; N, 9.8

Elemental analysis (%): Found- C, 5.22; H, 4.27; N, 5.32

Calculated- C, 5.01; H, 4.21; N, 5.85

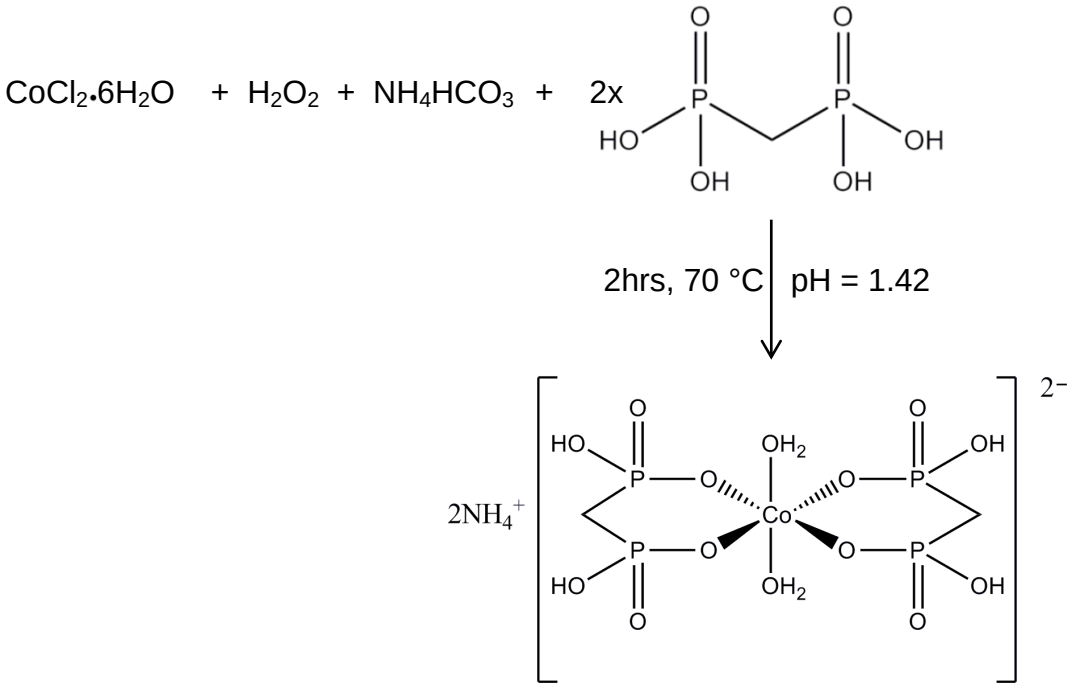

Figure 3.9 Reaction scheme of the formation of $(NH_4)_2[Co(CH_4O_6P_2)_2(H_2O)_2]$.

3.7.2.5 Synthesis of disodium $(Na)_2[Co(CH_4O_6P_2)_2(H_2O)_2]\cdot 2H_2O$

Disodium diaquabis(methylenediphosphonato)cobaltate(II) dihydrate was prepared by dissolving cobalt(II) chloride hexahydrate (0.169 g, 0.71 mmol) and methylene diphosphonate (0.3726 g, 2.12 mmol) in distilled water (5 mL). Sodium hydroxide (3 mL, 1 M) was added to the solution which became murk light pink in appearance. The pH of the solution was lowered to 1.23 using 1M hydrochloric acid, in order to get a clear solution. The mixture was heated for 3 days at 140 °C. It was then gradually cooled down to room temperature. The solution was centrifuged and the product was allowed to stand in the open air to evaporate the solvent slowly, depositing pink crystals.

Yield: 0.0984 g (27.61 %).

IR (ATR): υ (cm^{-1}) = 600 to 3700; (C-H) 2923.81 and 2990.81; (P=O) 1218.47; (P-C) 733.89; coordinated water (O-H) 3303.92-3500.[3,26,27,28,29,30,31]

XPS data displaying the percentage of each element present (%): P, 14.5; Co, 3.0; Na, 7.1

NMR: The complex is paramagnetic so NMR was not possible.

Elemental analysis (%): Found- C, 4.75; H, 3.19

Calculated- C, 4.79; H, 3.21

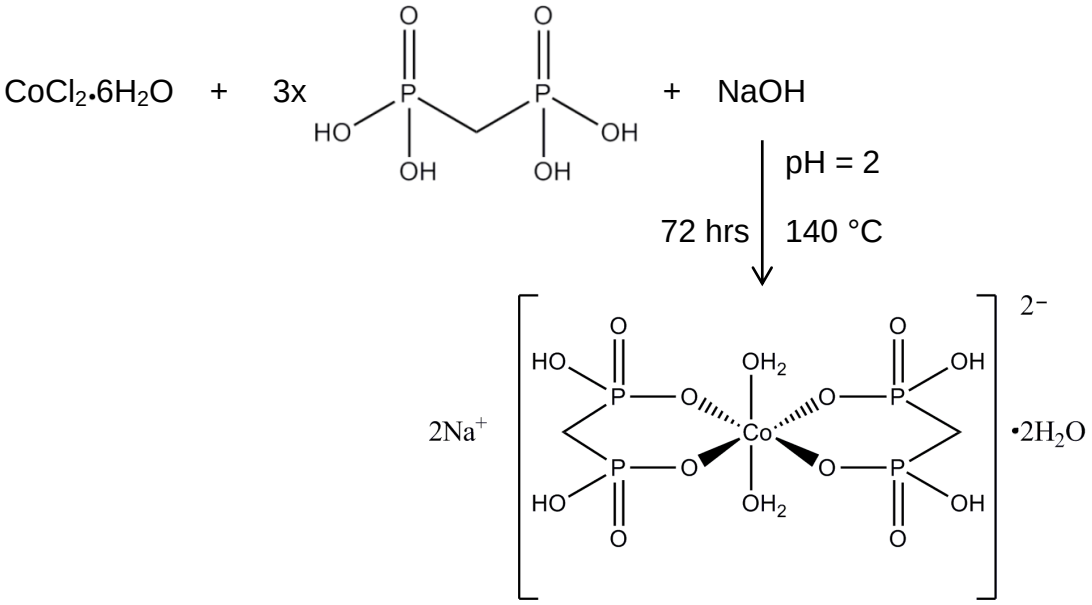

Figure 3.10 Reaction scheme of the formation of $(Na)_2[Co(CH_4O_6P_2)_2(H_2O)_2]\cdot 2H_2O$.

3.7.2.6 Synthesis of $(Cs)_2[Co(CH_4O_6P_2)_2(H_2O)_2]$

Dicesium diaquabis(methylenediphosphonato)cobaltate(II) was prepared by dissolving cobalt(II) chloride hexahydrate (0.1700 g, 0.714 mmol) in distilled water (10 mL). The pH was lowered to 1.87 using 1M hydrochloric acid (1 mL). The solution was heated for 30 minutes at 40 °C. Methylene diphosphonate (0.2510 g, 1.43 mmol) was dissolved in distilled water (7 mL) and the pH was elevated to 1.93 using cesium chloride. Both solutions were added together and the pH changed to 2.04. The pink solution was then heated at 80 °C for 3 hours. The solution was centrifuged and the product was allowed to stand in the open air to evaporate the solvent slowly, depositing pink crystals.

Yield: 0.0363 g (7.17 %).

IR (ATR): υ (cm^{-1}) = 600 to 3700; (C-H) 2906.20 and 2953.90; (P=O) 1149.92; (P-C) 810.04; coordinated water (O-H) 3183.29-3319.84.[3,26,27,28,29,30,31]

XPS data displaying the percentage of each element present (%): P, 11.0; Co, 3.3; Cs, 5.9

NMR: The complex is paramagnetic so NMR was not possible.

Elemental analysis (%): Found- C, 4.20; H, 1.75

Calculated- C, 3.39; H, 1.71

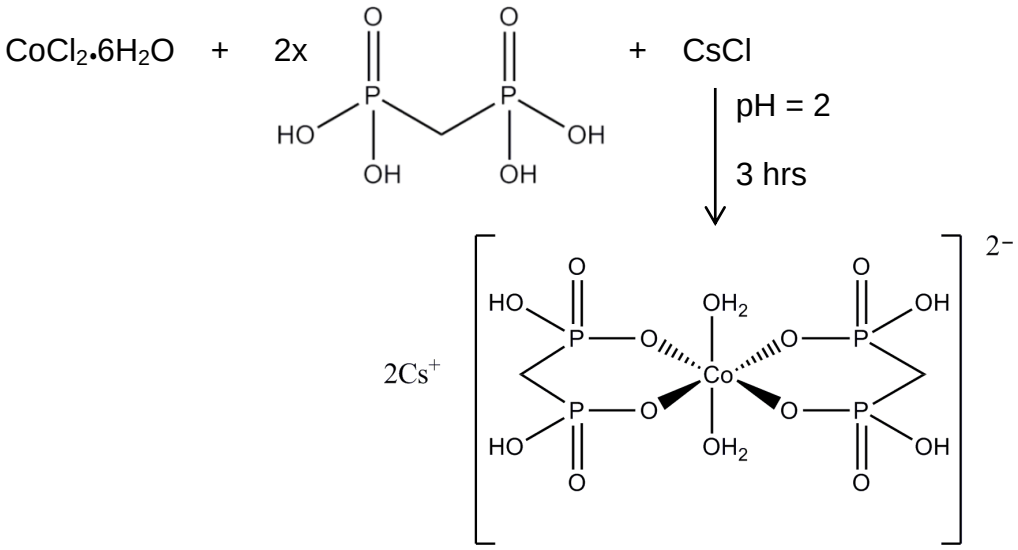

Figure 3.11 Reaction scheme of the formation of $(Cs)_2[Co(CH_4O_6P_2)_2(H_2O)_2]$.

3.7.3 Summary of XPS Data

Each complex was characterized using XPS, this technique is used to generate a graph like **Figure 3.12,** for each complex, from which the percentage of elements present in that complex can be determined. It displays how many electrons are emitted from a sample surface when irradiated by X-rays. The quantity of electrons which are emitted from the surface of the sample are recorded at a sequence of energies incorporating both the background signal and the resonance peaks, which are characteristic of the bound states of the electrons in the surface atoms. The resonance peaks above the background are crucial features in a XPS spectrum. Every element has a unique binding energy which is associated with each core

atomic orbital; therefore each element will generate a unique set of peaks in the photoelectron spectrum. The occurrence of peaks at specific energies signifies the presence of a certain element within the sample. The intensity of the peaks correlates to the concentration of the element within the sample.

This technique differs from elemental analysis as it is a surface technique. **Figure 3.12** illustrates that there is a substantial amount of oxygen and carbon present and the percentage values for these elements **(Table 3.1)** is high but the atmosphere also has an effect on the results. This technique is beneficial if you are analysing heavy elements other than oxygen and carbon.

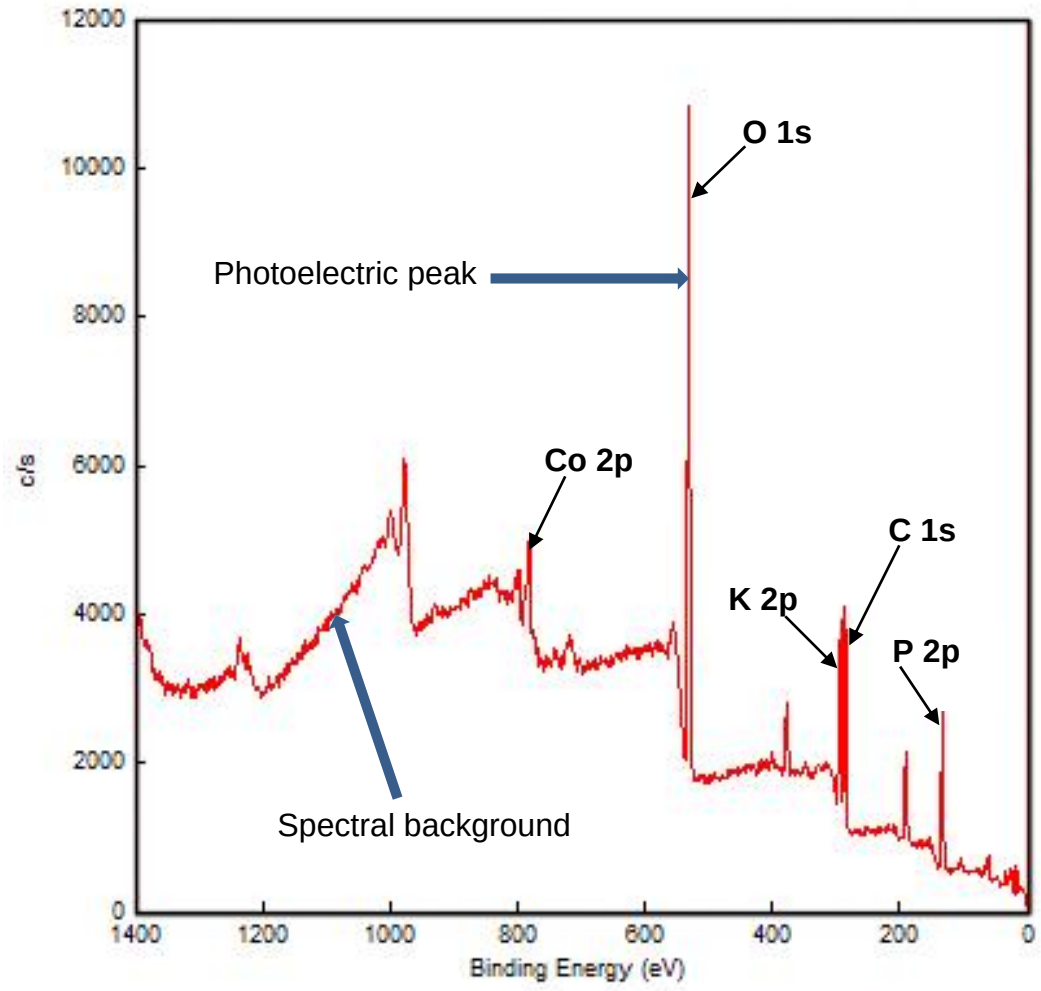

Figure 3.12 Survey scan of the XPS spectra of $K[Co(CH_4O_6P_2)_2(H_2O)_2]$ indicating all the elements present in the sample.

XPS spectra are quantified in terms of the intensities of the peaks as well as by the orientation of the peaks. Peak intensities determine how much of the material is

present at the surface and the peak positions indicate the elemental and chemical composition as displayed in **Table 3.1**.

Table 3.1 XPS data displaying the percentage of each species of element present (%), the binding energy (BE) and all the possible species or the orbital and/or oxidation state of the metal or atom present (OX).

Potassium diaquabis(methylenediphosphonato)cobaltate(III)														
Oxygen			Carbon			Potassium			Phosphorous			Cobalt		
BE (eV)	%	OX	BE (eV)	%	OX	BE (eV)	%	OX	BE (eV)	%	OX	BE (eV)	%	OX
530.6	9.82	OH_2	284.51	60.71	C-C	292.7	66.67	$2p_{3/2}$	132.79	66.67	$2p_{3/2}$	781.08	66.67	$2p_{3/2}$
530.86	31.28	O	285.24	24.45	C-O	295.5	33.33	$2p_{1/2}$	133.74	33.33	$2p_{1/2}$	796.13	33.33	$2p_{1/2}$
531.46	19.63	P-OH	286.37	4.9	C-P									
532.1	19.63	P-O	288.3	9.94	C=O									
532.88	19.63	P=O												

Table 3.1 displays the binding energy in eV, this denotes the position that each element will occupy and this value is unique for each element, for example oxygen will always have a binding energy around 530 eV. The binding energy for an electron is determined by not only the level from which the photoemission takes place but also on the formal oxidation state of the atom as well as the local physical and chemical environment. Alterations in the afore mentioned will give rise to small shifts in the peak positions in the spectrum, this is referred to as the *chemical shifts*. Atoms which have a higher positive oxidation state have a higher binding energy primarily because of the extra coulombic interaction between the photo emitted electron and the ion core.

3.8 Conclusion

A range of Co(II), Co(III) and Cr(III) complexes were successfully synthesized according to the methods described above but the yields were relatively low and this could be attributed to a variety of factors ranging from the solvent used, temperature, pH, etc. These compounds were characterized by IR, XPS as well as elemental analysis. NMR could only be performed on the potassium diaquadihydroxy-(methylenediphosphonato)cobaltate(III) complex because the other complexes either

had solubility issues or they were paramagnetic. ^{1}H NMR spectroscopy provided characteristic peaks at 1.95 ppm and also at 2.25 ppm. These proton NMR peaks were for the hydroxyl protons on the methylene diphosphonate ligand. ^{13}C NMR spectroscopy also provided a distinguishing C-P peak at 27.03 ppm and from the ^{31}P NMR spectroscopy only one peak was found at 27.63 ppm which means that the two phosphonates are symmetrical. IR analysis of these complexes revealed characteristic stretching frequencies at ± 730-820 cm^{-1} for the P-C groups, ± 1170-1220 cm^{-1} for the P=O groups, ± 2900-2990 cm^{-1} for the C-H groups, ± 3000-3100 cm^{-1} for the N-H groups and ± 3000-3500 cm^{-1} for the coordinated O-H groups.

All of the complexes provided suitable crystalline solids which were used for single crystal X-ray diffraction which are discussed in detail in Chapter 5 and 6.

4 Dissociation Constants of Methylene Diphosphonate in an Aqueous Medium

4.1 Introduction

Methylene diphosphonate (MDP) is a polyprotic acid and has four different K_a values. It is able to donate more than one proton per acid molecule. The ionizations of polyprotic acids is a stepwise process with the first ionization step being the easiest and with each consecutive ionization step it becomes more difficult to remove the protons, thus it becomes harder to predict the pH at which the next protonation will occur. The numerous K_a values will vary because it is energetically less favourable to lose a proton if the conjugated base is more negatively charged.[1,2]

Only a limited amount of studies relating to the pK_a values of methylene diphosphonate are found in literature. However some of the pK_a values differ considerably and this is because the methods used to determine the pK_a values differ with regards to the temperature, ionic strength, solvent media, etc.

The volumetric titration of methylene diphosphonate is dependent on the concentration as well as the pH, thus a large and constant ionic medium is vital to ensure that the activity coefficients does not change.[3] In this study the pK_a values for methylene diphosphonate were obtained by using three different methodologies, together with literature data and the values which were predicted by SPARC.

[1] J.C. Kotz, P.M. Treichel and J.R. Townsend. *Chemistry and Chemical Reactivity*, 7th Edition, p 787, Brooks/Cole, Canada, **2009**.

[2] K.W. Whitten, R.E. Davis, M.L. Peck and G.G. Stanley. *Chemistry*, 8th Edition, Thomson Brooks/Cole, United States of America, **2007**.

[3] W. Hummel. *Chemical thermodynamics of compounds and complexes of U, Np, Pu, Am, Tc, Se, Ni, and Zr, with selected organic ligands*, Elsevier, Netherlands, **2005**.

Three methodologies namely the geometric method, the first derivative method and lastly the second derivative method were used to determine the dissociation constants and the equivalence points of methylene diphosphonate.

SPARC, a computer program is used to determine the dissociation constants of a polyprotic substance like methylene diphosphonate, even when the pK_a values are close to each other.[4] It uses algorithms which are based on the fundamental chemical structure theory which incorporates principles of linear free-energy relationships (LFER), perturbation theory from quantum chemistry as well as quantitative structure activity relationships (QSAR). It is able to estimate the pK_a values of any organic compound but just examining the chemical structure.[5] SPARC was used as a "reference" to compare our values to as it only looks at the molecular formula to generate the various pK_a values, it does not take into account the presence of an ionic medium, the temperature or even the solvent utilised.

4.1.1 Relevance of pK_a values in the Radiopharmaceutical Industry.

The acid dissociation constant is an indicator to the extent of the ionization of a drug at various pH values and it is therefore a vital parameter that indicates the optimization of the drug structure.

The ionization of drugs is essential as it affects the physico-chemical properties of drugs, such as the solubility and lipophilicity as well as parameters that concern the cell-drug interaction, for instance the membrane permeability, plasma protein binding, metabolism, tissue penetration and target protein binding. Many compounds which are used for medication are weak bases or acids. The efficiency with which the compound enters the blood is dependent on the pK_a values and the water-octanol partition coefficient.[6]

[4] S. Şanli, N. Şanli and G. Alsancak. *Journal of the Brazilian Chemical Society*, 2009, **20**, 939-946.

[5] M. Kelen and N. Sanli. *Journal of the Brazilian Chemical Society*, 2009, **20**, 133-140.

[6] Yasushi Ishihama, Masahiro Nakamura, Toshinobu Miwa, Takashi Kajima and Naoki Asakawa. Journal of *Pharmaceutical Sciences*, 2002, **92**, 933-942.

4.2 Experimental Procedures

4.2.1 General Procedure

All chemicals and reagents were of analytical grade and distilled water was used in all of the experiments. Titrations were performed on a Compact Titrator G20 and standard buffer solutions were used to calibrate the machine. The SPARC program and Microsoft Office Excel 2010 were used to fit the data. The ionic strength of all the reaction solutions were kept constant by the addition of NaCl (0.1 M), unless otherwise stated.

4.2.2 Standard Deviation

All the titrations were done in triplicate and the standard deviations was determined. This is the measure of the average deviation of each value from the mean and it is the spread of data about the mean value.[7]

$$s = \sqrt{\frac{1}{N-1}\sum_{i=1}^{N}(x_i - \bar{x})^2}$$

… Eq. 4.1

In **Equation 4.1**, N is the number of measurements, x_i is each individual measurement and $\bar{x}$ is the mean of all the measurements. The quantity ($x_i - \bar{x}$) is referred to as the "residual" or the "deviation from the mean" for each measurement and N-1 is called the "degrees of freedom" or the Bessel's correction.[8]

[7] D.C. Howell. *Fundamental Statistics for the Behavioral Sciences*, 6th Edition, p 82-84, Thomson Wadsworth, United States of America, **2008**.

[8] W.J. DeCoursey. *Statistics and Probability for Engineering Applications with Microsoft Excel*, p 48, Elsevier Science, United States of America, **2003**.

4.2.3 Standardisation of Sodium Hydroxide with Potassium Hydrogen Phthalate

A small quantity of potassium hydrogen phthalate (0.6182 g, 3.03 mmol) was dissolved in distilled water (50 mL) and a few drops of phenanthroline indicator was added. The potassium hydrogen phthalate (KHP) solution was titrated with the sodium hydroxide (NaOH) of unknown concentration until the end point was reached. The procedure was repeated three times and the average concentration of sodium hydroxide was taken as the concentration of the standard base solution.

4.2.4 Preparation of Solutions

(a) The sodium hydroxide solution was prepared by dissolving sodium hydroxide (1.9932 g, 49.83 mmol) in distilled water (500 mL). This solution was standardised before being used.

(b) Methylene diphosphonate (0.0178 g, 0.1011 mmol) was dissolved in distilled water (50 mL) and sodium chloride (0.3017 g, 52.00 mmol), the background electrolyte, was added to this solution.

(c) Methylene diphosphonate (0.0174 g, 0.09886 mmol) was dissolved in distilled water (50 mL).

4.3 Methylene Diphosphonate

4.3.1 Introduction

The ligand methylene diphosphonate (MDP) is a polyprotic acid with four protonation constants. As each proton is lost, subtle changes in the electronic structure of MDP occurs. Each proton is lost according to the following reactions, where $X = CH_2P_2O_3^{-4}$.

:

$$H_4X_{(aq)} \overset{K_{a1}}{\rightleftharpoons} H_3X^{-1}_{(aq)} + H^+_{(aq)} \quad \text{... Eq. 4.2}$$

$$H_3X^{-1}_{(aq)} \overset{K_{a2}}{\rightleftharpoons} H_2X^{-2}_{(aq)} + H^+_{(aq)} \quad \text{... Eq. 4.3}$$

$$H_2X^{-2}_{(aq)} \overset{K_{a3}}{\rightleftharpoons} HX^{-3}_{(aq)} + H^+_{(aq)} \quad \text{... Eq. 4.4}$$

$$HX^{-3}_{(aq)} \overset{K_{a4}}{\rightleftharpoons} X^{-4}_{(aq)} + H^+_{(aq)} \quad \text{... Eq. 4.5}$$

In order to quantify the chemical equilibria, the equilibrium constants are determined, where $X = CH_2P_2O_3^{-4}$.

.

$$K_{a1} = \frac{[H_3X^{-1}][H^+]}{[H_4X]} \quad \text{... Eq. 4.6}$$

$$K_{a2} = \frac{[H_2X^{-2}][H^+]}{[H_3X^{-1}]} \quad \text{... Eq. 4.7}$$

$$K_{a3} = \frac{[HX^{-3}][H^+]}{[H_2X^{-2}]} \quad \text{... Eq. 4.8}$$

$$K_{a4} = \frac{[X^{-4}][H^+]}{[HX^{-3}]} \quad \text{... Eq. 4.9}$$

When an equilibrium constant is displayed as a concentration quotient, it means that the activity quotient is constant. In order for this to be valid the equilibrium constants must be determined in a medium comprised of a high ionic strength. In order to ascertain the concentrations of the chemical species, titrations are performed. From the titrations the equilibrium constants could be derived by fitting the experimental data.

The Henderson-Hasselbach equation is derived from the acid dissociation constant equation by the following steps:

$$\log_{10}K_{a1} = \log_{10}\left(\frac{[H_3X^{-1}][H^+]}{[H_4X]}\right) \quad \text{... Eq. 4.10}$$

$$\log_{10}K_{a1} = \log_{10}[H^+] + \log_{10}\left(\frac{[H_3X^{-1}]}{[H_4X]}\right) \quad \text{... Eq. 4.11}$$

$$-pK_{a1} = -pH + \log_{10}\left(\frac{[H_3X^{-1}]}{[H_4X]}\right) \quad \text{... Eq. 4.12}$$

$$pH = pK_{a1} + \log_{10}\left(\frac{[H_3X^{-1}]}{[H_4X]}\right) \quad \text{... Eq. 4.13}$$

$X = CH_2P_2O_3^{-4}$

Three methods were utilised to determine the equivalence points and the pK_a values; the first is referred to as the geometric method, the second method involves

generating the first derivative graph and the third method is to make a second derivative plot.

4.4 Determination of the Acid Dissociation Constants and Equivalence Points of MDP

4.4.1 Volumetric Titration Curve of MDP

A volumetric titration is an analytical technique employed to quantitatively determine how much analyte is dissolved in a sample. The titrant (NaOH) is gradually added to the analyte (MDP) and this results in a chemical reaction between the analyte and the titrant (the concentration of the titrant is known). The titrant is gradually added till the reaction is complete. The pH alters gradually until the end point, where a sharp change is observed.

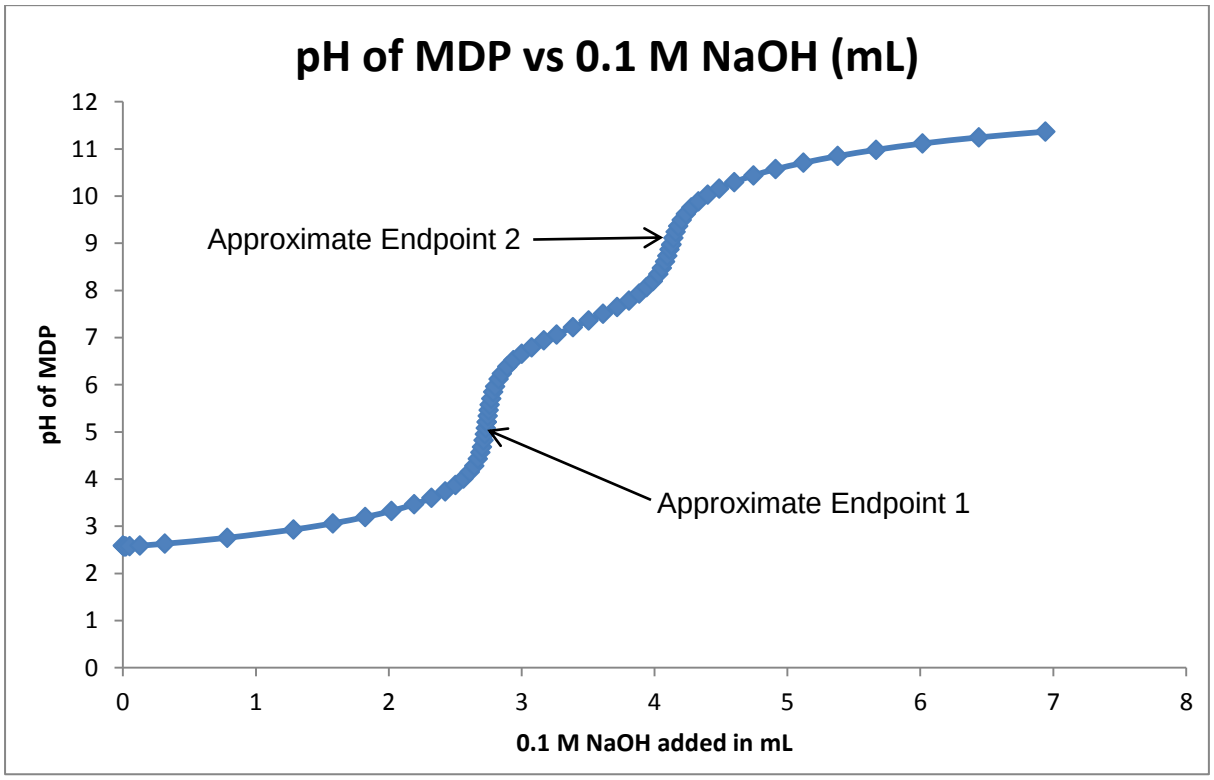

Figure 4.1 Plot of pH versus the volume of base added (0.1 M sodium hydroxide, no NaCl) for methylene diphosphonate at 18.0 ºC.

The titration curve as depicted in **Figure 4.1** has a distinctive sigmoid shape and a fundamental task in any titration is the determination of the equivalence point. Normally this is the section of the curve where a large amount of change takes place, a steep rise, and is referred to as the equivalence point. This is the point at which the quantity of titrant added is stoichiometrically equal to the amount of analyte present in the original sample.

The first method used to determine the equivalence points as well as the pK_a values is referred to as the geometric method. This is a graphical method which is the simplest method used to interpret pH titration data.

The steep rise (equivalence point) is followed by a shallow gradient which is formed due to the reaction between the methylene diphosphonate and the sodium hydroxide.

The midpoint of a steep change in pH marks the equivalence point. By inspection the curve in **Figure 4.1** shows two different equivalence points, the first after the addition of 2.74 mL NaOH and the second after the addition of 4.13 mL.

The Henderson-Hasselbach equation (**Equation 4.13**) displays how the pH changes as base is added and the equation is utilised to determine the pK_a values. According to **Equation 4.13** the pK_a value is equal to half of the equivalence point. The pK_a value was determined to be 2.96(8), which according to literature (2.87 without and ionic medium and 2.75 with and ionic medium of 0.1 M $C_4H_{12}BrN$) is the pK_{a2} value.[9] The quantity of base required to go from the first equivalence point to the second one, determines the new half equivalence point. The pH at this point is equivalent to the pK_{a3} value of 7.29(5) which correlated to literature (7.45 without and ionic medium and 7.33 with and ionic medium of 0.1 M $C_4H_{12}BrN$).[9]

The reason why these pK_a values differ slightly from literature is because there was no ionic medium (NaCl) present, water was the solvent in these titrations and the temperature at which the titrations were performed was 18.0 ºC.

[9] K. Moedritzer and R.R. Irani. *Journal of Inorganic and Nuclear Chemistry*, 1962, **22**, 297.

4.4.2 First Derivative Method

The second method can't be used to determine the pK_a values it is only utilised to ascertain the equivalence points. This method is more accurate in determining the equivalence points compared to the geometric method and is referred to as the first derivative method. A first derivative plot is constructed by using **Equation 4.14**.

$$\frac{\Delta pH}{\Delta V} = \frac{pH_2 - pH_1}{V_2 - V_1} \qquad \text{... Eq. 4.14}$$

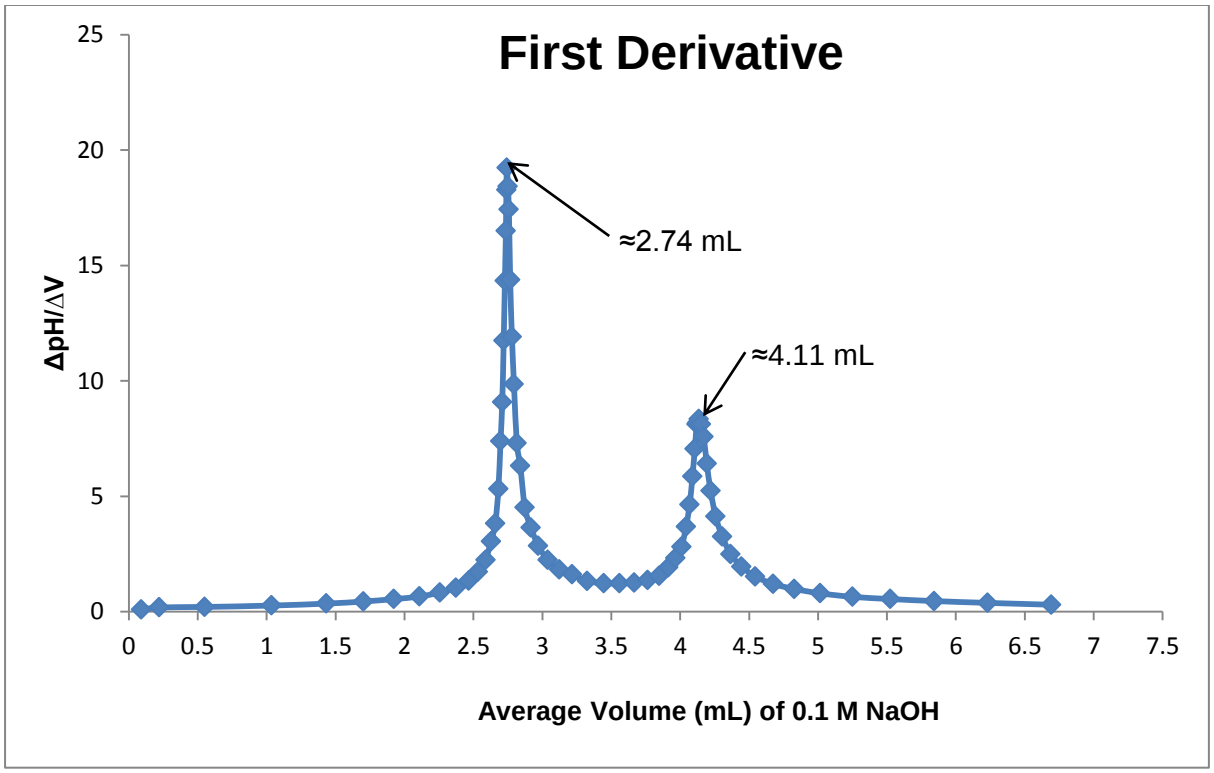

Figure 4.2 Plot of the first derivative versus the average volume of base added (0.1 M sodium hydroxide, no NaCl) for methylene diphosphonate at 18.0 ºC.

In order to acquire a better approximation of the volumes at the equivalence points the first derivative plot is constructed based on **Equation 4.14**. It displays the change in slope of the titration curve as a function of the added volume of sodium hydroxide. The inflections points in the curve are the points of maximum slope as

displayed in **Figure 4.2**. The first inflection point is at 2.74 mL which is identical to the equivalence point determined using the geometric method. The second inflection point is at 4.11 mL which correlates to the equivalence point obtained using the geometric method which was 4.13 mL.

4.4.3 Second Derivative Method

The third method used to determine the equivalence points and the pK_a values is referred to as the second derivative method. A second derivative plot is constructed by using **Equation 4.15**.

$$\frac{\Delta^2 pH}{\Delta V^2} = \frac{(\Delta pH_2/\Delta V_2) - (\Delta pH_1/\Delta V_1)}{\Delta V_2 - \Delta V_1} \quad \text{... Eq. 4.15}$$

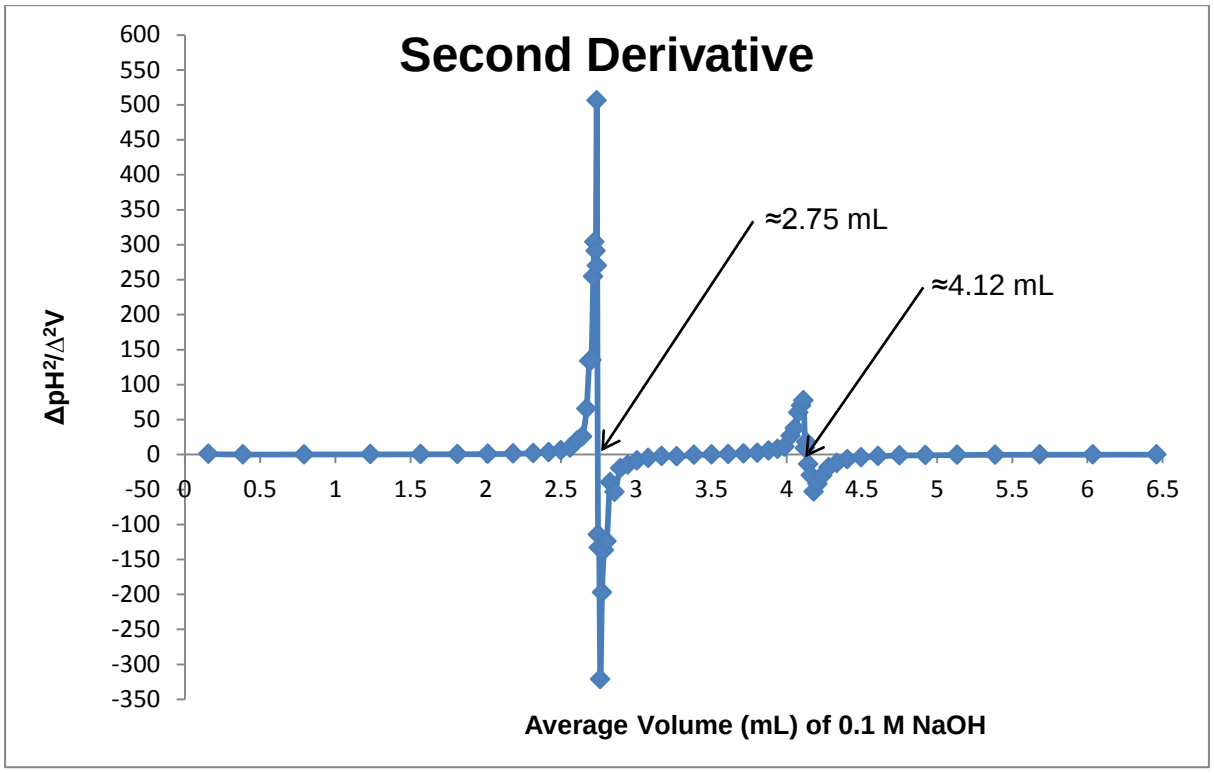

Figure 4.3 Plot of the second derivative versus the average volume of base added (0.1 M sodium hydroxide, no NaCl) for methylene diphosphonate at 18.0 ºC.

This method is used to calculate the differences between adjacent first derivative values in a titration. With the second derivative method the end points (equivalence points) are equivalent to the inflection points in the curve; this is where the second derivative crosses the x-axis. In **Figure 4.3** the graph intersects the x-axis twice; the first equivalence point is at 2.75 mL which correlates well with the values acquired from the first derivative method and the geometric method. The second equivalence point is at 4.12 mL which is similar to the values which were obtained using the other methods.

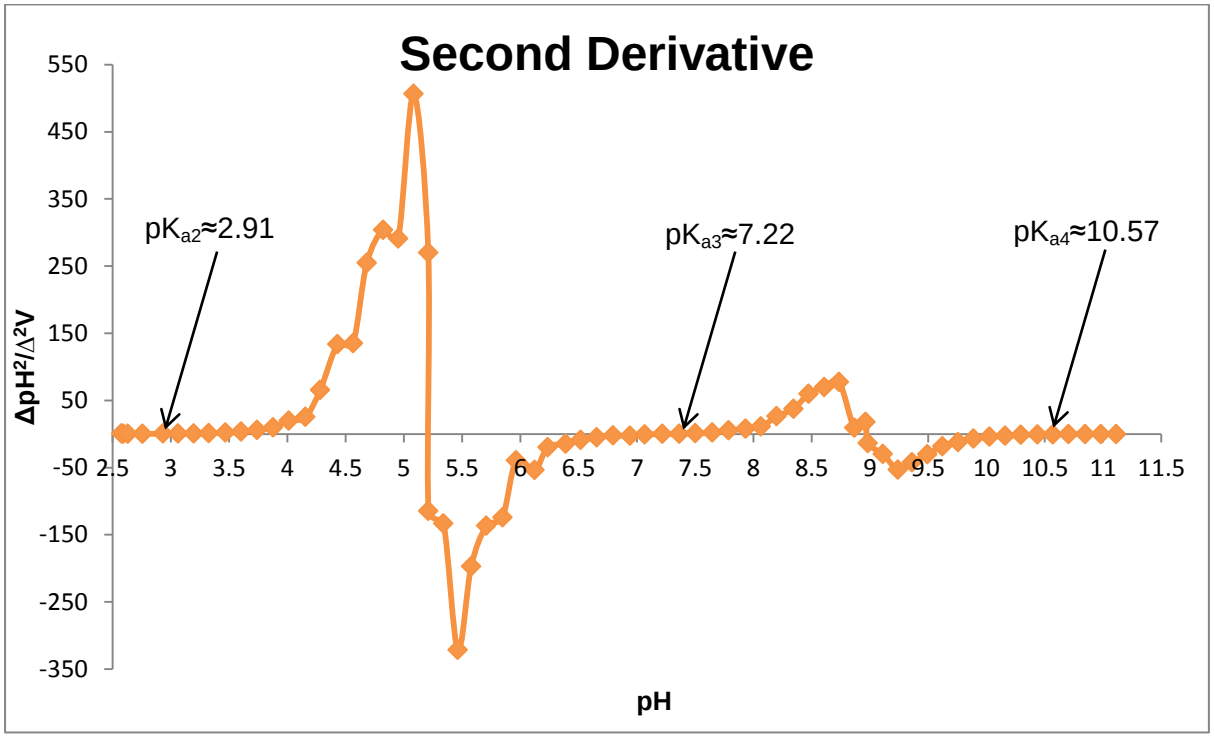

Figure 4.4 The second derivative plot of methylene diphosphonate versus the pH (no NaCl) for methylene diphosphonate at 18.0 ºC.

The second derivative function (**Equation 4.15**) can be employed to acquire more precise pK_{a2}, pK_{a3} and pK_{a4} values by plotting $\Delta pH/\Delta V$ versus the pH values which were acquired during the titration. Where the graph intersects the x-axis the pH value is equal to the pK_a values. If more than one point intersects the x-axis for a specific pK_a value then the average pK_a value is determined. Based on **Figure 4.4** the pK_{a2} value is 2.91(8) and pK_{a3} value is equal to 7.22(5). Both values differ

slightly from the ones determined using the geometric method. Using the second derivative method the pK_{a4} value of 10.57(1) was acquired while the geometric method was unable to ascertain the pK_{a4} value. A reason why the geometric method could not pick up the pK_{a4} value is because the third and fourth equivalence points were so close together. All the pK_a values acquired using this method correlated to literature.[9]

All three methodologies produced pK_a values that were very similar to each other and the same applied for the equivalence points. Unfortunately the pK_{a1} value could not be determined, the reason for this is that the Compact Titrator G20 is unable to perform titrations below pH 2 and the pK_{a1} value according to literature ranges from 1.30-2.20.[9,13,14]

4.4.4 SPARC Software

This software which has been used in numerous publications, performs automated reasoning in chemistry.[5,10,11,12] It is able to estimate the ionization pK_a values of a vast amount of molecules by examining their molecular structure. The software performs a computational algorithm which is based on the fundamental chemical structure theory.

It is able to determine the pK_a values of polyprotic acids, generate a mechanism as well as the species distribution curve. The only negative aspect regarding the software is that it only works for ligands and not complexes.

[10] S.H. Hilal, Y. El-Shabrawy, L.A. Carreira, S.W. Karickhoff, S.S. Toubar and M. Rizk. *Talanta*, 1996, **43**, 607-619.

[11] J.M. Herrero-Martínez, M. Sanmartin, M. Rosés, E. Bosch and C. Ràfols. *Electrophoresis*, 2005, **26**, 1886-1895.

[12] C.J. Jackson, K. Weir, A. Herlt, J. Khurana, T.D. Sutherland, I. Horne, C. Easton, R.J. Russell, C. Scott and J.G. Oakeshott. *Applied and Environmentatl Microbiology*, 2009, **75**, 5153-5156.

For methylene diphosphonate, SPARC was able to determine the four pK_a values:

$$pK_{a1} = 1.60$$

$$pK_{a2} = 2.90$$

$$pK_{a3} = 7.50$$

$$pK_{a4} = 8.53$$

These values are similar to literature[9,13,14] but also correlated to the pK_{a2} and pK_{a3} values which were acquired using the Compact Titrator G20. The pK_{a4} value differs a lot and a reason for this is that the software does not take into consideration the concentration of the analyte and the titrant, the ionic medium or the temperature. It purely looks at the simplified molecular input line entry specification (SMILE) to generate the data. According to literature there is always a large error present on the last pK_a value.

SPARC could determine which proton dissociates in each step and from this the general protonation mechanism could be constructed as depicted in **Figure 4.5**. The sequence in which proton dissociation takes place is dependent on the acidity of the proton. The most acidic proton, the one with the lowest pK_a value will dissociate first while the removal of successive protons become more complicated.

[13] K.L. Nash and E.P. Horwitz. *Inorganica Chimica Acta*, 1990, **169**, 245-252.

[14] E.C. Lisic, M. Phillips, D. Ensor, K.L. Nash, A. Beets and F.F. Knapp Jr. *Nuclear Medicine and Biology*, 2001, **28**, 419-424.

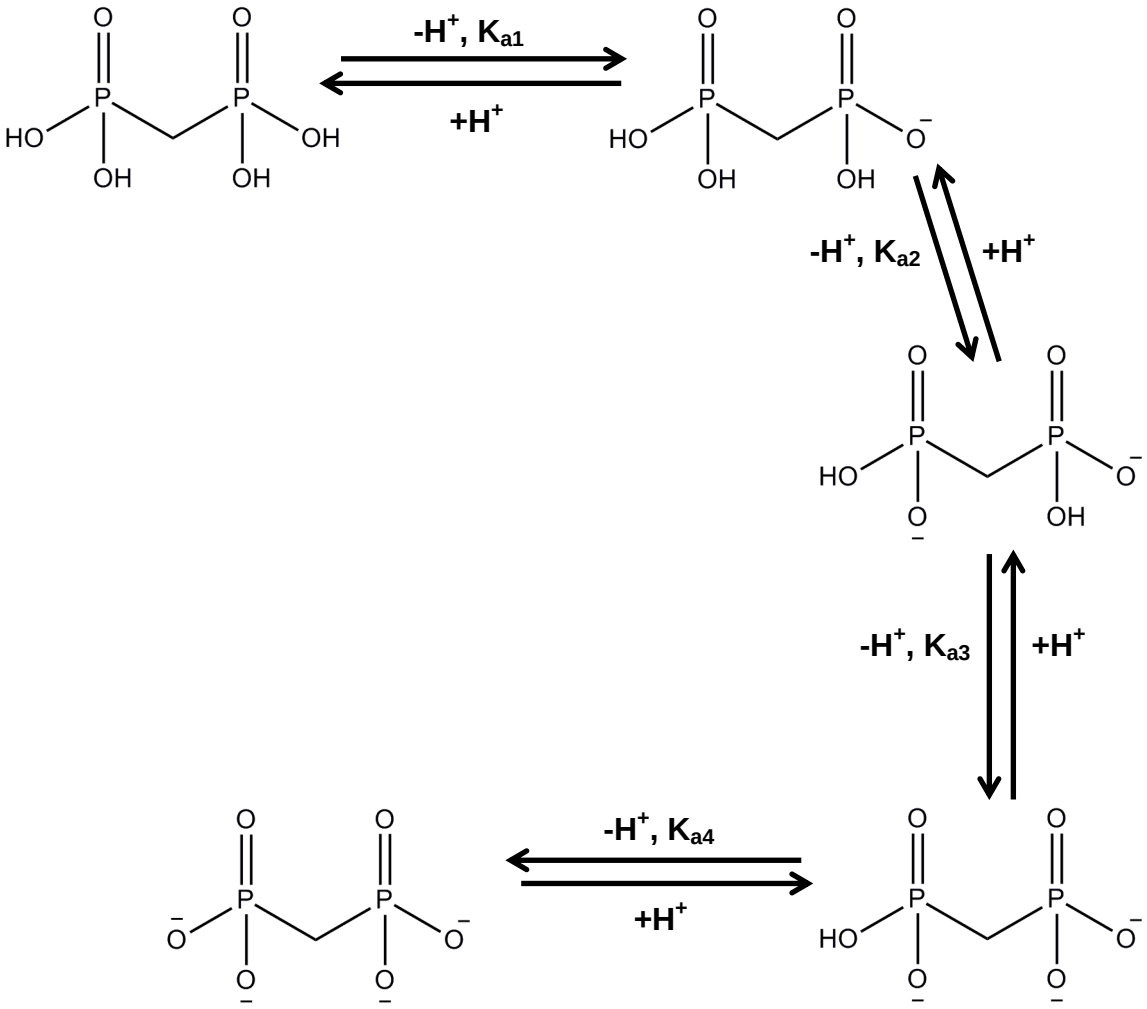

Figure 4.5 General protonation mechanism for methylene diphosphonate using SPARC.

Initially the solution is comprised of $CH_2P_2O_3H_4$ but once sodium hydroxide is added, then $CH_2P_2O_3H_3^-$ and $CH_2P_2O_3H_4$ are found in the solution. After more base is added then only $CH_2P_2O_3H_3^-$ is found in the solution and this is when the first equivalence point is reached. The addition of more base does not "drown" the system with OH^- ions as it does in monoprotic acids. The hydroxide ion is employed to expel the next proton which is a lot harder. The solution is now comprised of $CH_2P_2O_3H_3^-$ as well as $CH_2P_2O_3H_2^{-2}$. As more base is added only $CH_2P_2O_3H_2^{-2}$ remains present in the solution thus the second equivalence point has been reached. As more base is introduced to the analyte then $CH_2P_2O_3H_2^{-2}$ as well as $CH_2P_2O_3H^{-3}$ are present in the solution. But after more base is added then only $CH_2P_2O_3H^{-3}$ is present, therefore the third equivalence point has been attained. Again more base is

added to the solution which is composed of $CH_2P_2O_3H^{-3}$ and $CH_2P_2O_3^{-4}$ so in order to get the last equivalence point extra base is added.

4.4.5 Summary of the Results

Table 4.1 Protonation constants for the ligand methylene diphosphonate.

Equilibrium	pK_a	μ (ionic medium)	Temperature	Reference
$H_4X = H_3X^{-1} + H^+$	-	None	18 ºC	This work
$H_3X^{-1} = H_2X^{-2} + H^+$	2.91(8)			
$H_2X^{-2} = HX^{-3} + H+$	7.22(5)			
$HX^{-3} = X^{-4} + H^+$	10.57(1)			
$H_4X = H_3X^{-1} + H^+$	-	0.1 M NaCl	18 ºC	This work
$H_3X^{-1} = H_2X^{-2} + H^+$	2.95(1)			
$H_2X^{-2} = HX^{-3} + H+$	6.81(5)			
$HX^{-3} = X^{-4} + H^+$	10.41(2)			
$H_4X = H_3X^{-1} + H^+$	1.6			SPARC
$H_3X^{-1} = H_2X^{-2} + H^+$	2.9			
$H_2X^{-2} = HX^{-3} + H+$	7.5			
$HX^{-3} = X^{-4} + H^+$	8.53			
$H_4X = H_3X^{-1} + H^+$	2.2	None	25 ºC	[9]
$H_3X^{-1} = H_2X^{-2} + H^+$	2.87			
$H_2X^{-2} = HX^{-3} + H+$	7.45			
$HX^{-3} = X^{-4} + H^+$	10.69			
$H_4X = H_3X^{-1} + H^+$	1.7	0.1 M $C_4H_{12}BrN$	25 ºC	[9]
$H_3X^{-1} = H_2X^{-2} + H^+$	2.75			
$H_2X^{-2} = HX^{-3} + H+$	7.33			
$HX^{-3} = X^{-4} + H^+$	10.42			
$H_4X = H_3X^{-1} + H^+$	1.30(0.01)	0.1 M NaCl	25 ºC	[13] & [14]
$H_3X^{-1} = H_2X^{-2} + H^+$	2.35(0.01)			
$H_2X^{-2} = HX^{-3} + H+$	6.34(0.01)			
$HX^{-3} = X^{-4} + H^+$	8.90(0.01)			

The protonation constants for the ligand MDP are comparable to the reported values as displayed in **Table 4.1.** The slight differences in the protonation constants are because different ionic solutions as well as varying ionic strengths (NaCl) and temperatures were used. The ionic strength ensures that minimal changes occur to the solution during a titration. In order to investigate the effect of the ionic medium on the determination of the ionization constants, it was decided to perform the volumetric titrations in an ionic medium of 0.1 M NaCl and compare these values with data obtained without any adjustments to the ionic medium, the temperature for all of the reactions was kept constant at 18.0 ºC. The result is that the pK_{a2} values (2.91(8) no ionic medium present and 2.95(1) with and ionic medium (0.1 M NaCl)) and pK_{a4} values (10.57(1) no ionic medium present and 10.41(2) with and ionic medium (0.1 M NaCl)) compare to each other and to literature.[9] The major difference arises in the pK_{a3} values, of 7.22(5) without and ionic medium and 6.81(5) with an ionic medium (0.1 M NaCl), where there is a noticeable difference. Therefore a large and constant ionic medium is vital to ensure that the activity coefficients does not change.

4.4.6 Species Distribution Curve

The distribution curve, which is an effective visual tool, is used to display the fraction of each species present within the solution which is plotted against the pH.

From **Figure 4.6** the three pK_a values can be identified, where the two graphs intersect each other. The graph also displays which species are dominant and over what pH range. At, for instance, pH = 2.91, the concentrations of H_3X^{-1} and H_2X^{-2} are roughly equivalent to each other and the concentrations of HX^{-3} and X^{-4} are insignificant, therefore H_3X^{-1} and H_2X^{-2} are the dominant species over the pH range of 0-5.

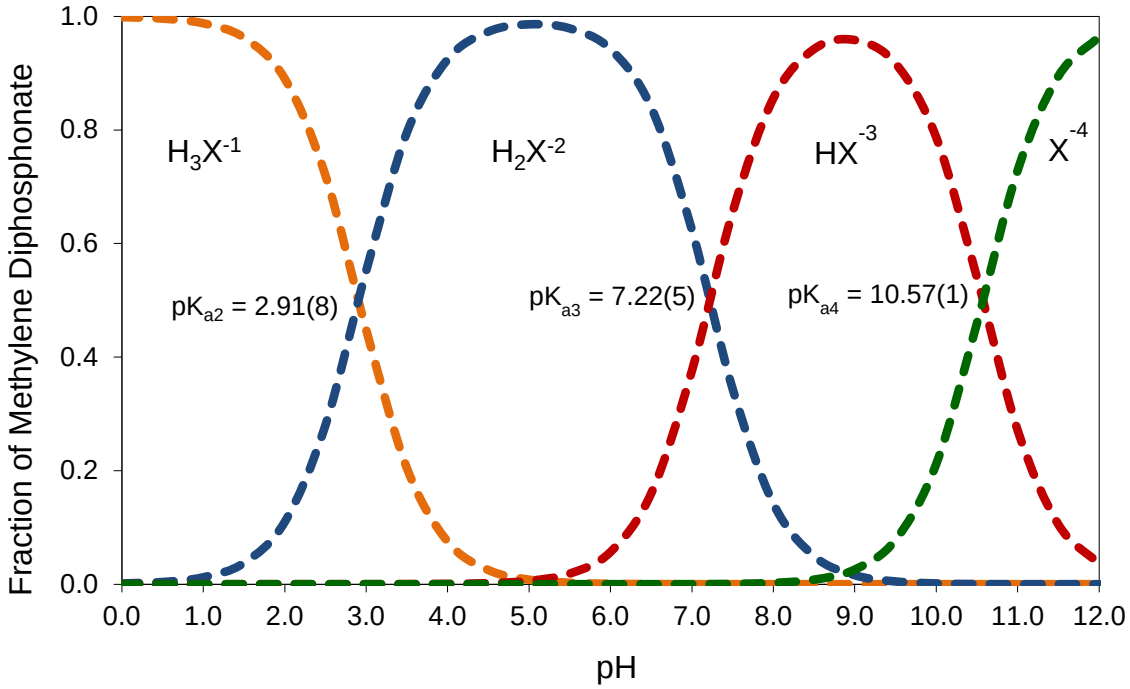

Figure 4.6 Species distribution curve of methylene diphosphonate.

4.5 Conclusion

The determination of the pK_a values is vital for the characterization of a potential drug. In this work numerous volumetric titrations were performed on methylene diphosphonate with and without and ionic medium (NaCl) present. The protonation constants and the equivalence points for the methylene diphosphonate ligand were determined using three methods which were compared to the protonation constants generated from the SPARC software as well as literature values. The reported protonation constant values as depicted in **Table 4.1** correlated despite the fact that they were determined at different temperatures, ionic mediums (NaCl) and strengths as well as with different solvents. Unfortunately the pK_{a1} value could not be attained due to the fact that the Compact Titrator G20 is unable to perform titrations below pH 2. If the protonation constants for a potential new drug are known then the distribution plots can be determined, which displays the extent that a potential drug is ionized at the physiological pH (i.e., pH=7.40 in the blood).

5 Crystallographic Study of Cobalt(III) and Chromium(III) complexes

5.1 Introduction

This chapter deals with the solid state characterization of Co(III)- and Cr(III) methylene diphosphonate (MDP) complexes.[1] Methylene diphosphonate is an important bidentate ligand as it is predominately used in the preparation of skeletal imaging agents. Very few metal derivatives of methylene diphosphonate have been structurally characterized.

The solid state characterization provides a better understanding of how the methylene diphosphonate coordinates to a metal complex and this will provide information with regard to the crystal packing orientation and molecular interactions. Illustrated in **Figure 5.1** are the Co(III)- and Cr(III) methylene diphosphonate complexes evaluated in this crystallographic study.

[1] K. Libson, E. Deutsch and B.L. Barnett. *Journal of American Chemical Society*, 1980, **7**, 2476-2478.

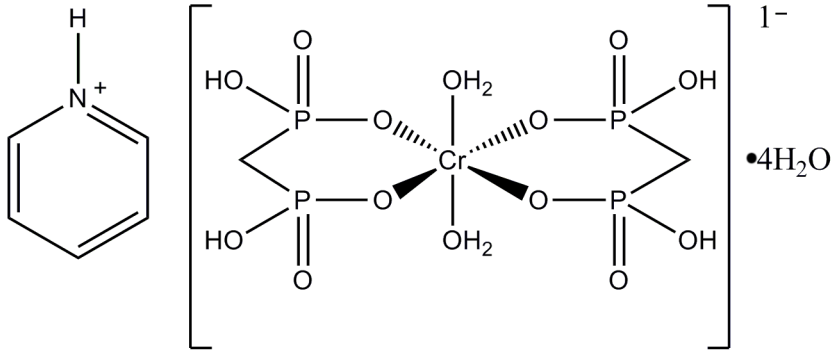

1

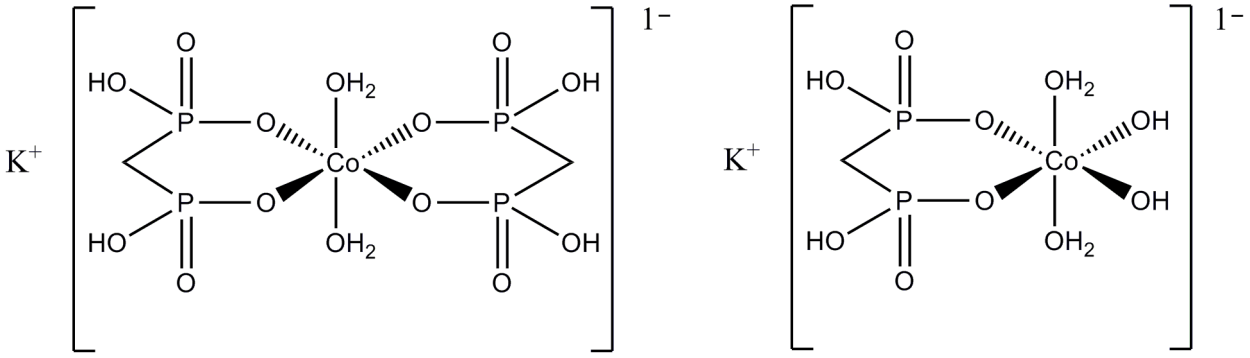

2 **3**

Figure 5.1 Schematic representation of all the complexes discussed in this single crystal X-ray crystallographic study. 1. $(C_5H_6N)[Cr(CH_4O_6P_2)_2(H_2O)_2]\cdot 4H_2O$, 2. $K[Co(CH_4O_6P_2)_2(H_2O)_2]$ and 3. $K[Co(CH_4O_6P_2)(OH)_2(H_2O)_2]$.

5.2 Experimental

The reflection data for all the structures were compiled on a Bruker X8 ApexII 4K Kappa CCD diffractometer which utilises a graphite monochromated Mo Kα radiation and applies ω- and φ-scans at 100K.[2] COSMO[3] was employed in order to optimise the collection of more than a hemisphere of reciprocal space. To ensure that no decomposition of the crystals took place during the collection the initial 50 frames were repeated after the collection was complete. All the crystals remained stable throughout the data collection. The frames were combined using a narrow-frame integration algorithm and then reduced with the Bruker SAINT-Plus[4] and XPREP[4] software packages, respectively. The multi-scan technique SADABS[5] was utilised to correct data which had adsorption effects. SIR97[6] which is a direct method package was used to solve all the structures and refinement was done on the WinGX,[7] software package which incorporates SHELXL.[8] All the graphical representations of the crystal structures were generated using DIAMOND.[9] Unless otherwise stated all the structures are shown with thermal ellipsoids drawn at 50% probability level. diphosphonate have been structurally characterized.

All non-hydrogen atoms were refined anisotropically, while all the methyl and aromatic H atoms were placed in geometrically idealised positions (C-H = 0.95-0.98 Å) and constrained to ride on their parent atoms

[2] Bruker, APEX2 (Version 1.0-27), Bruker AXS Inc., Madison, Wisconsin, United States of America, **2005**.

[3] Bruker, COSMO, (Version 1.48), Bruker AXS Inc., Madison, Wisconsin, United States of America, **2003**.

[4] Bruker, SAINT-Plus (Version 7.12) (including XPREP), Bruker AXS Inc., Madison, Wisconsin, United States of America, **2004**.

[5] Bruker, SADABS, (Version 2004/1), Bruker AXS Inc., Madison, Wisconsin, United States of America, **1998**.

[6] A. Altomare, M.C. Burla, M. Camalli, G.L. Cascarano, C. Giacovazzo, A. Guagliardi, A.G.G. Moliterni, G. Polidori and R. Spagna. *J. Appl. Cryst*., 1999, **32**, 115.

[7] L.J. Farrugia. *J. Appl. Cryst*., 1999, **32**, 837.

[8] G.M. Sheldrick, SHELXL97, *Program for Solving Crystal Structures*, University of Göttingen, Germany, **1997**.

[9] K. Brandenburg and H. Putz, DIAMOND, Release 3.0c, Crystal Impact GbR, Bonn, Germany, **2005**.

(U_{iso}(H) = 1.5U_{eq}(C) and 1.2U_{eq}(C)). The hydrogen atoms attached to the hydroxyl groups and aqueous molecules were located on a different Fourier map, restrained to a reasonable O-H distances using DFIX and refined isotropically.

A summary of the general crystal data and the refinement parameters of the three structures are given in **Table 5.1.** The supplementary data in Appendix A contains the complete list of atomic coordinates, equivalent isotropic parameters, bond distances and angles, the hydrogen coordinates for each individual dataset and the anisotropic displacement parameters.

Table 5.1: General crystal data and refinement parameters for the three studied structures.

Compound	$(C_5H_6N)[Cr(CH_4O_6P_2)_2(H_2O)_2]\cdot 4H_2O$	$K[Co(CH_4O_6P_2)_2(H_2O)_2]$	$K[Co(CH_4O_6P_2)(OH)_2(H_2O)_2]$
Empirical Formula	Cr1 N1 C7 P4 H26 O18	Co1 K1 C2 P4 H12 O14	Co1 K1 C1 P2 H10 O10
Formula Weight (g.mol^{-1})	588.17	482.02	340.04
Wavelength (Å)	0.71073	0.71073	0.71073
Crystal System	Triclinic	Triclinic	Orthorhombic
Space Group	$P\bar{1}$	$P\bar{1}$	*Pnma*
Unit Cell Dimensions			
***a* (Å)**	7.206(5)	6.4523(3)	14.034(5)
***b* (Å)**	7.485(4)	8.7056(3)	9.322(6)
***c* (Å)**	10.984(5)	13.193(5)	8.504(4)
***α* (°)**	107.085(5)	91.334(2)	90.000(5)
***β* (°)**	106.128(6)	93.304(3)	90.000(5)
***γ* (°)**	94.496(4)	93.333(2)	90.000(5)
Volume (Å^3)	535.7(6)	738.32(5)	1112.5(1)
Z	1	2	4
Density (calculated) (g.cm^{-3})	1.823 Mg/m^3	2.186 Mg/m^3	2.030 Mg/m^3
Absorption Coefficient (mm^{-1})	0.92	1.95	2.237
***F*(000)**	303	485	680
Crystal Size (mm^3)	0.22 x 0.16 x 0.08	0.28 x 0.17 x 0.17	0.25 x 0.21 x 0.07
Crystal Colour	Green	Pink	Purple
Crystal Morphology	Cuboid	Cuboid	Platelet
Theta Range (°)	4.09 - 28.27	1.55 – 28.34	2.80 - 28.42
Completeness (%)	99.1	98.9	99.8
Index Ranges	-9 ≤ h ≤ 9	-8 ≤ h ≤ 8	-18 ≤ h ≤ 18
	-9 ≤ k ≤ 6	-11 ≤ k ≤ 9	-12 ≤ k ≤ 12
	-14 ≤ l ≤ 14	-16 ≤ l ≤ 17	-11 ≤ l ≤ 11
Reflections Collected	8784	13499	24843
Independent Reflections	2632	3648	1483
R_{int}	0.02	0.04	0.02
Absorption Correction	Multiscan	Multiscan	Multiscan
Refinement Method	Full-matrix least-squares on F^2	Full-matrix least-squares on F^2	Full-matrix least-squares on F^2
Data/Restraints/Parameters	2632 / 16 / 179	3648 / 10 / 244	1483 / 7 / 94
Goodness-of-fit of F^2	1.053	1.223	1.197
Final *R* Indices [*I*>2sigma(*I*)]	R1 = 0.0240	R1 = 0.0402	R1 = 0.0376
	wR2 = 0.0690	wR2 = 0.1068	wR2 = 0.1129
***R* Indices (all data)**	R1 = 0.0252	R1 = 0.0463	R1 = 0.0395
	wR2 = 0.0697	wR2 = 0.1178	wR2 = 0.1257
ρ_{max} and ρ_{min} (e.Å^{-3})	0.473 and -0.623	1.040 and -0.613	0.760 and -0.954

5.3 Crystal structure of: Pyridinium diaquabis(methylenediphosphonato)chromate(III) tetrahydate.[10]

5.3.1 Introduction

The complex pyridinium diaquabis(methylenediphosphonato)chromate(III) tetrahydrate, $(C_5H_6N)[Cr(CH_4O_6P_2)_2(H_2O)_2]\cdot 4H_2O$, was synthesized according to the procedure described in Section 3.7.2.1. Green single crystals were harvested and a summary of the general crystal data is provided for in **Table 5.1**. The numbering scheme and molecular structure of $(C_5H_6N)[Cr(CH_4O_6P_2)_2(H_2O)_2]\cdot 4H_2O$ is presented in **Figure 5.2.** Significant bond distances and non-hydrogen interactions are referred to in **Table 5.2** and important bond angles and torsion angles are reported in **Table 5.3.** The anisotropic displacement parameters, atom coordinates as well as all the bond distances, bond angles and hydrogen coordination are provided in the supplementary data (Appendix A).

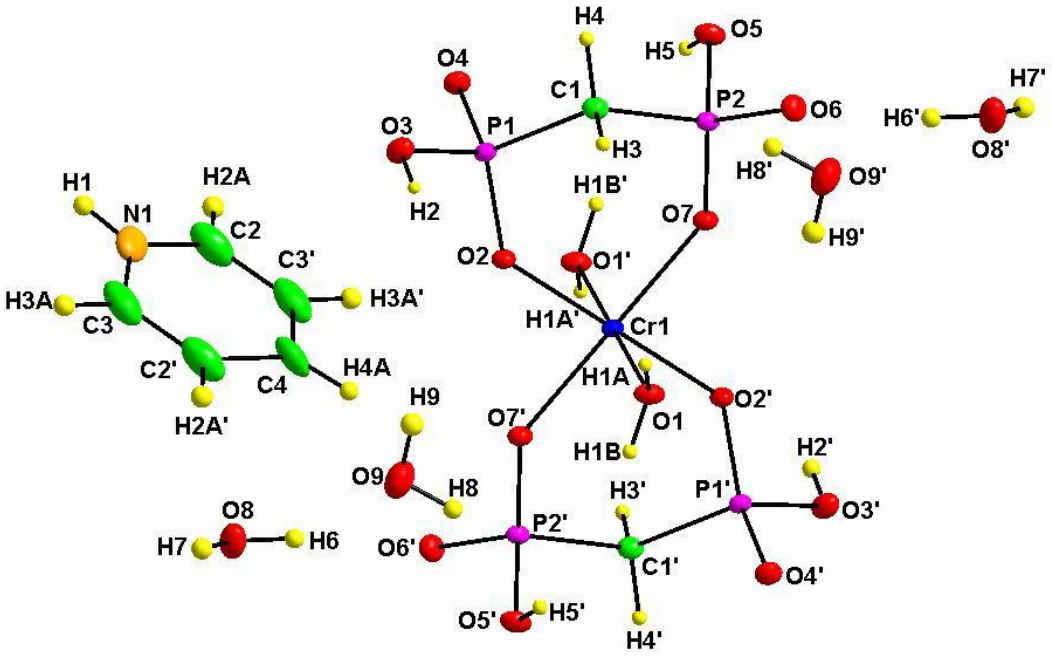

Figure 5.2 Graphical illustration of pyridinium diaquabis(MDP)chromate(III) tetrahydrate displaying the numbering scheme of the atoms in the molecule (ellipsoid probability = 50% except for hydrogen atoms).

[10] K. van der Merwe, H.G. Visser and J.A. Venter. *Acta Cryst.*, 2010, **E66**, m1011-m1012.

Table 5.2: Selected bond lengths and non-hydrogen bonding interactions of pyridinium diaquabis(MDP)chromate(III) tetrahydrate.

Chromium Distances (Å)		**Non-Hydrogen Bonding Interactions to 3,3 Å**	
Cr1-O1	1.991(4)	P1----P2	3.033(3)
Cr1-O2	1.956(4)	O1----O2	2.804(7)
Cr1-O7	1.964(4)	O1----O7	2.777(6)
		O2----O3	2.504(6)
Diphosphonate Distances (Å)		O2----O4	2.561(7)
P1-O3	1.568(4)	O2----O7	2.812(6)
P1-O4	1.512(4)	O3----O4	2.491(5)
P1-C1	1.797(6)	O5----O6	2.479(7)
P2-O5	1.568(4)	O5----O7	2.524(6)
P2-O6	1.499(4)	O6----O7	2.544(7)
P2-C1	1.804(5)		
Pyridinium Distances (Å)			
N1-C2	1.340(5)		
N1-C3	1.360(4)		
C2-C4	1.410(5)		
C3-C4	1.400(5)		

Table 5.3: Selected bond angles and torsion angles of pyridinium diaquabis(MDP)chromate(III) tetrahydrate.

Chromium Angles (°)		**Diphosphonate Angles (°)**	
O1-Cr1-O2	90.51(2)	P1-C1-P2	114.8(3)
O1-Cr1-O7	89.20(2)	O2-P1-O3	108.6(2)
O2-Cr1-O7	91.66(2)	O2-P1-O4	115.5(2)
		O5-P2-O7	109.7(2)
Torsion Angles (°)		O6-P2-O7	114.8(2)
O3-P1-C1-P2	171.1(3)		
O6-P2-C1-P1	-164.9(3)		

5.3.2 Results and Discussion

The title compound, $(C_5H_6N)[Cr(CH_4O_6P_2)_2(H_2O)_2]\cdot 4H_2O$, crystallised in the triclinic crystal system in the $P\bar{1}$ space group. The asymmetric unit is composed of two non-coordinated aqueous molecules, half of a pyridinium cation with the N1 and C4 atoms orientated on a center of symmetry as well as half of a molecule which is made up of one methylene diphosphonate ligand and one aqueous molecule coordinated to a chromium atom which is also orientated on a center of symmetry.

Two methylene diphosphonate anions coordinate to the central metal ion via four oxygen atoms from two bidentate ligands and this leads to the formation of two six-membered rings. Two water molecules complement the distorted octahedral coordination environment of the Cr in a *trans*-position. The crystal structure also contains four uncoordinated water molecules.

Two pairs of phosphonate oxygen atoms (O2, O7, O2', O7') from two equivalent methylene diphosphonate ligands define the equatorial plane, whereas the two equivalent water molecules (O1 and O1') reside in the axial positions.

The chromium aqua (Cr1-O1) distance is 1.991(4) Å, which is longer in comparison to the Cr1-O2 and the Cr1-O7 distances of 1.956(4) Å and 1.964(4) Å respectively, and this correlates closely to literature values.[11,12]

The O1-Cr1-O2, O1-Cr1-O7 and O2-Cr1-O7 angles have respective values of 90.51(2)°, 89.20(2)° and 91.66(2)°, this indicates that the complex has a slightly distorted octahedral geometry.

The pyridinium cation is located on an inversion center resulting in the N1 atom and the C4 atom sharing a position; hence both atoms only have half occupation (50%). The C-C bond lengths which range from 1.400(5) Å to 1.410(5) Å and are longer in comparison to literature values.[13] The N-C bond lengths which vary from 1.340(5) Å

[11] A.E. Ceniceros-Gómez, N. Barba-Behrens, M.E. Quiroz-Castro, S. Bernès, H. Nöth and S.E. Castillo-Blum. *Polyhedron*, 2000, **19**, 1821-1827.

[12] L. Tang, Z. Wang, J. Chai and J. Wang. *Journal of Chemical Crystallography*, 2002, **32**, 261-265.

[13] M.E. Glaoui, R. Kefi, O. Amri, E. Jeanneau and C.B. Nasr. *Acta Cryst.*, 2008, **E64**, o2204.

to 1.360(4) Å respectively are slightly longer compared to literature values.[13] The difference in values from literature could be explained by the presence of the 50% positional disorder.

There are two types of P-O bonds, the P-OH bond with distances of 1.568(4) Å for P1-O3 and 1.568(4) Å for P2-O5 and the P=O bond with distances of 1.512(4) Å for P1-O4 and 1.499(4) Å for P2-O6.[14,15]

The presence of a double bond between the phosphorous and the oxygen also influences the bond angles. The O-P=O angles are 115.5(2)° for O2-P1-O4 and 114.8(2)° for O6-P2-O7 while the O-P-O angles are 108.6(2)° for O2-P1-O3 and 109.7(2)° for O5-P2-O7. The O-P=O angles are larger in comparison to the O-P-O angles and this confirms that there is a partial double-bond present at O4 and O6; which corresponds to results found for related molecules.[16,17,18,19]

In order to investigate the bent nature of the P-C-P ligand a plane was constructed through C1, P1, P2, O7, Cr1, O2 as well as through C1', P1', P2', O7', O2' as displayed in **Figure 5.3.** It is clear to ascertain that P1-O4 and P2-O6 have a staggered conformation and this also applies to P1-O3 and P2-O5.

[14] V.V. Bon, A.V. Dudko, A.N. Kozachkova, V.I. Pekhnyo and N.V. Tsaryk. *Acta Crystallographica Section E*, 2010, **E66**, m537-m538.

[15] S.S. Jurisson, J.J. Benedict, R.C. Elder, R. Whittle and E. Deutsch. *Inorganic Chemistry*, 1983, **22**, 1332-1338.

[16] V.M. Coiro and D. Lamba. *Acta Cryst.*, 1989, **C45**, 446-448.

[17] D. Vega, R. Baggio and M.T. Garland. *Acta Cryst.*, 1996, **C52**, 2198-2201.

[18] D. Vega, R. Baggio and O. Piro. *Acta Cryst.*, 1998, **C54**, 324-327.

[19] E. Freire, D.R. Vega and R. Biaggo. *Acta Cryst.*, 2010, **C66**, m166-m170.

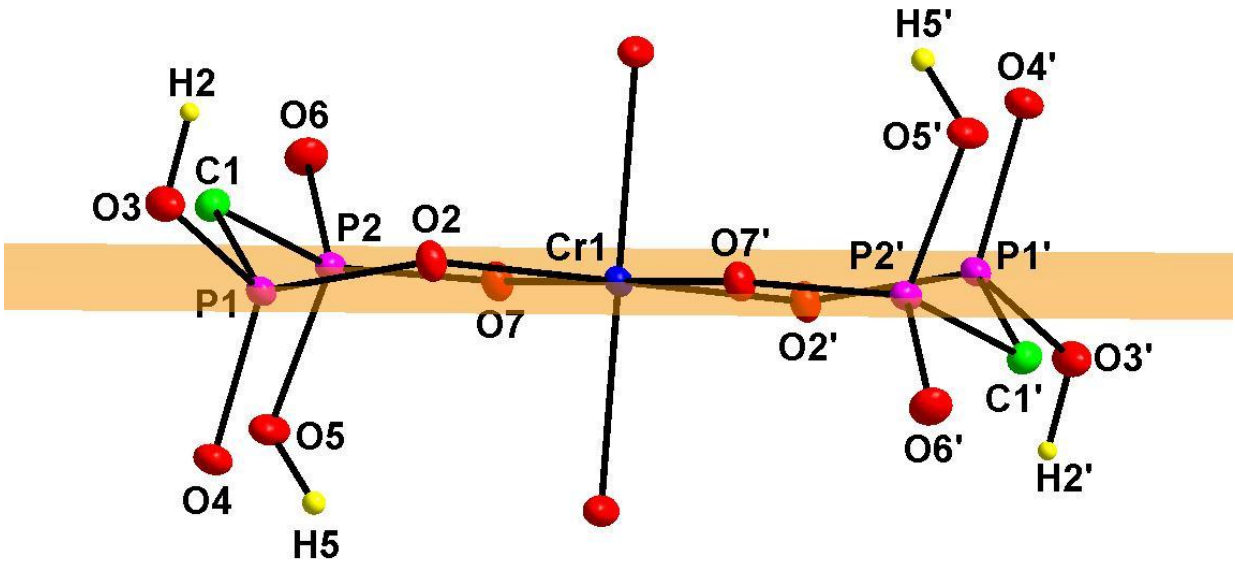

Figure 5.3 Partial structure of pyridinium diaquabis(MDP)chromate(III) tetrahydrate displaying the configuration of the P-O and P=O atoms as well as the orientation of the atoms on the plane (water molecules, certain hydrogens and the cation have been removed for clarity).

P1-O3 and P2-O6 are orientated on the same side of the plane, pointing upwards whilst P1-O4 and P2-O5 are directed on the opposite side of the plane, pointing downwards.

C1 has a distance of 0.604(6) Å and O2 a distance of 0.234(5) Å from the plane. Both lie on the same side and deviate the most from the plane. P1 and P2 lie on the plane and O7 are orientated slightly below the plane with a distance of 0.100(5) Å from the plane.

Table 5.4: Selected distances between specific atoms and the horizontal plane constructed through C1, P1, P2, O7, Cr1, O2 as well as through C1', P1', P2', O7', O2'.

Atom	Distance Å	Atom	Distance Å
O2	-0.234(5)	O2'	0.234(5)
P1	0.045(2)	P1'	-0.045(2)
C1	-0.604(6)	C1'	0.604(6)
P2	0.009(2)	P2'	-0.009(2)
O7	0.100(5)	O7'	-0.100(5)
Cr1	0.000(3)		

Bisphosphonates can be differentiated from pyrophosphates as they have a P-C-P bond which is biologically resistant in comparison to the P-O-P bridge found in

pyrophosphates.[20] The P-C-P bond is an essential component for a potential drug as there is no known enzyme which is able to break-up the P-C-P bond.[21]

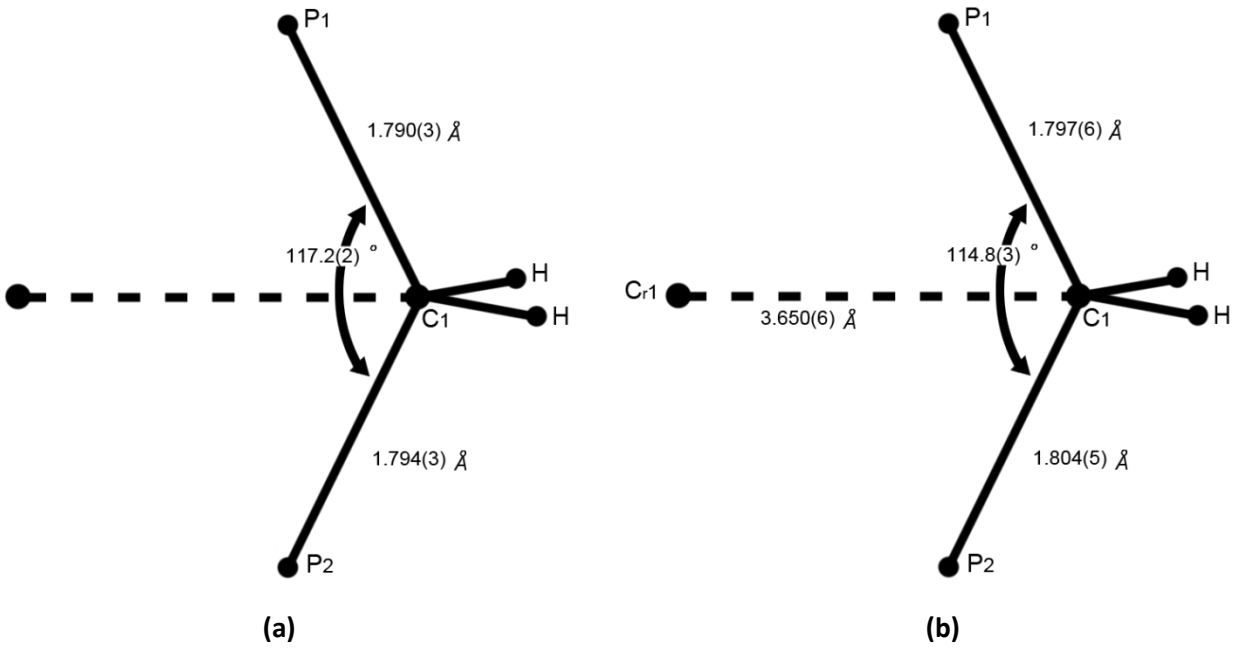

Figure 5.4 Graphical comparison of the P-C-P bond in (a) methylene diphosphonate and (b) pyridinium diaquabis(MDP)chromate(III) tetrahydrate.

Figure 5.4(a) displays the P-C-P bond present in the MDP ligand which is not coordinated to a metal.[22] By coordinating chromium to the MDP ligand a few deviations are notable as depicted in **Figure 5.4(b)**. Although not significantly, the P-C bond lengths in **Figure 5.4(b)** appear to be slightly elongated while the P-C-P angle is 3° smaller in comparison to that of **Figure 5.4(a)**. A reason for the reduction in the P-C-P angle could be due to the ring strain.

The phosphonate-carbon-phosphonate backbone is present in all bisphosphonates and this core structure allows the bisphosphonates to bond tightly to the bone material. The two phosphonate groups are referred to as the “bone hooks” and are

[20] J.B. Catterall and T.E. Cawston. *Arthritis Research and Therapy*, 2003, **5**, 12-24.

[21] T.P. Haromy, W.B. Knight, D. Dunaway-Mariano and M. Sundaralingam. *Inorganic Chemistry*, 1984, **23**, 2412-2415.

[22] D. DeLaMatter, J.J. McCullough and C. Calvo. *The Journal of Physical Chemistry*, 1973, **77**, 1146-1148.

vital because they are not only responsible for the binding to the hydroxyapatite but also for the biochemical mechanism of action.[23]

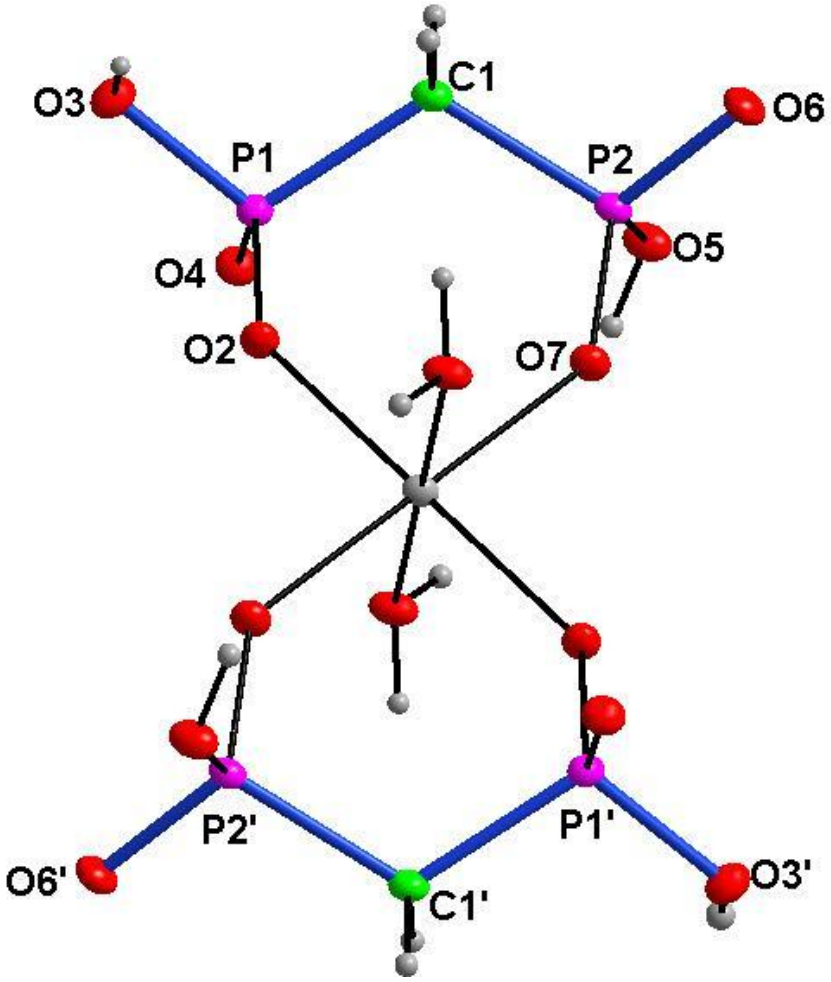

Figure 5.5 Molecular diagram of pyridinium diaquabis(MDP)chromate(III) tetrahydrate displaying the "W" configuration (cation and water molecules have been omitted for clarity).

The orientation of the $-PO_3$ group with regard to the P-C-P plane is a significant feature of the MDP ligand. The term "W" configuration is used when O3-P1-C1-P2-O6 forms a planar "W" which can easily be observed in **Figure 5.5**. Not only is the "W" shape significant for the biological activity of the bisphosphonate,[24] but it allows the MDP ligand to be doubly bidentate,[1] with O2 and O7 on the one side of the "W" coordinated to the metal center while there is a

[23] L. Wilder, K.A. Jaeggi, M. Glatt, K. Müller, R. Bachmann, M. Bisping, A. Born, R. Cortesi, G. Guiglia, H. Jeker, R. Klein, U. Ramseier, J. Schmid, G. Schreiber, Y. Seltenmeyer and J.R. Green. *Journal of Medical Chemistry*, 2002, **45**, 3721-3738.

[24] D. Fernández, D. Vega and J.A. Ellena. *Acta Cryst.*, 2003, **C59**, o289-o292.

possibility for O4 and O5 to coordinate to the metal center on the other side of the "W". The O-P-C-P torsion angles which characterize the "W" shape are 171.1(3)° and -164.9(3)° respectively.

Table 5.5: Hydrogen bond lengths and angles for pyridinium diaquabis(MDP)chromate(III) tetrahydrate [Å and °].

D-H…A	d(D-H)	D(H…A)	D(D…A)	<(DHA)
N1-H1…O9^{iii}	0.86	2.32	3.030(5)	140.5
O1-H1A…O6^{ii}	0.80(6)	1.83(6)	2.634(6)	176(9)
O1-H1B…O4^{iv}	0.83(6)	1.87(6)	2.704(6)	177(9)
O3-H2…O8^{v}	0.82	1.83	2.629(6)	162.9
C4-H4A…O9^{iii}	0.93	2.16	2.930(6)	140.1
O5-H5…O4^{iii}	0.83(5)	1.80(5)	2.619(6)	175(1)
O8-H6…O6^{vi}	0.83(6)	1.86(6)	2.687(6)	171(9)
O8-H7…O9^{i}	0.85(7)	1.94(8)	2.748(7)	158(1)
O9-H8…O4^{i}	0.83(6)	2.00(6)	2.833(6)	179(1)
O9-H9…O8^{vii}	0.84(7)	1.99(7)	2.820(7)	174(1)
C1-H3…O6^{ii}	0.97	2.49	3.346(7)	146.8

Symmetry transformations used to generate equivalent atoms:

(i) x, y, z; (ii) –x+1, -y+2, -z+1; (iii) –x, -y+1, -z+1; (iv) x+1, y, z; (v) –x+1, -y+2, -z+2;

(vi) x, y, z+1; (vii) –x, -y+2, -z+2.

The complete list of all the hydrogen bond distances and angles is given in **Table 5.5**. All the intermolecular hydrogen bonding interactions are shown in **Figure 5.6(a)** and **(b)**.

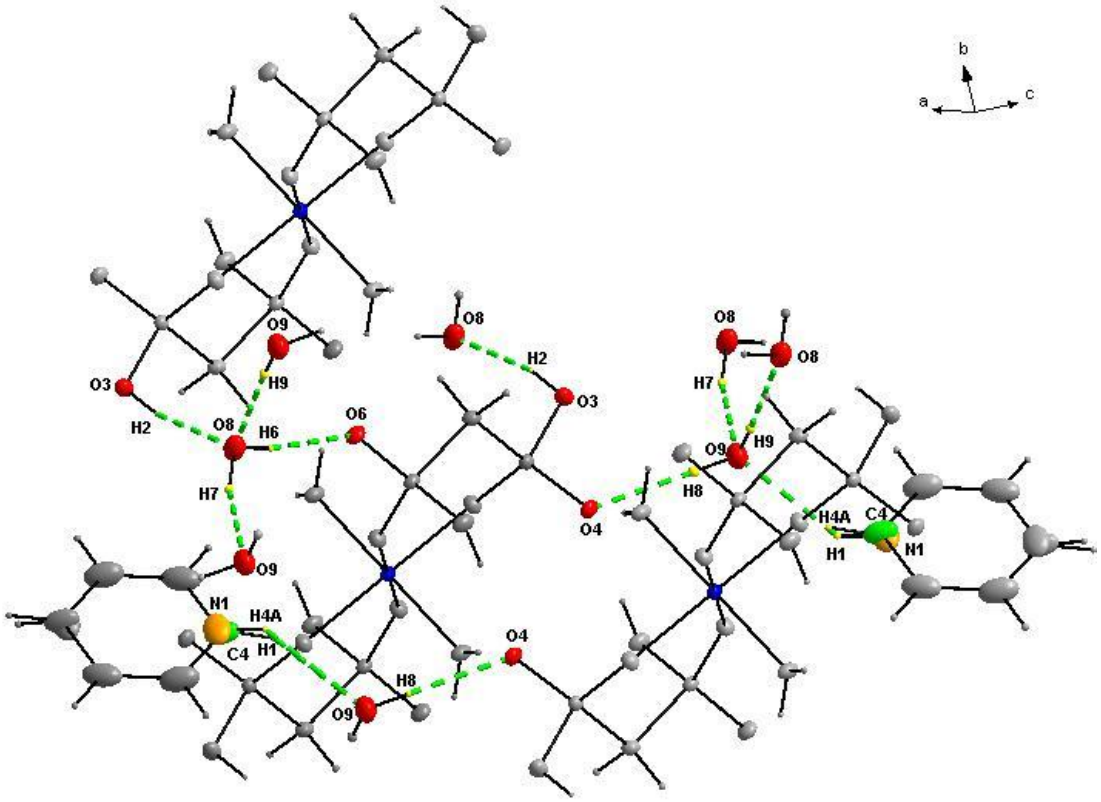

(a)

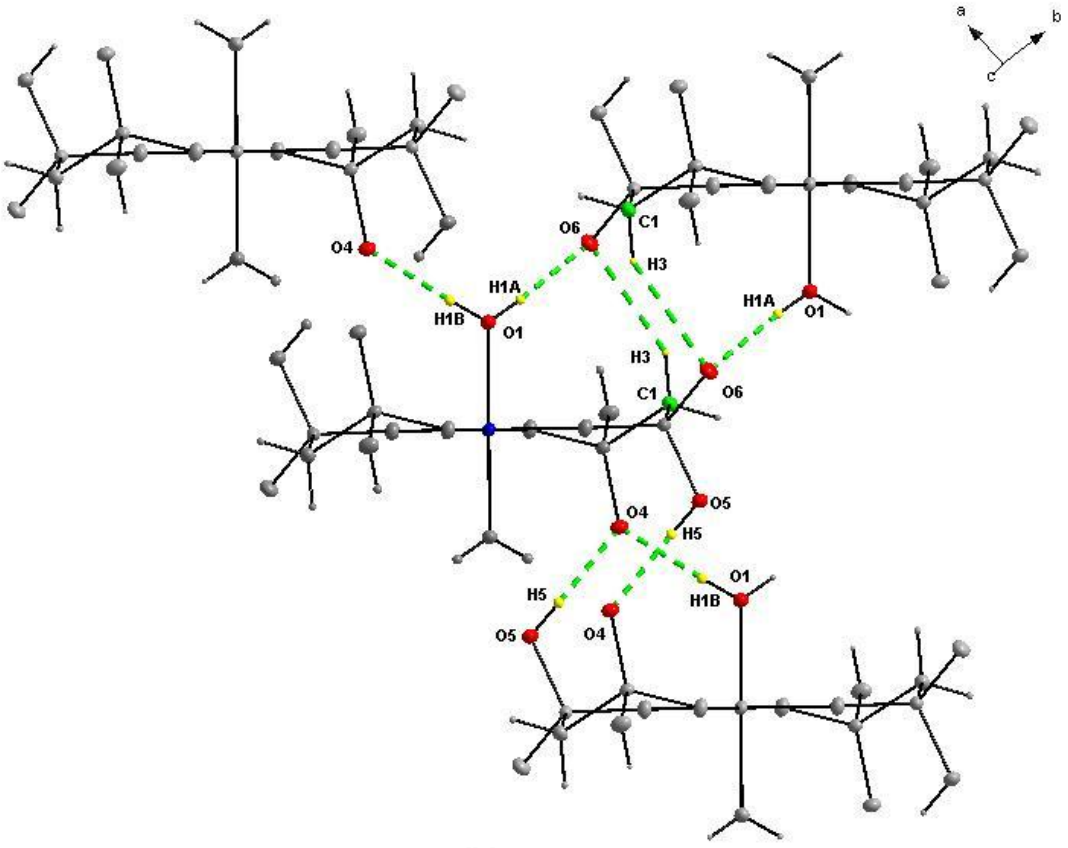

(b)

Figure 5.6(a) and (b) A breakdown of the all the intermolecular hydrogen bonding of pyridinium diaquabis(MDP)chromate(III) tetrahydrate.

Water plays an essential role in the structure. The water molecules that are trapped between layers, influences the terminal oxygen atoms which are coordinated to the phosphorous atoms via hydrogen bonds and this leads to a stable crystal structure. An elaborate amount of hydrogen bonding is observed among the coordinated and lattice water molecules together with the phosphonate and hydroxyl oxygen atoms. Intermolecular hydrogen bonding is also noted on the disordered cation. In **Figure 5.6(a)** and **(b)** the two oxygen atoms (O4 and O6) within the phosphonate groups of the one MDP ligand behave like hydrogen-bond acceptors towards a bifurcated hydrogen bond which originates from the coordinated water molecule. Metal aqua-ions can act as hydrogen bond donors with limited acceptor properties. Numerous novel complexes with metal aqua-ions have been reported.[25]

The molecules are linked through O-H···O and N-H···O hydrogen-bonding interactions resulting in a 3-D supramolecular network.[26]

The $-P(O)_2(OH)-$ group has the ability to act as a hydrogen-bond donor as well as an acceptor.[27] All the O-H and N-H groups act as hydrogen-bond donors in the crystal structure.[27] The acceptors are the oxygen atoms of the anions. The removal of a proton causes hydrogen aggregations from stronger P-O-H···O-P (P2-O5-H5···O4-P1) to weaker C-H···O (C1-H3···O6) hydrogen bonds.[28]

The hydrogen bonding interactions present appear to enhance the solid state ordering of the compound. In this P-C-P compound no [29] intramolecular hydrogen bonding exists despite the extensive amount of intramolecular O···O interactions which are 2.479(7)-2.804(7) Å (from **Table 5.2)** and appear to further stabilise the complex.

[25] H. Xu and F. Wang. *Acta Cryst.*, 2008, **E64**, m493.

[26] J.D. Wuest. *Chemical Communications*, 2005, **47**, 5830-5837.

[27] Z. Yuan and W. Clegg. *Acta Cryst.*, 2005, **E61**, o2635-o2637.

[28] M. Li, J. Xiang, S. Chen, S. Wu, L. Yuan, H. Li, H. He and J. Sun. *Journal of Coordination Chemistry*, 2008, **61**, 372-383.

[29] S.W. Peterson, E. Gebert, A.H. Reis, M.E. Druyan, G.W. Mason and D.F. Peppard. *The Journal of Physical Chemistry*, 1977, **81**, 466-471.

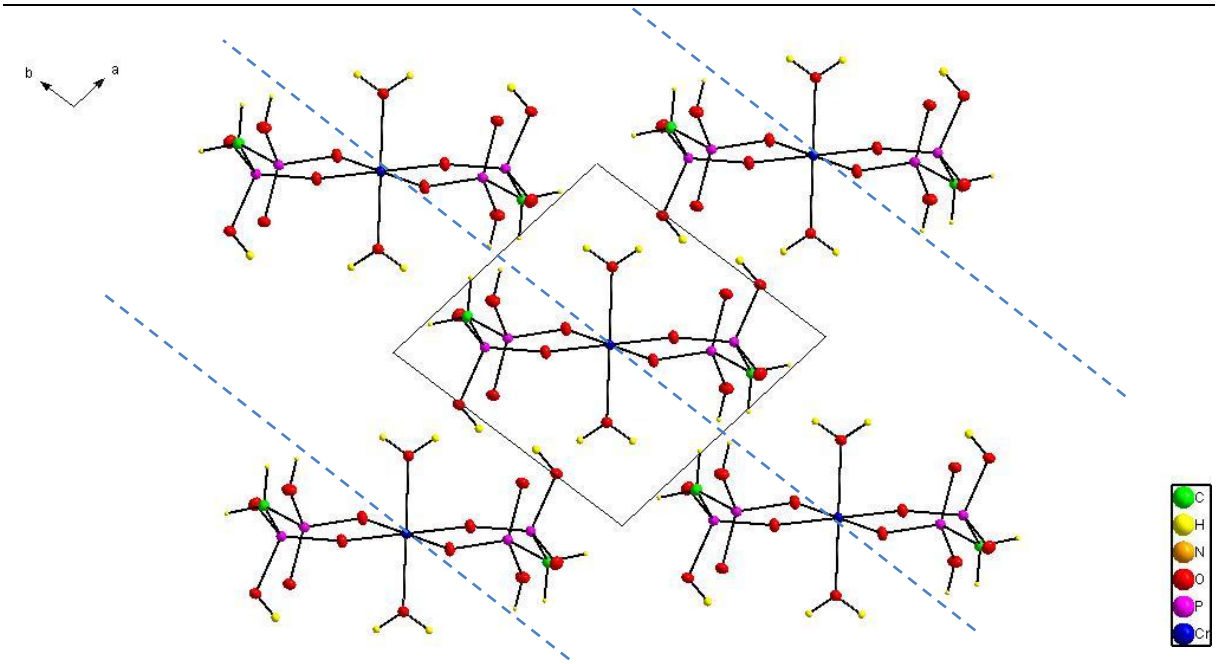

Figure 5.7 The crystal packing of pyridinium diaquabis(MDP)chromate(III) tetrahydrate, the unit is viewed along the c-axis (water molecules and pyridinium cation have been omitted for clarity).

Figure 5.7 displays how the molecules orientate themselves in parallel layers. The blue dotted line indicates that the molecules also appear to pack diagonally.

5.4 Crystal structure of: Potassium diaquabis(methylenediphosphonato)cobaltate(III).[30]

5.4.1 Introduction

The synthesis of potassium diaquabis(methylenediphosphonato)cobaltate(III), $K[Co(CH_4O_6P_2)_2(H_2O)_2]$, was according to the procedure described in Section 3.7.2.2 from which pink crystals were harvested. A summary of the general crystal data is given in **Table 5.1**. The numbering scheme and molecular structure of $K[Co(CH_4O_6P_2)_2(H_2O)_2]$ is represented in **Figure 5.8.** Significant bond distances and non-hydrogen interactions are referred to in **Table 5.6** and important bond angles and torsion angles are reported in **Table 5.7.** The anisotropic displacement parameters, atom coordinates as well as all the bond distances, bond angles and hydrogen coordination are provided as supplementary data (Appendix A).

[30] H.G. Visser, J.A. Venter and K.A. van der Merwe. *Acta Cryst*., 2010, **E66**, m159.

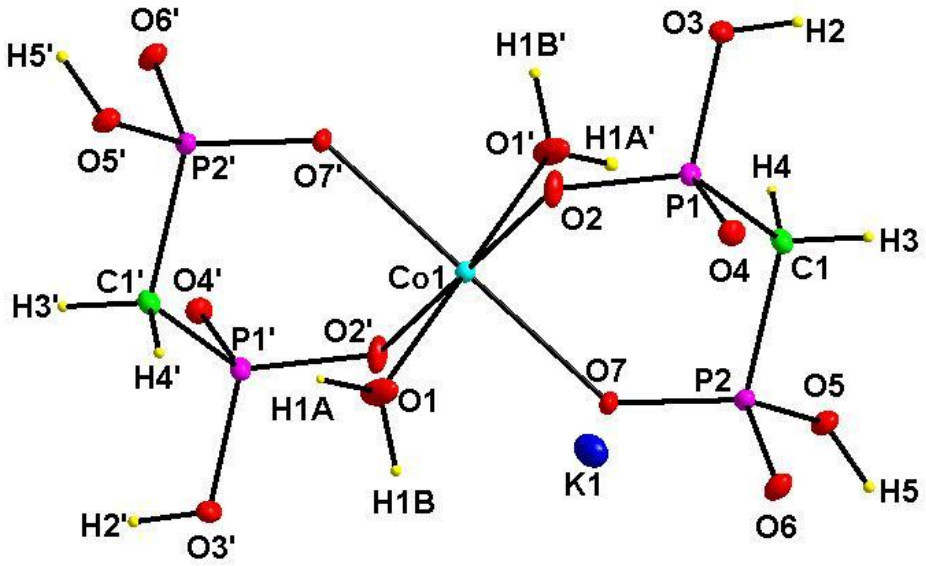

Figure 5.8 Molecular diagram of potassium diaquabis(MDP)cobaltate(III) displaying the numbering scheme of the atoms in the Co1 molecule (ellipsoid probability = 50% except for hydrogen atoms).

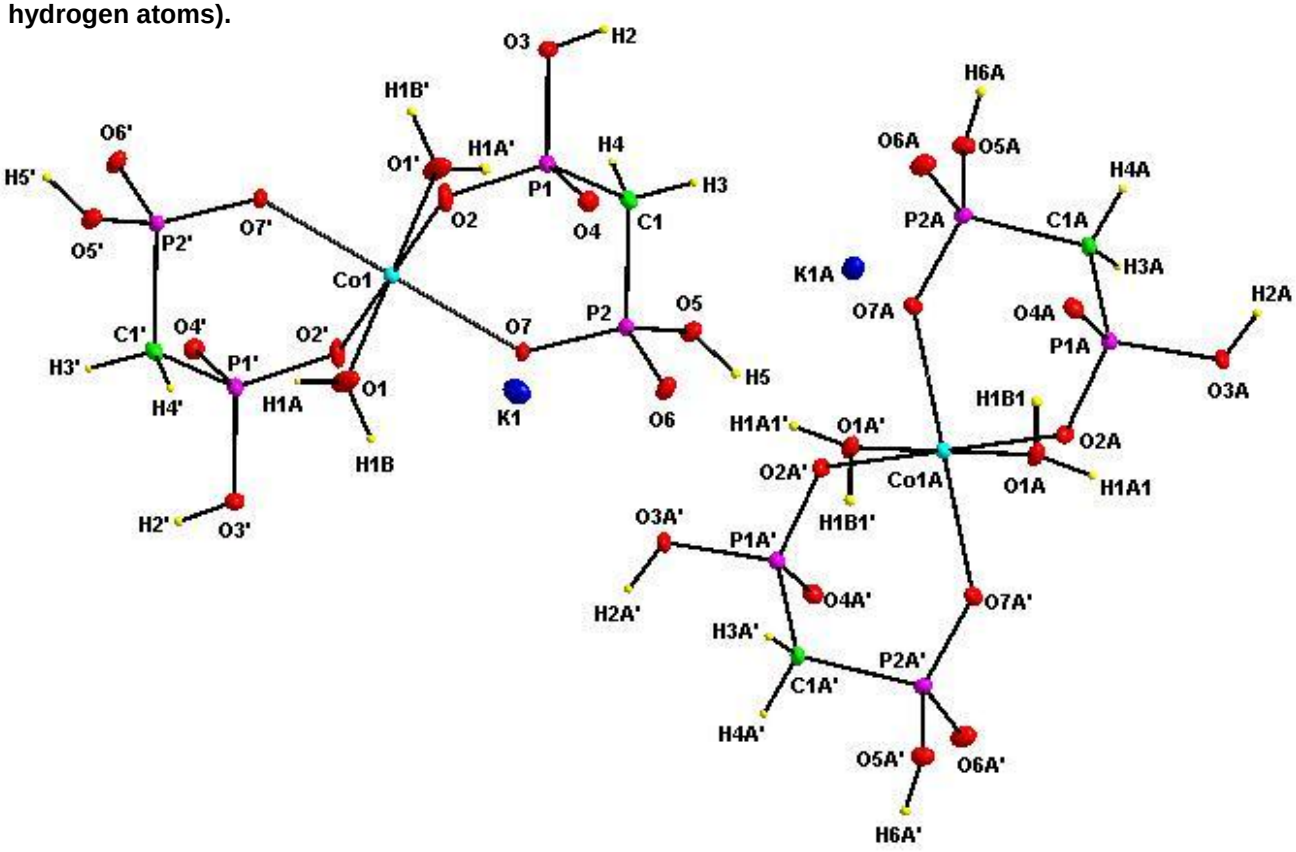

Figure 5.9 Graphical illustration of potassium diaquabis(MDP)cobaltate(III) displaying the numbering scheme of the atoms in the Co1 and the Co1A molecules (ellipsoid probability = 50% except for hydrogen atoms).

Table 5.6: Selected bond lengths and non-hydrogen bonding interactions of potassium diaquabis(MDP)cobaltate(III).

Cobalt Distances (Å)			
Co1-O1	2.083(3)	Co1A-O1A	2.126(3)
Co1-O2	2.065(3)	Co1A-O2A	2.132(3)
Co1-O7	2.117(3)	Co1A-O7A	2.052(3)
Diphosphonate Distances (Å)			
P1-O3	1.575(3)	P1A-O3A	1.575(3)
P1-O4	1.522(3)	P1A-O4A	1.517(3)
P1-C1	1.803(4)	P1A-C1A	1.794(4)
P2-O5	1.581(3)	P2A-O5A	1.581(3)
P2-O6	1.502(3)	P2A-O6A	1.501(3)
P2-C1	1.807(4)	P2A-C1A	1.806(4)
Non-Hydrogen Bonding Interactions to 3,3 Å			
P1----P2	3.047(9)	P1A----P2A	3.044(3)
O1----O2	2.899(4)	O1A----O2A	3.033(4)
O1----O7	2.962(4)	O1A----O7A	3.063(4)
O2----O3	2.498(5)	O2A----O3A	2.457(5)
O2----O4	2.531(2)	O2A----O4A	2.545(2)
O2----O7	3.043(4)	O2A----O7A	3.114(9)
O3----O4	2.540(2)	O3A----O4A	2.549(8)
O5----O6	2.562(2)	O5A----O6A	2.540(7)
O5----O7	2.503(5)	O5A----O7A	2.438(4)
O6----O7	2.548(1)	O6A----O7A	2.577(6)

Table 5.7: Selected bond angles and torsion angles of potassium diaquabis(MDP)cobaltate(III).

Cobalt Angles (°)			
O1-Co1-O2	88.66(1)	O1A-Co1A-O2A	90.86(1)
O1-Co1-O7	89.69(1)	O1A-Co1A-O7A	94.29(1)
O2-Co1-O7	93.34(1)	O2A-Co1A-O7A	96.22(1)
Diphosphonate Angles (°)			
P1-C1-P2	115.20(2)	P1A-C1A-P2A	115.50(2)
O2-P1-O3	108.30(2)	O2A-P1A-O3A	105.61(2)
O2-P1-O4	113.35(2)	O2A-P1A-O4A	114.51(2)
O5-P2-O7	107.38(2)	O5A-P2A-O7A	104.53(2)
O6-P2-O7	114.64(2)	O6A-P2A-O7A	118.24(2)
Torsion Angles (°)			
O3-P1-C1-P2	-169.8(2)	O3A-P1A-C1A-P2A	176.6(2)
O5-P2-C1-P1	171.8(2)	O5A-P2A-C1A-P1A	-170.1(2)

5.4.2 Results and Discussion

The title complex, $K[Co(CH_4O_6P_2)_2(H_2O)_2]$, crystallised in the triclinic space group, $P\bar{1}$. The asymmetric unit is composed of two potassium cations as well as two halves of a molecule each comprising of one methylene diphosphonate ligand and one aqueous molecule coordinated to a cobalt atom which is orientated on a center of symmetry. The two complete molecules are generated by inversion symmetry with each molecule comprised of a slightly distorted $Co^{III}O_6$ octahedron defined by two bidentate methylene diphosphonate ligands and two water molecules. The water molecules are orientated in a *trans* configuration.

Two pairs of phosphonate oxygen atoms, (O2, O7, O2', O7' for Co1) and (O2A, O7A, O2A', O7A' for Co1A) from two equivalent methylene diphosphonate ligands, define the equatorial plane, whereas the two equivalent water molecules, (O1 and O1' for Co1) and (O1A and O1A' for Co1A) reside in the axial positions.

The axial distances (the aqua oxygens) for Co1/A-O1/A range from 2.083(3) Å to 2.126(3) Å. The Co-O distances for the equatorial bonds for Co1/A-O2/A range from

2.065(3) Å to 2.132(3) Å and for Co1/A-O7/A are from 2.052(3) Å to 2.117(3) Å.[31,32,33]

The bite angles for the Co1and Co1A atoms range from 88.66(1)° to 96.22(1)°, therefore the two molecules have a slightly distorted octahedral geometry.

Each MDP ligand contains two phosphonate groups made up of the P-OH and the P=O bonds. The P-OH bond distances for the two molecules are almost the same with a distance of 1.575(3) Å for P1-O3 and 1.581(3) Å for P2-O5.[19,34] The P=O bond distances for the two molecules range from 1.517(3) Å to 1.522(3) Å for P1/A-O4/A[35] but for P2/A-O6/A the bond distances are 1.502(3) Å and 1.501(3) Å respectively.[36] All these values compare well with similar structures.[19]

The P-OH and P=O bonds differ slightly from literature, but this could be a result of the two molecules interacting with one another or because they are in close proximity with regards to one another and this affects not only their bond distances but also the angles. One distinguishing aspect of the P-OH distances are that they are always notably longer than the P=O distances.

The O-P-O angles for the two molecules range from 105.61(2)° to 108.30(2)° for O2/A-P1/A-O3/A and 104.53(2)°-107.38(2)° for O5/A-P2/A-O7/A, these values correlate to related structures.[17,18] The O-P=O angles for O2/A-P1/A-O4/A vary from 113.35(2)° to 114.51(2)° and for O6/A-P2/A-O7/A they range between 114.64(2)° and 118.24(2)°, which correspond well to similar compounds.[17,18] The O-P=O angles are more sizable in comparison to the O-P-O angles, this confirms the presence of a partial double-bond at O4/O4A and O6/O6A; which corresponds to related molecules.[16,17,18,19]

In order to investigate the bent nature of the P-C-P ligand a plane can be constructed through C1, P1, P2, O7, Co1, O2 as well as through C1', P1', P2', O7',

[31] P. Yin, X. Wang, S. Gao and L. Zheng. *Journal of Solid State Chemistry*, 2005, **178**, 1049-1053.

[32] Y. Gong, W. Tang, W. Hou, Z. Zha and C. Hu. *Inorganic Chemistry*, 2006, **45**, 4987-4995

[33] P. Yin, S. Gao, L. Zheng and X. Xin. *Chem. Mater.*, 2003, **15**, 3233-3236.

[34] E. Freire and D.R. Vega. *Acta Cryst.,* 2009, **E65**, m1428-m1429.

[35] Z. Zhang, S. Gao and L. Zheng. *Dalton Transactions*, 2007, 4681-4684.

[36] Z. Zhang, R. Li and Y. Zhang. *Acta Cryst.*, 2009, **E65**, m1701-m1702.

O2' as displayed in **Figure 5.10.** It is clear to observe that P1-O4 and P2-O6 have an eclipsed conformation and this also applies to P1-O3 and P2-O5. P1-O3 and P2-O5 are orientated on the same side of the plane, pointing downwards. P1-O4 and P2-O6 are directed on the opposite side of the plane, pointing upwards. The same holds for the Co1A molecule.

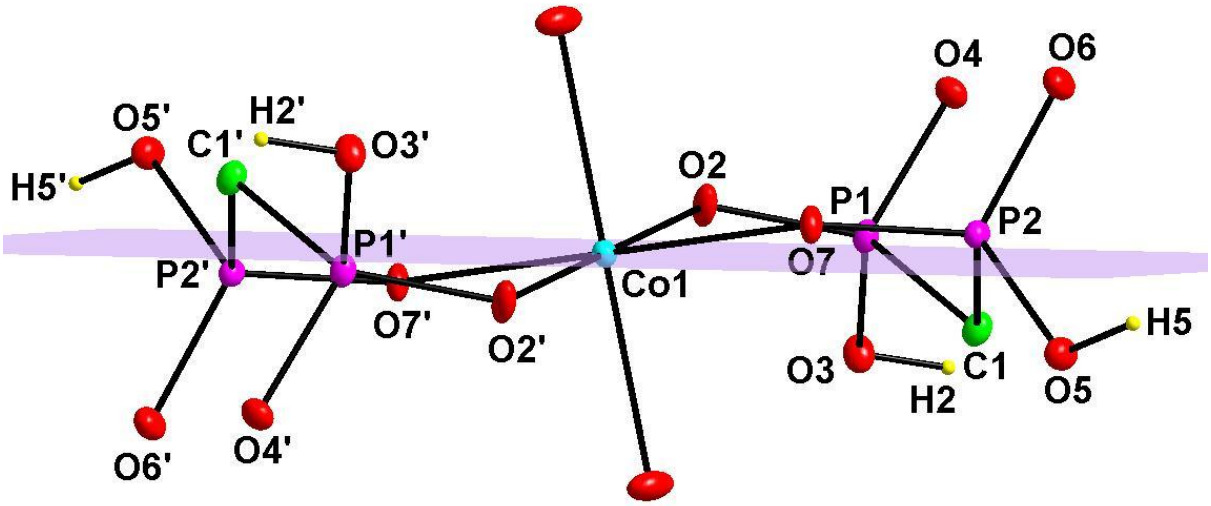

Figure 5.10 Partial structure of potassium diaquabis(MDP)cobaltate(III) displaying the configuration of the P-O and P=O atoms as well as the orientation of the atoms on the plane (certain hydrogens and the cation have been removed for clarity).

C1 has a distance of 0.618(4) Å with regard to the plane and it deviates the most from the plane. O2 (0.403(8) Å), P1 (0.149(7) Å), P2 (0.239(4) Å) and O7 (0.305(2) Å) are orientated on the same side of the plane. O7, P2, C1, P1, O2, Co1, O2', P1', C1', P2', O7' forms a type of a chair conformation and C1 and C1' are staggered with regard to one another. The same is noted for the Co1A molecule.

Table 5.8: Selected distances between specific atoms and the horizontal plane constructed through C1, P1, P2, O7, Co1, O2 as well as through C1', P1', P2', O7', O2'.

Atom	Distance, Å	Atom	Distance, Å
O2	0.403(8)	O2'	-0.403(8)
P1	0.149(7)	P1'	-0.149(7)
C1	-0.618(4)	C1'	0.618(4)
P2	0.239(4)	P2'	-0.239(4)
O7	0.305(2)	O7'	-0.305(2)
Co1	0.000		

The relevance of the P-C-P bond is explained in detail in Paragraph **5.3.2**. **Figure 5.11(a)** depicts the P-C-P bond for an uncoordinated MDP ligand.[22] By coordinating cobalt to the MDP ligand a few deviations are notable as displayed in **Figure 5.11(b)** and **Figure 5.11(c)**. The P-C bond lengths for **Figure 5.11(b)** and **Figure 5.11(c)** are slightly elongated compared to **Figure 5.11(a).**

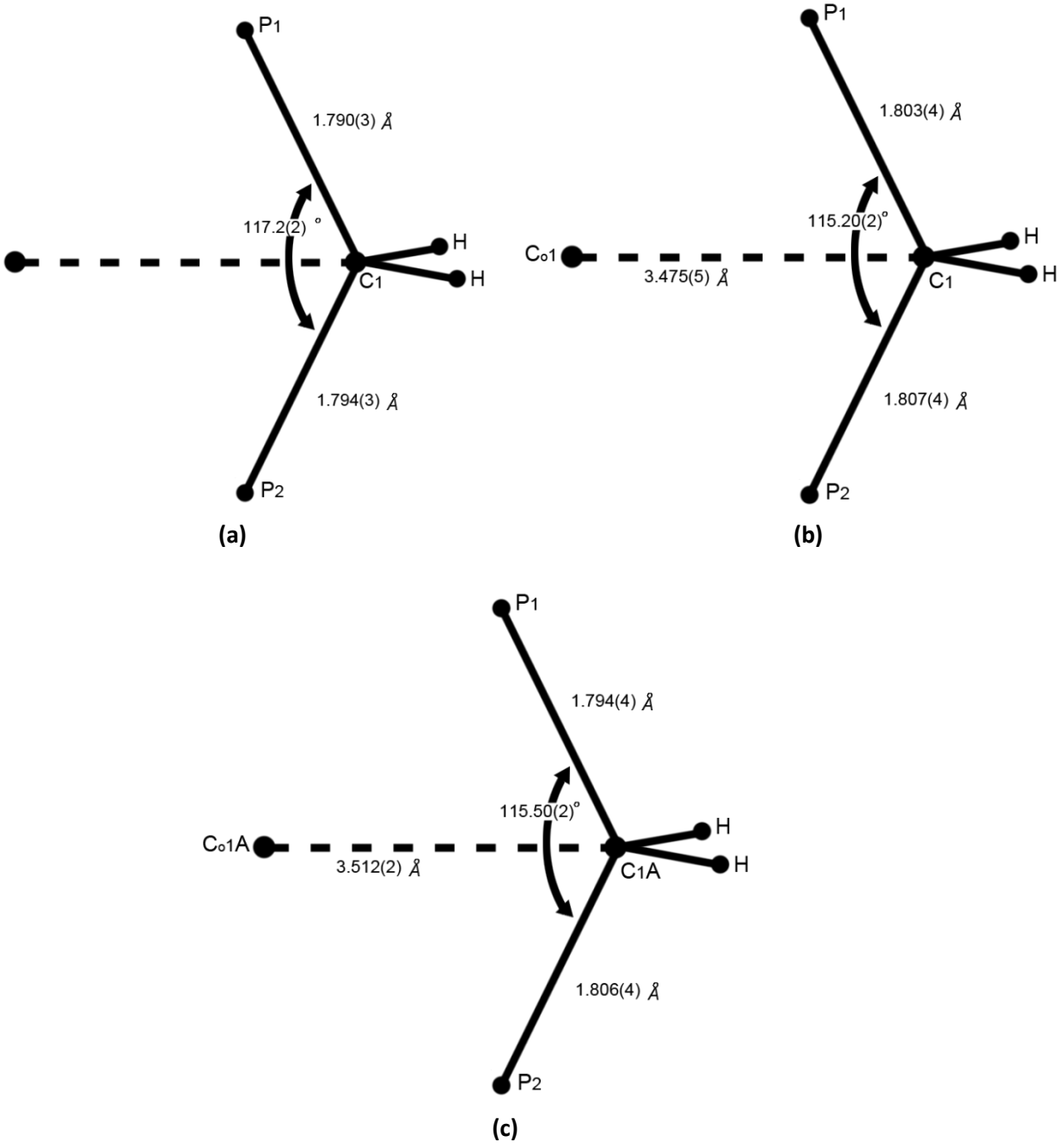

Figure 5.11 Graphical comparison of the P-C-P bond in (a) methylene diphosphonate, (b) potassium diaquabis(MDP)cobaltate(III) of the Co1 molecule and (c) potassium diaquabis(MDP)cobaltate(III) of the Co1A molecule.

The P-C-P angle for both the Co1 and the Co1A molecules reduced by 2° in comparison to **Figure 5.11(a)**. A reason for the reduction in the P-C-P angle could be because of ring strain.

The Co-C distance for Co1 is 3.475(5) Å and for Co1A is 3.512(2) Å. These values compare well with one another but they are slightly shorter in comparison to a value of 3.63 Å in literature.[21] The primary reason for this slight decrease in Co-C distance is because unlike in literature where there was only one MDP ligand coordinated to the cobalt metal center,[21] in our case there are two MDP ligands bonded to the cobalt metal center. Another reason could be that when the Co(II) coordinated to the MDP ligands the cobalt oxidizes from Co(II) to Co(III). The Co1 and Co1A are so close in proximity this could also have an effect on the Co-C distances and P-C-P angles.

The significance of the "W" configuration is explained in detail in Paragraph **5.3.2**. The term "W" configuration is applied when O3-P1-C1-P2-O6 forms a planar "W" which can easily be observed in **Figure 5.12**.

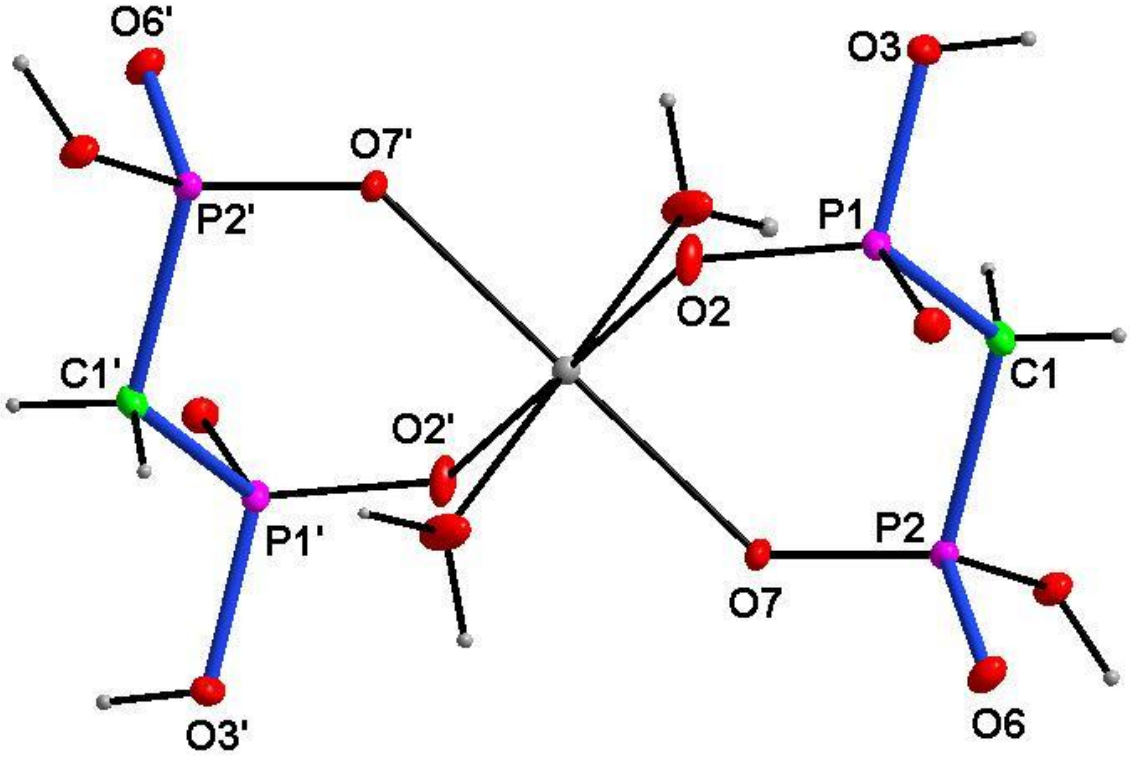

Figure 5.12 Molecular diagram of potassium diaquabis(MDP)cobaltate(III) for the Co1 molecule displaying the "W" configuration (the cation has been omitted for clarity).

The “W” shape enables the MDP ligand to be doubly bidentate,[1] with O2 and O7 on the one side of the “W” coordinated to the metal center while there is a possibility for O4 and O5 to coordinate to the metal center on the other side of the “W”. The O-P-C-P torsion angles which characterize the “W” shape for Co1 are -169.8(2)° for O3-P1-C1-P2 and 171.8(2)° for O5-P2-C1-P1 and for Co1A they are 176.6(2)° for O3A-P1A-C1A-P2A and -170.1(2)° for O5A-P2A-C1A-P1A.

Table 5.9: Hydrogen bonds for potassium diaquabis(MDP)cobaltate(III) [Å and °].

D-H…A	d(D-H)	D(H…A)	D(D…A)	<(DHA)
O1A-H1A1…O6^{iv}	0.84(2)	1.84(2)	2.679(4)	175(7)
O1-H1A…O4^{ii}	0.87(2)	1.84(2)	2.687(4)	168(5)
O1-H1B…O6A^{iii}	0.87(2)	1.83(3)	2.676(4)	164(6)
O3-H2…O4^{vi}	0.85(2)	1.73(2)	2.559(4)	170(7)
O1A-H1B1…O4A^{v}	0.85(2)	1.90(2)	2.737(4)	169(7)
O3A-H2A…O4A^{vii}	0.85(2)	1.71(2)	2.567(4)	179(7)
O5-H5…O2A^{iv}	0.84(2)	1.78(2)	2.617(4)	172(7)
O5A-H6A…O7^{i}	0.83(2)	1.83(3)	2.633(4)	161(7)

Symmetry transformations used to generate equivalent atoms:

(i) x, y+1, z; (ii) –x+2, -y-1, -z+2; (iii) x, y-1, z; (iv) -x+1, -y, -z+1; (v) x-1, y, z;

(vi) –x+2, -y, -z+2; (vii) –x+2, -y+1, -z+1.

The complete list of all the hydrogen bond distances and angles is given in **Table 5.9**. All the intermolecular hydrogen bonding interactions are observed in **Figure 5.13(a)** and **(b)**.

Water plays an important role in the structure; this was explained in detail in Paragraph **5.3.2**. An extensive amount of hydrogen bonding is observed among the coordinated as well as the phosphonate and hydroxyl oxygen atoms. The molecules are linked through O-H···O hydrogen-bonding interactions resulting in a 3-D supramolecular network. In **Figure 5.13(a)** there is hydrogen-bonding present between both molecules at H1A1···O6 and in **Figure 5.13(b)** at H5···O2A.

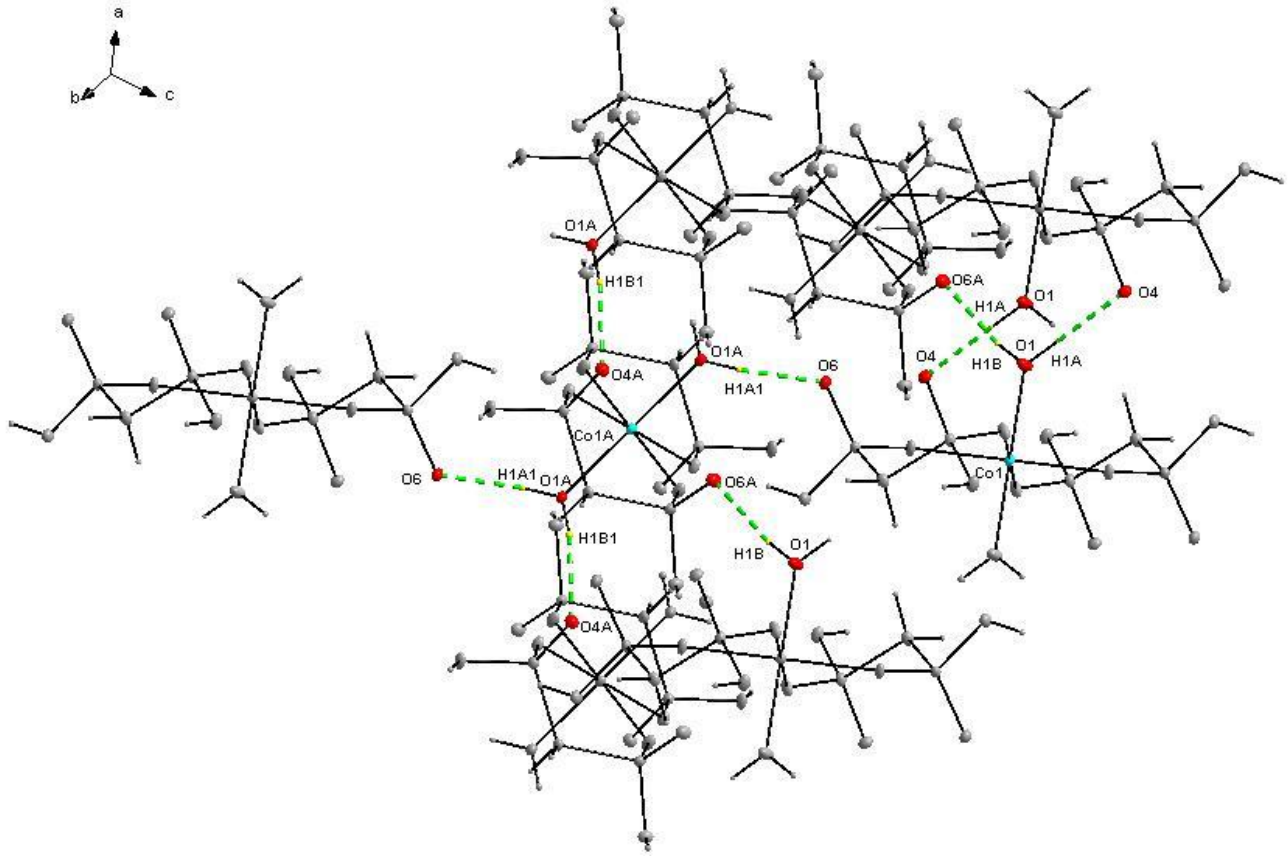

(a)

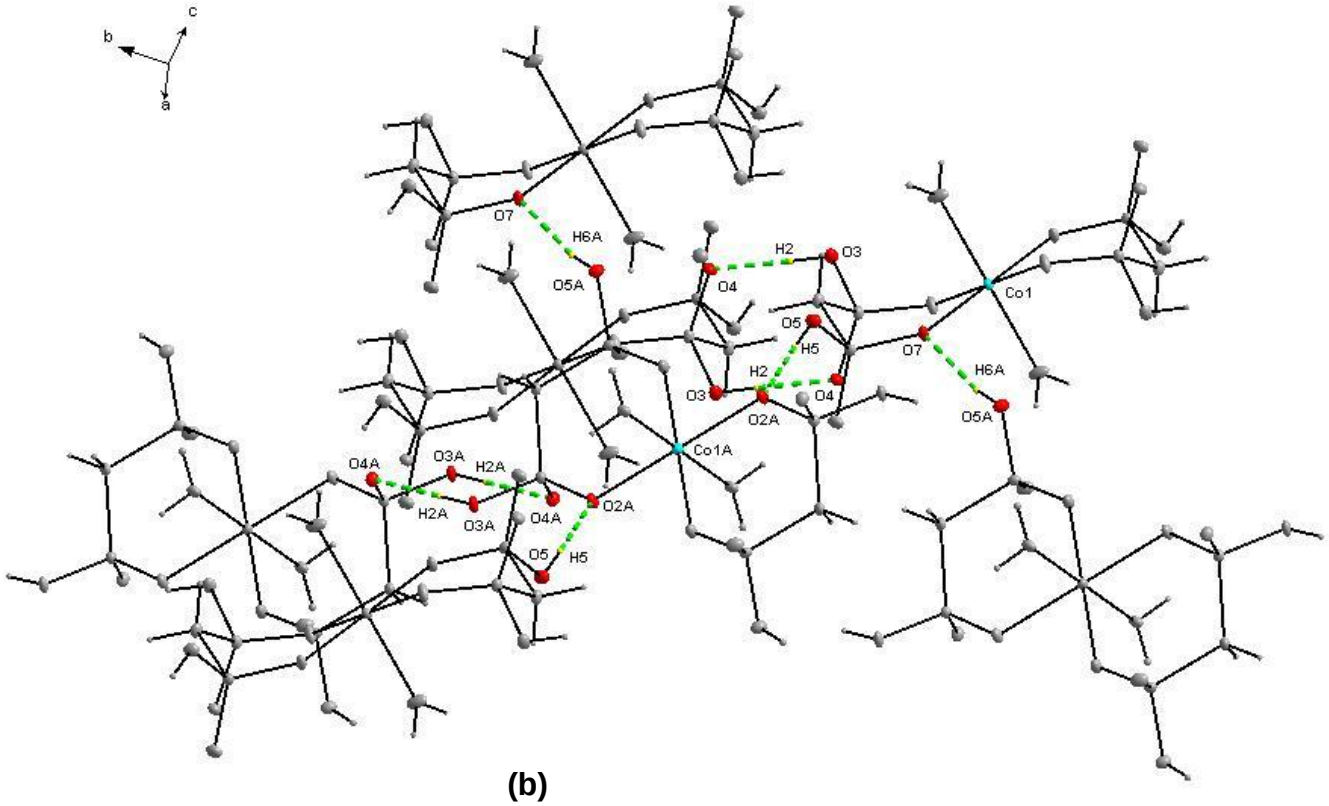

(b)

Figure 5.13(a) and (b) displays a breakdown of the intermolecular hydrogen bonding of potassium diaquabis(MDP)cobaltate(III).

The P=O bonds (P1/A=O4/A or P2/A=O6/A) influences most of the hydrogen-bonding either bonding to the hydrogen originating from the P-OH or to the hydrogen corresponding to the coordinated water. In **Figure 5.13(a)** and **(b)** the oxygen atoms (O4/O4A and O6/O6A) within the phosphonate groups of the one MDP ligand behave like hydrogen-bond acceptors towards the bifurcated hydrogen bond which originates from the coordinated water molecule. Metal aqua-ions can behave as hydrogen bond donors with limited acceptor properties. The $–P(O)_2(OH)-$ group has the ability to act as a hydrogen-bond donor as well as an acceptor which is clearly evident in this case. However all the P-OH and coordinated water behave as hydrogen-bond donors in the crystal structure. Therefore each P=O oxygen is an acceptor for intermolecular hydrogen bonding and each P-O(H) oxygen is linked to a single hydrogen.

In this P-C-P compound no intramolecular hydrogen bonding[29] exists despite the extensive amount of intramolecular O···O interactions in **Table 5.6**, which range from 2.498(5)-3.043(4) Å for Co1 and 2.438(4)-3.114(9) Å for Co1A. The intramolecular O···O interactions enhance the stability of the molecules.

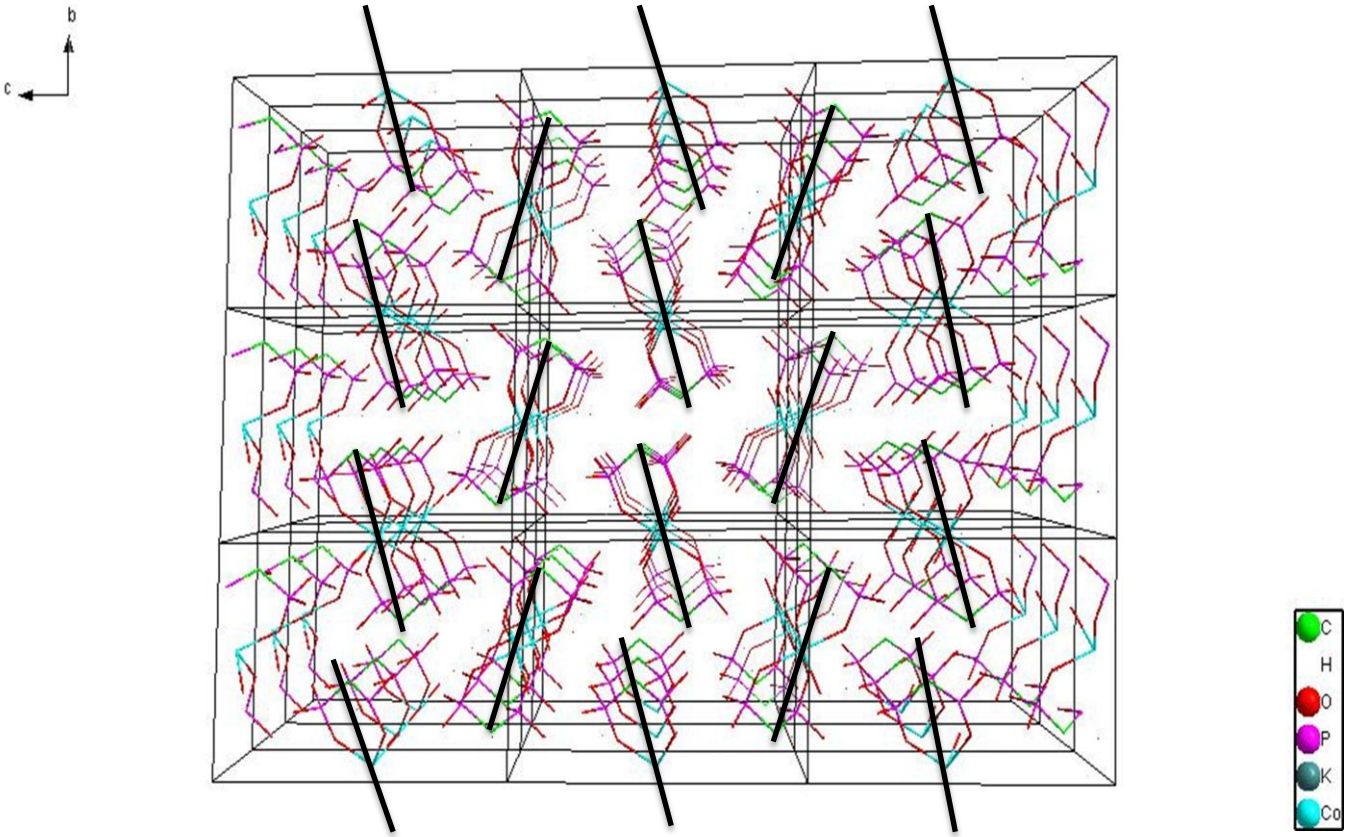

Figure 5.14 A 3x3 matrix displaying the crystal packing of potassium diaquabis(MDP)cobaltate(III). The matrix is viewed along the a-axis (hydrogens have been omitted for clarity).

In **Figure 5.14** no distinctive pattern is observed until the packing is expanded to a 3x3 matrix. The molecules orientate themselves along the sides of the unit cell and appear to pack in a herring-bone fashion. The octahedral cation is positioned in the center of the cell edges.

5.5 Crystal structure of: Potassium diaquadihydroxy(methylenediphosphonato)cobaltate(III).

5.5.1 Introduction

The complex, potassium diaquadihydroxy(methylenediphosphonato)cobaltate(III), $K[Co(CH_4O_6P_2)(H_2O)_2(OH)_2]$, was synthesized according to the procedure described in Section 3.7.2.3 and purple crystals were successfully harvested. The numbering scheme and molecular structure of $K[Co(CH_4O_6P_2)(H_2O)_2(OH)_2]$ are represented in **Figure 5.15.** Significant bond distances and non-hydrogen interactions are displayed in **Table 5.10** and important bond angles and torsion angles are reported in **Table 5.11.**

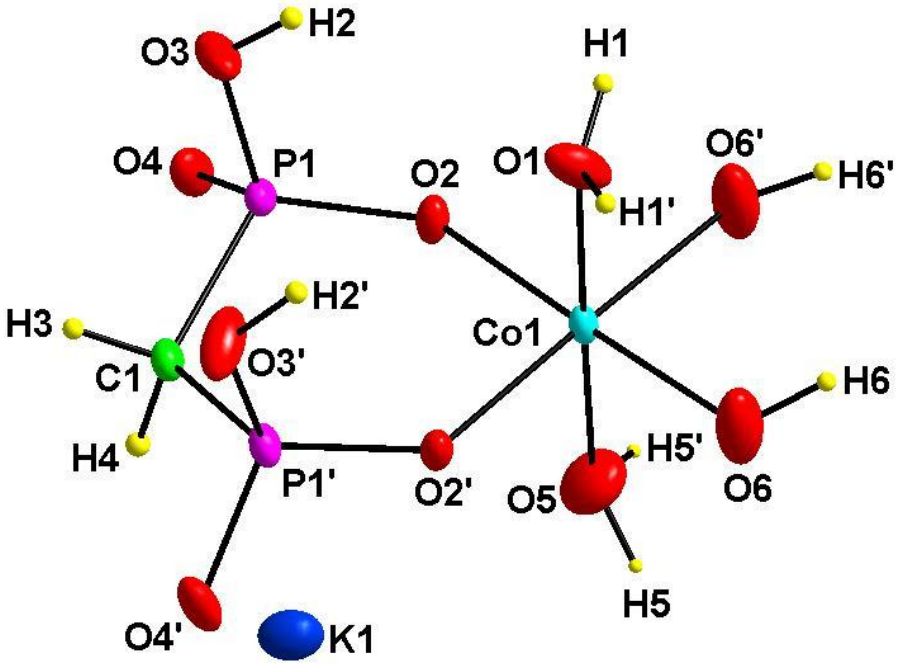

Figure 5.15 Graphical illustration of potassium diaquadihydroxy(MDP)cobaltate(III), displaying the numbering scheme of the atoms in the molecule.

Table 5.10: Selected bond lengths and non-hydrogen bonding interactions present in potassium diaquadihydroxy(MDP)cobaltate(III).

Cobalt Distances (Å)		**Non-Hydrogen Bonding Interactions to 3,3 Å**	
Co1-O1	1.946(4)	O1----O2	2.795(1)
Co1-O2	1.928(2)	O1----O6	2.679(8)
Co1-O5	1.938(5)	O2----O3	2.537(9)
Co1-O6	1.931(3)	O2----O4	2.502(1)
		O2----O5	2.697(8)
Diphosphonate Distances (Å)		O3----O4	2.488(8)
P1-O2	1.512(2)	O5----O6	2.778(1)
P1-O3	1.563(3)		
P1-O4	1.513(3)		
P1-C1	1.799(8)		

Table 5.11: Selected bond angles and torsion angles for the complex potassium diaquadihydroxy(MDP)cobaltate(III).

Cobalt Angles (°)		**Diphosphonate Angles (°)**	
O1-Co1-O2	92.33(1)	P1-C1-P1'	116.11(1)
O1-Co1-O5	178.86(2)	O2-P1-O3	111.13(1)
O1-Co1-O6	87.44(2)	O2-P1-O4	111.61(1)
O2-Co1-O5	88.45(1)	O3-P1-O4	107.98(2)
O2-Co1-O6	178.24(1)		
O5-Co1-O6	91.77(2)	**Torsion Angle (°)**	
		O4-P1-C1-P1'	162.7(2)

5.5.2 Results and Discussion

The asymmetric unit of the title compound, $K[Co(CH_4O_6P_2)(H_2O)_2(OH)_2]$, crystallised in the orthorhombic crystal system and the space group, *Pnma*. The unit cell is composed of four molecules. The complete molecule as displayed in **Figure 5.15** is composed of a distorted $Co^{III}O_6$ octahedron which is derived from the coordination of one bidentate MDP ligand, two hydroxyls and two aqua molecules. The two phosphonates and the two hydroxyl groups are orientated in the equatorial positions and two water molecules reside in the axial positions.

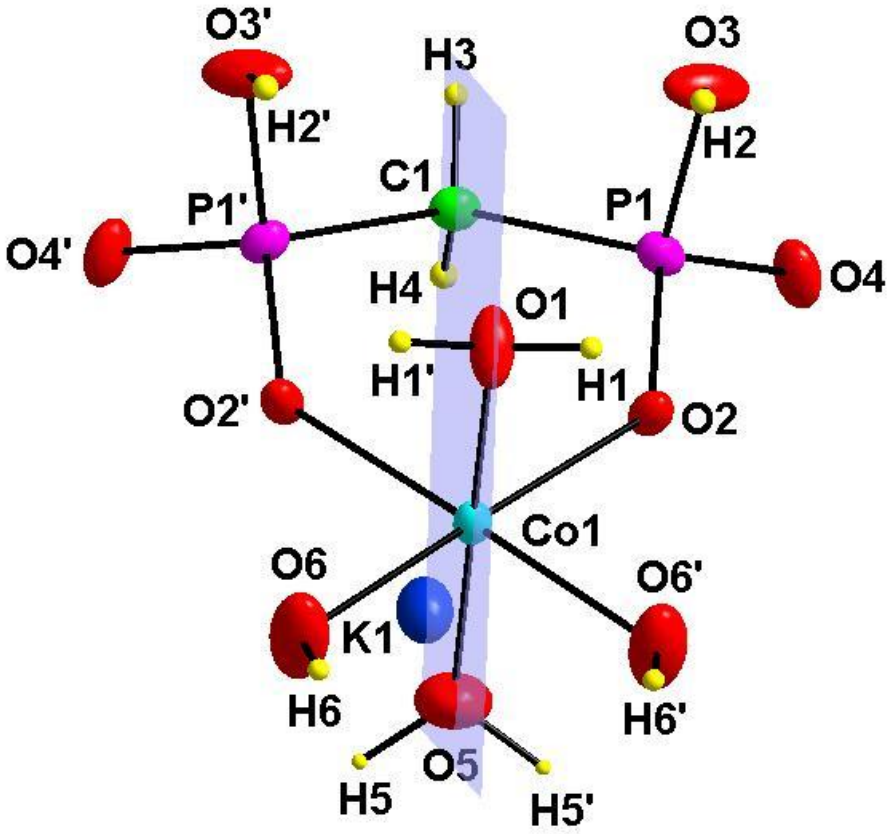

Figure 5.16 Graphical representation of potassium diaquadihydroxy(MDP)cobaltate(III), with a plane constructed through O5, K1, Co1, O1, H4, C1 and H3 atoms.

It is evident from **Figure 5.16** that there is a mirror plane running through the center of the O5, K1, Co1, O1, H4, C1 and H3 atoms. The H1 and H5 atoms are disordered (50% occupancy) around the mirror plane (which can be divided into H1, H1', H5 and H5').

The bidentate methylene diphosphonate coordinates to the central cobalt metal via two oxygen atoms (O2 and O2') from the phosphonate groups, this results in the formation of a six-membered ring and two water molecules reside in a *trans* configuration. The atoms orientated on the axial positions, (Co1-O1 with a distance of 1.946(4) Å and Co1-O5 which has a distance of 1.938(5) Å), are more elongated in comparison to the atoms positioned along the equatorial axis, (Co1-O2 with a distance of 1.928(2) Å and Co1-O6 which has a distance of 1.931(3) Å). These values are similar to values in literature.[15] The O-Co-O angles range from 87.44(2)°

to 178.86(2)° and deviate from the values of an ideal octahedron, resulting in a slightly distorted geometry.[35,37,38]

Two separate P-O bond distances can be distinguished, namely the P-OH bonds and the P=O bonds. P1-O3 is a P-OH bond with a bond distance of 1.563(3) Å while P1-O4 is a P=O bond and has a bond distance of 1.513(3) Å.[10,14,15] It is essential to note that the P-OH distance is more elongated than the P=O distance. The O-P-O angle for O2-P1-O3 is 111.13(1)° and the O-P=O angle for O2-P1-O4 is 111.61(1)°.[10,14,15] The O-P-O-H angle is slightly smaller in comparison to the O-P=O angle.

In order to investigate the bent nature of the P-C-P ligand a plane was constructed through O6', Co1, O2, P1, C1, P1', O2' and O6 as displayed in **Figure 5.17**. It is clear to ascertain that P1-O3 and P1'-O3' have an eclipsed conformation and point upwards while P1-O4 and P1'-O4' which also have and eclipsed conformation but they are pointing downwards.

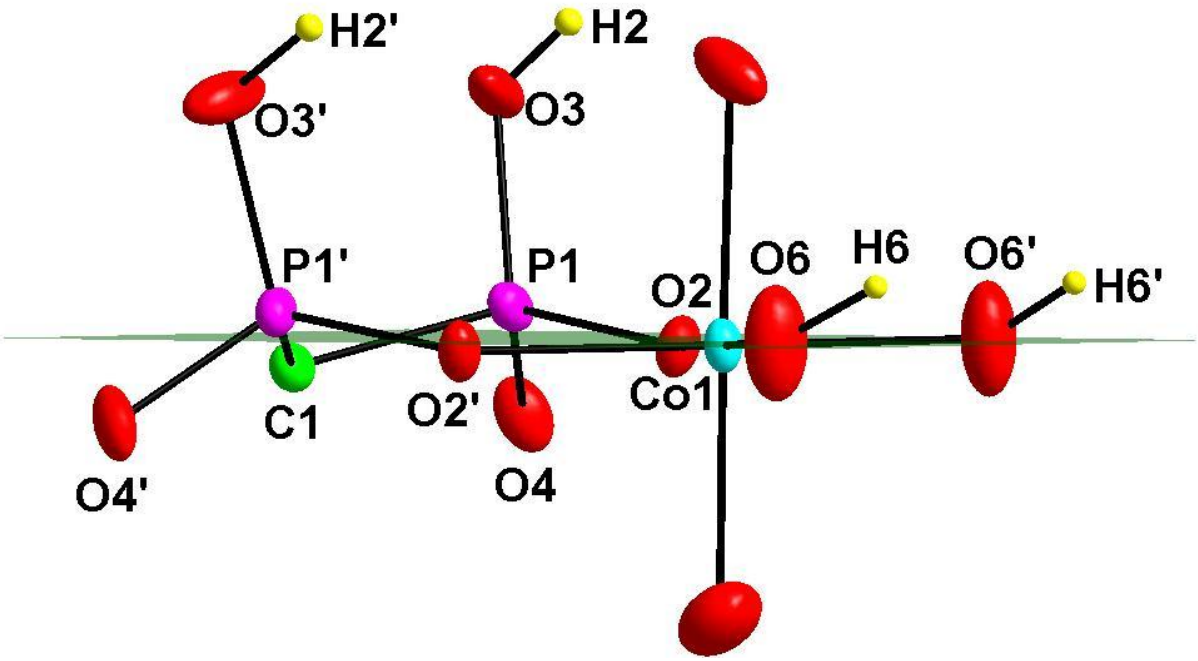

Figure 5.17 Partial structure of potassium diaquadihydroxy(MDP)cobaltate(III) displaying the configuration of the P-O and P=O atoms as well as the orientation of the atoms on the plane (certain hydrogens and the cation have been removed for clarity).

[37] S. Bao, L. Zheng, Y. Liu, W. Xu and S. Feng. *Inorganic Chemistry*, 2003, **42**, 5037-5039.

[38] J. Xiang, M. Li, S. Wu, L. Yuan and J. Sun. *Journal of Molecular Structure*, 2007, **826**, 143-149.

Atom C1 is the furthest from the plane with a distance of 0.229(2) Å and P1 lies 0.190(2) Å from the plane. O2, O6 and Co1 lie on the plane but diverge only slightly with O2 being 0.073(2) Å, O6 is 0.014(2) Å and Co1 0.033(2) Å away from the plane. O2 and Co1 are orientated on the same side of the plane, with the atoms pointing downwards. P1 and O6 are positioned on the opposite side of the plane, pointing upwards.

Table 5.12: Distances between the atoms and the horizontal plane constructed through O6', Co1, O2, P1, C1, P1', O2' and O6.

Atom	Distance Å	Atom	Distance Å
O2	-0.073(2)	O2'	-0.073(2)
P1	0.190(2)	P1'	0.190(2)
O6	0.014(2)	O6'	0.014(2)
C1	-0.229(2)		
Co1	-0.033(2)		

The relevance of the P-C-P bond is explained thoroughly in Paragraph **5.3.2**. The P-C-P bond helps to stabilize the MDP ligand against enzymatic attack and it plays a vital role in enabling it to selectively block the action of resorbing osteoclasts.[35,39]

Figure 5.18(a) displays the P-C-P bond for an uncoordinated MDP ligand.[40] By coordinating cobalt to the MDP ligand a few deviations are notable as depicted in **Figure 5.18(b)**. The P-C bond is a bit longer in **Figure 5.18(b)** and the P-C-P angle is around 1° smaller in comparison to **Figure 5.18(a)**. A reason for the reduction in the P-C-P angle may be due to ring strain. The P-C-P angle for the complex doesn't deviate too much from the MDP ligand and this could also be because only one MDP ligand coordinates to the metal (cobalt).

[39] H. Fleisch. *Metabolic Bone Disease and Related Research*, 1981, **3**, 279-287.

[40] D. DeLaMatter, J.J. McCullough and C. Calvo. *The Journal of Physical Chemistry*, 1973, **77**, 1146-1148.

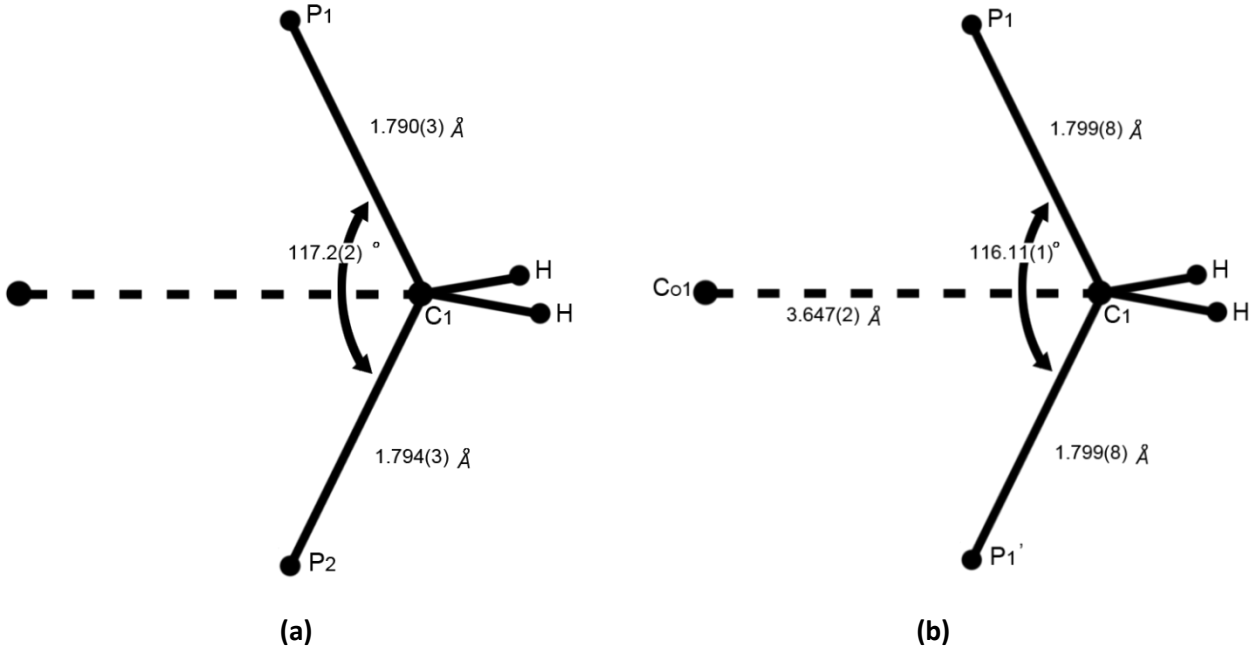

Figure 5.18 An illustration comparing the P-C-P bond for (a) methylene diphosphonate and (b) potassium diaquadihydroxy(MDP)cobaltate(III).

The Co-C distance for Co1 is 3.647(2) Å is almost identical to literature (3.63 Å).[21] The primary reason for similarity in the Co-C distance is because both structures only have one MDP ligand coordinated to the cobalt metal center.

The significance of the "W" configuration is explained in detail in Paragraph **5.3.2**. The term "W" configuration is applied when O4-P1-C1-P1'-O4' forms a planar "W" which can be observed in **Figure 5.19**. The "W" shape allows the MDP ligand to be 'doubly' bidentate,[1] with regard to O3 and O3'. The "W" shape is delineated by the O-P-C-P torsion angles which are -162.7(2)° for O4'-P1'-C1-P1 and 162.7(2)° for O4-P1-C1-P1'.

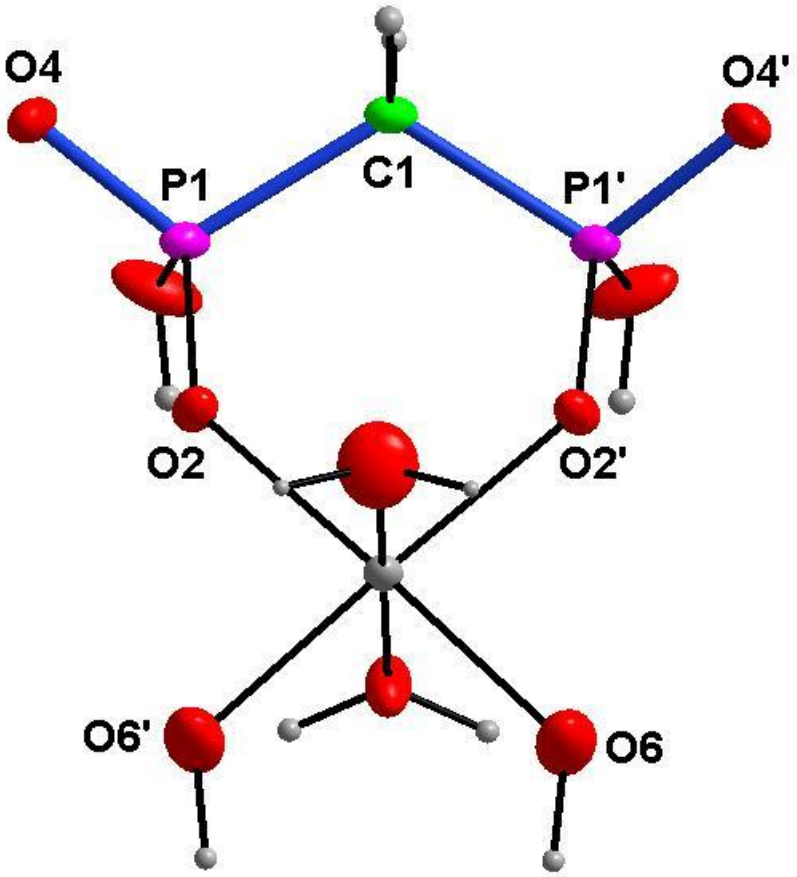

Figure 5.19 Graphical illustration of potassium diaquadihydroxy(MDP)cobaltate(III) featuring the "W" configuration (the cation has not been displayed for clarity).

Table 5.13: Hydrogen bonds for potassium diaquadihydroxy(MDP)cobaltate(III) [Å and °].

D-H…A	d(D-H)	D(H…A)	D(D…A)	<(DHA)
O1-H1…O3^{i}	0.82	2.56	3.376(4)	172.9
O1-H1…O4^{i}	0.82	2.28	2.763(4)	118.6
O3-H2…O4^{i}	0.84(1)	1.72(2)	2.537(4)	163(5)
O5-H5…O4^{ii}	0.86(6)	2.31(8)	3.100(5)	153(8)

Symmetry transformations used to generate equivalent atoms:

(i) –x+1/2, -y+1, z-1/2; (ii) –x, y+1/2, -z+1.

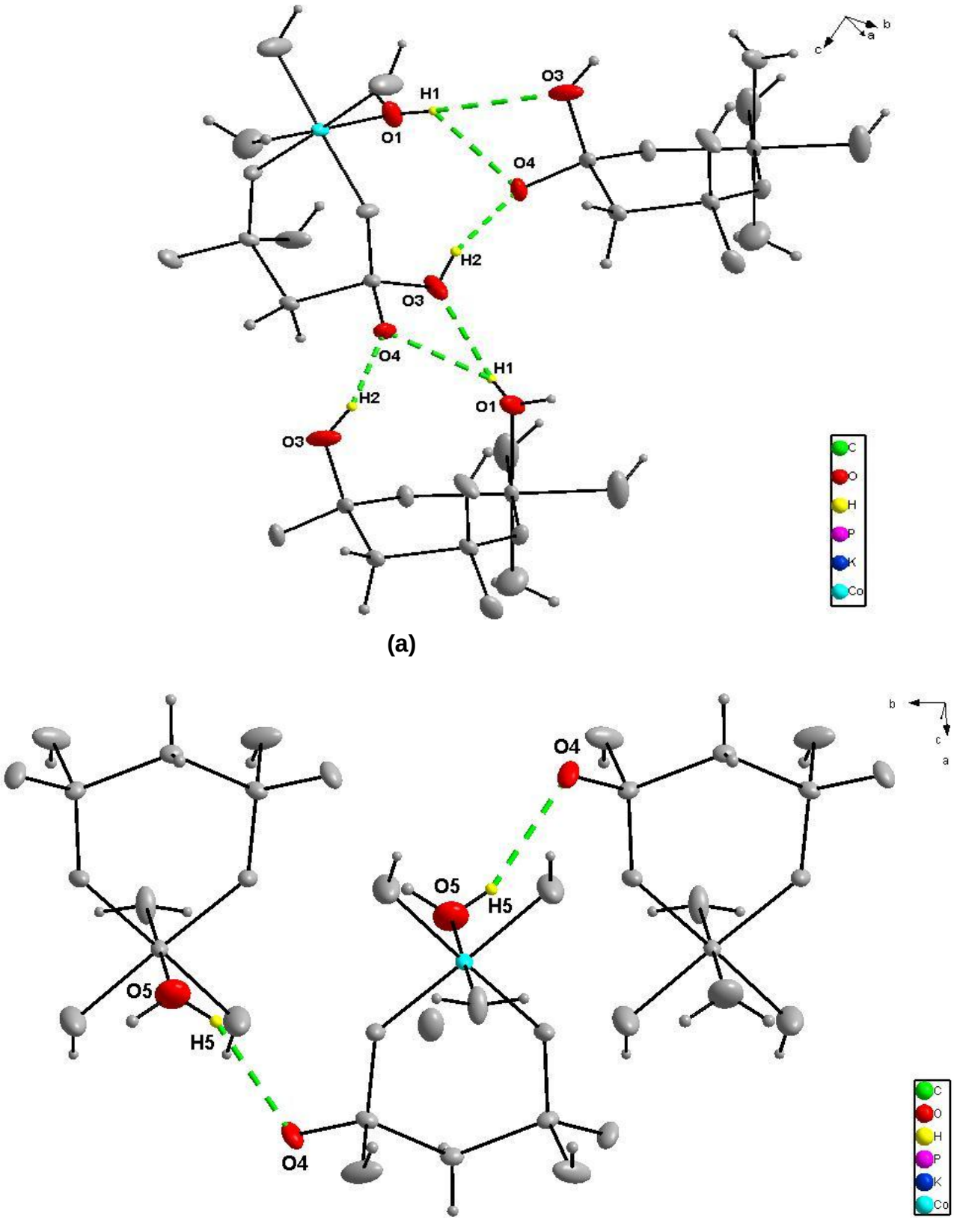

Figure 5.20 A breakdown of the intermolecular hydrogen bonding for potassium diaquadihydroxy(MDP)cobaltate(III), as displayed in (a) and (b).

The complete list of all the hydrogen bond distances and angles is given in **Table 5.13**. All the intermolecular hydrogen bonding interactions are displayed in in **Figure 5.20 (a)** and **(b)**.

The significance of the coordinated water is explained in Paragraph **5.3.2**. Hydrogen bonding interactions are present between the coordinated aqueous molecules as well as the phosphonate and hydroxyl oxygen atoms. The molecules are linked through O-H···O hydrogen-bonding interactions resulting in a 3-D supramolecular network. In **Figure 5.20 (a)** and **(b)** the oxygen atom, O4, which is coordinated to the phosphonate P1 of the MDP ligand, is the prominent hydrogen-bond acceptor with regard to a bifurcated hydrogen bond which originates from the coordinated water molecule, or the hydrogen from the hydroxyl group. In **Figure 5.20 (b)** the molecules are positioned in a head-to-tail fashion connected through O5-H5 intermolecular hydrogen bonding. These metal aqua-ions can act as hydrogen bond donors but have limited acceptor properties.

The $-P(O)_2(OH)-$ group has the ability to act as a hydrogen-bond donor as well as an acceptor, unlike the protons present on the methylene which are not involved in the hydrogen-bonding scheme.[27] The hydrogen bonding interactions present appear to enhance the solid state ordering of the compound and no intramolecular hydrogen bonding exists[29] in the P-C-P compound despite the extensive amount of intramolecular O···O interactions which range from 2.488(8) Å to 2.795(1) Å (from **Table 5.10**).

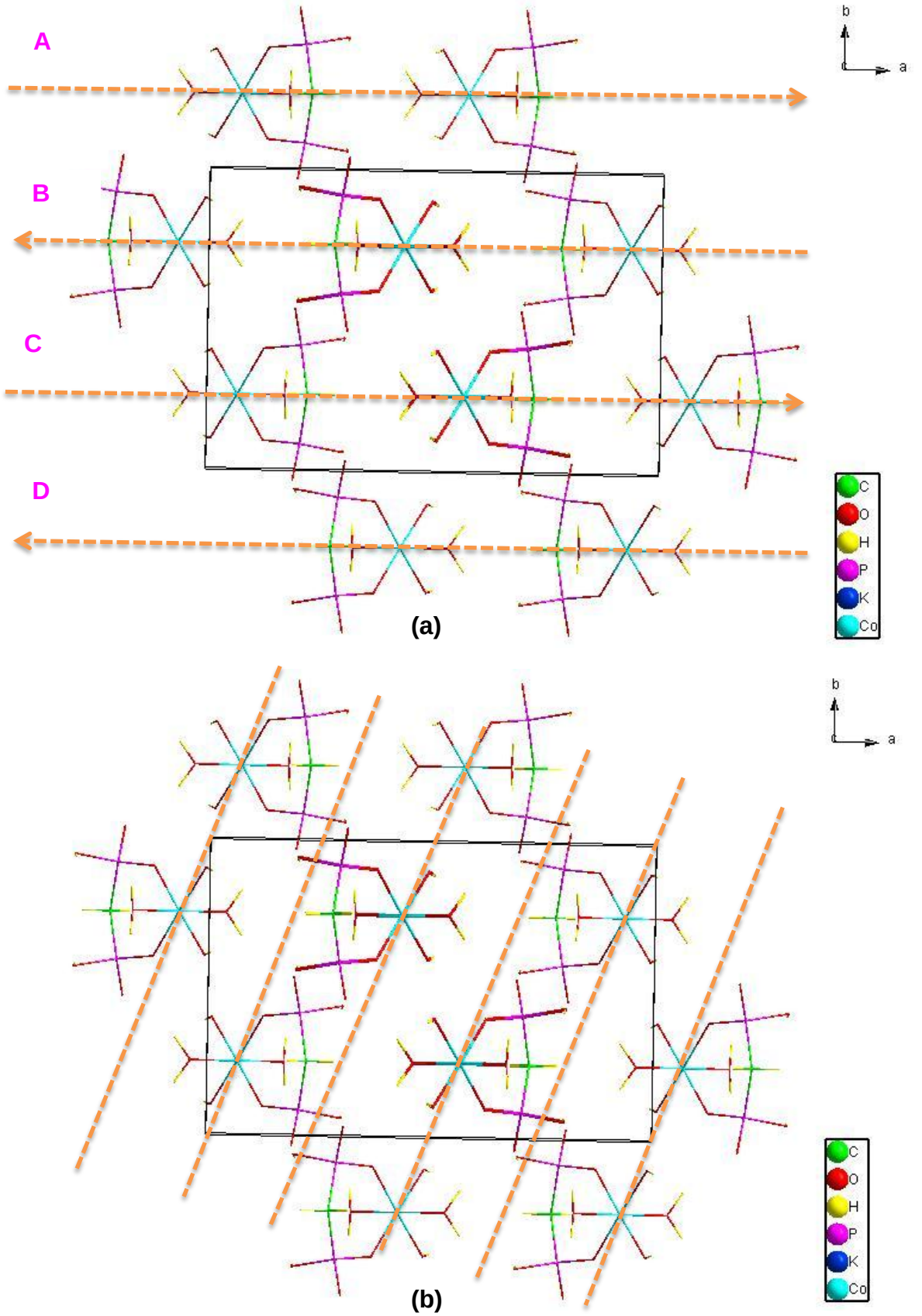

Figure 5.21 (a) and (b) the packing diagrams viewed along the c-axis (the cation has been omitted for clarity).

In **Figure 5.21 (a)** the molecules are orientated horizontally (the horizontal lines are labeled a, b, c and d) but the molecules which are positioned on line a and c are facing in the same direction (for instance to the right) and the molecules on row b and d are facing in the opposite direction (for example to the left). These molecule pack in a zig-zag fashion. **Figure 5.21 (b)** displays that the molecules pack also appear to pack in a diagonal fashion.

5.6 Conclusion

A new range of cobalt(III) and chromium(III) complexes comprising of a O,O' bidentate ligand (MDP) and aqueous molecules were successfully synthesized and characterized by means of X-ray crystallography. Pyridinium diaquabis(methylenediphosphonato)chromate(III) tetrahydrate and potassium diaquabis(methylenediphosphonato)cobaltate(III) have already been published. A limited amount of similar structures were available in literature and this indicated that there was an opening in this field of study.

Table 5.14: Summary comparing the bond distances for 1. $(C_5H_6N)[Cr(CH_4O_6P_2)_2(H_2O)_2]\cdot 4H_2O$, 2. $K[Co(CH_4O_6P_2)_2(H_2O)_2]$ and 3. $K[Co(CH_4O_6P_2)(OH)_2(H_2O)_2]$.

Complex	$M\text{-}O_{(axial)}$ Distances (Å)		$M\text{-}O_{(equatorial)}$ Distances (Å)	
$(C_5H_6N)[Cr(CH_4O_6P_2)_2(H_2O)_2]\cdot 4H_2O$	Cr1-O1	1.991(4)	Cr1-O2 & Cr1-O7	1.956(4) & 1.964(5)
$K[Co(CH_4O_6P_2)_2(H_2O)_2]$	Co1-O1	2.083(3)	Co1-O2 & Co1-O7	2.065(3) & 2.117(3)
	Co1A-O1A	2.126(3)	Co1A-O2A & Co1A-O7A	2.132(3) & 2.052(3)
$K[Co(CH_4O_6P_2)(OH)_2(H_2O)_2]$	Co1-O1	1.946(4)	Co1-O2 & Co1-O6	1.928(2) &1.931(3)
	Co1-O5	1.938(5)		

A summary of the certain geometrical differences between these three complexes are provided in **Table 5.14** and **Table 5.15**. Small differences in the bond lengths of all the complexes are observed. The potassium diaquadihydroxy-(methylenediphosphonato)cobaltate(III) has the smallest axial and equatorial bond distances, the bite angle differed substantially in comparison to the other complexes and it has the largest P-C-P angle. However the Cr(III) complex differed from the other two complexes as the axial bond distance in the Cr(III)- compound is more elongated compared to the equatorial bond distances which could be due to pseudo

Jahn-Teller distortions.[41] The O-M-O angles for all of the complexes deviated from the ideal angle of 90° which explained why the octahedron complexes were distorted.

Table 5.15: Summary comparing the bond angles for 1. $(C_5H_6N)[Cr(CH_4O_6P_2)_2(H_2O)_2]\cdot 4H_2O$, 2. $K[Co(CH_4O_6P_2)_2(H_2O)_2]$ and 3. $K[Co(CH_4O_6P_2)(OH)_2(H_2O)_2]$.

Complex	O-M-O Angle (°)	P-C-P Angle (°)
$(C_5H_6N)[Cr(CH_4O_6P_2)_2(H_2O)_2]\cdot 4H_2O$	89.20(2)-91.66(2)	114.8(3)
$K[Co(CH_4O_6P_2)_2(H_2O)_2]$	88.66(1)-93.34(1)	115.2(2)
	90.86(1)-96.22(1)	115.5(2)
$K[Co(CH_4O_6P_2)(OH)_2(H_2O)_2]$	87.44(2)-178.86(2)	116.11(1)

With the aid of X-ray crystallography it was possible to determine how the MDP ligand co-crystallised to the cobalt(III) and chromium(III) complexes. Altering the metal (cobalt or chromium) did not affect the how the MDP ligand coordinated, their geometries and P-C-P angles were comparable to each other and to literature. The P-C-P bond angle is responsible for stabilizing the MDP ligand against enzymatic attack and it plays a vital role in enabling it to selectively block the action of resorbing osteoclasts.[39,42]

[41] L.R. Falvello, *Journal of the Chemical Society, Dalton Transactions,* 1997, **23**, 4463-4476.

[42] D. Fernández, D. Vega and J.A. Ellena. *Acta Cryst.*, 2003, **C59**, o289-o292.

6 Crystallographic Study of Cobalt(II) complexes

6.1 Introduction

In the past 20 years numerous diphosphonate compounds have undergone intensive pharmacological studies primarily because of their possible use in treating bone diseases. This can be attributed to the fact that bisphosphonic acids are excellent anti-hypercalcemics and have a high affinity for bone tissue.[1]

In the previous chapters (Chapter 2 and Chapter 5) the significance of the bidentate ligand MDP was discussed. Understanding how the ligand coordinates to transition metals and functions may provide essential information with regard to these metal-ligand systems. It is also important to know how they can be adjusted in order to use them for radiotherapy.

The solid state characterization of Co(II) methylene diphosphonate (MDP) complexes are presented in Chapter 6. The solid state characterization provides a better understanding of how the methylene diphosphonate coordinates to a metal complex and this will provide important information with regard to the crystal packing, orientation and molecular interactions.

The Co(II) methylene diphosphonate complexes evaluated in this crystallographic study are presented in **Figure 6.1**.

[1] D. Vega, R. Baggio and M.T. Garland. *Acta Cryst*., 1996, **C52**, 2198-2201.

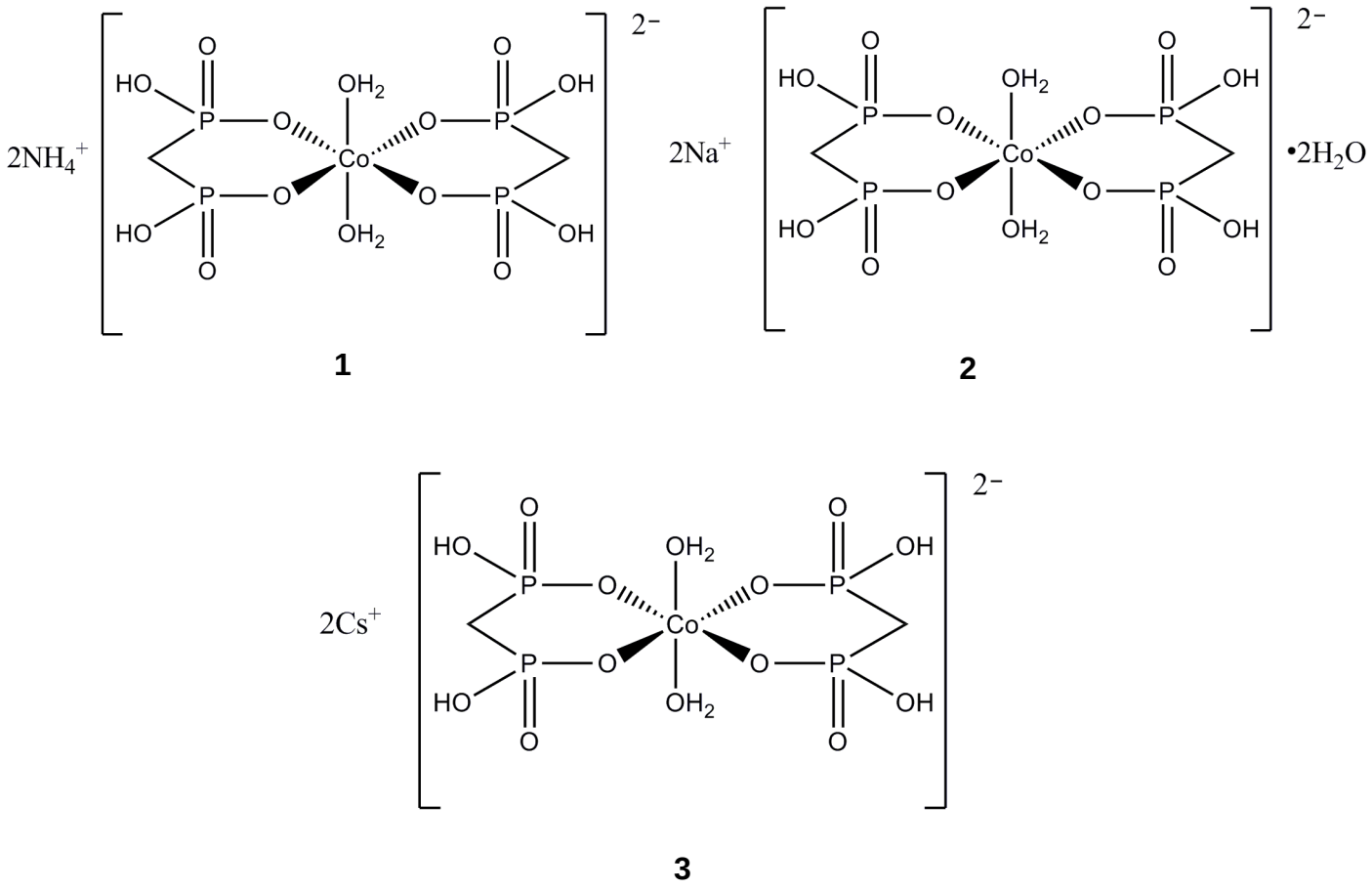

1 **2** **3**

Figure 6.1 Schematic representation of all the complexes discussed in this single crystal X-ray crystallographic study. 1. $(NH_4)_2[Co(CH_4O_6P_2)_2(H_2O)_2]$, 2. $Na_2[Co(CH_4O_6P_2)_2(H_2O)_2]\cdot 2H_2O$ and 3. $Cs_2[Co(CH_4O_6P_2)_2(H_2O)_2]$.

6.2 Experimental

The reflection data for the above mentioned structures were collected on a Bruker X8 ApexII 4K Kappa CCD diffractometer which utilises a graphite monochromated Mo Kα radiation and applies ω- and φ-scans at 100K.[2] COSMO[3] was employed in order to optimise the collection of more than a hemisphere of reciprocal space. To ensure that no decomposition of the crystals took place during the collection the initial 50 frames were repeated after the collection was complete. All the crystals remained stable throughout the data collection. The frames were combined using a narrow-frame integration algorithm and then reduced with the Bruker SAINT-Plus[4] and XPREP[4] software packages, respectively. The multi-scan technique SADABS[5] was utilised to correct data which had adsorption effects. The structures were solved using the direct methods package SIR97[6] and all the refinement were done on WinGX[7] which incorporates SHELXL.[8] All the graphical representations of the crystal structures were generated using DIAMOND.[9] Unless otherwise stated all the structures are shown with thermal ellipsoids drawn at 50% probability level.

All non-hydrogen atoms were refined anisotropically, while the methyl and aromatic H atoms were placed in geometrically idealised positions (C-H = 0.95-0.98 Å) and constrained to ride on their parent atoms (U_{iso}(H) = 1.5U_{eq}(C) and 1.2U_{eq}(C)). The

[2] Bruker, APEX2 (Version 1.0-27), Bruker AXS Inc., Madison, Wisconsin, United States of America, **2005**.

[3] Bruker, COSMO, (Version 1.48), Bruker AXS Inc., Madison, Wisconsin, United States of America, **2003**.

[4] Bruker, SAINT-Plus (Version 7.12) (including XPREP), Bruker AXS Inc., Madison, Wisconsin, United States of America, **2004**.

[5] Bruker, SADABS, (Version 2004/1), Bruker AXS Inc., Madison, Wisconsin, United States of America, **1998**.

[6] A. Altomare, M.C. Burla, M. Camalli, G.L. Cascarano, C. Giacovazzo, A. Guagliardi, A.G.G. Moliterni, G. Polidori and R. Spagna. *J. Appl. Cryst*., 1999, **32**, 115.

[7] L.J. Farrugia. *J. Appl. Cryst*., 1999, **32**, 837.

[8] G.M. Sheldrick, SHELXL97, *Program for Solving Crystal Structures*, University of Göttingen, Germany, **1997**.

[9] K. Brandenburg and H. Putz, DIAMOND, Release 3.0c, Crystal Impact GbR, Bonn, Germany, **2005**.

hydrogen atoms attached to the hydroxyl groups and aqueous molecules were located on a different Fourier map, restrained to a reasonable O-H distances using DFIX and refined isotropically.

A summary of the general crystal data and the refinement parameters for all the complexes is given in **Table 6.1**. The supplementary data in Appendix B contains the complete list of atomic coordinates, equivalent isotropic parameters, bond distances and angles, the hydrogen coordinates for each individual dataset and the anisotropic displacement parameters.

Table 6.1: General crystal data and refinement parameters for the following compounds:

Compound	$(NH_4)_2[Co(CH_4O_6P_2)_2(H_2O)_2]$	$Na_2[Co(CH_4O_6P_2)_2(H_2O)_2]\cdot 2H_2O$	$Cs_2[Co(CH_4O_6P_2)_2(H_2O)_2]$
Empirical Formula	Co1 N2 C2 P4 H20 O14	Co1 Na2 C2 P4 H16 O16	Co1 Cs2 C2 P4 H12 O14
Formula Weight (g.mol^{-1})	479.01	524.96	708.75
Wavelength (Å)	0.71069	0.71073	0.71073
Crystal System	Triclinic	Monoclinic	Triclinic
Space Group	$P\bar{1}$	$P2_1/c$	$P\bar{1}$
Unit Cell Dimensions			
***a* (Å)**	7.455(5)	6.869(2)	7.333(5)
***b* (Å)**	7.560(5)	13.286(4)	7.412(5)
***c* (Å)**	8.035(5)	8.354(3)	7.666(5)
***α* (°)**	88.282(5)	90.000(5)	74.621(5)
***β* (°)**	62.450(5)	91.375(10)	83.064(5)
***γ* (°)**	71.834(5)	90.000(5)	86.496(5)
Volume (Å^3)	378.0(4)	762.23(4)	398.6(5)
Z	1	2	1
Density (calculated) (g.cm^{-3})	2.069 Mg/m^3	2.287 Mg/m^3	2.286 Mg/m^3
Absorption Coefficient (mm^{-1})	1.63	1.669	5.963
***F*(000)**	237	530	253
Crystal Size (mm^3)	0.28 x 0.16 x 0.11	0.52 x 0.24 x 0.09	0.38 x 0.07 x 0.047
Crystal Colour	Pink	Pink	Pink
Crystal Morphology	Rod	Platelet	Needle
Theta Range (°)	2.86 - 28.41	2.88 - 28.43	2.77 - 28.00
Completeness (%)	99.1	99.2	99.2
Index Ranges	-9 ≤ h ≤ 9	-8 ≤ h ≤ 9	-9 ≤ h ≤ 9
	-9≤ k ≤ 10	-17 ≤ k ≤ 16	-9 ≤ k ≤ 9
	-10 ≤ l ≤ 9	-11 ≤ l ≤ 8	-10 ≤ l ≤ 10
Reflections Collected	8436	8743	4208
Independent Reflections	1877	1902	1906
R_{int}	0.03	0.02	0.02
Absorption Correction	Multiscan	Multiscan	Multiscan
Refinement Method	Full-matrix least-squares on F^2	Full-matrix least-squares on F^2	Full-matrix least-squares on F^2
Data/Restraints/Parameters	1877 / 6 / 134	1902 / 5 / 139	1906/ 4 / 122
Goodness-of-fit of F^2	1.258	1.271	1.361
Final *R* Indices [*I*>2sigma(*I*)]	R1 = 0.0264	R1 = 0.0195	R1 = 0.0162
	wR2 = 0.0912	wR2 = 0.0641	wR2 = 0.0465
***R* Indices (all data)**	R1 = 0.0314	R1 = 0.0214	R1 = 0.0186
	wR2 = 0.1225	wR2 = 0.0800	wR2 = 0.0791
ρ_{max} and ρ_{min} (e.Å^{-3})	0.744 and -0.682	0.495 and -0.768	1.029 and -0.827

6.3 Crystal structure of: Diammonium diaquabis(methylenediphosphonato)cobaltate(II).[10]

6.3.1 Introduction

The preparation of diammonium diaquabis(methylenediphosphonato)cobaltate(II), $(NH_4)_2[Co(CH_4O_6P_2)_2(H_2O)_2]$, was according to the procedure described in Section 3.7.2.4 from which pink crystals were acquired. A summary of the general crystal data is given in **Table 6.1**. The numbering scheme and molecular structure of $(NH_4)_2[Co(CH_4O_6P_2)_2(H_2O)_2]$ is represented in **Figure 6.2.** Significant bond distances and non-hydrogen interactions are referred to in **Table 6.2** and consequential bond angles and torsion angles are reported in **Table 6.3.** The anisotropic displacement parameters, atom coordinates as well as all the bond distances, bond angles and hydrogen coordination are provided in the supplementary data (Appendix B).

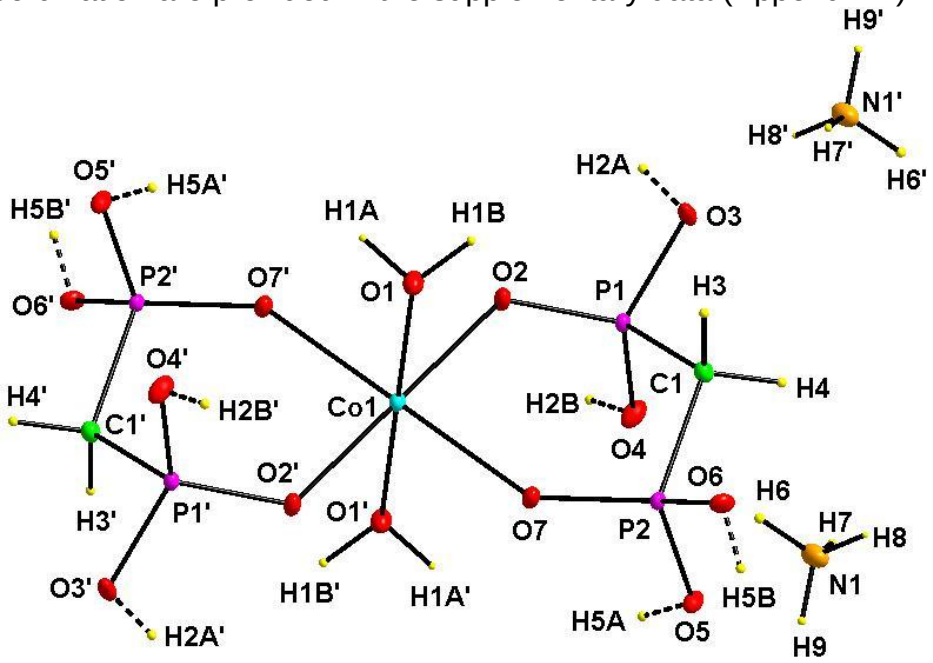

Figure 6.2 Molecular diagram of diammonium diaquabis(MDP)cobaltate(II) displaying the numbering scheme of the atoms in the molecule (ellipsoid probability = 50% except for hydrogen atoms). The dotted lines display the 50% positional disorder present on the protons.

[10] K.A. van der Merwe, H.G. Visser and J.A. Venter. *Acta Cryst.*, 2009, **E65**, m1394.

Table 6.2: Selected bond lengths and non-hydrogen bonding interactions of diammonium diaquabis(MDP)cobaltate(II).

Cobalt Distances (Å)		Non-Hydrogen Bonding Interactions to 3,3 Å	
Co1-O1	2.103(2)	P1----P2	3.059(2)
Co1-O2	2.072(2)	O1----O2	2.887(4)
Co1-O7	2.136(2)	O1----O7	2.969(4)
		O2----O3	2.534(1)
Diphosphonate Distances (Å)		O2----O4	2.528(2)
P1-O3	1.547(2)	O2----O7	3.108(4)
P1-O4	1.536(2)	O3----O4	2.536(1)
P1-C1	1.795(4)	O5----O6	2.522(1)
P2-O5	1.541(2)	O5----O7	2.532(1)
P2-O6	1.530(2)	O6----O7	2.521(1)
P2-C1	1.795(4)		

Table 6.3: Selected bond angles and torsion angles of diammonium diaquabis(MDP)cobaltate(II).

Cobalt Angles (°)		Diphosphonate Angles (°)	
O1-Co1-O2	87.47(9)	P1-C1-P2	116.90(2)
O1-Co1-O7	88.91(8)	O2-P1-O3	112.43(1)
O2-Co1-O7	95.23(9)	O2-P1-O4	112.63(1)
		O5-P2-O7	111.80(1)
(d) Torsion Angles (°)		O6-P2-O7	111.69(1)
O3-P1-C1-P2	-178.87(1)		
O6-P2-C1-P1	-165.90(1)		

6.3.2 Results and Discussion

The title compound, $(NH_4)_2[Co(CH_4O_6P_2)_2(H_2O)_2]$, crystallised in the triclinic crystal system in the space group $P\bar{1}$. The assymetric unit is composed of an ammonium cation as well as half of a molecule made up of one methylene diphosphonate ligand and one aqueous molecule coordinating to a cobalt atom. It features a cobalt atom which is located at a special position and the entire molecule is generated by inversion symmetry. This compound has a slightly distorted $Co^{II}O_6$ octahedron configuration and the four equatorial binding sites are occupied by phosphonate

oxygens (O2, O7, O2' and O7') from two bidentate methylene diphosphonate ligands and two water molecules (O1 and O1') occupy the axial positions. The water molecules are orientated in a *trans* configuration.

The axial distance for Co1-O1(cobalt aqua distance) is 2.103(2) Å. Two equatorial distances are present in the molecule, the Co1-O2 distance of 2.072(2) Å and the Co1-O7 distance of 2.136(2) Å. These values are in agreement with those in other cobalt phosphonate compounds.[11]

The O-Co-O bite angles of relevance range between 87.47(9)° and 95.23(9)° and this confirms that the cobalt(II) complex has a slightly distorted octahedral geometry.

There are two unique types of P-O bonds: the P-OH and the P=O bonds which can be differentiated as the P-OH distances are always notably longer in comparison to the P=O distances. The P-O bond distances range from 1.530(2) Å to 1.547(2) Å but no distinction between the P=O and P-OH can be made because there is a 50% positional disorder present on the protons coordinated to O3, O4, O5 and O6 and this results in the bond lengths being similar.

The O-P-O angles are similar because of the 50% positional disorder so no distinction between the O-P-OH and O-P=O angles can be made. The best fits were obtained when the protons were placed with a 50% positional disorder.

In order to investigate the bent nature of the P-C-P ligand a plane was constructed through C1, P1, P2, O7, Co1, O2 as well as through C1', P1', P2', O7', O2' as displayed in **Figure 6.3**. P1-O4/P1'-O4' and P2-O5/P2'-O5' have an eclipsed conformation but P1-O3/P1'-O3' and P2-O6/P2'-O6' don't display a staggered or eclipsed conformation. An observation that can be made based on all the past structures discussed, there was always a notable pattern observed for the P=O and the P-OH bonds. There is a pattern for the P1-O4/P1'-O4' and P2-O5/P2'-O5' bonds which might be because these are the P=O bonds. Due to the positional disorder, the P-OH bonds don't display a specific conformation as the hydrogens are not fixed and crystallized in a range of possible positions which resulted in the P1-O3/P1'-O3' and P2-O6/P2'-O6' not having a specific conformation.

[11] E.V. Bakhmutova, X. Ouyang, D.G. Medvedev and A. Clearfield. *Inorganic Chemistry*, 2003, **42**, 7046-7051.

P1-O3 and P2-O6 are orientated on the same side of the plane, pointing upwards, while P1-O4 and P2-O5 are directed on the opposite side of the plane, pointing downwards.

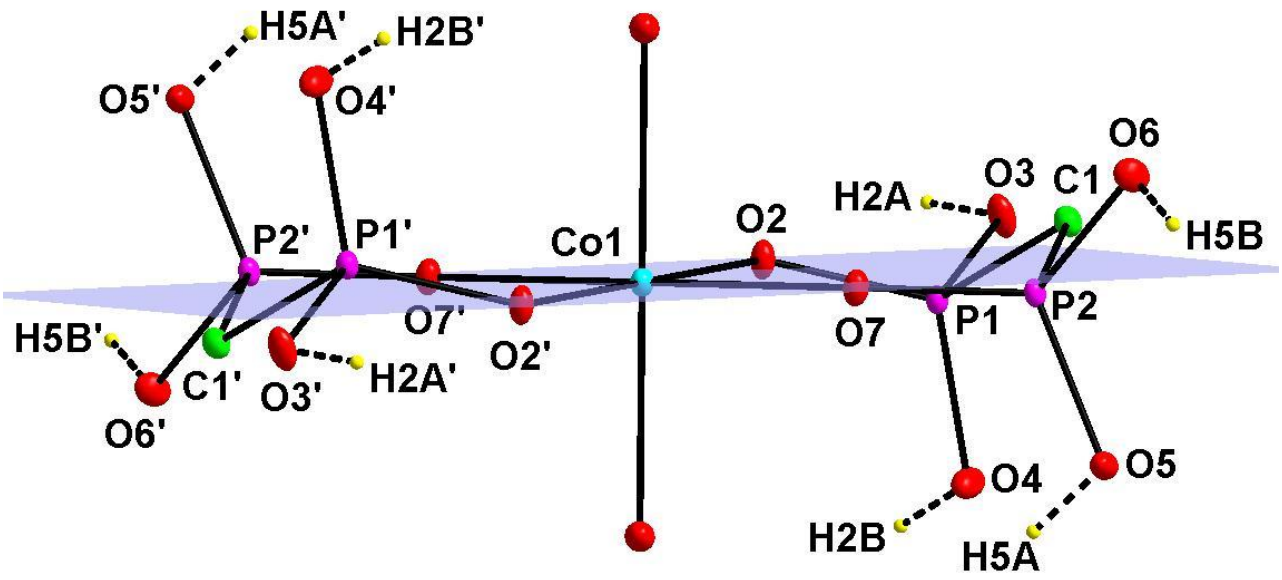

Figure 6.3 Partial structure of ammonium diaquabis(MDP)cobaltate(II) displaying the configuration of the P-O and P=O atoms as well as the orientation of the atoms on the plane (certain hydrogens and the cations have been removed for clarity).

C1 has a distance of 0.358(3) Å and O2 a distance of 0.081(3) Å with regards to the plane. Both C1 and O2 are orientated on the same side of the plane while C1 deviates the most from the plane. O2 and O7 lie on the plane but O2 and O7 are orientated on opposite sides of the plane. P1 and P2 are located on the same side of the plane with P1 being 0.308(3) Å from the plane and P2 is 0.156(3) Å from the plane. O7, P2, C1, P1, O2, Co1, O2', P1', C1', P2', O7' forms a type of a chair conformation, C1 and C1' are staggered with regards to one another.

Table 6.4: Selected distances between specific atoms and the horizontal plane constructed through C1, P1, P2, O7, Co1, O2 as well as through C1', P1', P2', O7', O2'.

Atom	Distance Å	Atom	Distance Å
O2	-0.081(3)	O2'	0.081(3)
P1	0.308(3)	P1'	-0.308(3)
C1	-0.358(3)	C1'	0.358(3)
P2	0.156(3)	P2'	-0.156(3)
O7	0.051(3)	O7'	-0.051(3)
Co1	0.0000		

The importance of the P-C-P bond is explained comprehensively in Paragraph **5.3.2**. **Figure 6.4(a)** illustrates the P-C-P bond present in the uncoordinated MDP ligand.[12] By bonding cobalt to the MDP ligand a few differences are notable as displayed in **Figure 6.4(b)**. The P2-C1 bond lengths for **Figure 6.4(a)** and **(b)** are almost identical to each other but the P1-C1 bond length in **Figure 6.4(b)** is almost 0.005 Å longer in comparison to the P1-C1 bond length in **Figure 6.4(a)**.

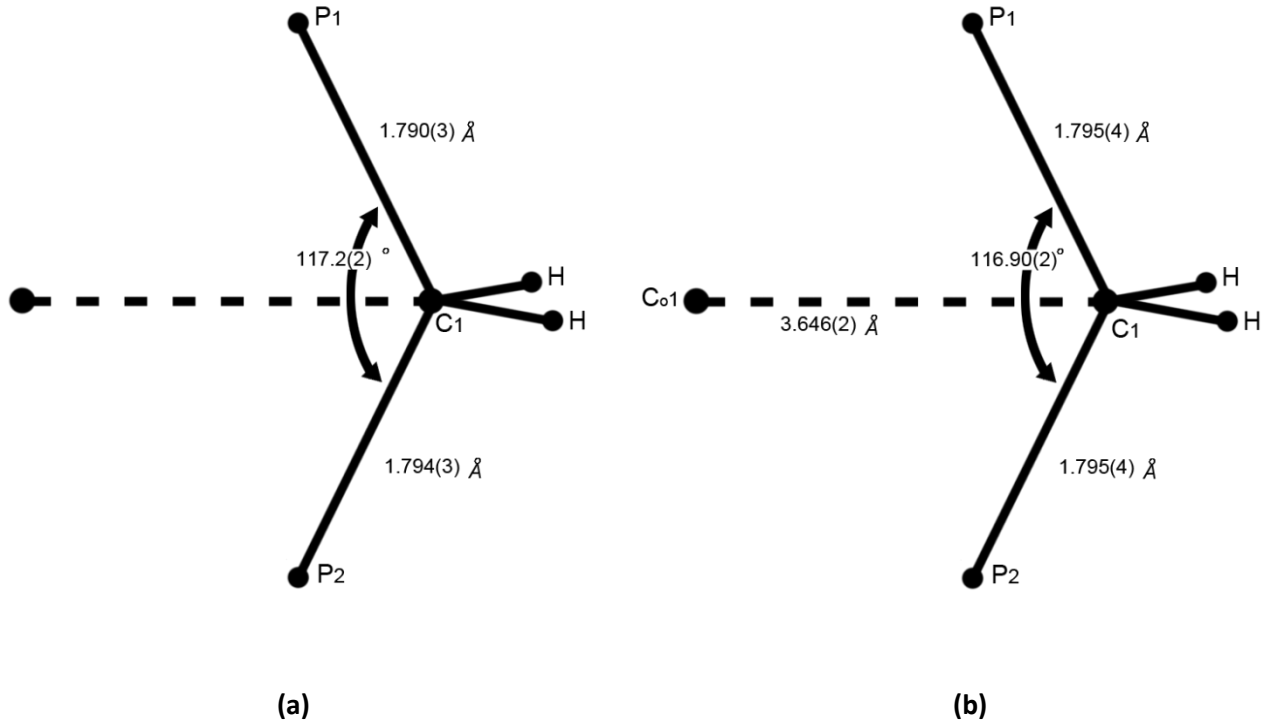

Figure 6.4 Graphical comparison of the P-C-P bond in (a) methylene diphosphonate and (b) ammonium diaquabis(MDP)cobaltate(II).

[12] D. DeLaMatter, J.J. McCullough and C. Calvo. The Journal of Physical Chemistry, 1973, **77**, 1146-1148.

The P-C-P angle in **Figure 6.4(b)** is practically identical to **Figure 6.4(a)** as well as to the literature value.[13] A reason for the similarity in the P-C-P angles[12,13] for **Figure 6.4(a)** and **(b)** could be because in ammonium diaquabis(MDP)cobaltate(II). the cobalt metal coordinates to the MDP ligand but doesn't undergo a change in charge.

The Co-C distance is 3.646(2) Å which is slightly longer compared to the value of 3.63 Å in literature.[13] This complex differs to the one described in literature as it has two methylene diphosphonate ligand coordinating to the cobalt atom instead of one which is reported in literature.

The relevance of the "W" configuration is explained in detail in Paragraph **5.3.2**. The term "W" configuration is applied when O3-P1-C1-P2-O6 forms a planar "W" which can be observed in **Figure 6.5**.

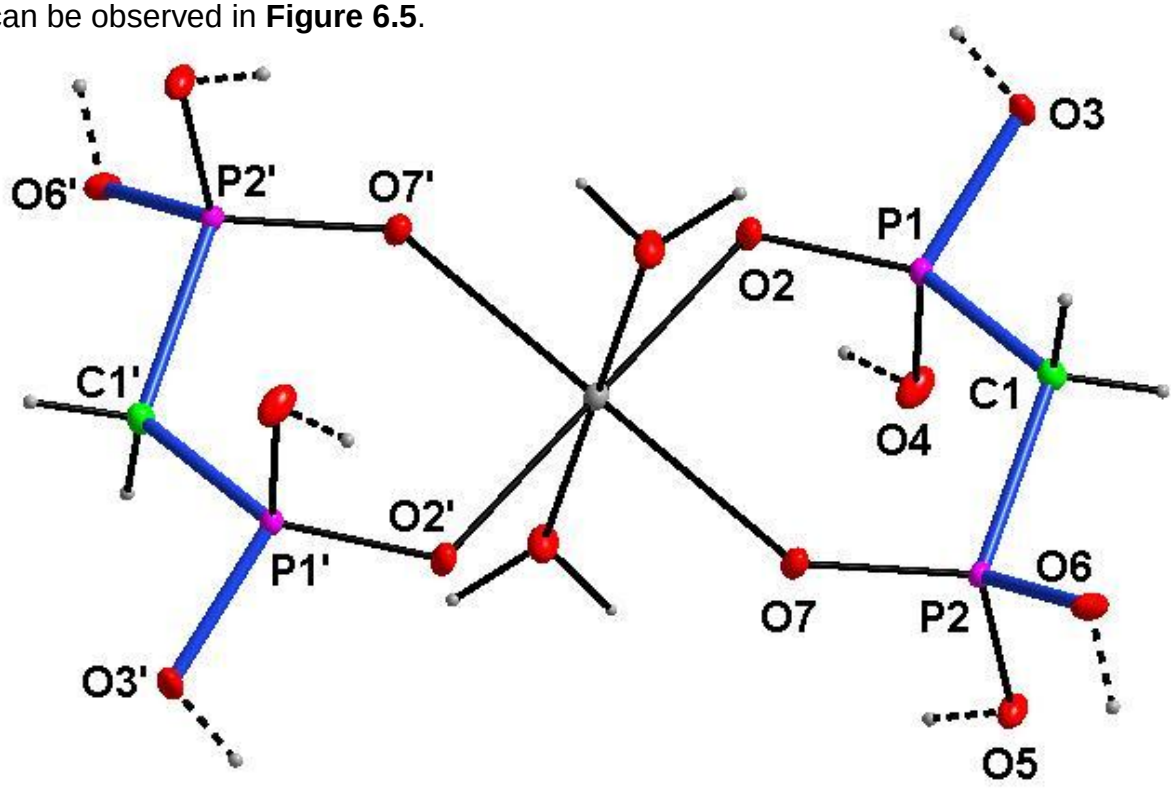

Figure 6.5 Molecular diagram of ammonium diaquabis(MDP)cobaltate(II) displaying the "W" configuration (cations have been omitted for clarity).

[13] T.P. Harmony, W.B. Knight, D. Dunaway-Mariano and M. Sundaralingam. *Inorganic Chemistry*, 1984, **23**, 2412-2415.

The “W” shape allows the MDP ligand to be doubly bidentate,[14] with O2 and O7 on the one side of the “W” coordinated to one metal center while there is a potential for O4 and O5 to coordinate to a metal center on the other side of the “W”. The O-P-C-P torsion angles which characterize the “W” shape are -178.87(1)° for O3-P1-C1-P2 and -165.90(1)° for O6-P2-C1-P1.

Table 6.5: Hydrogen bonds for ammonium diaquabis(MDP)cobaltate(II) [Å and °].

D-H…A	d(D-H)	D(H…A)	D(D…A)	<(DHA)
O1-H1A…O5^{vi}	0.83(2)	1.98(2)	2.794(3)	165(4)
O1-H1B…O6^{ii}	0.85(2)	1.98(2)	2.826(3)	179(5)
O3-H2A…O6^{iii}	0.82	1.66	2.436(3)	157.3
O5-H5A…O5^{iv}	0.82	1.66	2.464(4)	164.7
O6-H5B…O3^{v}	0.82	1.67	2.436(3)	153.5
N1-H7…O7^{vii}	0.81(2)	2.16(2)	2.968(4)	173(4)
N1-H8…O3^{i}	0.84(2)	2.06(2)	2.891(4)	170(4)
N1-H9…O7^{iv}	0.81(2)	2.18(2)	2.960(3)	161(4)
N1-H9…O2^{viii}	0.81(2)	2.60(4)	3.104(4)	122(4)

Symmetry transformations used to generate equivalent atoms:

(i) –x+1, -y+1, -z+1; (ii) –x+1, -y+1, -z+2; (iii) x-1, y, z; (iv) -x+2, -y, -z+1; (v) x+1, y, z;

(vi) x-1, y, z+1; (vii) x, y, z-1; (viii) x+1, y, z-1.

[14] K. Lisbon, E. Deutsch and B.L. Barnett. *Journal of American Chemical Society*, 1980, **7**, 2476-2478.

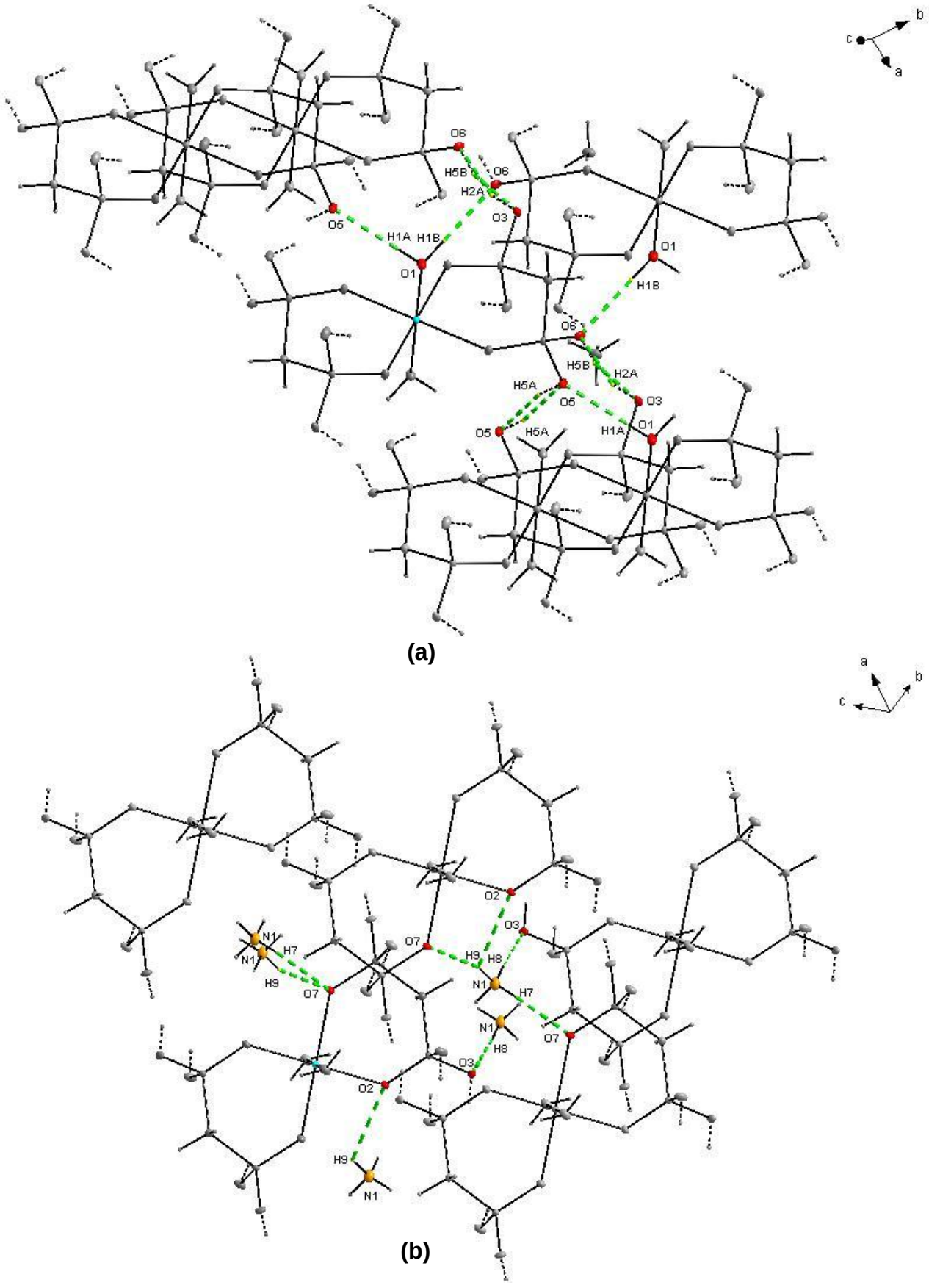

Figure 6.6(a) and (b) A breakdown of the intermolecular hydrogen bonding of ammonium diaquabis(MDP)cobaltate(II).

The complete list of all the hydrogen bond distances and angles is provided for in **Table 6.5**. All the intermolecular hydrogen bonding interactions are observed in **Figure 6.6(a)** and **(b)**.

Numerous hydrogen bonds are observed amongst the coordinated water molecules, the hydroxyl oxygen atoms and the cations. All the phosphonyl hydrogens are asymmetrically coordinated to two oxygen atoms in order to create an extensive three-dimensional network of hydrogen bonds which incorporates all the molecules of the unit cell. The molecules are connected through O-H···O and N-H···O hydrogen-bonding interactions and all of the N-H groups act as hydrogen-bond donors in the crystal structure.

Hydrogen bonds occur on all the phosphonate oxygen's except for P1-O4. In **Figure 6.6(a)** the oxygen atoms with a 50% positional disorder (O5/O5A and O6/O6A) behave like hydrogen-bond acceptors towards a bifurcated hydrogen bond which originates from the coordinated water molecule. Metal aqua-ions can act as hydrogen bond donors with limited acceptor properties. The $–P(O)_2(OH)-$ group has the ability to act as a hydrogen-bond donor as well as an acceptor which is clearly evident in this case.

In this P-C-P compound no intramolecular hydrogen bonding exists despite the numerous amount of intramolecular O···O interactions which are within 2.521(1)-3.108(4) Å as summarized in **Table 6.2**.[15] The intramolecular O···O interactions enhance the stability of the molecules.

[15] S.W. Peterson, E. Gebert, A.H. Reis, M.E. Druyan, G.W. Mason and D.F. Peppard. *The Journal of Physical Chemistry*, 1977, **81**, 466-471.

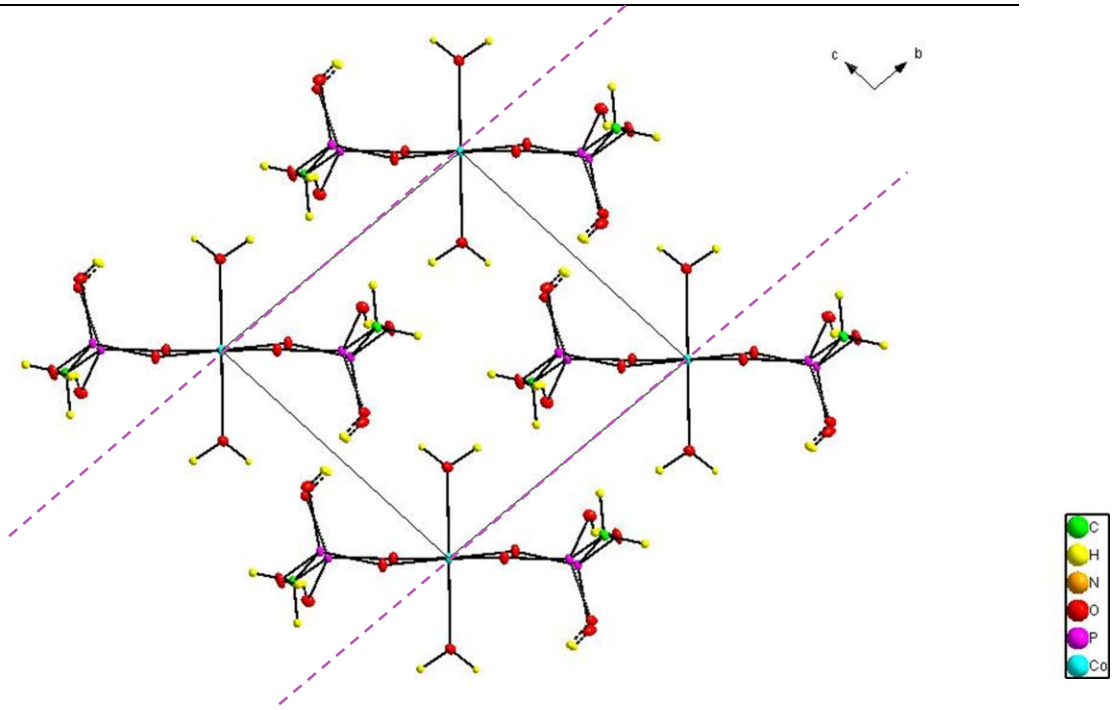

Figure 6.7 Crystal packing of ammonium diaquabis(MDP)cobaltate(II). The unit cell is viewed along the a-axis (cations have been removed for clarity).

The packing of the molecules as displayed in **Figure 6.7** appears to be in a 'sheet like' fashion. The molecules orientate themselves in parallel layers with each octahedral cation positioned in the center of the cell edges in the b-direction. The purple dotted line clearly indicates that the molecules also appear to pack diagonally.

6.4 Crystal structure of: Disodium diaquabis(methylenediphosphonato)cobaltate(II) dihydrate.

6.4.1 Introduction

The synthesis of disodium diaquabis(methylenediphosphonato)cobaltate(II) dihydrate, $Na_2[Co(CH_4O_6P_2)_2(H_2O)_2]\cdot 2H_2O$, was according to the procedure described in Section 3.7.2.5 and pink crystals were successfully harvested. The numbering scheme and molecular structure of $Na_2[Co(CH_4O_6P_2)_2(H_2O)_2]\cdot 2H_2O$ is presented in **Figure 6.8.** Important bond distances and non-hydrogen interactions are referred to in **Table 6.6** and essential bond angles and torsion angles are reported in **Table 6.7**.

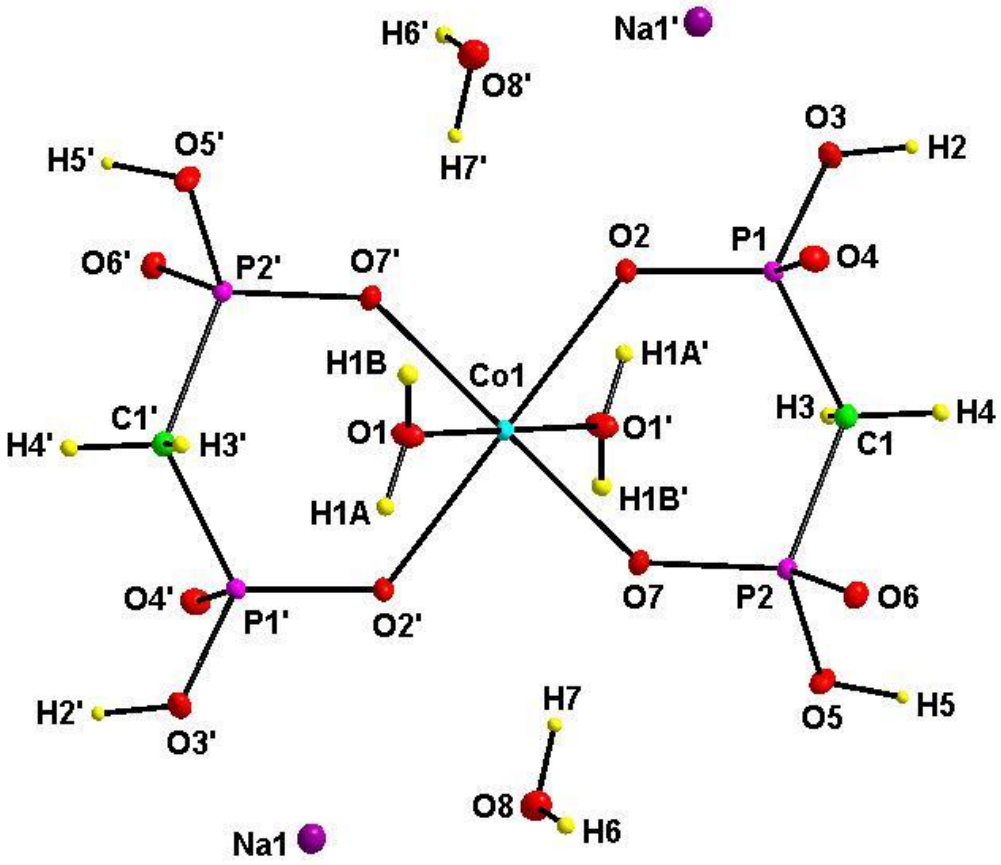

Figure 6.8 Molecular diagram of disodium diaquabis(methylenediphosphonato)cobaltate(II) dihydrate, displaying the numbering scheme of the atoms in the molecule. (ellipsoid probability = 50% except for the hydrogen atoms).

Table 6.6: Selected bond lengths and non-hydrogen bonding interactions present in disodium diaquabis(methylenediphosphonato)cobaltate(II) dihydrate.

Cobalt Distances (Å)		**Non-Hydrogen Bonding Interactions to 3,3 Å**	
Co1-O1	2.089(1)	P1----P2	3.025(1)
Co1-O2	2.115(1)	O1----O2	3.053(2)
Co1-O7	2.090(1)	O1----O7	2.867(2)
		O2----O3	2.465(1)
Diphosphonate Distances (Å)		O2----O7	2.980(2)
P1-O3	1.578(1)	O3----O4	2.539(1)
P1-O4	1.497(1)	O5----O6	2.530(1)
P1-C1	1.802(2)	O5----O7	2.478(1)
P2-O5	1.581(1)	O6----O7	2.557(1)
P2-O6	1.517(1)		
P2-C1	1.797(2)		

Table 6.7: Selected bond angles and torsion angles for disodium diaquabis-(methylenediphosphonato)cobaltate(II) dihydrate.

Cobalt Angles (°)		**Diphosphonate Angles (°)**	
O1-Co1-O2	93.16(4)	P1-C1-P2	114.36(8)
O1-Co1-O7	86.62(5)	O2-P1-O3	105.44(7)
O2-Co1-O7	90.25(5)	O2-P1-O4	115.28(7)
		O5-P2-O7	106.64(7)
Torsion Angles (°)		O6-P2-O7	115.47(7)
O3-P1-C1-P2	-174.16(8)		
O5-P2-C1-P1	161.81(8)		

6.4.2 Results and Discussion

The title compound, $Na_2[Co(CH_4O_6P_2)_2(H_2O)_2]\cdot 2H_2O$, crystallised in a monoclinic crystal system, in the *$P2_1/c$* space group. The asymmetric unit is composed of a non-coordinated water molecule, one sodium cation, one methylene diphosphonate ligand as well as one aqueous molecule coordinated to the cobalt atom.

In **Figure 6.8** the distorted $Co^{II}O_6$ is represented by two bidentate MDP ligands which are coordinated to the cobalt metal center (orientated on a special position)

along the equatorial axis and two aqueous molecules which are orientated along the axial axis.

The two methylene diphosphonate anions coordinate to the cobalt via four oxygen atoms (O2/O2' and O7/O7') originating from the phosphonate groups. This coordination leads to the formation of two six-membered rings. The last two positions are occupied by the two water molecules which are in a *trans* configuration.

The Co1-O1 atoms positioned along the axial axis have a distance of 2.089(1) Å. An interesting observation is that the atoms orientated on the equatorial axis are longer in length, Co1-O2 (2.115(1) Å) and Co1-O7 (2.090(1) Å), in comparison to the atoms on the axial axis. These distances correspond well with literature values.[16,17,18,19,20]

The O-Co-O bite angles of importance are O1-Co1-O2 (93.16(4)°), O1-Co1-O7 (86.62(5)°) and O2-Co1-O7 (90.25(5)°), which compare well with other corresponding structures.[16,18,19]

The compound consists of four phosphonates and each phosphonate has two unique types of P-O bonds present, namely the P-OH bonds and the P=O bonds. The P-OH bond distances are 1.578(1) Å for P1-O3 and 1.581(1) Å for P2-O5. The P=O bond distances are 1.497(1) Å for P1-O4 and 1.517(1) Å for P2-O6. These values relate well to literature values.[1,21,22] A distinguishing characteristic of the P-OH bonds is that they are more elongated compared to the P=O bonds.

The O-P-OH angles are 105.44(7)° for O2-P1-O3 and 106.64(7)° for O5-P2-O7, while the O-P=O angles are 115.28(7)° for O2-P1-O4 and 115.47(7) ° for O6-P2-O7. These values correlate well with other phosphonate complexes.[1,21,22,23]

[16] S. Bao, L. Zheng, Y. Liu, W. Xu and S. Feng. *Inorganic Chemistry*, 2003, **42**, 5037-5039.

[17] D. Cao, Y. Li and L. Zheng. *Inorganic Chemistry*, 2007, **46**, 7571-7578.

[18] Y. Gong, W. Tang, W. Hou, Z. Zha and C. Hu. *Inorganic Chemistry*, 2006, **45**, 4987-4995.

[19] P. Yin, S. Gao, L. Zheng and X. Xin. *Chem. Mater.*, 2003, **15**, 3233-3236.

[20] H.G. Visser, J.A. Venter and K.A. van der Merwe. *Acta Cryst.*, 2010, **E66**, m159.

[21] E. Freire and D.R. Vega. *Acta Cryst.*, 2009, **E65**, m1428-m1429.

[22] D. Vega, R. Baggio and O. Piro. *Acta Cryst.*, 1998, **C54**, 324-327.

[23] V.V. Bon, A.V. Dudko, A.N. Kozachkova, V.I. Pekhnyo and N.V. Tsaryk. *Acta Crystallographica Section E*, 2010, **E66**, m537-m538.

The O-P=O angles are larger in comparison to the O-P-OH angles and this is because of the partial double bond present.

In order to investigate the bent nature of the P-C-P ligand a plane was constructed through C1, P1, P2, O7, Co1, O2 as well as through C1', P1', P2', O7', O2' as displayed in **Figure 6.9.** It is clear to ascertain that P1-O3 and P2-O5 have an eclipsed conformation and this also applies to P1-O4 and P2-O6. P1-O3 and P2-O5 are pointing upwards, while P1-O4 and P2-O6 are directed downwards.

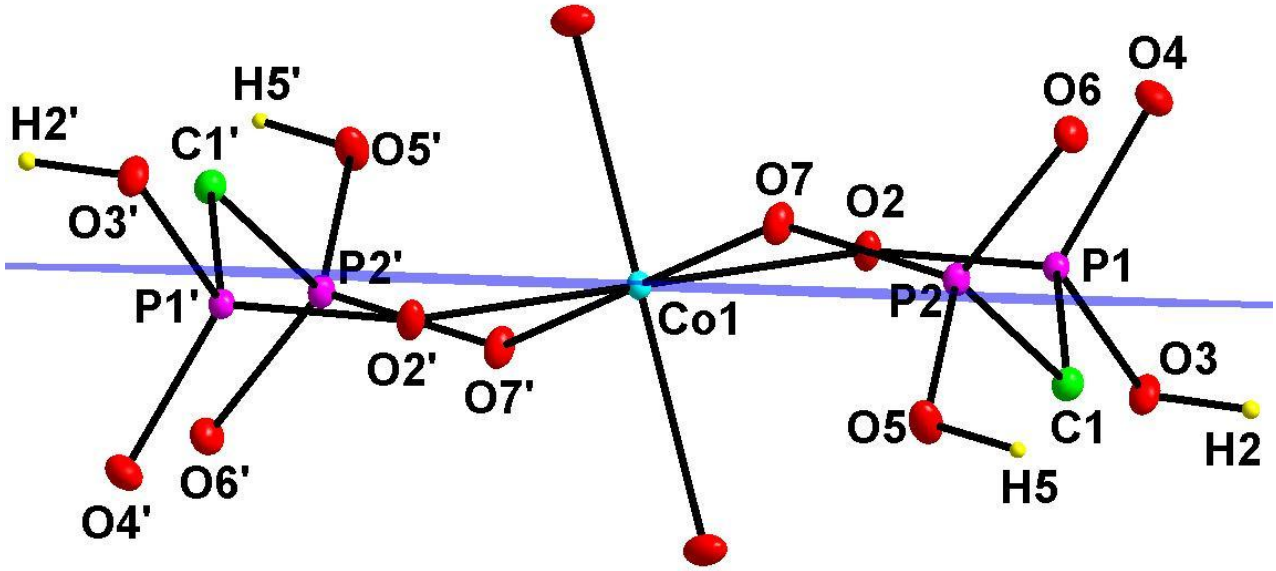

Figure 6.9 Illustration of disodium diaquabis(MDP)cobaltate(II) dihydrate, indicating the configuration of the P-O and P=O atoms as well as the orientation of the atoms on the plane (certain hydrogens, cations and non-coordinated water molecules have been omitted for clarity).

C1 is the most distant atom from the plane with a distance of 0.653(1) Å from the plane and is the only atom orientated on the one side of the plane, pointing downwards. P2 diverges a little with regards to the plane with a distance of 0.249(6) Å from the plane. Atoms O2, P1, P2 and O7 lie on the opposite side of the plane, pointing upwards. Atoms O7, P2, C1, P1, O2, Co1, O2', P1', C1', P2', O7' displays a form of a chair conformation while C1 and C1' are staggered with regards to one another.

Table 6.8: The expanse between the atoms and the horizontal plane constructed through C1, P1, P2, O7, Co1, O2 as well as through C1', P1', P2', O7', O2'.

Atom	Distance Å	Atom	Distance Å
O2	-0.328(7)	O2'	0.328(7)
P1	-0.249(6)	P1'	0.249(6)
C1	0.653(1)	C1'	-0.653(1)
P2	-0.111(4)	P2'	0.111(4)
O7	-0.497(2)	O7'	0.497(2)
Co1	0.000		

The significance of the P-C-P bond is explained thoroughly in Paragraph **5.3.2**. The P-C-P bond for an uncoordinated MDP ligand is displayed in **Figure 6.10(a)**.[12] By coordinating cobalt to the MDP ligand a few differences are observed as illustrated in **Figure 6.10(b)**. The P-C bonds as depicted in **Figure 6.10(b)** are almost identical to the P-C bond distances in **Figure 6.10(a).** The only noticeable difference is in the angles, the P-C-P angle in **Figure 6.10(b)** is 3° smaller in relation to that of **Figure 6.10(a)**. An explanation for the smaller P-C-P angle is because of ring strain.

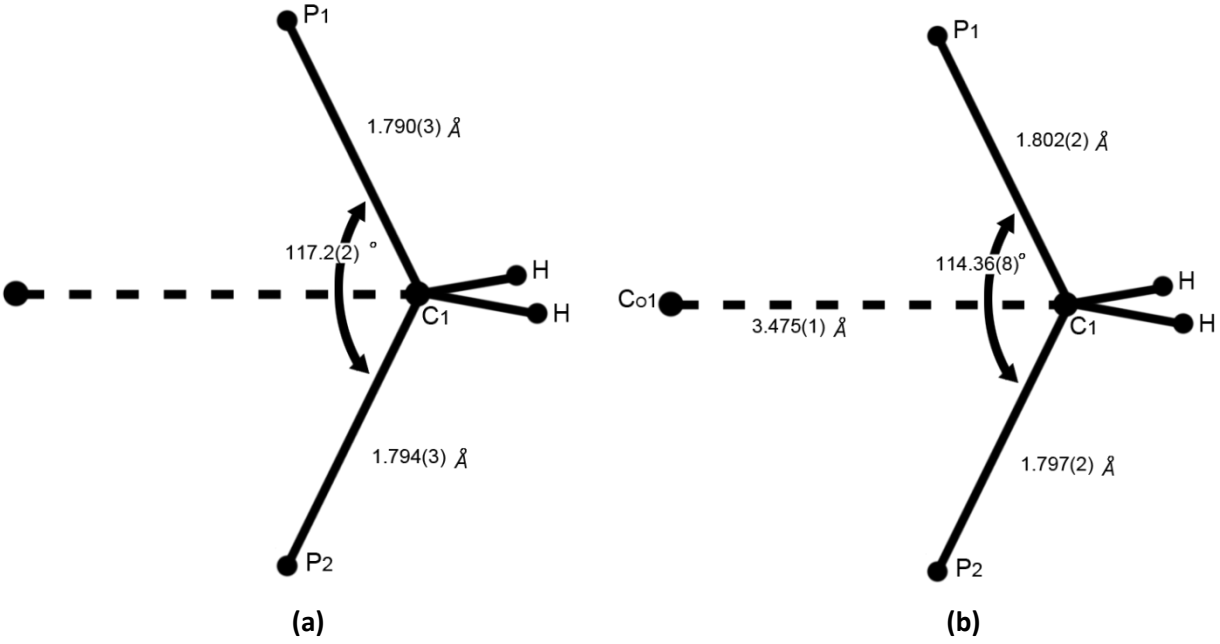

Figure 6.10 Graphical comparison of the P-C-P bond in (a) methylene diphosphonate and (b) disodium diaquabis(MDP)cobaltate(II) dihydrate.

The Co-C distance is 3.475(1) Å which is slightly shorter compared to the value of 3.63 Å in literature.[13] This complex differs to the one described in literature as it has two methylene diphosphonate ligand coordinating to the cobalt atom.

The importance of the "W" configuration is explained thoroughly in Paragraph **5.3.2**. The use of the term, "W" configuration is exercised when O3-P1-C1-P2-O5 forms a planar "W" which can clearly be seen in **Figure 6.11**. The "W" shape enables the MDP ligand to be doubly bidentate,[14] with regards to O2 and O7 on the one side of the "W" which is coordinating to the metal center and there is a possibility for O4 and O6 to coordinate to the same metal center on the other side. This "W" shape is determined by the O-P-C-P torsion angles which are -174.16(8)° for O3-P1'-C1-P2 and 161.81(8)° for O5-P2-C1-P1.

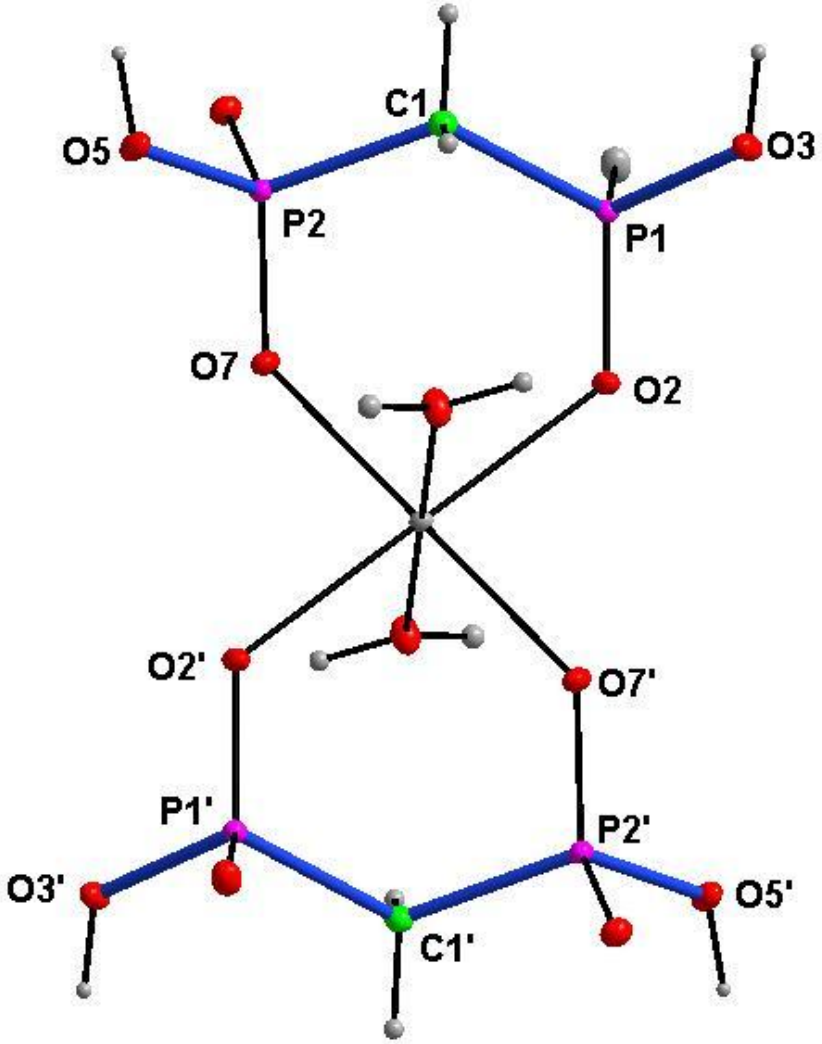

Figure 6.11 Molecular diagram of disodium diaquabis(MDP)cobaltate(II) dihydrate displaying the "W" configuration (cations and non-coordinated water molecules have been omitted for clarity).

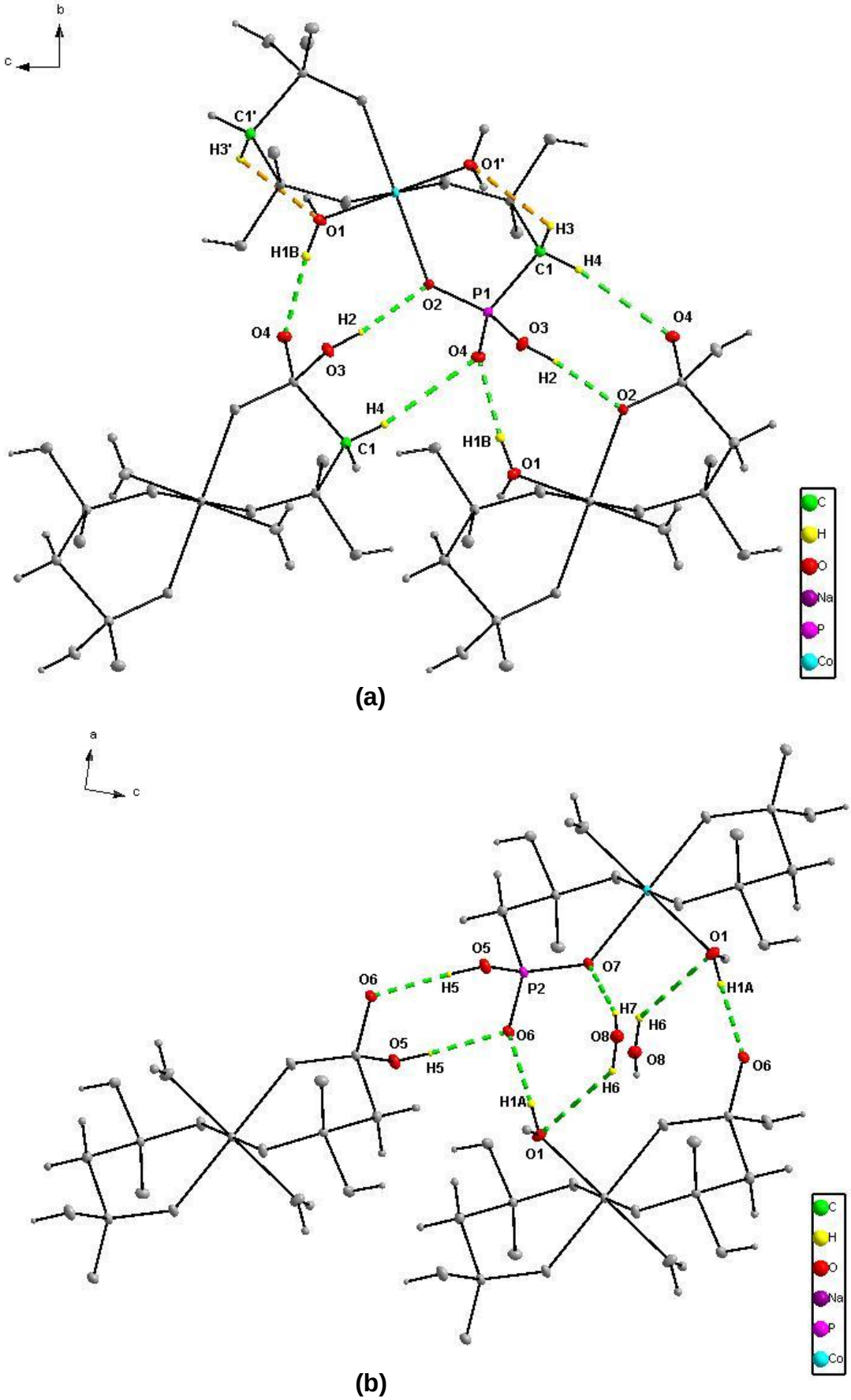

Figure 6.12 A breakdown of the intermolecular and intramolecular hydrogen bonding for disodium diaquabis(MDP)cobaltate(II) dihydrate, as shown in (a) and (b).

Table 6.9: The hydrogen bonding for disodium diaquabis(MDP)cobaltate(II) dihydrate [Å and°].

D-H…A	d(D-H)	D(H…A)	D(D…A)	<(DHA)
O1-H1A…O6^{v}	0.85(2)	1.95(2)	2.800(2)	176(3)
O1-H1B…O4^{vi}	0.84(2)	1.83(2)	2.664(2)	172(3)
O3-H2…O2^{iv}	0.84(2)	1.81(2)	2.639(2)	170(3)
O5-H5…O6^{vii}	0.83(2)	1.80(2)	2.626(2)	176(3)
O8-H6…O1^{v}	0.83(2)	2.57(3)	3.276(2)	143(3)
O8-H7…O7^{i,v}	0.85(3)	1.89(3)	2.716(2)	165(2)
C1-H3…O1^{ii,iii}	0.97	2.51	3.145(2)	123.2
C1-H4…O4^{iv}	0.97	2.5	3.435(2)	162.7

Symmetry transformations used to generate equivalent atoms:

(i) x, y, z; (ii) –x+1, -y+1, -z; (iii) x, y, z-1; (iv) x, -y+1/2, z-1/2; (v) –x, -y+1, -z; (vi) x, -y+1/2, z+1/2;

(vii) –x, -y+1, -z-1.

The complete list of all the hydrogen bond distances and angles is reported in **Table 6.9**. All the intermolecular and intramolecular hydrogen bonding interactions are illustrated in **Figure 6.12 (a)** and **(b)**.

The significance of water within a structure is explained in Paragraph **5.3.2**. Hydrogen bonding interactions or “soft contacts” cause O-H···O linkages between molecules and this leads to the formation of a three dimensional supramolecular network. Numerous intermolecular as well as intramolecular hydrogen bonding are present.

Figure 6.12 (a) which is viewed along the a-axis displays both intermolecular as well as intramolecular hydrogen bonding. The only intramolecular bonding which is represented by orange dashed lines occurs between the carbon atom C1 and the oxygen atom O1. The D-H···A angle which the intramolecular hydrogen bonding, (C1-H3…O1 angle is 123°), makes is smaller in comparison to all the intermolecular hydrogen bonding angles.

The O4, oxygen atom which is coordinated to the phosphonate P1 of the MDP ligand is the prominent hydrogen-bond acceptor towards a bifurcated hydrogen bond, which originates from the coordinated water molecule or the carbon from the methylene group. In **Figure 6.12 (b)** which is viewed along the b-axis, the O6 oxygen atom

from the phosphonate P2 is the main hydrogen bond acceptor, while the hydrogen coordinated to the aqueous molecule as well as the oxygen O5 from the phosphonate P2 are the hydrogen bond donors.

Based on this it is evident that the $–P(O)_2(OH)-$ group is able to be a hydrogen-bond donor as well as an acceptor. The soft contacts present seem to enhance the solid state ordering of the compound. **Table 6.6** displays that this P-C-P compound exhibits an extensive amount of intramolecular O···O interactions which range between 2.465(1) to 3.053(2) Å. Therefore the molecular packing of the complex is stabilized by intermolecular soft contacts as well as the intramolecular soft contact.

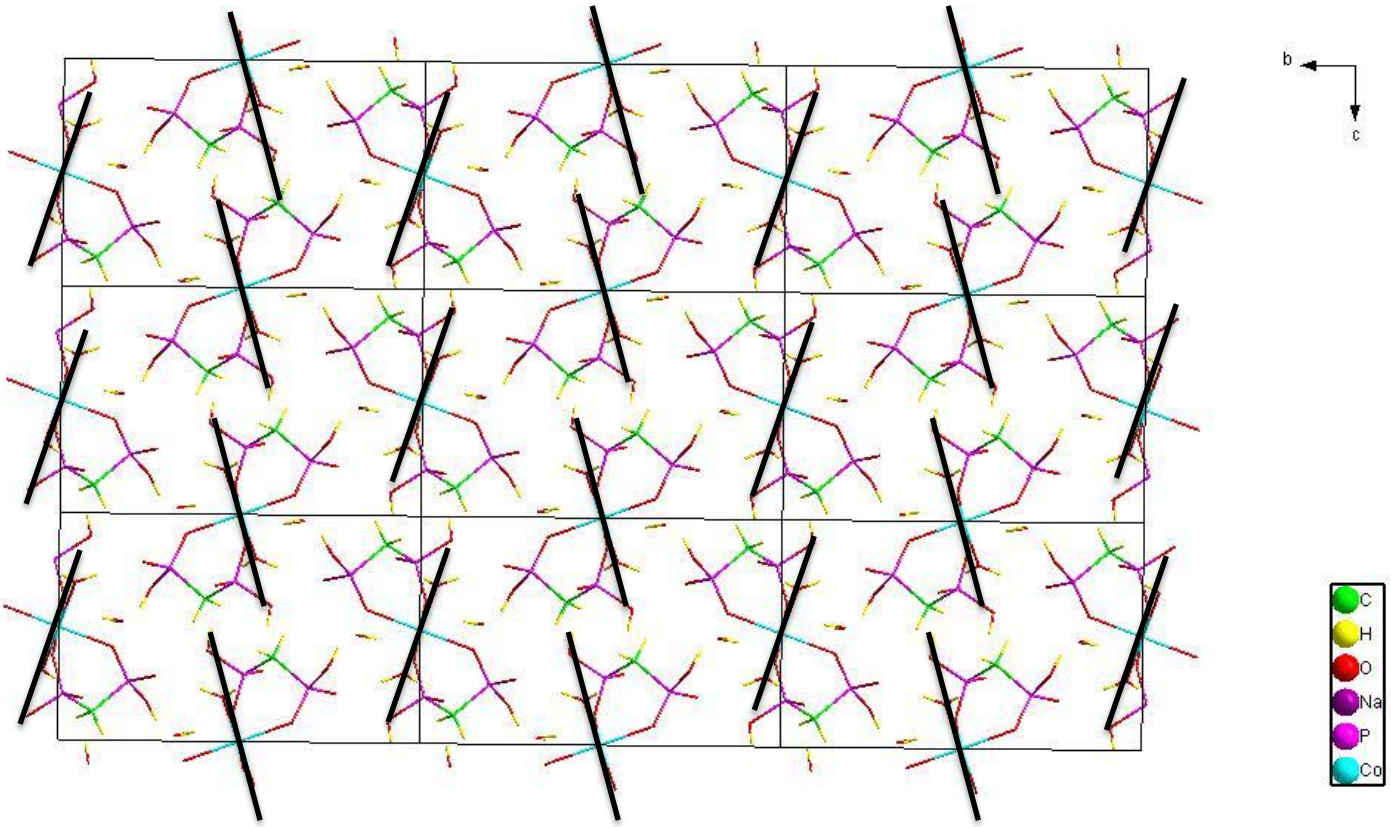

Figure 6.13 A 3x3 matrix displaying the crystal packing of disodium diaquabis(MDP)cobaltate(II) dihydrate. The matrix is viewed along the a-axis.

In **Figure 6.13** the molecules orientate themselves along the sides of the unit cell but no distinctive pattern is observable until the packing is expanded to a 3x3 matrix. The molecules appear to pack in a herring-bone fashion with the octahedral cation positioned in the center of the cell edges.

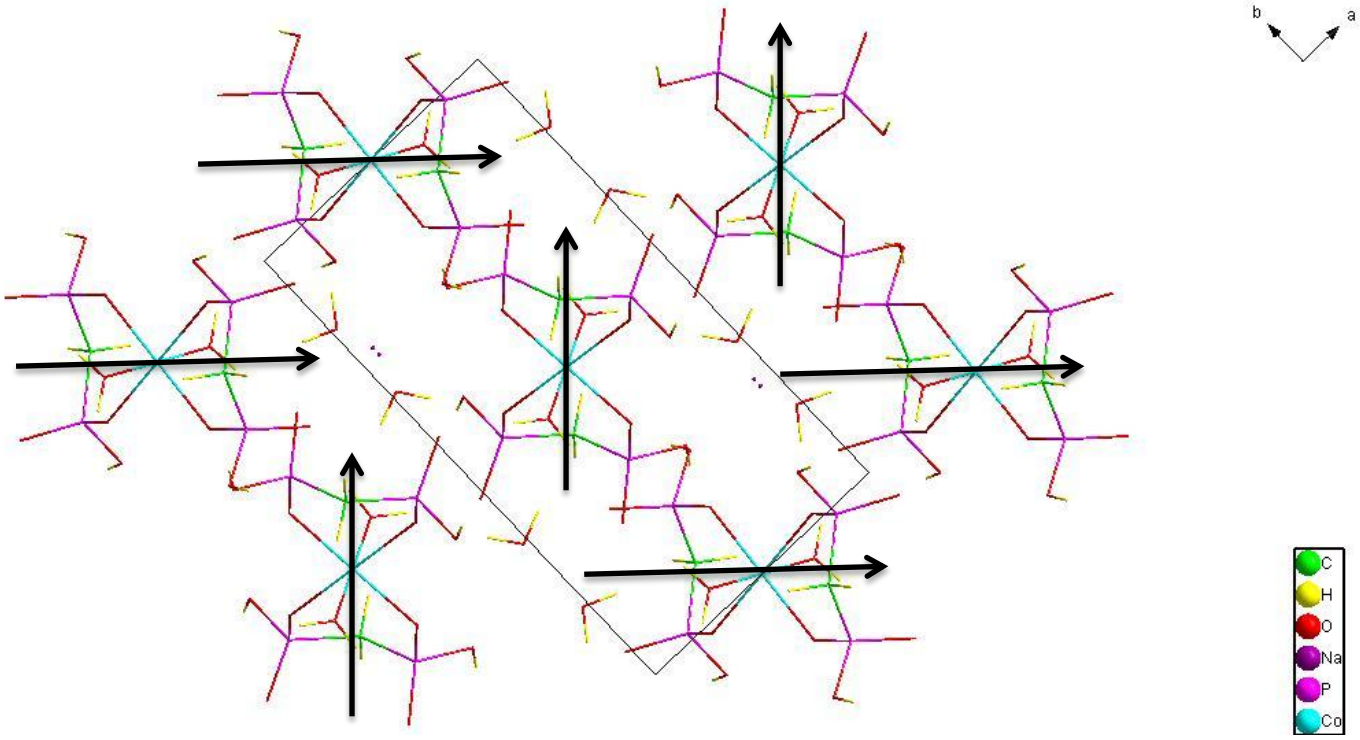

Figure 6.14 Stick packing diagrams of disodium diaquabis(MDP)cobaltate(II) dihydrate viewed along the c-axis.

Figure 6.14 displays the packing of the molecule as a stick diagram in order to clearly note the orientation of the molecules. The molecules pack in parallel lines horizontally but also appear to packing perpendicularly (within a row) with one molecule positioned horizontally and the molecule next to it lying vertically.

6.5 Crystal structure of: Dicesium diaquabis(methylenediphosphonato)cobaltate(II).

6.5.1 Introduction

The synthesis of dicesium diaquabis(methylenediphosphonato)cobaltate(II), $Cs_2[Co(CH_4O_6P_2)_2(H_2O)_2]$, was according to the procedure described in Section 3.7.2.6 from which pink crystals were harvested. The numbering scheme and molecular structure of $Cs_2[Co(CH_4O_6P_2)_2(H_2O)_2]$ is depicted in **Figure 6.15**. Important bond distances and non-hydrogen interactions are provided in **Table 6.10** and relevant bond angles and torsion angles are reported in **Table 6.11.**

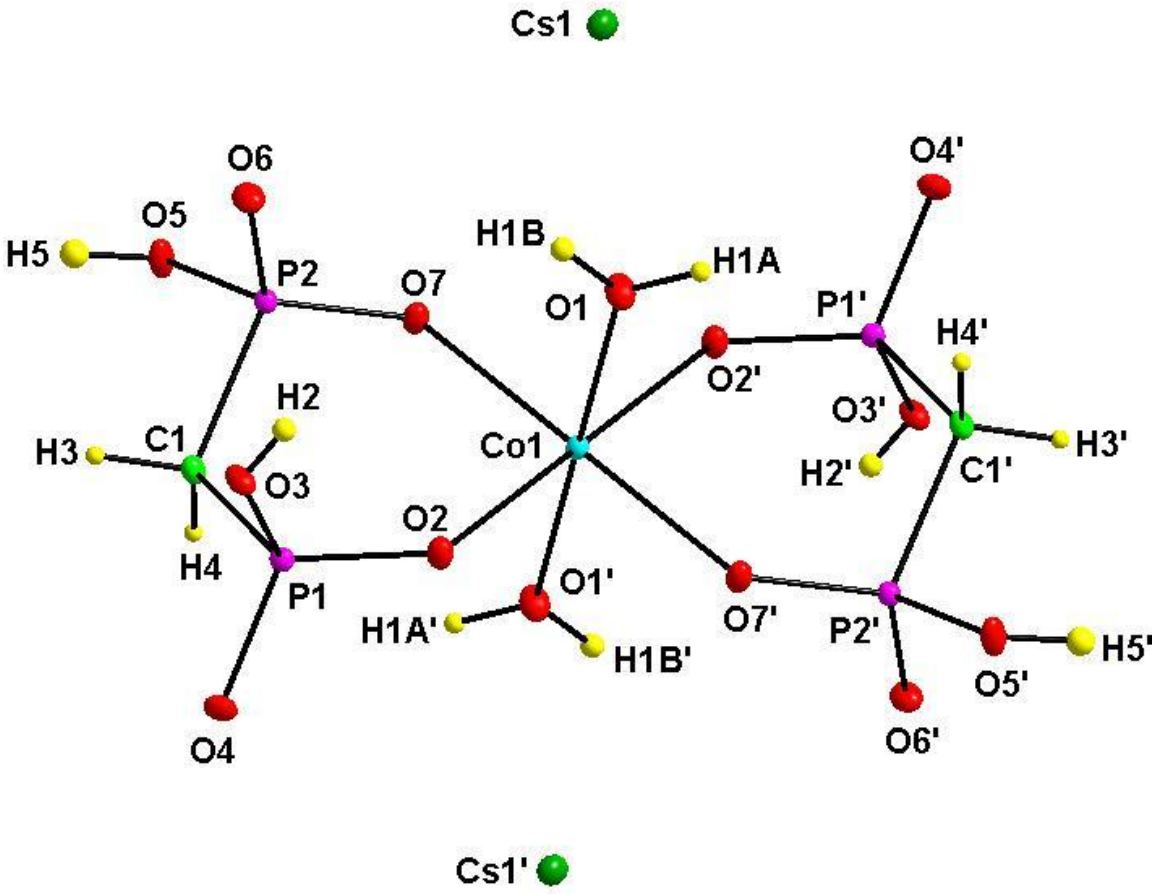

Figure 6.15 Graphical representation of dicesium diaquabis(MDP)cobaltate(II), displaying the numbering scheme of the atoms in the molecule (ellipsoid probability = 50% except for the hydrogen atoms).

Table 6.10: Selected bond lengths and non-hydrogen bonding interactions present in dicesium diaquabis(MDP)cobaltate(II).

Cobalt Distances (Å)		Non-Hydrogen Bonding Interactions to 3,3 Å	
Co1-O1	2.125(3)	P1----P2	3.062(2)
Co1-O2	2.079(3)	O1----O2	2.991(5)
Co1-O7	2.128(3)	O1----O7	3.046(5)
		O2----O3	2.523(2)
Diphosphonate Distances (Å)		O2----O7	3.090(5)
P1-O3	1.573(3)	O3----O4	2.491(1)
P1-O4	1.516(3)	O5----O6	2.518(1)
P1-C1	1.797(4)	O5----O7	2.546(1)
P2-O5	1.568(3)	O6----O7	2.548(2)
P2-O6	1.516(3)		
P2-C1	1.801(4)		

Table 6.11: Selected bond angles and torsion angles for the complex dicesium diaquabis(MDP)cobaltate(II).

Cobalt Angles (°)		Diphosphonate Angles (°)	
O1-Co1-O2	90.70(1)	P1-C1-P2	116.70(2)
O1-Co1-O7	91.44(1)	O2-P1-O3	109.97(2)
O2-Co1-O7	94.52(1)	O2-P1-O4	114.88(2)
		O5-P2-O7	111.69(2)
Torsion Angles (°)		O6-P2-O7	114.84(2)
O4-P1-C1-P2	-169.7(2)		
O5-P2-C1-P1	-179.6(2)		

6.5.2 Results and Discussion

$Cs_2[Co(CH_4O_6P_2)_2(H_2O)_2]$ is the title compound which crystallised in a triclinic crystal system, with a $P\bar{1}$ space group. The asymmetric unit is comprised of one cesium cation and half of a molecule which consists of one methylene diphosphonate ligand and one water molecule which are coordinated to a cobalt atom. The cobalt ion is located on a special position.

Figure 6.15 displays the $Co^{II}O_6$ which is a distorted octahedron comprised of two bidentate MDP ligands which coordinate to the cobalt metal center along the

equatorial axis and two aqueous molecules which are orientated along the axial axis and are in a *trans* configuration.

The two MDP ligands chelate to the cobalt via four oxygen atoms (O2/O2' and O7/O7') which arise from the phosphonate groups. This coordination results in two six-membered rings being formed.

The Co1-O1 atoms lie along the axial axis and have a distance of 2.125(3) Å. Co1-O2 with a distance of 2.079(3) Å and Co1-O7 with a distance of 2.128(3) Å are positioned on the equatorial axis and the Co1-O7 bond distance is surprisingly longer than the axial bond distance. These results correspond to other cobalt complexes.[16,17,18,19]

The relevant cobalt angles are the O1-Co1-O2 (90.70(1)°), O1-Co1-O7 (91.44(1)°) and finally the O2-Co1-O7 (94.52(1)°), these values deviate from the desired value of 90° for an octahedral and this results in the distorted geometry of the complex. The values also correlate to related literature values.[16,18,19,20]

$Cs_2[Co(CH_4O_6P_2)_2(H_2O)_2]$ has two types of P-O bonds, the P-OH and the P=O bonds. The P-OH bond distance for P1-O3 is 1.573(3) Å and for P2-O5. It is 1.568(3) Å. The P=O bond distances are 1.516(3) Å for P1-O4 and 1.516(3) Å for P2-O6, these values are similar to literature values.[13,24] A unique feature of the P-OH bonds is that they are longer in comparison to the P=O bonds.

There are two types of O-P-O angles, the O-P-OH angles: O2-P1-O3 (109.97(2)°), O5-P2-O7 (111.69(2)°), and the O-P=O angles: O2-P1-O4 (114.88(2)°) and O6-P2-O7 (114.84(2)°). These values correlate to other phosphonate complexes.[1,22,23] The reason for the O-P=O angles being larger in comparison to the O-P-OH angles is because of partial double bond present on O4 and O6. An interesting observation with regards to the P=O bond lengths and the O-P=O bond angles for O4/O4' and O6/O6' is that there bond lengths are equal and the bonds angles are almost identical.

[24] K. Stahl, J. Oddershede, H. Preikschat, E. Fischer and J.S. Bennekou. *Acta. Cryst.*, 2006, **C62**, m112-m115.

In order to evaluate the bent nature of the P-C-P ligand a plane was generated to pass through atoms C1, P1, P2, O7, Co1, O2 as well as through C1', P1', P2', O7', O2'. **Figure 6.16** displays that P1-O3 and P2-O5 has a staggered conformation with P1-O3 on the one side of the plane, pointing upwards and P2-O5 on the opposite side, pointing downwards. The same applies to P1-O4 and P2-O6.

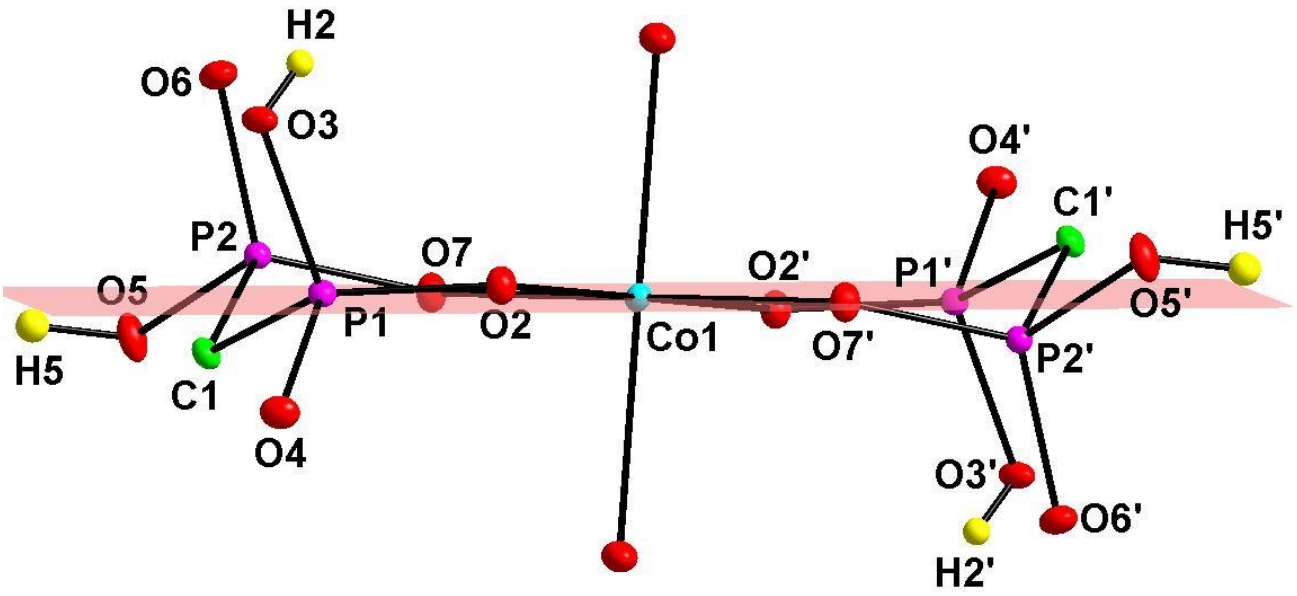

Figure 6.16 Partial structure of dicesium diaquabis(MDP)cobaltate(II) demonstrating the configuration of the P-O and P=O atoms as well as the orientation of the atoms on the plane (certain hydrogens and the cations have been removed for clarity).

Atom C1 is orientated the farthest with a distance of 0.421(3) Å, from the plane. Atom O7 lies almost on the plane with a distance of 0.008(3) Å, both C1 and O7 occur on the same side of the plane, pointing downwards. P2 which is positioned on the opposite side of the plane, pointing upwards diverges quite a bit with a distance of 0.316(3) Å from the plane. O2 (0.172(3) Å) and P1 (0.125(3) Å) are orientated on the same side of the plane and point upwards. O7, P2, C1, P1, O2, Co1, O2', P1', C1', P2', O7' forms a type of a chair conformation, with C1 and C1' displaying a staggered orientation.

Table 6.12: The distance between the atoms and the horizontal plane, which was constructed through C1, P1, P2, O7, Co1, O2 as well as through C1', P1', P2', O7', O2'.

Atom	Distance Å	Atom	Distance Å
O2	-0.172(3)	O2'	0.172(3)
P1	-0.125(3)	P1'	0.125(3)
C1	0.421(3)	C1'	-0.421(3)
P2	-0.316(3)	P2'	0.316(3)
O7	0.008(3)	O7'	-0.008(3)
Co1	0.000		

The relevance of the P-C-P bond is explained in detail in Paragraph **5.3.2**. **Figure 6.17(a)** illustrates the P-C-P bond for an uncoordinated MDP ligand,[12] once the MDP ligand is coordinated to the metal center (cobalt) differences in the P-C-P bond are observed as displayed in **Figure 6.17(b)**. The P-C bonds as depicted in **Figure 6.17(b)** are almost identical to the P-C bond distances in **Figure 6.17(a)**. Even the P-C-P angle in **Figure 6.17(b)** is almost identical to that of the MDP ligand with a difference of less than one degree.

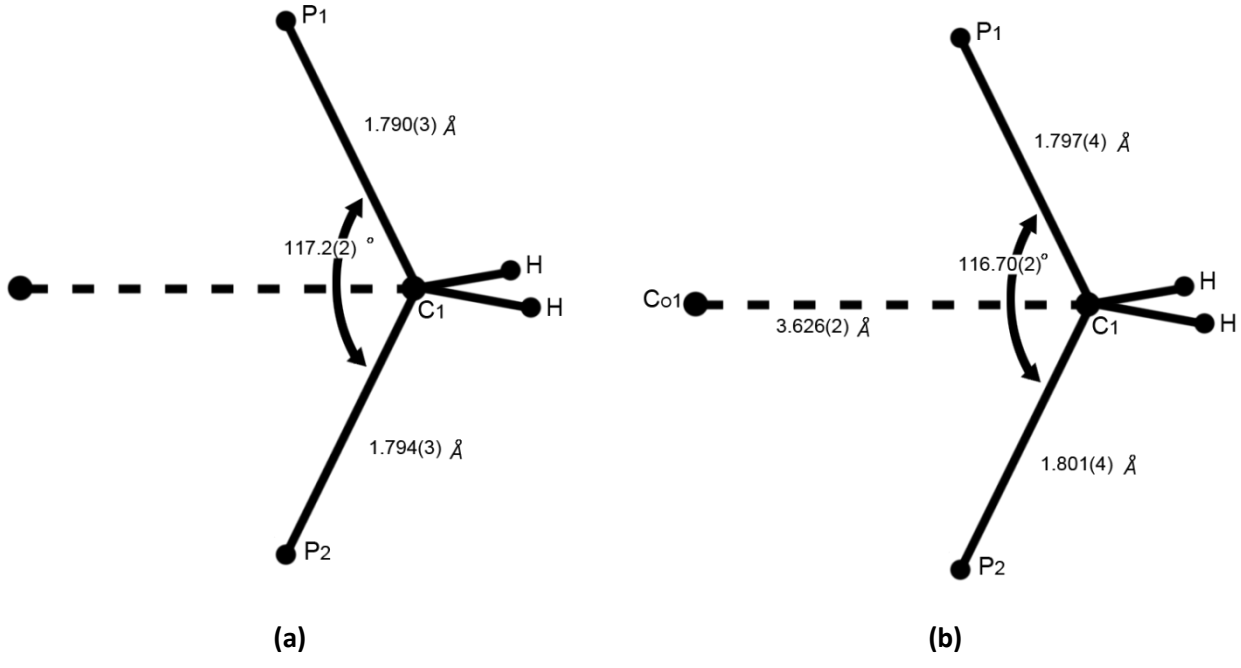

Figure 6.17 Schematic representation comparing the P-C-P linkage for (a) methylene diphosphonate and (b) dicesium diaquabis(MDP)cobaltate(II).

The Co-C distance is 3.626(2) Å which is practically identical to the value of 3.63 Å in literature, despite the fact that this complex has two methylene diphosphonate ligands coordinated to the metal center.[13]

The significance of the "W" configuration is explained in Paragraph **5.3.2.** The term, "W" configuration is employed when O4-P1-C1-P2-O5 forms a planar "W" shape which can clearly be observed in **Figure 6.18**. It allows the MDP ligand to be doubly bidentate,[14] which means that the O2 and O7 on the one side of the "W" can coordinate to the metal center and there is a possibility for O3 and O6 to attach to the metal center on the other side of the "W". O4-P1-C1-P2 (-169.7(2)°) and O5-P2-C1-P1 (-179.6(2)°) are the two torsion angles which make up the "W" configuration.

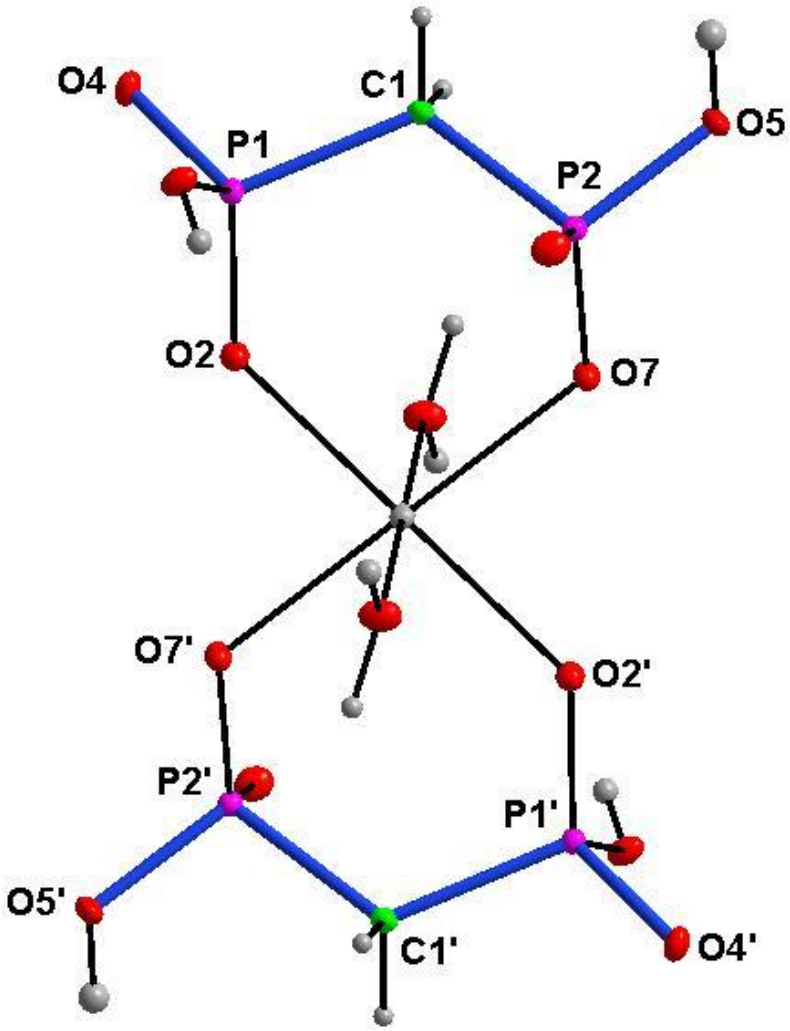

Figure 6.18 Molecular diagram of dicesium diaquabis(MDP)cobaltate(II) displaying the "W" shape (cations have been omitted for clarity).

Table 6.13: The soft contact present in dicesium diaquabis(MDP)cobaltate(II) [Å and °].

D-H…A	d(D-H)	D(H…A)	D(D…A)	<(DHA)
O1-H1A…O4^{iii}	0.87(2)	1.99(2)	2.856(5)	171(6)
O1-H1B…O6^{ii}	0.88(2)	1.97(7)	2.725(4)	142(1)
O3-H2…O6^{ii}	0.64(6)	1.91(6)	2.549(5)	175(7)
O5-H5…O5^{iv}	0.85(2)	2.44(6)	3.232(6)	156(1)
C1-H4…O4^{i}	0.97	2.56	3.481(5)	159

Symmetry transformations used to generate equivalent atoms:

(i) –x+1, -y, -z; (ii) –x, -y, -z+1; (iii) x, y, z+1; (iv) -x, -y+1, -z.

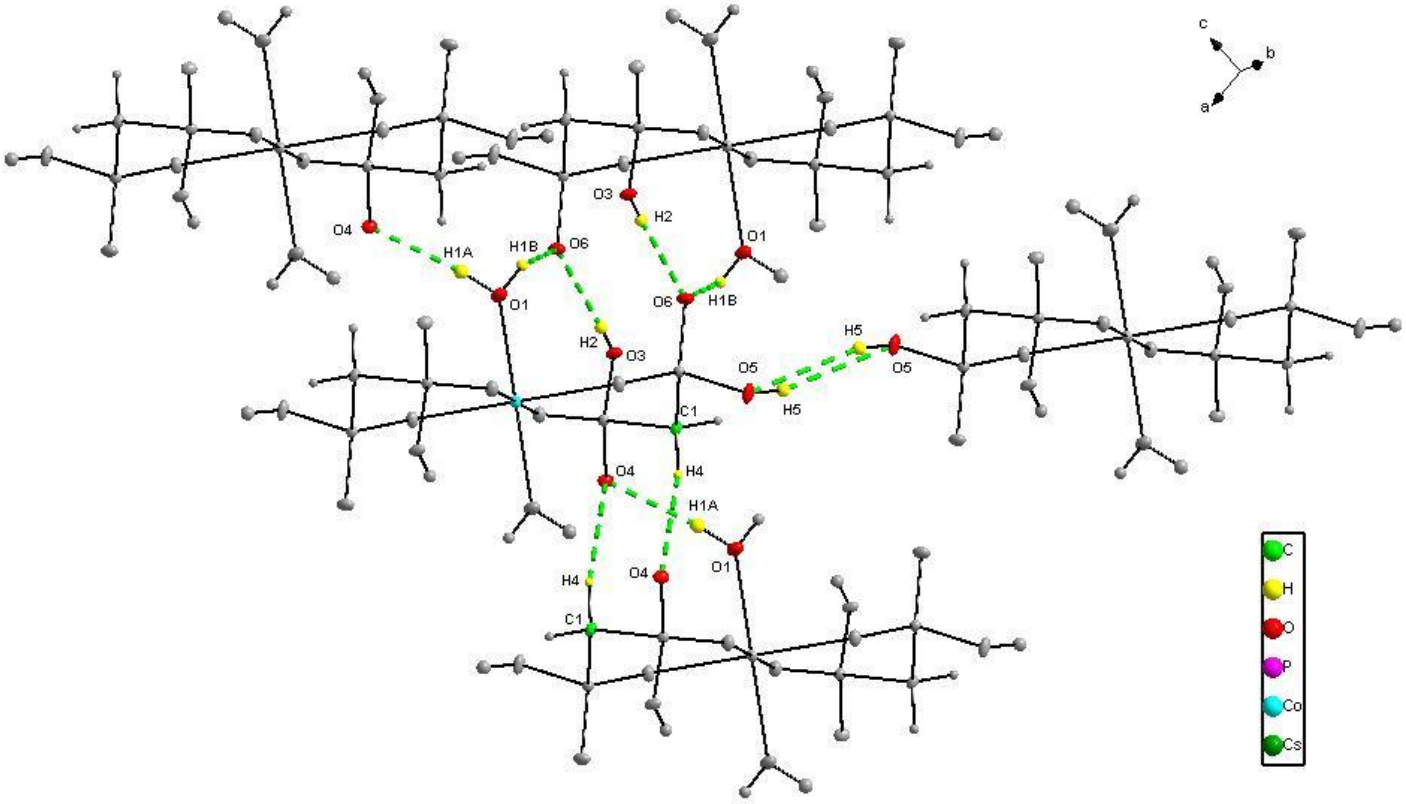

Figure 6.19 Graphical representation of the intermolecular hydrogen bond interactions found in dicesium diaquabis(MDP)cobaltate(II). The green fragmented lines indicate the intermolecular hydrogen interactions.

The complete list of all the hydrogen bond distances and angles is provided for in **Table 6.13**. All the intermolecular hydrogen bonding interactions are illustrated in **Figure 6.19**.

The significance of water present within a complex is explained in detail in Paragraph **5.3.2**. The “soft contacts” present result in O-H···O linkages between molecules and this leads to a three dimensional supramolecular network forming.

The packing of the dicesium diaquabis(MDP)cobaltate(II) compound is largely influenced by the various intermolecular hydrogen bonding interactions.

The phosphonate group is capable of being hydrogen bond donors or acceptors. The oxygen atoms O4 and O6 from the phosphonate groups P1 and P2 respectively are the hydrogen bond acceptors for all the intermolecular hydrogen bonds. The coordinated water molecule, as well as the oxygen atoms O3 and O6 and the C1 atom from the methylene group are the hydrogen bond donors. These soft contacts appear to enhance the solid state ordering of the compound. **Table 6.10** displays that the compound has a vast amount of intramolecular O···O interactions which range from 2.491(1) Å to 3.090(5) Å.

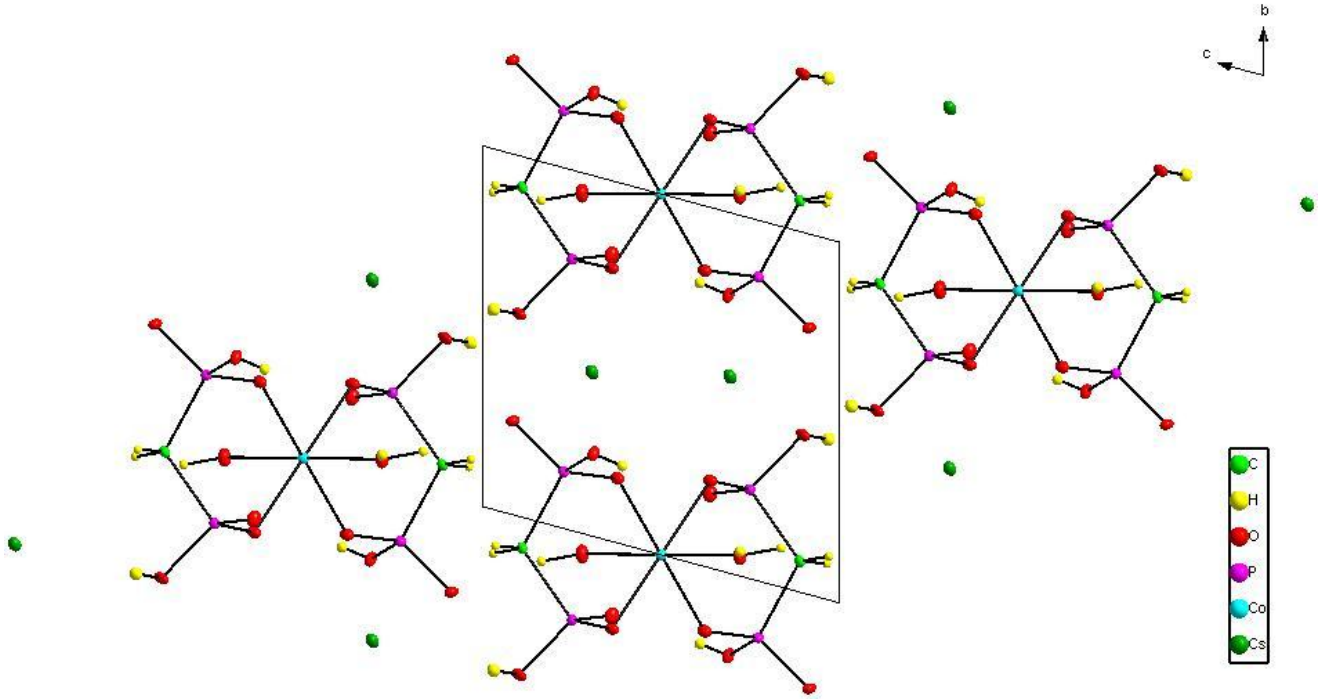

(a)

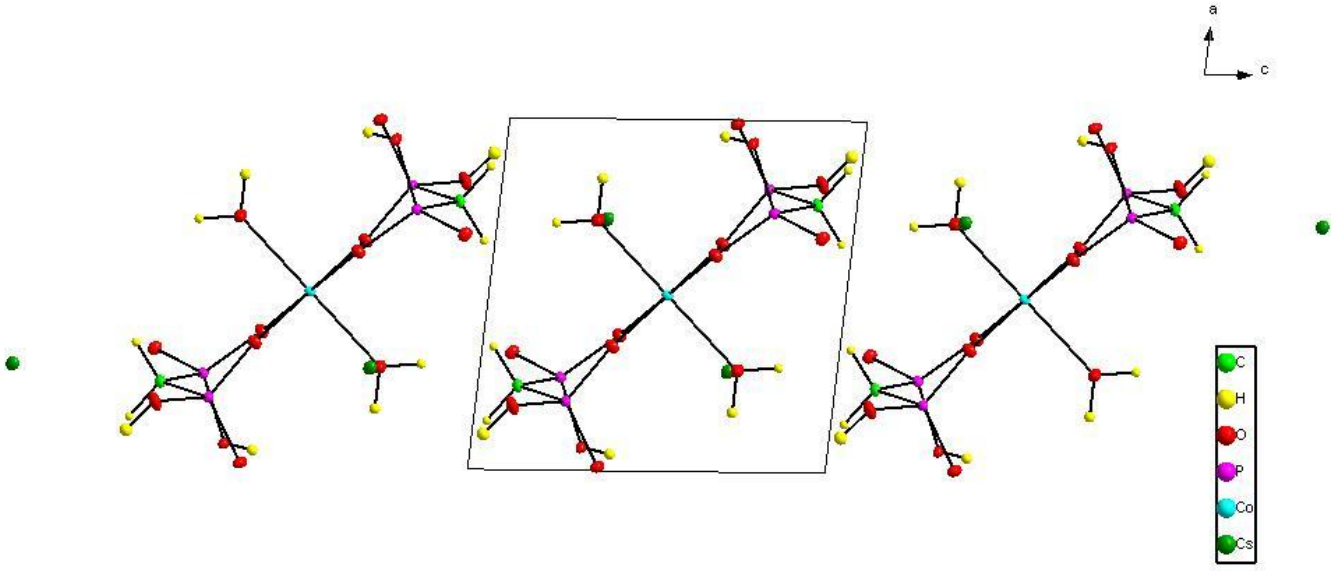

(b)

Figure 6.20 Perspective view of the unit cell of dicesium diaquabis(MDP)cobaltate(II) viewed along (a) the a-axis and (b) the b-axis.

The molecules pack in parallel lines horizontally as displayed in **Figure 6.20(a)** but also appear to packing diagonally as depicted in **Figure 6.20(b)**.

6.6 Conclusion

Three new of cobalt(II) complexes namely:

1. diammonium diaquabis(methylenediphosphonato)cobaltate(II),
2. disodium diaquabis(methylenediphosphonato)cobaltate(II) dihydrate and
3. dicesium diaquabis(methylenediphosphonato)cobaltate(II)

Each consisting of a O,O' bidentate ligand (MDP) were synthesized and characterised successfully by means of X-ray crystallography. A limited amount of related structures were available in literature and this indicated that there was an opening in this field of study.

Table 6.14: Summary comparing the bond distances for 1. $(NH_4)_2[Co(CH_4O_6P_2)_2(H_2O)_2]$, 2. $Na_2[Co(CH_4O_6P_2)_2(H_2O)_2]\cdot 2H_2O$ and 3. $Cs_2[Co(CH_4O_6P_2)_2(H_2O)_2]$.

Complex	$M\text{-}O_{(axial)}$ Distances (Å)		$M\text{-}O_{(equatorial)}$ Distances (Å)	
$(NH_4)_2[Co(CH_4O_6P_2)_2(H_2O)_2]$	Co1-O1	2.104(3)	Co1-O2 & Co1-O7	2.072(3) & 2.135(3)
$Na_2[Co(CH_4O_6P_2)_2(H_2O)_2]\cdot 2H_2O$	Co1-O1	2.089(1)	Co1-O2 & Co1-O7	2.115(1) & 2.090(1)
$Cs_2[Co(CH_4O_6P_2)_2(H_2O)_2]$	Co1-O1	2.125(3)	Co1-O2 & Co1-O7	2.079(3) & 2.128(3)

A summary of the geometrical deviations present between these complexes are provided in **Table 6.14** and **Table 6.15**. The Co(II) complexes have similar bond lengths as well as O-M-O angles but the P-C-P angle differs in these complexes and this might be due to the influence of the different cations.

Table 6.15: Summary comparing the bond angles for 1. $(NH_4)_2[Co(CH_4O_6P_2)_2(H_2O)_2]$, 2. $Na_2[Co(CH_4O_6P_2)_2(H_2O)_2]\cdot 2H_2O$ and 3. $Cs_2[Co(CH_4O_6P_2)_2(H_2O)_2]$.

Complex	O-M-O Angle (°)	P-C-P Angle (°)
$(NH_4)_2[Co(CH_4O_6P_2)_2(H_2O)_2]$	87.49(9)-95.23(9)	116.90(2)
$Na_2[Co(CH_4O_6P_2)_2(H_2O)_2]\cdot 2H_2O$	86.62(5)-93.16(4)	114.36(8)
$Cs_2[Co(CH_4O_6P_2)_2(H_2O)_2]$	90.70(1)-94.52(1)	116.70(2)

X-ray crystallography provided essential information regarding how the MDP ligand coordinated to the cobalt(II) complexes. Altering the cation did not influence the complex substantially.

It is clear from **Table 6.16** that the aqueous bond distances for all the cobalt(II) complexes as well as for $K[Co(CH_4O_6P_2)_2(H_2O)_2]$ are similar. For $K[Co(CH_4O_6P_2)(OH)_2(H_2O)_2]$ the $M\text{-}O_{(axial)}$ bond distance is the smallest because only one MDP ligand coordinates to the metal center. The P-C-P angles for all of the complexes are comparable to each other. By altering the quantity of bidentate ligands which coordinate to the metal as well as the metal employed will have a major influence on the $M\text{-}O_{(axial)}$ distances. All of these novel complexes could be utilized in the radiopharmaceutical industry but might also be employes as metal-organic frameworks.

Table 6.16: Comparison of the selected bond lengths as well as the selected bond angles for all the complexes.

Complex	$M\text{-}O_{(axial)}$ Distances (Å)		P-C-P Angle (°)
$(C_5H_6N)[Cr(CH_4O_6P_2)_2(H_2O)_2]\cdot 4H_2O$	Cr1-O1	1.991(4)	114.8 (3)
$K[Co(CH_4O_6P_2)_2(H_2O)_2]$	Co1-O1 & Co1A-O1A	2.083(3) & 2.126(4)	115.2(2)
$K[Co(CH_4O_6P_2)(OH)_2(H_2O)_2]$	Co1-O1 & Co1-O5	1.946(4) & 1.938(5)	116.11(1)
$(NH_4)_2[Co(CH_4O_6P_2)_2(H_2O)_2]$	Co1-O1	2.104(3)	116.90(2)
$Na_2[Co(CH_4O_6P_2)_2(H_2O)_2]\cdot 2H_2O$	Co1-O1	2.089(1)	114.36(8)
$Cs_2[Co(CH_4O_6P_2)_2(H_2O)_2]$	Co1-O1	2.125(3)	116.70(2)

7 Critical Evaluation of Study

7.1 Introduction

This chapter summarizes the results and the scientific relevance of the M.Sc. study and includes a discussion of future research possibilities.

7.2 Evaluation

The initial motivation for this M.Sc. study was to expand on the current knowledge regarding the chemistry and properties of the methylene diphosphonate ligand. A range of [M(MDP)] (M= Co(II), Co(III) and Cr(III)) complexes were synthesized. A large degree of the initial aims have successfully been attained.

Six novel MDP complexes have successfully been characterized by various spectroscopic techniques. The complexes were also characterized by X-ray crystallography in order to determine the coordination mode of the MDP ligand. The bond distances and angles correlated to each other and to other similar complexes. These characterizations were essential in contributing to the existing data pool.

All attempts to study the aqueous behaviour of these complexes were unsuccessful, mainly due to solubility issues. These challenges were somewhat alleviated with the synthesis of $K[Co(CH_4O_6P_2)(H_2O)_2(OH)_2]$, which contains only one MDP ligand (as opposed to two for the other complexes) and which is soluble over a wider pH range. However, the aqueous behaviour of this complex involves ten possible acid dissociation constants (two each for the aqua and hydroxo ligands and two for the MDP ligand) which put it outside of the scope of this study.

In order to circumvent the solubility problems we employed other means to characterize these complexes. Through XPS we were able to determine the charge of the metal present in each complex as well as the ratio between the metal to the metallic cations (counter ions) employed. The results from the elemental analysis correlated well with that of the assumed theoretical values. The protonation constants and equivalence points for methylene diphosphonate were successfully determined using three methodologies namely, the geometic method, the first derivative method and finally the second derivative method.

An extensive amount of intermolecular hydrogen bonding is present in each of the complexes which might also have an effect on the solubility of the complexes. To date no kinetic studies have been published on any MDP complexes and this could be due to solubility issues. Although not all of the aims in this study were attained, six new novel crystal structures with potential radiopharmaceutical applications were successfully obtained and characterized. These complexes might also be utilized as metal-organic frameworks.

7.3 Future Research

The evaluation of more water soluble complexes should be a major objective in future research which might be achieved by introducing different metal centers. Synthesis of the monodentate and bidentate MDP complexes in different solvents could possibly improve the solubility of the complex. Theoretical computational calculations could be used to determine the various K_a values to which the experimental K_a values could be correlated to.

APPENDIX A

A. Data for $(C_5H_6N)[Cr(CH_4O_6P_2)_2(H_2O)_2]\cdot 4H_2O$

Table 1.A: Atomic coordinates ($x10^4$) and equivalent isotropic displacement parameters ($Å^2 \times 10^3$) for $(C_5H_6N)[Cr(CH_4O_6P_2)_2(H_2O)_2]\cdot 4H_2O$. U(eq) is defined as one third of the trace of the orthogonalized U^{ij} tensor.

	x	y	z	U(eq)
C(1)	2683(8)	9145(8)	5903(6)	11(1)
C(2)	3206(12)	3837(11)	-627(8)	32(2)
C(3)	5612(13)	5896(11)	1367(8)	31(2)
N(1)	3810(70)	4790(80)	700(50)	28(12)
C(4)	3810(80)	4660(100)	780(50)	24(10)
O(1)	7325(6)	6953(6)	5401(4)	12(1)
O(2)	4491(6)	6457(6)	6635(4)	11(1)
O(3)	3700(6)	8943(6)	8418(4)	13(1)
O(4)	957(6)	6494(6)	6673(4)	12(1)
O(5)	-69(6)	7069(6)	3539(4)	13(1)
O(6)	2543(6)	9385(6)	3492(4)	13(1)
O(7)	3373(6)	6353(6)	3947(4)	11(1)
O(8)	2601(7)	9720(7)	11133(5)	20(1)
O(9)	-373(8)	7358(7)	8942(5)	24(1)
P(1)	2936(2)	7622(2)	6914(1)	9(1)
P(2)	2173(2)	7936(2)	4133(1)	9(1)
Cr(1)	5000	5000	5000	8(1)

Table 2.A: Bond distances (Å) and angles (º) for $(C_5H_6N)[Cr(CH_4O_6P_2)_2(H_2O)_2]\cdot 4H_2O$

Bond	Distance (Å)	Bond Angle	Angle(º)
C(1)-P(1)	1.797(6)	P(1)-C(1)-P(2)	114.8(3)
C(1)-P(2)	1.804(5)	P(1)-C(1)-H(3)	108.6
C(1)-H(3)	0.97	P(2)-C(1)-H(3)	108.6
C(1)-H(4)	0.97	P(1)-C(1)-H(4)	108.6
C(2)-N(1)	1.34(5)	P(2)-C(1)-H(4)	108.6
C(2)-C(3)^{viii}	1.371(13)	H(3)-C(1)-H(4)	107.5
C(2)-C(4)	1.41(5)	N(1)-C(2)-C(3)^{viii}	119(2)
C(2)-H(2A)	0.93	N(1)-C(2)-C(4)	6(6)
C(3)-N(1)	1.36(4)	C(3)viii-C(2)-C(4)	122(2)
C(3)-C(2)^{viii}	1.371(13)	N(1)-C(2)-H(2A)	120.7
C(3)-C(4)	1.40(5)	C(3)^{viii}-C(2)-H(2A)	120.7

C(3)-H(3A)	0.93	C(4)-C(2)-H(2A)	117.1
N(1)-H(1)	0.86	N(1)-C(3)-C(2)^{viii}	118(2)
C(4)-H(4A)	0.93	N(1)-C(3)-C(4)	6(6)
O(1)-Cr(1)	1.991(4)	C(2)^{viii}-C(3)-C(4)	122(3)
O(1)-H(1A)	0.80(6)	N(1)-C(3)-H(3A)	121.1
O(1)-H(1B)	0.83(6)	C(2)^{viii}-C(3)-H(3A)	121.1
O(2)-P(1)	1.515(4)	C(4)-C(3)-H(3A)	116.7
O(2)-Cr(1)	1.956(4)	C(2)-N(1)-C(3)	123(4)
O(3)-P(1)	1.568(4)	C(2)-N(1)-H(1)	118.3
O(3)-H(2)	0.82	C(3)-N(1)-H(1)	118.3
O(4)-P(1)	1.512(4)	C(3)-C(4)-C(2)	116(5)
O(5)-P(2)	1.568(4)	C(3)-C(4)-H(4A)	122.1
O(5)-H(5)	0.83(5)	C(2)-C(4)-H(4A)	122.1
O(6)-P(2)	1.499(4)	Cr(1)-O(1)-H(1A)	120(6)
O(7)-P(2)	1.519(4)	Cr(1)-O(1)-H(1B)	119(6)
O(7)-Cr(1)	1.964(4)	H(1A)-O(1)-H(1B)	107(9)
O(8)-H(6)	0.83(6)	P(1)-O(2)-Cr(1)	134.1(2)
O(8)-H(7)	0.85(7)	P(1)-O(3)-H(2)	109.5
O(9)-H(8)	0.83(6)	P(2)-O(5)-H(5)	114(5)
O(9)-H(9)	0.84(7)	P(2)-O(7)-Cr(1)	140.0(3)
P(1)-O(4)^{i}	1.512(4)	H(6)-O(8)-H(7)	114(10)
Cr(1)-O(2)^{ix}	1.956(4)	H(8)-O(9)-H(9)	108(10)
Cr(1)-O(7)^{ix}	1.964(4)	O(4)^{i}-P(1)-O(2)	115.5(2)
Cr(1)-O(1)^{ix}	1.991(4)	O(4)-P(1)-O(2)	115.5(2)
		O(4)^{i}-P(1)-O(3)	107.9(2)
		O(4)-P(1)-O(3)	107.9(2)
		O(2)-P(1)-O(3)	108.6(2)
		O(4)^{i}-P(1)-C(1)	110.1(2)
		O(4)-P(1)-C(1)	110.1(2)
		O(2)-P(1)-C(1)	107.6(2)
		O(3)-P(1)-C(1)	106.9(3)
		O(6)-P(2)-O(7)	114.8(2)
		O(6)-P(2)-O(5)	107.8(2)
		O(7)-P(2)-O(5)	109.7(2)
		O(6)-P(2)-C(1)	108.2(3)
		O(7)-P(2)-C(1)	109.0(2)
		O(5)-P(2)-C(1)	107.1(2)
		O(2)^{ix}-Cr(1)-O(2)	180.00(15)
		O(2)^{ix}-Cr(1)-O(7)	88.35(17)
		O(2)-Cr(1)-O(7)	91.65(17)
		O(2)^{ix}-Cr(1)-O(7)^{ix}	91.65(17)
		O(2)-Cr(1)-O(7)^{ix}	88.35(17)
		O(7)-Cr(1)-O(7)^{ix}	180.0(2)
		O(2)^{ix}-Cr(1)-O(1)^{ix}	90.51(17)

		O(2)-Cr(1)-O(1)^{ix}	89.49(17)
		O(7)-Cr(1)-O(1)^{ix}	90.81(18)
		O(7)^{ix}-Cr(1)-O(1)^{ix}	89.19(18)
		O(2)^{ix}-Cr(1)-O(1)	89.49(17)
		O(2)-Cr(1)-O(1)	90.51(17)
		O(7)-Cr(1)-O(1)	89.19(18)
		O(7)^{ix}-Cr(1)-O(1)	90.81(18)
		O(1)^{ix}-Cr(1)-O(1)	180.0(3)

Symmetry transformations used to generate equivalent atoms:

(i) x, y, z; (ii) –x+1, -y+2, -z+1; (iii) –x, -y+1, -z+1; (iv) x+1, y, z; (v) –x+1, -y+2, -z+2; (vi) x, y, z+1; (vii) –x, -y+2, -z+2; (viii) -x+1,-y+1,-z; ; (ix) -x+1, -y+1, -z+1

Table 3.A: Anisotropic displacement parameters for $(C_5H_6N)[Cr(CH_4O_6P_2)_2(H_2O)_2]\cdot 4H_2O$ ($Å^2$ x 10^3)

	U11	U22	U33	U23	U13	U12
C(1)	10(2)	8(2)	13(3)	3(2)	3(2)	1(2)
C(2)	33(4)	23(4)	29(4)	9(3)	-8(3)	0(3)
C(3)	42(5)	20(3)	21(3)	6(3)	-4(3)	7(3)
N(1)	40(20)	28(18)	33(19)	23(13)	19(16)	19(13)
C(4)	26(18)	19(15)	18(15)	8(13)	-8(12)	-1(12)
O(1)	8(2)	9(2)	19(2)	4(2)	3(2)	1(2)
O(2)	10(2)	12(2)	12(2)	4(2)	4(2)	5(2)
O(3)	11(2)	13(2)	13(2)	1(2)	4(2)	0(2)
O(4)	9(2)	11(2)	15(2)	4(2)	4(2)	0(1)
O(5)	8(2)	11(2)	19(2)	5(2)	2(2)	0(2)
O(6)	15(2)	11(2)	16(2)	7(2)	5(2)	2(2)
O(7)	10(2)	12(2)	14(2)	5(2)	5(2)	5(2)
O(8)	18(2)	26(2)	13(2)	5(2)	3(2)	-3(2)
O(9)	29(3)	24(3)	21(2)	7(2)	14(2)	4(2)
P(1)	7(1)	8(1)	10(1)	2(1)	3(1)	1(1)
P(2)	7(1)	8(1)	12(1)	4(1)	3(1)	2(1)
Cr(1)	7(1)	8(1)	11(1)	4(1)	4(1)	2(1)

Table 4.A: Hydrogen coordinates (x 10^4) and isotropic displacement parameters ($Å^2$ x 10^3) for $(C_5H_6N)[Cr(CH_4O_6P_2)_2(H_2O)_2]\cdot 4H_2O$

	x	y	z	U(eq)
H(3)	3885	10063	6226	13
H(4)	1633	9841	6027	13
H(2A)	2008	3014	-1034	39
H(3A)	6025	6454	2295	37
H(1)	3025	4691	1145	34
H(4A)	3051	4405	1294	29
H(2)	4774	9569	8570	20
H(1A)	7310(130)	8060(90)	5730(80)	25
H(1B)	8440(100)	6770(120)	5770(80)	30(20)
H(5)	-320(110)	5970(80)	3520(90)	30(30)
H(6)	2620(140)	9500(130)	11840(70)	30(20)
H(7)	1930(160)	8820(130)	10420(90)	60(30)
H(8)	20(130)	7100(130)	8280(80)	30(20)
H(9)	-1100(170)	8170(160)	8880(140)	70(40)

Table 5.A: Hydrogen bonds for $(C_5H_6N)[Cr(CH_4O_6P_2)_2(H_2O)_2]\cdot 4H_2O$

D-H...A	d(D-H)	d(H...A)	d(D...A)	<(DHA)
O(8)-H(7)...O(9)^{i}	0.85(7)	1.94(8)	2.748(7)	158(11)
O(9)-H(8)...O(4)^{i}	0.83(6)	2.00(6)	2.833(6)	179(10)
C(1)-H(3)...O(6)^{ii}	0.97	2.49	3.346(7)	146.8
O(1)-H(1A)...O(6)^{ii}	0.80(6)	1.83(6)	2.634(6)	176(9)
N(1)-H(1)...O(9)^{iii}	0.86	2.32	3.03(5)	140.5
C(4)-H(4A)...O(9)^{iii}	0.93	2.16	2.93(6)	140.1
O(5)-H(5)...O(4)^{iii}	0.83(5)	1.80(5)	2.619(6)	175(10)
O(1)-H(1B)...O(4)^{iv}	0.83(6)	1.87(6)	2.704(6)	177(9)
O(3)-H(2)...O(8)^{v}	0.82	1.83	2.629(6)	162.9
O(8)-H(6)...O(6)^{vi}	0.83(6)	1.86(6)	2.687(6)	171(9)
O(9)-H(9)...O(8)^{vii}	0.84(7)	1.99(7)	2.820(7)	174(13)

Symmetry transformations used to generate equivalent atoms:

(i) x, y, z; (ii) –x+1, -y+2, -z+1; (iii) –x, -y+1, -z+1; (iv) x+1, y, z; (v) –x+1, -y+2, -z+2; (vi) x, y, z+1; (vii) –x, -y+2, -z+2; (viii) -x+1,-y+1,-z; ; (ix) -x+1, -y+1, -z+1

Table 6.A: Torsion angles (º) for $(C_5H_6N)[Cr(CH_4O_6P_2)_2(H_2O)_2]\cdot 4H_2O$

Torsion Angle (º)	
C(3)^{viii}-C(2)-N(1)-C(3)	-5(7)
C(4)-C(2)-N(1)-C(3)	123(51)
C(2)^{viii}-C(3)-N(1)-C(2)	5(7)
C(4)-C(3)-N(1)-C(2)	-129(50)
N(1)-C(3)-C(4)-C(2)	43(42)
C(2)^{viii}-C(3)-C(4)-C(2)	-5(8)
N(1)-C(2)-C(4)-C(3)	-49(44)
C(3)^{viii}-C(2)-C(4)-C(3)	5(8)
Cr(1)-O(2)-P(1)-O(4)^{i}	76.5(4)
Cr(1)-O(2)-P(1)-O(4)	76.5(4)
Cr(1)-O(2)-P(1)-O(3)	-162.2(3)
Cr(1)-O(2)-P(1)-C(1)	-46.9(4)
P(2)-C(1)-P(1)-O(4)^{i}	-72.0(3)
P(2)-C(1)-P(1)-O(4)	-72.0(3)
P(2)-C(1)-P(1)-O(2)	54.7(4)
P(2)-C(1)-P(1)-O(3)	171.1(3)
Cr(1)-O(7)-P(2)-O(6)	132.7(4)
Cr(1)-O(7)-P(2)-O(5)	-105.8(4)
Cr(1)-O(7)-P(2)-C(1)	11.1(5)
P(1)-C(1)-P(2)-O(6)	-164.9(3)
P(1)-C(1)-P(2)-O(7)	-39.4(4)
P(1)-C(1)-P(2)-O(5)	79.2(3)
P(1)-O(2)-Cr(1)-O(2)^{ix}	-128(100)
P(1)-O(2)-Cr(1)-O(7)	19.2(4)
P(1)-O(2)-Cr(1)-O(7)^{ix}	-160.8(4)
P(1)-O(2)-Cr(1)-O(1)^{ix}	-71.6(4)
P(1)-O(2)-Cr(1)-O(1)	108.4(4)
P(2)-O(7)-Cr(1)-O(2)^{ix}	-177.9(4)
P(2)-O(7)-Cr(1)-O(2)	2.1(4)
P(2)-O(7)-Cr(1)-O(7)^{ix}	25(80)
P(2)-O(7)-Cr(1)-O(1)^{ix}	91.6(4)
P(2)-O(7)-Cr(1)-O(1)	-88.4(4)

Symmetry transformations used to generate equivalent atoms:

(i) x, y, z; (ii) –x+1, -y+2, -z+1; (iii) –x, -y+1, -z+1; (iv) x+1, y, z; (v) –x+1, -y+2, -z+2; (vi) x, y, z+1; (vii) –x, -y+2, -z+2; (viii) -x+1,-y+1,-z; ; (ix) -x+1, -y+1, -z+1

B. Data for $K[Co(CH_4O_6P_2)_2(H_2O)_2]$

Table 1.B: Atomic coordinates ($x10^4$) and equivalent isotropic displacement parameters ($Å^2 \times 10^3$) for $K[Co(CH_4O_6P_2)_2(H_2O)_2]$. U(eq) is defined as one third of the trace of the orthogonalized U^{ij} tensor.

	x	y	z	U(eq)
C(1)	6165(6)	-1336(4)	9122(3)	8(1)
C(1A)	6299(6)	3839(4)	5776(3)	8(1)
O(1)	6909(5)	-6649(4)	9462(2)	14(1)
O(1A)	2453(5)	1119(3)	4316(2)	9(1)
O(2)	7627(4)	-3576(3)	10354(2)	11(1)
O(2A)	7149(4)	1643(3)	4400(2)	8(1)
O(3)	8299(5)	-826(3)	10925(2)	10(1)
O(3A)	8190(5)	4320(3)	4026(2)	9(1)
O(4)	10208(4)	-1875(3)	9452(2)	9(1)
O(4A)	10178(4)	2998(3)	5451(2)	9(1)
O(5)	3411(4)	-1878(3)	7569(2)	9(1)
O(5A)	3898(4)	3337(3)	7356(2)	9(1)
O(6)	7069(4)	-2784(3)	7346(2)	10(1)
O(6A)	7656(5)	2613(3)	7543(2)	11(1)
O(7)	4598(4)	-4160(3)	8513(2)	9(1)
O(7A)	4857(5)	1095(3)	6386(2)	10(1)
P(1)	8178(2)	-1986(1)	9986(1)	7(1)
P(1A)	8066(2)	3124(1)	4901(1)	7(1)
P(2)	5370(2)	-2644(1)	8069(1)	7(1)
P(2A)	5762(2)	2612(1)	6826(1)	7(1)
K(1)	262(1)	-4595(1)	8129(1)	13(1)
K(1A)	804(1)	769(1)	6992(1)	11(1)
Co(1)	5000	-5000	10000	6(1)
Co(1A)	5000	0	5000	7(1)

Table 2.B: Bond distances (Å) and angles (º) for $K[Co(CH_4O_6P_2)_2(H_2O)_2]$.

Bond	Distance (Å)	Bond Angle	Angle(º)
C(1)-P(1)	1.803(4)	P(1)-C(1)-P(2)	115.2(2)
C(1)-P(2)	1.807(4)	P(1)-C(1)-H(3)	108.5
C(1)-H(3)	0.97	P(2)-C(1)-H(3)	108.5
C(1)-H(4)	0.97	P(1)-C(1)-H(4)	108.5
C(1A)-P(1A)	1.794(4)	P(2)-C(1)-H(4)	108.5
C(1A)-P(2A)	1.806(4)	H(3)-C(1)-H(4)	107.5
C(1A)-H(3A)	0.97	P(1A)-C(1A)-P(2A)	115.5(2)
C(1A)-H(4A)	0.97	P(1A)-C(1A)-H(3A)	108.4
O(1)-Co(1)	2.083(3)	P(2A)-C(1A)-H(3A)	108.4
O(1)-K(1)^{viii}	3.333(3)	P(1A)-C(1A)-H(4A)	108.4
O(1)-H(1A)	0.864(19)	P(2A)-C(1A)-H(4A)	108.4
O(1)-H(1B)	0.865(19)	H(3A)-C(1A)-H(4A)	107.5
O(1A)-Co(1A)	2.126(3)	Co(1)-O(1)-K(1)^{viii}	103.16(11)
O(1A)-K(1A)^{ix}	3.024(3)	Co(1)-O(1)-H(1A)	131(3)
O(1A)-H(1A1)	0.84(2)	K(1)^{viii}-O(1)-H(1A)	101(4)
O(1A)-H(1B1)	0.85(2)	Co(1)-O(1)-H(1B)	122(3)
O(2)-P(1)	1.507(3)	K(1)^{viii}-O(1)-H(1B)	65(4)
O(2)-Co(1)	2.065(3)	H(1A)-O(1)-H(1B)	107(3)
O(2)-K(1)^{x}	2.913(3)	Co(1A)-O(1A)-K(1A)^{ix}	118.87(12)
O(2A)-P(1A)	1.509(3)	Co(1A)-O(1A)-H(1A1)	118(5)
O(2A)-Co(1A)	2.132(3)	K(1A)^{ix}-O(1A)-H(1A1)	85(5)
O(2A)-K(1A)^{iv}	3.154(3)	Co(1A)-O(1A)-H(1B1)	113(5)
O(3)-P(1)	1.575(3)	K(1A)^{ix}-O(1A)-H(1B1)	109(5)
O(3)-K(1A)^{xi}	2.774(3)	H(1A1)-O(1A)-H(1B1)	111(7)
O(3)-H(2)	0.846(15)	P(1)-O(2)-Co(1)	129.18(17)
O(3A)-P(1A)	1.575(3)	P(1)-O(2)-K(1)^{x}	130.56(16)
O(3A)-K(1)^{iv}	3.077(3)	Co(1)-O(2)-K(1)^{x}	100.08(10)
O(3A)-H(2A)	0.85(2)	P(1A)-O(2A)-Co(1A)	127.64(16)
O(4)-P(1)	1.522(3)	P(1A)-O(2A)-K(1A)^{iv}	130.13(15)
O(4)-K(1)^{viii}	2.911(3)	Co(1A)-O(2A)-K(1A)^{iv}	94.86(9)
O(4A)-P(1A)	1.517(3)	P(1)-O(3)-K(1A)^{xi}	139.97(16)
O(4A)-K(1A)^{viii}	2.871(3)	P(1)-O(3)-H(2)	109(5)
O(5)-P(2)	1.581(3)	K(1A)^{xi}-O(3)-H(2)	105(5)
O(5)-K(1A)	3.017(3)	P(1A)-O(3A)-K(1)^{iv}	139.87(15)
O(5)-K(1)	3.157(3)	P(1A)-O(3A)-H(2A)	116(4)
O(5)-H(5)	0.84(2)	K(1)^{iv}-O(3A)-H(2A)	91(4)
O(5A)-P(2A)	1.581(3)	P(1)-O(4)-K(1)^{viii}	107.38(14)
O(5A)-K(1A)	2.922(3)	P(1A)-O(4A)-K(1A)^{viii}	121.20(15)
O(5A)-K(1)^{i}	3.235(3)	P(2)-O(5)-K(1A)	155.11(16)

O(5A)-H(6A)	0.83(2)	P(2)-O(5)-K(1)	93.88(13)
O(6)-P(2)	1.502(3)	K(1A)-O(5)-K(1)	106.18(9)
O(6)-K(1)^{viii}	2.830(3)	P(2)-O(5)-H(5)	119(5)
O(6A)-P(2A)	1.501(3)	K(1A)-O(5)-H(5)	68(5)
O(6A)-K(1A)^{viii}	2.779(3)	K(1)-O(5)-H(5)	110(5)
O(6A)-K(1)^{xii}	2.937(3)	P(2A)-O(5A)-K(1A)	98.21(13)
O(7)-P(2)	1.525(3)	P(2A)-O(5A)-K(1)^{i}	168.12(16)
O(7)-Co(1)	2.117(3)	K(1A)-O(5A)-K(1)^{i}	88.82(8)
O(7)-K(1)	2.816(3)	P(2A)-O(5A)-H(6A)	107(5)
O(7A)-P(2A)	1.502(3)	K(1A)-O(5A)-H(6A)	151(5)
O(7A)-Co(1A)	2.052(3)	K(1)^{i}-O(5A)-H(6A)	69(5)
O(7A)-K(1A)	2.779(3)	P(2)-O(6)-K(1)^{viii}	112.04(14)
P(1)-K(1)^{viii}	3.6663(14)	P(2A)-O(6A)-K(1A)^{viii}	116.85(15)
P(2)-K(1)	3.6247(14)	P(2A)-O(6A)-K(1)^{xii}	123.21(16)
P(2)-K(1)^{viii}	3.6678(13)	K(1A)^{viii}-O(6A)-K(1)^{xii}	97.96(9)
P(2A)-K(1A)	3.5148(13)	P(2)-O(7)-Co(1)	130.61(17)
P(2A)-K(1A)^{viii}	3.7080(13)	P(2)-O(7)-K(1)	109.59(14)
K(1)-O(6)^{v}	2.830(3)	Co(1)-O(7)-K(1)	101.82(11)
K(1)-O(4)^{v}	2.911(3)	P(2A)-O(7A)-Co(1A)	133.29(17)
K(1)-O(2)^{x}	2.913(3)	P(2A)-O(7A)-K(1A)	106.53(14)
K(1)-O(6A)^{xiii}	2.937(3)	Co(1A)-O(7A)-K(1A)	108.91(12)
K(1)-O(3A)^{iv}	3.077(3)	O(2)-P(1)-O(4)	113.34(16)
K(1)-O(5A)^{iii}	3.235(3)	O(2)-P(1)-O(3)	108.29(17)
K(1)-O(1)^{v}	3.333(3)	O(4)-P(1)-O(3)	110.16(17)
K(1)-P(1)^{v}	3.6663(14)	O(2)-P(1)-C(1)	111.55(18)
K(1)-P(2)^{v}	3.6678(13)	O(4)-P(1)-C(1)	107.70(17)
K(1A)-O(3)^{xi}	2.774(3)	O(3)-P(1)-C(1)	105.53(17)
K(1A)-O(6A)^{v}	2.779(3)	O(2)-P(1)-K(1)^{viii}	75.36(12)
K(1A)-O(4A)^{v}	2.871(3)	O(4)-P(1)-K(1)^{viii}	49.27(11)
K(1A)-O(1A)^{ix}	3.024(3)	O(3)-P(1)-K(1)^{viii}	155.42(12)
K(1A)-O(2A)^{iv}	3.154(3)	C(1)-P(1)-K(1)^{viii}	95.03(13)
K(1A)-P(2A)^{v}	3.7080(13)	O(2A)-P(1A)-O(4A)	114.50(16)
K(1A)-Co(1A)	3.9535(9)	O(2A)-P(1A)-O(3A)	105.60(16)
K(1A)-K(1)^{i}	4.3142(13)	O(4A)-P(1A)-O(3A)	111.04(16)
K(1A)-H(5)	2.82(7)	O(2A)-P(1A)-C(1A)	109.74(18)
Co(1)-O(2)^{x}	2.065(3)	O(4A)-P(1A)-C(1A)	109.11(17)
Co(1)-O(1)^{x}	2.083(3)	O(3A)-P(1A)-C(1A)	106.51(17)
Co(1)-O(7)^{x}	2.117(3)	O(6)-P(2)-O(7)	114.63(17)
Co(1)-K(1)^{x}	3.8544(9)	O(6)-P(2)-O(5)	112.37(16)
Co(1A)-O(7A)^{iv}	2.052(3)	O(7)-P(2)-O(5)	107.37(16)
Co(1A)-O(1A)^{iv}	2.126(3)	O(6)-P(2)-C(1)	111.66(18)
Co(1A)-O(2A)^{iv}	2.132(3)	O(7)-P(2)-C(1)	107.34(17)
Co(1A)-K(1A)^{iv}	3.9535(9)	O(5)-P(2)-C(1)	102.63(17)
		O(6)-P(2)-K(1)	131.67(13)

		O(7)-P(2)-K(1)	47.05(11)
		O(5)-P(2)-K(1)	60.32(11)
		C(1)-P(2)-K(1)	116.55(13)
		O(6)-P(2)-K(1)^{viii}	45.65(11)
		O(7)-P(2)-K(1)^{viii}	81.46(11)
		O(5)-P(2)-K(1)^{viii}	156.64(11)
		C(1)-P(2)-K(1)^{viii}	94.89(13)
		K(1)-P(2)-K(1)^{viii}	124.44(4)
		O(6A)-P(2A)-O(7A)	118.23(17)
		O(6A)-P(2A)-O(5A)	111.02(16)
		O(7A)-P(2A)-O(5A)	104.52(16)
		O(6A)-P(2A)-C(1A)	109.52(18)
		O(7A)-P(2A)-C(1A)	107.35(18)
		O(5A)-P(2A)-C(1A)	105.36(17)
		O(6A)-P(2A)-K(1A)	130.05(12)
		O(7A)-P(2A)-K(1A)	49.28(11)
		O(5A)-P(2A)-K(1A)	55.36(11)
		C(1A)-P(2A)-K(1A)	120.39(14)
		O(6A)-P(2A)-K(1A)^{viii}	41.97(11)
		O(7A)-P(2A)-K(1A)^{viii}	85.98(12)
		O(5A)-P(2A)-K(1A)^{viii}	150.43(12)
		C(1A)-P(2A)-K(1A)^{viii}	97.39(13)
		K(1A)-P(2A)-K(1A)^{viii}	126.55(4)
		O(7)-K(1)-O(6)^{v}	135.51(9)
		O(7)-K(1)-O(4)^{v}	83.18(8)
		O(6)^{v}-K(1)-O(4)^{v}	72.44(8)
		O(7)-K(1)-O(2)^{x}	60.11(8)
		O(6)^{v}-K(1)-O(2)^{x}	155.41(9)
		O(4)^{v}-K(1)-O(2)^{x}	94.72(9)
		O(7)-K(1)-O(6A)^{xiii}	130.52(9)
		O(6)^{v}-K(1)-O(6A)^{xiii}	89.50(9)
		O(4)^{v}-K(1)-O(6A)^{xiii}	139.63(9)
		O(2)^{x}-K(1)-O(6A)^{xiii}	87.25(8)
		O(7)-K(1)-O(3A)^{iv}	77.77(8)
		O(6)^{v}-K(1)-O(3A)^{iv}	83.23(8)
		O(4)^{v}-K(1)-O(3A)^{iv}	120.34(8)
		O(2)^{x}-K(1)-O(3A)^{iv}	121.22(8)
		O(6A)^{xiii}-K(1)-O(3A)^{iv}	91.79(8)
		O(7)-K(1)-O(5)	49.16(8)
		O(6)^{v}-K(1)-O(5)	86.66(8)
		O(4)^{v}-K(1)-O(5)	66.23(8)
		O(2)^{x}-K(1)-O(5)	107.69(8)
		O(6A)^{xiii}-K(1)-O(5)	150.35(8)
		O(3A)^{iv}-K(1)-O(5)	58.57(8)

		O(7)-K(1)-O(5A)^{iii}	51.00(8)
		O(6)^{v}-K(1)-O(5A)^{iii}	140.22(8)
		O(4)^{v}-K(1)-O(5A)^{iii}	134.14(8)
		O(2)^{x}-K(1)-O(5A)^{iii}	63.28(8)
		O(6A)^{xiii}-K(1)-O(5A)^{iii}	82.17(8)
		O(3A)^{iv}-K(1)-O(5A)^{iii}	58.41(7)
		O(5)-K(1)-O(5A)^{iii}	82.14(8)
		O(7)-K(1)-O(1)^{v}	127.52(8)
		O(6)^{v}-K(1)-O(1)^{v}	91.36(8)
		O(4)^{v}-K(1)-O(1)^{v}	93.55(8)
		O(2)^{x}-K(1)-O(1)^{v}	68.08(8)
		O(6A)^{xiii}-K(1)-O(1)^{v}	50.04(8)
		O(3A)^{iv}-K(1)-O(1)^{v}	141.60(8)
		O(5)-K(1)-O(1)^{v}	159.33(8)
		O(5A)^{iii}-K(1)-O(1)^{v}	111.58(8)
		O(7)-K(1)-P(2)	23.36(6)
		O(6)^{v}-K(1)-P(2)	112.34(7)
		O(4)^{v}-K(1)-P(2)	73.93(6)
		O(2)^{x}-K(1)-P(2)	82.72(6)
		O(6A)^{xiii}-K(1)-P(2)	145.87(7)
		O(3A)^{iv}-K(1)-P(2)	66.56(6)
		O(5)-K(1)-P(2)	25.80(5)
		O(5A)^{iii}-K(1)-P(2)	64.17(6)
		O(1)^{v}-K(1)-P(2)	147.33(6)
		O(7)-K(1)-P(1)^{v}	103.49(6)
		O(6)^{v}-K(1)-P(1)^{v}	64.97(6)
		O(4)^{v}-K(1)-P(1)^{v}	23.35(6)
		O(2)^{x}-K(1)-P(1)^{v}	94.86(7)
		O(6A)^{xiii}-K(1)-P(1)^{v}	116.28(6)
		O(3A)^{iv}-K(1)-P(1)^{v}	135.91(6)
		O(5)-K(1)-P(1)^{v}	88.49(6)
		O(5A)^{iii}-K(1)-P(1)^{v}	151.73(6)
		O(1)^{v}-K(1)-P(1)^{v}	72.12(6)
		P(2)-K(1)-P(1)^{v}	97.08(3)
		O(7)-K(1)-P(2)^{v}	143.93(7)
		O(6)^{v}-K(1)-P(2)^{v}	22.31(6)
		O(4)^{v}-K(1)-P(2)^{v}	63.99(6)
		O(2)^{x}-K(1)-P(2)^{v}	133.12(7)
		O(6A)^{xiii}-K(1)-P(2)^{v}	85.55(6)
		O(3A)^{iv}-K(1)-P(2)^{v}	105.28(6)
		O(5)-K(1)-P(2)^{v}	100.93(6)
		O(5A)^{iii}-K(1)-P(2)^{v}	159.03(6)
		O(1)^{v}-K(1)-P(2)^{v}	72.02(5)
		P(2)-K(1)-P(2)^{v}	124.44(4)

		P(1)^{v}-K(1)-P(2)^{v}	49.11(2)
		O(3)^{xi}-K(1A)-O(7A)	98.13(9)
		O(3)^{xi}-K(1A)-O(6A)^{v}	82.19(9)
		O(7A)-K(1A)-O(6A)^{v}	138.94(9)
		O(3)^{xi}-K(1A)-O(4A)^{v}	136.48(9)
		O(7A)-K(1A)-O(4A)^{v}	81.59(8)
		O(6A)^{v}-K(1A)-O(4A)^{v}	71.37(8)
		O(3)^{xi}-K(1A)-O(5A)	75.49(9)
		O(7A)-K(1A)-O(5A)	50.57(8)
		O(6A)^{v}-K(1A)-O(5A)	90.85(9)
		O(4A)^{v}-K(1A)-O(5A)	71.12(8)
		O(3)^{xi}-K(1A)-O(5)	69.89(8)
		O(7A)-K(1A)-O(5)	66.29(8)
		O(6A)^{v}-K(1A)-O(5)	146.11(9)
		O(4A)^{v}-K(1A)-O(5)	142.51(8)
		O(5A)-K(1A)-O(5)	99.99(8)
		O(3)^{xi}-K(1A)-O(1A)^{ix}	130.80(9)
		O(7A)-K(1A)-O(1A)^{ix}	119.64(9)
		O(6A)^{v}-K(1A)-O(1A)^{ix}	87.57(9)
		O(4A)^{v}-K(1A)-O(1A)^{ix}	82.86(8)
		O(5A)-K(1A)-O(1A)^{ix}	152.98(9)
		O(5)-K(1A)-O(1A)^{ix}	96.21(8)
		O(3)^{xi}-K(1A)-O(2A)^{iv}	119.68(8)
		O(7A)-K(1A)-O(2A)^{iv}	55.76(8)
		O(6A)^{v}-K(1A)-O(2A)^{iv}	154.69(9)
		O(4A)^{v}-K(1A)-O(2A)^{iv}	96.22(8)
		O(5A)-K(1A)-O(2A)^{iv}	106.24(8)
		O(5)-K(1A)-O(2A)^{iv}	50.11(8)
		O(1A)^{ix}-K(1A)-O(2A)^{iv}	68.67(8)
		O(3)^{xi}-K(1A)-P(2A)	86.09(7)
		O(7A)-K(1A)-P(2A)	24.19(6)
		O(6A)^{v}-K(1A)-P(2A)	116.55(7)
		O(4A)^{v}-K(1A)-P(2A)	76.25(6)
		O(5A)-K(1A)-P(2A)	26.43(6)
		O(5)-K(1A)-P(2A)	81.17(6)
		O(1A)^{ix}-K(1A)-P(2A)	139.92(6)
		O(2A)^{iv}-K(1A)-P(2A)	79.94(6)
		O(3)^{xi}-K(1A)-P(2A)^{v}	101.36(7)
		O(7A)-K(1A)-P(2A)^{v}	142.30(7)
		O(6A)^{v}-K(1A)-P(2A)^{v}	21.18(6)
		O(4A)^{v}-K(1A)-P(2A)^{v}	62.12(6)
		O(5A)-K(1A)-P(2A)^{v}	104.24(6)
		O(5)-K(1A)-P(2A)^{v}	151.22(6)
		O(1A)^{ix}-K(1A)-P(2A)^{v}	68.18(6)

		$O(2A)^{iv}$-K(1A)-$P(2A)^{v}$	133.53(6)
		P(2A)-K(1A)-$P(2A)^{v}$	126.55(4)
		$O(3)^{xi}$-K(1A)-Co(1A)	122.97(7)
		O(7A)-K(1A)-Co(1A)	29.41(6)
		$O(6A)^{v}$-K(1A)-Co(1A)	146.15(7)
		$O(4A)^{v}$-K(1A)-Co(1A)	74.84(6)
		O(5A)-K(1A)-Co(1A)	76.27(6)
		O(5)-K(1A)-Co(1A)	67.69(6)
		$O(1A)^{ix}$-K(1A)-Co(1A)	90.26(6)
		$O(2A)^{iv}$-K(1A)-Co(1A)	32.50(5)
		P(2A)-K(1A)-Co(1A)	51.53(2)
		$P(2A)^{v}$-K(1A)-Co(1A)	133.28(3)
		$O(3)^{xi}$-K(1A)-$K(1)^{i}$	71.82(6)
		O(7A)-K(1A)-$K(1)^{i}$	98.40(6)
		$O(6A)^{v}$-K(1A)-$K(1)^{i}$	42.39(7)
		$O(4A)^{v}$-K(1A)-$K(1)^{i}$	65.28(6)
		O(5A)-K(1A)-$K(1)^{i}$	48.57(6)
		O(5)-K(1A)-$K(1)^{i}$	135.66(6)
		$O(1A)^{ix}$-K(1A)-$K(1)^{i}$	125.97(6)
		$O(2A)^{iv}$-K(1A)-$K(1)^{i}$	151.45(6)
		P(2A)-K(1A)-$K(1)^{i}$	74.72(3)
		$P(2A)^{v}$-K(1A)-$K(1)^{i}$	58.64(2)
		Co(1A)-K(1A)-$K(1)^{i}$	118.96(2)
		$O(3)^{xi}$-K(1A)-H(5)	85.6(5)
		O(7A)-K(1A)-H(5)	58.7(13)
		$O(6A)^{v}$-K(1A)-H(5)	159.9(10)
		$O(4A)^{v}$-K(1A)-H(5)	127.6(6)
		O(5A)-K(1A)-H(5)	101.5(14)
		O(5)-K(1A)-H(5)	16.1(4)
		$O(1A)^{ix}$-K(1A)-H(5)	88.4(12)
		$O(2A)^{iv}$-K(1A)-H(5)	34.1(5)
		P(2A)-K(1A)-H(5)	78.3(14)
		$P(2A)^{v}$-K(1A)-H(5)	154.2(14)
		Co(1A)-K(1A)-H(5)	53.5(8)
		$K(1)^{i}$-K(1A)-H(5)	145.6(12)
		O(2)-Co(1)-$O(2)^{x}$	180
		O(2)-Co(1)-$O(1)^{x}$	91.34(12)
		$O(2)^{x}$-Co(1)-$O(1)^{x}$	88.66(12)
		O(2)-Co(1)-O(1)	88.66(12)
		$O(2)^{x}$-Co(1)-O(1)	91.34(12)
		$O(1)^{x}$-Co(1)-O(1)	180.000(1)
		O(2)-Co(1)-$O(7)^{x}$	86.66(11)
		$O(2)^{x}$-Co(1)-$O(7)^{x}$	93.34(11)
		$O(1)^{x}$-Co(1)-$O(7)^{x}$	89.69(11)

		O(1)-Co(1)-O(7)^{x}	90.31(11)
		O(2)-Co(1)-O(7)	93.34(11)
		O(2)^{x}-Co(1)-O(7)	86.66(11)
		O(1)^{x}-Co(1)-O(7)	90.31(11)
		O(1)-Co(1)-O(7)	89.69(11)
		O(7)^{x}-Co(1)-O(7)	180.000(1)
		O(2)-Co(1)-K(1)^{x}	48.07(8)
		O(2)^{x}-Co(1)-K(1)^{x}	131.93(8)
		O(1)^{x}-Co(1)-K(1)^{x}	110.62(9)
		O(1)-Co(1)-K(1)^{x}	69.38(9)
		O(7)^{x}-Co(1)-K(1)^{x}	45.66(8)
		O(7)-Co(1)-K(1)^{x}	134.34(8)
		O(2)-Co(1)-K(1)	131.93(8)
		O(2)^{x}-Co(1)-K(1)	48.07(8)
		O(1)^{x}-Co(1)-K(1)	69.38(9)
		O(1)-Co(1)-K(1)	110.62(9)
		O(7)^{x}-Co(1)-K(1)	134.34(8)
		O(7)-Co(1)-K(1)	45.66(8)
		K(1)^{x}-Co(1)-K(1)	180
		O(7A)-Co(1A)-O(7A)^{iv}	180
		O(7A)-Co(1A)-O(1A)^{iv}	85.71(11)
		O(7A)^{iv}-Co(1A)-O(1A)^{iv}	94.29(11)
		O(7A)-Co(1A)-O(1A)	94.29(11)
		O(7A)^{iv}-Co(1A)-O(1A)	85.71(11)
		O(1A)^{iv}-Co(1A)-O(1A)	180.000(1)
		O(7A)-Co(1A)-O(2A)	96.22(11)
		O(7A)^{iv}-Co(1A)-O(2A)	83.78(11)
		O(1A)^{iv}-Co(1A)-O(2A)	89.14(11)
		O(1A)-Co(1A)-O(2A)	90.86(11)
		O(7A)-Co(1A)-O(2A)^{iv}	83.78(11)
		O(7A)^{iv}-Co(1A)-O(2A)^{iv}	96.22(11)
		O(1A)^{iv}-Co(1A)-O(2A)^{iv}	90.86(11)
		O(1A)-Co(1A)-O(2A)^{iv}	89.14(11)
		O(2A)-Co(1A)-O(2A)^{iv}	180.00(11)
		O(7A)-Co(1A)-K(1A)	41.68(8)
		O(7A)^{iv}-Co(1A)-K(1A)	138.32(8)
		O(1A)^{iv}-Co(1A)-K(1A)	110.99(8)
		O(1A)-Co(1A)-K(1A)	69.01(8)
		O(2A)-Co(1A)-K(1A)	127.35(8)
		O(2A)^{iv}-Co(1A)-K(1A)	52.65(8)
		O(7A)-Co(1A)-K(1A)^{iv}	138.32(8)
		O(7A)^{iv}-Co(1A)-K(1A)^{iv}	41.68(8)
		O(1A)^{iv}-Co(1A)-K(1A)^{iv}	69.01(8)
		O(1A)-Co(1A)-K(1A)^{iv}	110.99(8)

		O(2A)-Co(1A)-K(1A)^{iv} O(2A)^{iv}-Co(1A)-K(1A)^{iv} K(1A)-Co(1A)-K(1A)^{iv}	52.65(8) 127.35(8) 180

Symmetry transformations used to generate equivalent atoms:

(i) x, y+1, z; (ii) –x+2, -y-1, -z+2; (iii) x, y-1, z; (iv) -x+1, -y, -z+1; (v) x-1, y, z; (vi) –x+2, -y, -z+2; (vii) –x+2, -y+1, -z+1; (viii) x+1,y,z; (ix) -x,-y,-z+1; (x) -x+1,-y-1,-z+2; (xi) -x+1,-y,-z+2; (xii) x+1,y+1,z; (xiii) x-1,y-1,z.

Table 3.B: Anisotropic displacement parameters (Å^2 x 10^3) for K[Co($CH_4O_6P_2$)$_2$(H_2O)$_2$].

	U11	U22	U33	U23	U13	U12
C(1)	9(2)	6(2)	9(2)	0(1)	-1(1)	0(1)
C(1A)	10(2)	6(2)	7(2)	2(1)	2(1)	1(1)
O(1)	15(2)	18(2)	9(1)	-1(1)	-1(1)	10(1)
O(1A)	10(2)	11(2)	7(2)	3(1)	3(1)	3(1)
O(2)	9(1)	9(1)	14(1)	6(1)	-1(1)	-1(1)
O(2A)	10(1)	7(1)	7(1)	0(1)	0(1)	-3(1)
O(3)	13(1)	8(1)	7(1)	-1(1)	0(1)	-2(1)
O(3A)	14(1)	5(1)	8(1)	2(1)	0(1)	-2(1)
O(4)	8(1)	10(1)	9(1)	0(1)	2(1)	-1(1)
O(4A)	8(1)	8(1)	10(1)	0(1)	-1(1)	0(1)
O(5)	10(1)	11(1)	6(1)	1(1)	0(1)	2(1)
O(5A)	8(1)	10(1)	9(1)	-2(1)	0(1)	1(1)
O(6)	11(1)	13(1)	7(1)	2(1)	2(1)	2(1)
O(6A)	11(1)	14(1)	9(1)	-1(1)	-1(1)	3(1)
O(7)	14(1)	6(1)	6(1)	2(1)	1(1)	-1(1)
O(7A)	14(1)	6(1)	9(1)	0(1)	3(1)	-2(1)
P(1)	8(1)	6(1)	7(1)	1(1)	-1(1)	-1(1)
P(1A)	7(1)	6(1)	6(1)	1(1)	1(1)	0(1)
P(2)	8(1)	6(1)	6(1)	1(1)	1(1)	1(1)
P(2A)	8(1)	7(1)	6(1)	-1(1)	1(1)	1(1)
K(1)	11(1)	12(1)	16(1)	-1(1)	-2(1)	2(1)
K(1A)	11(1)	12(1)	11(1)	2(1)	1(1)	3(1)
Co(1)	7(1)	6(1)	6(1)	1(1)	1(1)	0(1)
Co(1A)	8(1)	6(1)	6(1)	0(1)	1(1)	0(1)

Table 4.B: Hydrogen coordinates (x 10^4) and isotropic displacement parameters (Å^2 x 10^3) for $K[Co(CH_4O_6P_2)_2(H_2O)_2]$.

	x	y	z	U(eq)
H(3)	6649	-360	8854	10
H(4)	4956	-1152	9502	10
H(3A)	4994	4005	5404	9
H(4A)	6864	4831	6048	9
H(1A)	7730(70)	-7240(50)	9790(30)	18(14)
H(1A1)	2650(100)	1600(70)	3780(30)	34(18)
H(1B)	6900(90)	-6910(70)	8826(16)	33(17)
H(1B1)	1840(110)	1670(70)	4730(40)	50(20)
H(2)	8690(100)	60(30)	10740(50)	36(18)
H(2A)	8730(90)	5220(40)	4190(50)	32(17)
H(5)	3340(100)	-1750(80)	6939(17)	37(18)
H(6A)	4400(100)	4090(50)	7700(50)	50(20)

Table 5.B: Hydrogen bonds for $K[Co(CH_4O_6P_2)_2(H_2O)_2]$.

D-H...A	d(D-H)	d(H...A)	d(D...A)	<(DHA)
O(5A)-H(6A)...O(7)^{i}	0.83(2)	1.83(3)	2.633(4)	161(7)
O(1)-H(1A)...O(4)^{ii}	0.864(19)	1.84(2)	2.687(4)	168(5)
O(1)-H(1B)...O(6A)^{iii}	0.865(19)	1.83(3)	2.676(4)	164(6)
O(5)-H(5)...O(2A)^{iv}	0.84(2)	1.78(2)	2.617(4)	172(7)
O(1A)-H(1A1)...O(6)^{iv}	0.84(2)	1.84(2)	2.679(4)	175(7)
O(1A)-H(1B1)...O(4A)^{v}	0.85(2)	1.90(2)	2.737(4)	169(7)
O(3)-H(2)...O(4)^{vi}	0.846(15)	1.723(19)	2.559(4)	170(7)
O(3A)-H(2A)...O(4A)^{vii}	0.85(2)	1.71(2)	2.567(4)	179(7)

Symmetry transformations used to generate equivalent atoms:

(i) x, y+1, z; (ii) –x+2, -y-1, -z+2; (iii) x, y-1, z; (iv) -x+1, -y, -z+1; (v) x-1, y, z; (vi) –x+2, -y, -z+2; (vii) –x+2, -y+1, -z+1; (viii) x+1,y,z; (ix) -x,-y,-z+1; (x) -x+1,-y-1,-z+2; (xi) -x+1,-y,-z+2; (xii) x+1,y+1,z; (xiii) x-1, y-1, z.

Table 6.B: Torsion angles (º) for $K[Co(CH_4O_6P_2)_2(H_2O)_2]$.

Torsion Angle (º)	
Co(1)-O(2)-P(1)-O(4)	-121.6(2)
$K(1)^{x}$-O(2)-P(1)-O(4)	64.1(2)
Co(1)-O(2)-P(1)-O(3)	115.8(2)
$K(1)^{x}$-O(2)-P(1)-O(3)	-58.4(2)
$K(1)^{x}$-O(2)-P(1)-C(1)	-174.10(19)
Co(1)-O(2)-P(1)-$K(1)^{viii}$	-89.5(2)
$K(1)^{x}$-O(2)-P(1)-$K(1)^{viii}$	96.23(18)
$K(1)^{viii}$-O(4)-P(1)-O(2)	42.71(19)
$K(1)^{viii}$-O(4)-P(1)-O(3)	164.21(13)
$K(1)^{viii}$-O(4)-P(1)-C(1)	-81.18(17)
$K(1A)^{xi}$-O(3)-P(1)-O(2)	28.7(3)
$K(1A)^{xi}$-O(3)-P(1)-O(4)	-95.8(3)
$K(1A)^{xi}$-O(3)-P(1)-C(1)	148.3(2)
$K(1A)^{xi}$-O(3)-P(1)-$K(1)^{viii}$	-66.0(4)
P(2)-C(1)-P(1)-O(2)	-52.4(3)
P(2)-C(1)-P(1)-O(4)	72.5(2)
P(2)-C(1)-P(1)-O(3)	-169.8(2)
P(2)-C(1)-P(1)-$K(1)^{viii}$	23.8(2)
Co(1A)-O(2A)-P(1A)-O(4A)	95.2(2)
$K(1A)^{iv}$-O(2A)-P(1A)-O(4A)	-47.0(2)
Co(1A)-O(2A)-P(1A)-O(3A)	-142.30(19)
$K(1A)^{iv}$-O(2A)-P(1A)-O(3A)	75.5(2)
Co(1A)-O(2A)-P(1A)-C(1A)	-27.9(3)
$K(1A)^{iv}$-O(2A)-P(1A)-C(1A)	-170.07(17)
$K(1A)^{viii}$-O(4A)-P(1A)-O(2A)	-55.1(2)
$K(1A)^{viii}$-O(4A)-P(1A)-O(3A)	-174.56(15)
$K(1A)^{viii}$-O(4A)-P(1A)-C(1A)	68.3(2)
$K(1)^{iv}$-O(3A)-P(1A)-O(2A)	-49.3(3)
$K(1)^{iv}$-O(3A)-P(1A)-O(4A)	75.3(3)
$K(1)^{iv}$-O(3A)-P(1A)-C(1A)	-166.0(2)
P(2A)-C(1A)-P(1A)-O(2A)	62.8(3)
P(2A)-C(1A)-P(1A)-O(4A)	-63.4(3)
P(2A)-C(1A)-P(1A)-O(3A)	176.6(2)
$K(1)^{viii}$-O(6)-P(2)-O(7)	-47.4(2)
$K(1)^{viii}$-O(6)-P(2)-O(5)	-170.37(14)
$K(1)^{viii}$-O(6)-P(2)-C(1)	74.93(19)
$K(1)^{viii}$-O(6)-P(2)-K(1)	-100.88(14)
Co(1)-O(7)-P(2)-O(6)	108.8(2)
K(1)-O(7)-P(2)-O(6)	-124.92(16)

Co(1)-O(7)-P(2)-O(5)	-125.6(2)
K(1)-O(7)-P(2)-O(5)	0.69(18)
Co(1)-O(7)-P(2)-C(1)	-15.8(3)
K(1)-O(7)-P(2)-C(1)	110.43(16)
Co(1)-O(7)-P(2)-K(1)	-126.3(3)
Co(1)-O(7)-P(2)-K(1)^{viii}	76.65(19)
K(1)-O(7)-P(2)-K(1)^{viii}	-157.08(12)
K(1A)-O(5)-P(2)-O(6)	-89.6(4)
K(1)-O(5)-P(2)-O(6)	126.36(15)
K(1A)-O(5)-P(2)-O(7)	143.5(3)
K(1A)-O(5)-P(2)-C(1)	30.5(4)
K(1)-O(5)-P(2)-C(1)	-113.55(15)
K(1A)-O(5)-P(2)-K(1)	144.1(4)
K(1A)-O(5)-P(2)-K(1)^{viii}	-107.1(4)
K(1)-O(5)-P(2)-K(1)^{viii}	108.8(3)
P(1)-C(1)-P(2)-O(6)	-67.6(3)
P(1)-C(1)-P(2)-O(7)	58.8(3)
P(1)-C(1)-P(2)-O(5)	171.8(2)
P(1)-C(1)-P(2)-K(1)	108.85(19)
P(1)-C(1)-P(2)-K(1)^{viii}	-23.8(2)
K(1A)^{viii}-O(6A)-P(2A)-O(7A)	44.3(2)
K(1)^{xii}-O(6A)-P(2A)-O(7A)	165.44(15)
K(1A)^{viii}-O(6A)-P(2A)-O(5A)	165.04(15)
K(1)^{xii}-O(6A)-P(2A)-O(5A)	-73.8(2)
K(1A)^{viii}-O(6A)-P(2A)-C(1A)	-79.0(2)
K(1)^{xii}-O(6A)-P(2A)-C(1A)	42.1(2)
K(1A)^{viii}-O(6A)-P(2A)-K(1A)	103.24(15)
K(1)^{xii}-O(6A)-P(2A)-K(1A)	-135.63(11)
K(1)^{xii}-O(6A)-P(2A)-K(1A)^{viii}	121.1(2)
Co(1A)-O(7A)-P(2A)-O(6A)	-101.8(3)
K(1A)-O(7A)-P(2A)-O(6A)	120.10(16)
Co(1A)-O(7A)-P(2A)-O(5A)	134.2(2)
K(1A)-O(7A)-P(2A)-O(5A)	-3.93(17)
Co(1A)-O(7A)-P(2A)-C(1A)	22.6(3)
K(1A)-O(7A)-P(2A)-C(1A)	-115.49(16)
Co(1A)-O(7A)-P(2A)-K(1A)	138.1(3)
Co(1A)-O(7A)-P(2A)-K(1A)^{viii}	-73.9(2)
K(1A)-O(7A)-P(2A)-K(1A)^{viii}	148.02(10)
K(1A)-O(5A)-P(2A)-O(6A)	-124.91(15)
K(1)^{i}-O(5A)-P(2A)-O(6A)	109.3(8)
K(1A)-O(5A)-P(2A)-O(7A)	3.62(16)
K(1)^{i}-O(5A)-P(2A)-O(7A)	-122.1(8)
K(1A)-O(5A)-P(2A)-C(1A)	116.61(16)
K(1)^{i}-O(5A)-P(2A)-C(1A)	-9.1(8)

K(1)^{i}-O(5A)-P(2A)-K(1A)	-125.8(8)
K(1A)-O(5A)-P(2A)-K(1A)^{viii}	-104.4(2)
K(1)^{i}-O(5A)-P(2A)-K(1A)^{viii}	129.8(7)
P(1A)-C(1A)-P(2A)-O(6A)	70.4(3)
P(1A)-C(1A)-P(2A)-O(7A)	-59.1(3)
P(1A)-C(1A)-P(2A)-O(5A)	-170.1(2)
P(1A)-C(1A)-P(2A)-K(1A)	-111.6(2)
P(1A)-C(1A)-P(2A)-K(1A)^{viii}	29.0(2)
P(2)-O(7)-K(1)-O(6)^{v}	-8.5(2)
Co(1)-O(7)-K(1)-O(6)^{v}	132.80(11)
P(2)-O(7)-K(1)-O(4)^{v}	-64.76(15)
Co(1)-O(7)-K(1)-O(4)^{v}	76.53(11)
P(2)-O(7)-K(1)-O(2)^{x}	-164.21(18)
Co(1)-O(7)-K(1)-O(2)^{x}	-22.92(9)
P(2)-O(7)-K(1)-O(6A)^{xiii}	140.13(14)
Co(1)-O(7)-K(1)-O(6A)^{xiii}	-78.58(14)
P(2)-O(7)-K(1)-O(3A)^{iv}	58.37(14)
Co(1)-O(7)-K(1)-O(3A)^{iv}	-160.34(11)
Co(1)-O(7)-K(1)-O(5)	140.85(15)
P(2)-O(7)-K(1)-O(5A)^{iii}	117.43(17)
Co(1)-O(7)-K(1)-O(5A)^{iii}	-101.28(12)
P(2)-O(7)-K(1)-O(1)^{v}	-154.01(12)
Co(1)-O(7)-K(1)-O(1)^{v}	-12.72(15)
Co(1)-O(7)-K(1)-P(2)	141.3(2)
P(2)-O(7)-K(1)-P(1)^{v}	-76.36(14)
Co(1)-O(7)-K(1)-P(1)^{v}	64.93(10)
P(2)-O(7)-K(1)-P(2)^{v}	-40.9(2)
Co(1)-O(7)-K(1)-P(2)^{v}	100.44(12)
K(1A)-O(5)-K(1)-O(7)	-164.70(14)
P(2)-O(5)-K(1)-O(6)^{v}	174.75(13)
K(1A)-O(5)-K(1)-O(6)^{v}	9.66(9)
P(2)-O(5)-K(1)-O(4)^{v}	102.48(13)
K(1A)-O(5)-K(1)-O(4)^{v}	-62.61(9)
P(2)-O(5)-K(1)-O(2)^{x}	15.13(15)
K(1A)-O(5)-K(1)-O(2)^{x}	-149.97(9)
P(2)-O(5)-K(1)-O(6A)^{xiii}	-102.15(18)
K(1A)-O(5)-K(1)-O(6A)^{xiii}	92.75(17)
P(2)-O(5)-K(1)-O(3A)^{iv}	-101.15(14)
K(1A)-O(5)-K(1)-O(3A)^{iv}	93.76(10)
P(2)-O(5)-K(1)-O(5A)^{iii}	-43.51(12)
K(1A)-O(5)-K(1)-O(5A)^{iii}	151.39(10)
P(2)-O(5)-K(1)-O(1)^{v}	89.8(2)
K(1A)-O(5)-K(1)-O(1)^{v}	-75.3(2)
K(1A)-O(5)-K(1)-P(2)	-165.10(18)

P(2)-O(5)-K(1)-P(1)^{v}	109.74(12)
K(1A)-O(5)-K(1)-P(1)^{v}	-55.35(8)
P(2)-O(5)-K(1)-P(2)^{v}	157.52(11)
K(1A)-O(5)-K(1)-P(2)^{v}	-7.57(9)
O(6)-P(2)-K(1)-O(7)	86.2(2)
O(5)-P(2)-K(1)-O(7)	-179.2(2)
C(1)-P(2)-K(1)-O(7)	-89.4(2)
K(1)^{viii}-P(2)-K(1)-O(7)	27.84(15)
O(6)-P(2)-K(1)-O(6)^{v}	-100.22(18)
O(7)-P(2)-K(1)-O(6)^{v}	173.58(16)
O(5)-P(2)-K(1)-O(6)^{v}	-5.67(14)
C(1)-P(2)-K(1)-O(6)^{v}	84.14(15)
K(1)^{viii}-P(2)-K(1)-O(6)^{v}	-158.59(7)
O(6)-P(2)-K(1)-O(4)^{v}	-162.97(17)
O(7)-P(2)-K(1)-O(4)^{v}	110.83(16)
O(5)-P(2)-K(1)-O(4)^{v}	-68.41(14)
C(1)-P(2)-K(1)-O(4)^{v}	21.39(15)
K(1)^{viii}-P(2)-K(1)-O(4)^{v}	138.66(7)
O(6)-P(2)-K(1)-O(2)^{x}	99.96(17)
O(7)-P(2)-K(1)-O(2)^{x}	13.76(16)
O(5)-P(2)-K(1)-O(2)^{x}	-165.48(14)
C(1)-P(2)-K(1)-O(2)^{x}	-75.68(15)
K(1)^{viii}-P(2)-K(1)-O(2)^{x}	41.59(8)
O(6)-P(2)-K(1)-O(6A)^{xiii}	25.9(2)
O(7)-P(2)-K(1)-O(6A)^{xiii}	-60.30(19)
O(5)-P(2)-K(1)-O(6A)^{xiii}	120.46(17)
C(1)-P(2)-K(1)-O(6A)^{xiii}	-149.73(17)
K(1)^{viii}-P(2)-K(1)-O(6A)^{xiii}	-32.46(14)
O(6)-P(2)-K(1)-O(3A)^{iv}	-28.71(16)
O(7)-P(2)-K(1)-O(3A)^{iv}	-114.92(16)
O(5)-P(2)-K(1)-O(3A)^{iv}	65.84(14)
C(1)-P(2)-K(1)-O(3A)^{iv}	155.65(15)
K(1)^{viii}-P(2)-K(1)-O(3A)^{iv}	-87.08(7)
O(6)-P(2)-K(1)-O(5)	-94.6(2)
O(7)-P(2)-K(1)-O(5)	179.2(2)
C(1)-P(2)-K(1)-O(5)	89.80(19)
K(1)^{viii}-P(2)-K(1)-O(5)	-152.92(13)
O(6)-P(2)-K(1)-O(5A)^{iii}	36.18(16)
O(7)-P(2)-K(1)-O(5A)^{iii}	-50.03(16)
O(5)-P(2)-K(1)-O(5A)^{iii}	130.73(14)
C(1)-P(2)-K(1)-O(5A)^{iii}	-139.47(15)
K(1)^{viii}-P(2)-K(1)-O(5A)^{iii}	-22.19(7)
O(6)-P(2)-K(1)-O(1)^{v}	126.29(18)
O(7)-P(2)-K(1)-O(1)^{v}	40.08(19)

O(5)-P(2)-K(1)-O(1)^{v}	-139.16(16)
C(1)-P(2)-K(1)-O(1)^{v}	-49.35(18)
K(1)^{viii}-P(2)-K(1)-O(1)^{v}	67.92(12)
O(6)-P(2)-K(1)-P(1)^{v}	-166.02(15)
O(7)-P(2)-K(1)-P(1)^{v}	107.78(15)
O(5)-P(2)-K(1)-P(1)^{v}	-71.46(13)
C(1)-P(2)-K(1)-P(1)^{v}	18.34(14)
K(1)^{viii}-P(2)-K(1)-P(1)^{v}	135.61(4)
O(6)-P(2)-K(1)-P(2)^{v}	-121.63(15)
O(7)-P(2)-K(1)-P(2)^{v}	152.17(15)
O(5)-P(2)-K(1)-P(2)^{v}	-27.08(13)
C(1)-P(2)-K(1)-P(2)^{v}	62.73(15)
K(1)^{viii}-P(2)-K(1)-P(2)^{v}	180
P(2A)-O(7A)-K(1A)-O(3)^{xi}	-60.91(15)
Co(1A)-O(7A)-K(1A)-O(3)^{xi}	150.02(11)
P(2A)-O(7A)-K(1A)-O(6A)^{v}	26.5(2)
Co(1A)-O(7A)-K(1A)-O(6A)^{v}	-122.56(13)
P(2A)-O(7A)-K(1A)-O(4A)^{v}	75.10(15)
Co(1A)-O(7A)-K(1A)-O(4A)^{v}	-73.97(12)
P(2A)-O(7A)-K(1A)-O(5A)	2.66(12)
Co(1A)-O(7A)-K(1A)-O(5A)	-146.41(16)
P(2A)-O(7A)-K(1A)-O(5)	-124.67(16)
Co(1A)-O(7A)-K(1A)-O(5)	86.26(12)
P(2A)-O(7A)-K(1A)-O(1A)^{ix}	151.87(13)
Co(1A)-O(7A)-K(1A)-O(1A)^{ix}	2.81(15)
P(2A)-O(7A)-K(1A)-O(2A)^{iv}	178.57(18)
Co(1A)-O(7A)-K(1A)-O(2A)^{iv}	29.51(9)
Co(1A)-O(7A)-K(1A)-P(2A)	-149.1(2)
P(2A)-O(7A)-K(1A)-P(2A)^{v}	59.77(19)
Co(1A)-O(7A)-K(1A)-P(2A)^{v}	-89.30(14)
P(2A)-O(7A)-K(1A)-Co(1A)	149.1(2)
P(2A)-O(7A)-K(1A)-K(1)^{i}	11.78(15)
Co(1A)-O(7A)-K(1A)-K(1)^{i}	-137.29(10)
P(2A)-O(5A)-K(1A)-O(3)^{xi}	111.25(14)
K(1)^{i}-O(5A)-K(1A)-O(3)^{xi}	-78.37(8)
P(2A)-O(5A)-K(1A)-O(7A)	-2.45(11)
K(1)^{i}-O(5A)-K(1A)-O(7A)	167.93(12)
P(2A)-O(5A)-K(1A)-O(6A)^{v}	-167.05(13)
K(1)^{i}-O(5A)-K(1A)-O(6A)^{v}	3.33(8)
P(2A)-O(5A)-K(1A)-O(4A)^{v}	-97.09(14)
K(1)^{i}-O(5A)-K(1A)-O(4A)^{v}	73.29(8)
P(2A)-O(5A)-K(1A)-O(5)	45.21(14)
K(1)^{i}-O(5A)-K(1A)-O(5)	-144.41(7)
P(2A)-O(5A)-K(1A)-O(1A)^{ix}	-80.7(2)

K(1)^{i}-O(5A)-K(1A)-O(1A)^{ix}	89.64(18)
P(2A)-O(5A)-K(1A)-O(2A)^{iv}	-5.97(15)
K(1)^{i}-O(5A)-K(1A)-O(2A)^{iv}	164.41(7)
K(1)^{i}-O(5A)-K(1A)-P(2A)	170.38(17)
P(2A)-O(5A)-K(1A)-P(2A)^{v}	-150.46(11)
K(1)^{i}-O(5A)-K(1A)-P(2A)^{v}	19.92(7)
P(2A)-O(5A)-K(1A)-Co(1A)	-18.69(11)
K(1)^{i}-O(5A)-K(1A)-Co(1A)	151.69(6)
P(2A)-O(5A)-K(1A)-K(1)^{i}	-170.38(17)
P(2)-O(5)-K(1A)-O(3)^{xi}	-55.6(4)
K(1)-O(5)-K(1A)-O(3)^{xi}	86.87(10)
P(2)-O(5)-K(1A)-O(7A)	53.4(4)
K(1)-O(5)-K(1A)-O(7A)	-164.15(12)
P(2)-O(5)-K(1A)-O(6A)^{v}	-92.0(4)
K(1)-O(5)-K(1A)-O(6A)^{v}	50.46(19)
P(2)-O(5)-K(1A)-O(4A)^{v}	86.8(4)
K(1)-O(5)-K(1A)-O(4A)^{v}	-130.80(12)
P(2)-O(5)-K(1A)-O(5A)	14.8(4)
K(1)-O(5)-K(1A)-O(5A)	157.27(9)
P(2)-O(5)-K(1A)-O(1A)^{ix}	173.1(4)
K(1)-O(5)-K(1A)-O(1A)^{ix}	-44.45(10)
P(2)-O(5)-K(1A)-O(2A)^{iv}	117.7(4)
K(1)-O(5)-K(1A)-O(2A)^{iv}	-99.86(11)
P(2)-O(5)-K(1A)-P(2A)	33.5(4)
K(1)-O(5)-K(1A)-P(2A)	175.91(8)
P(2)-O(5)-K(1A)-P(2A)^{v}	-132.2(3)
K(1)-O(5)-K(1A)-P(2A)^{v}	10.21(18)
P(2)-O(5)-K(1A)-Co(1A)	85.4(4)
K(1)-O(5)-K(1A)-Co(1A)	-132.17(9)
P(2)-O(5)-K(1A)-K(1)^{i}	-23.8(4)
K(1)-O(5)-K(1A)-K(1)^{i}	118.64(8)
O(6A)-P(2A)-K(1A)-O(3)^{xi}	24.61(17)
O(7A)-P(2A)-K(1A)-O(3)^{xi}	119.88(16)
O(5A)-P(2A)-K(1A)-O(3)^{xi}	-64.74(14)
C(1A)-P(2A)-K(1A)-O(3)^{xi}	-152.91(16)
K(1A)^{viii}-P(2A)-K(1A)-O(3)^{xi}	78.75(8)
O(6A)-P(2A)-K(1A)-O(7A)	-95.3(2)
O(5A)-P(2A)-K(1A)-O(7A)	175.4(2)
C(1A)-P(2A)-K(1A)-O(7A)	87.2(2)
K(1A)^{viii}-P(2A)-K(1A)-O(7A)	-41.13(15)
O(6A)-P(2A)-K(1A)-O(6A)^{v}	103.86(18)
O(7A)-P(2A)-K(1A)-O(6A)^{v}	-160.87(16)
O(5A)-P(2A)-K(1A)-O(6A)^{v}	14.51(15)
C(1A)-P(2A)-K(1A)-O(6A)^{v}	-73.66(17)

K(1A)^{viii}-P(2A)-K(1A)-O(6A)^{v}	158.00(7)
O(6A)-P(2A)-K(1A)-O(4A)^{v}	164.53(17)
O(7A)-P(2A)-K(1A)-O(4A)^{v}	-100.21(16)
O(5A)-P(2A)-K(1A)-O(4A)^{v}	75.17(14)
C(1A)-P(2A)-K(1A)-O(4A)^{v}	-13.00(16)
K(1A)^{viii}-P(2A)-K(1A)-O(4A)^{v}	-141.34(7)
O(6A)-P(2A)-K(1A)-O(5A)	89.4(2)
O(7A)-P(2A)-K(1A)-O(5A)	-175.4(2)
C(1A)-P(2A)-K(1A)-O(5A)	-88.2(2)
K(1A)^{viii}-P(2A)-K(1A)-O(5A)	143.49(14)
O(6A)-P(2A)-K(1A)-O(5)	-45.62(17)
O(7A)-P(2A)-K(1A)-O(5)	49.64(16)
O(5A)-P(2A)-K(1A)-O(5)	-134.98(14)
C(1A)-P(2A)-K(1A)-O(5)	136.85(16)
K(1A)^{viii}-P(2A)-K(1A)-O(5)	8.51(7)
O(6A)-P(2A)-K(1A)-O(1A)^{ix}	-134.79(18)
O(7A)-P(2A)-K(1A)-O(1A)^{ix}	-39.52(18)
O(5A)-P(2A)-K(1A)-O(1A)^{ix}	135.85(16)
C(1A)-P(2A)-K(1A)-O(1A)^{ix}	47.69(18)
K(1A)^{viii}-P(2A)-K(1A)-O(1A)^{ix}	-80.65(11)
O(6A)-P(2A)-K(1A)-O(2A)^{iv}	-96.46(17)
O(7A)-P(2A)-K(1A)-O(2A)^{iv}	-1.20(15)
O(5A)-P(2A)-K(1A)-O(2A)^{iv}	174.18(14)
C(1A)-P(2A)-K(1A)-O(2A)^{iv}	86.02(16)
K(1A)^{viii}-P(2A)-K(1A)-O(2A)^{iv}	-42.33(7)
O(6A)-P(2A)-K(1A)-P(2A)^{v}	125.87(15)
O(7A)-P(2A)-K(1A)-P(2A)^{v}	-138.87(15)
O(5A)-P(2A)-K(1A)-P(2A)^{v}	36.51(14)
C(1A)-P(2A)-K(1A)-P(2A)^{v}	-51.66(16)
K(1A)^{viii}-P(2A)-K(1A)-P(2A)^{v}	180
O(6A)-P(2A)-K(1A)-Co(1A)	-114.07(16)
O(7A)-P(2A)-K(1A)-Co(1A)	-18.81(14)
O(5A)-P(2A)-K(1A)-Co(1A)	156.57(13)
C(1A)-P(2A)-K(1A)-Co(1A)	68.40(15)
K(1A)^{viii}-P(2A)-K(1A)-Co(1A)	-59.94(4)
O(6A)-P(2A)-K(1A)-K(1)^{i}	96.82(16)
O(7A)-P(2A)-K(1A)-K(1)^{i}	-167.92(15)
O(5A)-P(2A)-K(1A)-K(1)^{i}	7.46(13)
C(1A)-P(2A)-K(1A)-K(1)^{i}	-80.70(15)
K(1A)^{viii}-P(2A)-K(1A)-K(1)^{i}	150.96(4)
P(1)-O(2)-Co(1)-O(2)^{x}	86.4(6)
K(1)^{x}-O(2)-Co(1)-O(2)^{x}	-98.0(4)
P(1)-O(2)-Co(1)-O(1)^{x}	-58.7(2)
K(1)^{x}-O(2)-Co(1)-O(1)^{x}	116.90(11)

P(1)-O(2)-Co(1)-O(1)	121.3(2)
K(1)^{x}-O(2)-Co(1)-O(1)	-63.10(11)
P(1)-O(2)-Co(1)-O(7)^{x}	-148.3(2)
K(1)$^{x-}$O(2)-Co(1)-O(7)^{x}	27.29(11)
P(1)-O(2)-Co(1)-O(7)	31.7(2)
K(1)^{x}-O(2)-Co(1)-O(7)	-152.71(11)
P(1)-O(2)-Co(1)-K(1)^{x}	-175.5(3)
P(1)-O(2)-Co(1)-K(1)	4.5(3)
K(1)^{x}-O(2)-Co(1)-K(1)	180
K(1)^{viii}-O(1)-Co(1)-O(2)	-43.76(11)
K(1)^{viii}-O(1)-Co(1)-O(2)^{x}	136.24(11)
K(1)^{viii}-O(1)-Co(1)-O(1)^{x}	159.4(7)
K(1)^{viii}-O(1)-Co(1)-O(7)^{x}	-130.41(11)
K(1)^{viii}-O(1)-Co(1)-O(7)	49.59(11)
K(1)^{viii}-O(1)-Co(1)-K(1)^{x}	-88.90(9)
K(1)^{viii}-O(1)-Co(1)-K(1)	91.10(9)
P(2)-O(7)-Co(1)-O(2)	-22.4(2)
K(1)-O(7)-Co(1)-O(2)	-151.51(11)
P(2)-O(7)-Co(1)-O(2)^{x}	157.6(2)
K(1)-O(7)-Co(1)-O(2)^{x}	28.49(11)
P(2)-O(7)-Co(1)-O(1)^{x}	68.9(2)
K(1)-O(7)-Co(1)-O(1)^{x}	-60.15(12)
P(2)-O(7)-Co(1)-O(1)	-111.1(2)
K(1)-O(7)-Co(1)-O(1)	119.85(12)
P(2)-O(7)-Co(1)-O(7)^{x}	171.2(14)
K(1)-O(7)-Co(1)-O(7)^{x}	42.1(12)
P(2)-O(7)-Co(1)-K(1)^{x}	-50.9(3)
K(1)-O(7)-Co(1)-K(1)^{x}	180
P(2)-O(7)-Co(1)-K(1)	129.1(3)
O(7)-K(1)-Co(1)-O(2)	39.79(15)
O(6)^{v}-K(1)-Co(1)-O(2)	-48.21(17)
O(4)^{v}-K(1)-Co(1)-O(2)	-57.95(13)
O(2)^{x}-K(1)-Co(1)-O(2)	180
O(6A)^{xiii}-K(1)-Co(1)-O(2)	162.37(13)
O(3A)^{iv}-K(1)-Co(1)-O(2)	60.07(13)
O(5)-K(1)-Co(1)-O(2)	10.35(13)
O(5A)^{iii}-K(1)-Co(1)-O(2)	98.32(13)
O(1)^{v}-K(1)-Co(1)-O(2)	-150.31(12)
P(2)-K(1)-Co(1)-O(2)	21.60(12)
P(1)^{v}-K(1)-Co(1)-O(2)	-78.44(12)
P(2)^{v}-K(1)-Co(1)-O(2)	-80.97(12)
O(7)-K(1)-Co(1)-O(2)^{x}	-140.21(15)
O(6)^{v}-K(1)-Co(1)-O(2)^{x}	131.79(17)
O(4)^{v}-K(1)-Co(1)-O(2)^{x}	122.05(13)

O(6A)^{xiii}-K(1)-Co(1)-O(2)^{x}	-17.63(13)
O(3A)^{iv}-K(1)-Co(1)-O(2)^{x}	-119.93(13)
O(5)-K(1)-Co(1)-O(2)^{x}	-169.65(13)
O(5A)^{iii}-K(1)-Co(1)-O(2)^{x}	-81.68(13)
O(1)^{v}-K(1)-Co(1)-O(2)^{x}	29.69(12)
P(2)-K(1)-Co(1)-O(2)^{x}	-158.40(12)
P(1)^{v}-K(1)-Co(1)-O(2)^{x}	101.56(12)
P(2)^{v}-K(1)-Co(1)-O(2)^{x}	99.03(12)
O(7)-K(1)-Co(1)-O(1)^{x}	112.08(14)
O(6)^{v}-K(1)-Co(1)-O(1)^{x}	24.07(16)
O(4)^{v}-K(1)-Co(1)-O(1)^{x}	14.34(11)
O(2)^{x}-K(1)-Co(1)-O(1)^{x}	-107.71(15)
O(6A)^{xiii}-K(1)-Co(1)-O(1)^{x}	-125.35(12)
O(3A)^{iv}-K(1)-Co(1)-O(1)^{x}	132.35(11)
O(5)-K(1)-Co(1)-O(1)^{x}	82.64(11)
O(5A)^{iii}-K(1)-Co(1)-O(1)^{x}	170.61(11)
O(1)^{v}-K(1)-Co(1)-O(1)^{x}	-78.03(12)
P(2)-K(1)-Co(1)-O(1)^{x}	93.88(10)
P(1)^{v}-K(1)-Co(1)-O(1)^{x}	-6.15(10)
P(2)^{v}-K(1)-Co(1)-O(1)^{x}	-8.69(10)
O(7)-K(1)-Co(1)-O(1)	-67.92(14)
O(6)^{v}-K(1)-Co(1)-O(1)	-155.93(16)
O(4)^{v}-K(1)-Co(1)-O(1)	-165.66(11)
O(2)^{x}-K(1)-Co(1)-O(1)	72.29(15)
O(6A)^{xiii}-K(1)-Co(1)-O(1)	54.65(12)
O(3A)^{iv}-K(1)-Co(1)-O(1)	-47.65(11)
O(5)-K(1)-Co(1)-O(1)	-97.36(11)
O(5A)^{iii}-K(1)-Co(1)-O(1)	-9.39(11)
O(1)^{v}-K(1)-Co(1)-O(1)	101.97(12)
P(2)-K(1)-Co(1)-O(1)	-86.12(10)
P(1)^{v}-K(1)-Co(1)-O(1)	173.85(10)
P(2)^{v}-K(1)-Co(1)-O(1)	171.31(10)
O(7)-K(1)-Co(1)-O(7)^{x}	180.000(1)
O(6)^{v}-K(1)-Co(1)-O(7)^{x}	92.00(16)
O(4)^{v}-K(1)-Co(1)-O(7)^{x}	82.26(12)
O(2)^{x}-K(1)-Co(1)-O(7)^{x}	-39.79(16)
O(6A)^{xiii}-K(1)-Co(1)-O(7)^{x}	-57.42(13)
O(3A)^{iv}-K(1)-Co(1)-O(7)^{x}	-159.72(12)
O(5)-K(1)-Co(1)-O(7)^{x}	150.56(12)
O(5A)^{iii}-K(1)-Co(1)-O(7)^{x}	-121.47(12)
O(1)^{v}-K(1)-Co(1)-O(7)^{x}	-10.10(12)
P(2)-K(1)-Co(1)-O(7)^{x}	161.81(11)
P(1)^{v}-K(1)-Co(1)-O(7)^{x}	61.77(11)
P(2)^{v}-K(1)-Co(1)-O(7)^{x}	59.24(12)

O(6)^{v}-K(1)-Co(1)-O(7)	-88.00(16)
O(4)^{v}-K(1)-Co(1)-O(7)	-97.74(12)
O(2)^{x}-K(1)-Co(1)-O(7)	140.21(16)
O(6A)^{xiii}-K(1)-Co(1)-O(7)	122.58(13)
O(3A)^{iv}-K(1)-Co(1)-O(7)	20.28(12)
O(5)-K(1)-Co(1)-O(7)	-29.44(12)
O(5A)^{iii}-K(1)-Co(1)-O(7)	58.53(12)
O(1)^{v}-K(1)-Co(1)-O(7)	169.90(12)
P(2)-K(1)-Co(1)-O(7)	-18.19(11)
P(1)^{v}-K(1)-Co(1)-O(7)	-118.23(11)
P(2)^{v}-K(1)-Co(1)-O(7)	-120.76(12)
O(7)-K(1)-Co(1)-K(1)^{x}	-114.4(6)
O(6)^{v}-K(1)-Co(1)-K(1)^{x}	157.6(6)
O(4)^{v}-K(1)-Co(1)-K(1)^{x}	147.9(6)
O(2)^{x}-K(1)-Co(1)-K(1)^{x}	25.8(6)
O(6A)^{xiii}-K(1)-Co(1)-K(1)^{x}	8.2(5)
O(3A)^{iv}-K(1)-Co(1)-K(1)^{x}	-94.1(6)
O(5)-K(1)-Co(1)-K(1)^{x}	-143.8(6)
O(5A)^{iii}-K(1)-Co(1)-K(1)^{x}	-55.9(5)
O(1)^{v}-K(1)-Co(1)-K(1)^{x}	55.5(5)
P(2)-K(1)-Co(1)-K(1)^{x}	-132.6(6)
P(1)^{v}-K(1)-Co(1)-K(1)^{x}	127.4(6)
P(2)^{v}-K(1)-Co(1)-K(1)^{x}	124.8(6)
P(2A)-O(7A)-Co(1A)-O(7A)^{iv}	-26.2(6)
K(1A)-O(7A)-Co(1A)-O(7A)^{iv}	111.2(3)
P(2A)-O(7A)-Co(1A)-O(1A)^{iv}	94.0(2)
K(1A)-O(7A)-Co(1A)-O(1A)^{iv}	-128.64(12)
P(2A)-O(7A)-Co(1A)-O(1A)	-86.0(2)
K(1A)-O(7A)-Co(1A)-O(1A)	51.36(12)
P(2A)-O(7A)-Co(1A)-O(2A)	5.3(3)
K(1A)-O(7A)-Co(1A)-O(2A)	142.69(11)
P(2A)-O(7A)-Co(1A)-O(2A)^{iv}	-174.7(3)
K(1A)-O(7A)-Co(1A)-O(2A)^{iv}	-37.31(11)
P(2A)-O(7A)-Co(1A)-K(1A)	-137.4(3)
P(2A)-O(7A)-Co(1A)-K(1A)^{iv}	42.6(3)
K(1A)-O(7A)-Co(1A)-K(1A)^{iv}	180
K(1A)^{ix}-O(1A)-Co(1A)-O(7A)	-135.69(13)
K(1A)^{ix}-O(1A)-Co(1A)-O(7A)^{iv}	44.31(13)
K(1A)^{ix}-O(1A)-Co(1A)-O(1A)^{iv}	30.3(6)
K(1A)^{ix}-O(1A)-Co(1A)-O(2A)	128.01(13)
K(1A)^{ix}-O(1A)-Co(1A)-O(2A)^{iv}	-51.99(13)
K(1A)^{ix}-O(1A)-Co(1A)-K(1A)	-101.89(12)
K(1A)^{ix}-O(1A)-Co(1A)-K(1A)^{iv}	78.11(12)
P(1A)-O(2A)-Co(1A)-O(7A)	-2.4(2)

K(1A)^{iv}-O(2A)-Co(1A)-O(7A)	149.54(10)
P(1A)-O(2A)-Co(1A)-O(7A)^{iv}	177.6(2)
K(1A)^{iv}-O(2A)-Co(1A)-O(7A)^{iv}	-30.46(10)
P(1A)-O(2A)-Co(1A)-O(1A)^{iv}	-88.0(2)
K(1A)^{iv}-O(2A)-Co(1A)-O(1A)^{iv}	63.95(10)
P(1A)-O(2A)-Co(1A)-O(1A)	92.0(2)
K(1A)^{iv}-O(2A)-Co(1A)-O(1A)	-116.05(10)
P(1A)-O(2A)-Co(1A)-K(1A)	28.1(2)
K(1A)^{iv}-O(2A)-Co(1A)-K(1A)	180
P(1A)-O(2A)-Co(1A)-K(1A)^{iv}	-151.9(2)
O(3)^{xi}-K(1A)-Co(1A)-O(7A)	-36.13(14)
O(6A)^{v}-K(1A)-Co(1A)-O(7A)	96.42(17)
O(4A)^{v}-K(1A)-Co(1A)-O(7A)	99.91(13)
O(5A)-K(1A)-Co(1A)-O(7A)	26.10(13)
O(5)-K(1A)-Co(1A)-O(7A)	-80.95(13)
O(1A)^{ix}-K(1A)-Co(1A)-O(7A)	-177.56(13)
O(2A)^{iv}-K(1A)-Co(1A)-O(7A)	-130.72(15)
P(2A)-K(1A)-Co(1A)-O(7A)	15.60(12)
P(2A)^{v}-K(1A)-Co(1A)-O(7A)	122.86(13)
K(1)^{i}-K(1A)-Co(1A)-O(7A)	50.08(12)
O(3)^{xi}-K(1A)-Co(1A)-O(7A)^{iv}	143.87(14)
O(7A)-K(1A)-Co(1A)-O(7A)^{iv}	180
O(6A)^{v}-K(1A)-Co(1A)-O(7A)^{iv}	-83.58(17)
O(4A)^{v}-K(1A)-Co(1A)-O(7A)^{iv}	-80.09(13)
O(5A)-K(1A)-Co(1A)-O(7A)^{iv}	-153.90(13)
O(5)-K(1A)-Co(1A)-O(7A)^{iv}	99.05(13)
O(1A)^{ix}-K(1A)-Co(1A)-O(7A)^{iv}	2.44(13)
O(2A)^{iv}-K(1A)-Co(1A)-O(7A)^{iv}	49.28(15)
P(2A)-K(1A)-Co(1A)-O(7A)^{iv}	-164.40(12)
P(2A)^{v}-K(1A)-Co(1A)-O(7A)^{iv}	-57.14(13)
K(1)^{i}-K(1A)-Co(1A)-O(7A)^{iv}	-129.92(12)
O(3)^{xi}-K(1A)-Co(1A)-O(1A)^{iv}	20.40(12)
O(7A)-K(1A)-Co(1A)-O(1A)^{iv}	56.53(15)
O(6A)^{v}-K(1A)-Co(1A)-O(1A)^{iv}	152.96(15)
O(4A)^{v}-K(1A)-Co(1A)-O(1A)^{iv}	156.44(11)
O(5A)-K(1A)-Co(1A)-O(1A)^{iv}	82.63(11)
O(5)-K(1A)-Co(1A)-O(1A)^{iv}	-24.42(11)
O(1A)^{ix}-K(1A)-Co(1A)-O(1A)^{iv}	-121.03(13)
O(2A)^{iv}-K(1A)-Co(1A)-O(1A)^{iv}	-74.19(13)
P(2A)-K(1A)-Co(1A)-O(1A)^{iv}	72.14(9)
P(2A)^{v}-K(1A)-Co(1A)-O(1A)^{iv}	179.40(10)
K(1)^{i}-K(1A)-Co(1A)-O(1A)^{iv}	106.61(9)
O(3)^{xi}-K(1A)-Co(1A)-O(1A)	-159.60(12)
O(7A)-K(1A)-Co(1A)-O(1A)	-123.47(15)

O(6A)^{v}-K(1A)-Co(1A)-O(1A)	-27.04(15)
O(4A)^{v}-K(1A)-Co(1A)-O(1A)	-23.56(11)
O(5A)-K(1A)-Co(1A)-O(1A)	-97.37(11)
O(5)-K(1A)-Co(1A)-O(1A)	155.58(11)
O(1A)^{ix}-K(1A)-Co(1A)-O(1A)	58.97(13)
O(2A)^{iv}-K(1A)-Co(1A)-O(1A)	105.81(13)
P(2A)-K(1A)-Co(1A)-O(1A)	-107.86(9)
K(1)^{i}-K(1A)-Co(1A)-O(1A)	-73.39(9)
O(3)^{xi}-K(1A)-Co(1A)-O(2A)	-85.41(12)
O(7A)-K(1A)-Co(1A)-O(2A)	-49.28(15)
O(6A)^{v}-K(1A)-Co(1A)-O(2A)	47.14(16)
O(4A)^{v}-K(1A)-Co(1A)-O(2A)	50.63(11)
O(5A)-K(1A)-Co(1A)-O(2A)	-23.18(11)
O(5)-K(1A)-Co(1A)-O(2A)	-130.23(11)
O(1A)^{ix}-K(1A)-Co(1A)-O(2A)	133.16(11)
O(2A)^{iv}-K(1A)-Co(1A)-O(2A)	180
P(2A)-K(1A)-Co(1A)-O(2A)	-33.68(10)
P(2A)^{v}-K(1A)-Co(1A)-O(2A)	73.58(10)
O(3)^{xi}-K(1A)-Co(1A)-O(2A)^{iv}	94.59(12)
O(7A)-K(1A)-Co(1A)-O(2A)^{iv}	130.72(15)
O(6A)^{v}-K(1A)-Co(1A)-O(2A)^{iv}	-132.86(16)
O(4A)^{v}-K(1A)-Co(1A)-O(2A)^{iv}	-129.37(11)
O(5A)-K(1A)-Co(1A)-O(2A)^{iv}	156.82(11)
O(5)-K(1A)-Co(1A)-O(2A)^{iv}	49.77(11)
O(1A)^{ix}-K(1A)-Co(1A)-O(2A)^{iv}	-46.84(11)
P(2A)-K(1A)-Co(1A)-O(2A)^{iv}	146.32(10)
P(2A)^{v}-K(1A)-Co(1A)-O(2A)^{iv}	-106.42(10)
K(1)^{i}-K(1A)-Co(1A)-O(2A)^{iv}	-179.20(10)
O(3)^{xi}-K(1A)-Co(1A)-K(1A)^{iv}	90.24(14)
O(7A)-K(1A)-Co(1A)-K(1A)^{iv}	126.37(17)
O(6A)^{v}-K(1A)-Co(1A)-K(1A)^{iv}	-137.21(19)
O(4A)^{v}-K(1A)-Co(1A)-K(1A)^{iv}	-133.72(14)
O(5A)-K(1A)-Co(1A)-K(1A)^{iv}	152.47(14)
O(5)-K(1A)-Co(1A)-K(1A)^{iv}	45.42(13)
O(1A)^{ix}-K(1A)-Co(1A)-K(1A)^{iv}	-51.19(13)
O(2A)^{iv}-K(1A)-Co(1A)-K(1A)^{iv}	-4.35(15)
P(2A)-K(1A)-Co(1A)-K(1A)^{iv}	141.98(13)
P(2A)^{v}-K(1A)-Co(1A)-K(1A)^{iv}	-110.76(14)
K(1)^{i}-K(1A)-Co(1A)-K(1A)^{iv}	176.45(14)

Symmetry transformations used to generate equivalent atoms:

(i) x, y+1, z; (ii) –x+2, -y-1, -z+2; (iii) x, y-1, z; (iv) -x+1, -y, -z+1; (v) x-1, y, z; (vi) –x+2, -y, -z+2; (vii) –x+2, -y+1, -z+1; (viii) x+1,y,z; (ix) -x,-y,-z+1; (x) -x+1,-y-1,-z+2; (xi) -x+1,-y,-z+2; (xii) x+1,y+1,z; (xiii) x-1, y-1, z.

C. Data for $K[Co(CH_4O_6P_2)_2(OH)_2(H_2O)_2]$

Table 1.C: Atomic coordinates ($x10^4$) and equivalent isotropic displacement parameters ($Å^2 \times 10^3$) for $K[Co(CH_4O_6P_2)_2(OH)_2(H_2O)_2]$. U(eq) is defined as one third of the trace of the orthogonalized U^{ij} tensor.

	x	y	z	U(eq)
C(1)	2225(3)	2500	6514(5)	13(1)
O(1)	1719(3)	2500	1557(4)	24(1)
O(2)	1248(2)	4025(2)	4277(3)	14(1)
O(3)	3031(2)	4399(4)	4548(3)	28(1)
O(4)	1923(2)	5353(3)	6578(3)	20(1)
O(5)	-377(3)	2500	4538(6)	36(1)
O(6)	92(3)	1017(3)	1813(4)	38(1)
P(1)	2068(1)	4137(1)	5425(1)	12(1)
K(1)	-74(1)	2500	8293(1)	26(1)
Co(1)	678(1)	2500	3068(1)	11(1)

Table 2.C: Bond distances (Å) and angles (º) for $K[Co(CH_4O_6P_2)_2(OH)_2(H_2O)_2]$.

Bond	Distance (Å)	Bond Angle	Angle(º)
C(1)-P(1)^{iii}	1.799(8)	P(1)^{iii}-C(1)-P(1)	116.11(1)
C(1)-P(1)	1.799(8)	P(1)^{iii}-C(1)-H(3)	107.7(16)
C(1)-H(3)	0.91(6)	P(1)-C(1)-H(3)	107.7(16)
C(1)-H(4)	1.07(7)	P(1)^{iii}-C(1)-H(4)	111.3(16)
O(1)-Co(1)	1.946(4)	P(1)-C(1)-H(4)	111.3(16)
O(1)-H(1)	0.82	H(3)-C(1)-H(4)	102(5)
O(2)-P(1)	1.512(2)	Co(1)-O(1)-H(1)	109.5
O(2)-Co(1)	1.928(2)	P(1)-O(2)-Co(1)	135.32(14)
O(3)-P(1)	1.563(3)	P(1)-O(3)-H(2)	115(3)
O(3)-H(2)	0.839(12)	Co(1)-O(5)-K(1)	122.57(19)
O(4)-P(1)	1.513(3)	Co(1)-O(5)-H(5)	114(7)
O(5)-Co(1)	1.938(5)	K(1)-O(5)-H(5)	97(7)
O(5)-K(1)	3.221(5)	Co(1)-O(6)-K(1)^{iv}	137.23(13)
O(5)-H(5)	0.86(2)	Co(1)-O(6)-K(1)^{v}	103.35(13)
O(6)-Co(1)	1.931(3)	K(1)^{iv}-O(6)-K(1)^{v}	113.14(9)
O(6)-K(1)^{iv}	3.280(4)	Co(1)-O(6)-H(6)	124(4)
O(6)-K(1)^{v}	3.306(4)	K(1)^{iv}-O(6)-H(6)	94(4)
O(6)-H(6)	0.89(2)	K(1)^{v}-O(6)-H(6)	20(4)

K(1)-O(6)^{iv}	3.280(4)	O(2)-P(1)-O(4)	111.61(14)
K(1)-O(6)^{vi}	3.280(4)	O(2)-P(1)-O(3)	111.13(14)
K(1)-O(6)^{vii}	3.306(4)	O(4)-P(1)-O(3)	107.97(17)
K(1)-O(6)^{vii}	3.306(4)	O(2)-P(1)-C(1)	111.53(16)
K(1)-H(4)	2.71(7)	O(4)-P(1)-C(1)	108.59(16)
Co(1)-O(2)^{iii}	1.928(2)	O(3)-P(1)-C(1)	105.77(18)
Co(1)-O(6)^{iii}	1.931(3)	O(5)-K(1)-O(6)^{iv}	88.39(6)
		O(5)-K(1)-O(6)^{vi}	88.39(6)
		O(6)^{iv}-K(1)-O(6)^{vi}	176.76(11)
		O(5)-K(1)-O(6)^{vii}	155.08(6)
		O(6)^{iv}-K(1)-O(6)^{vii}	116.32(7)
		O(6)^{vi}-K(1)-O(6)^{vii}	66.86(9)
		O(5)-K(1)-O(6)^{vii}	155.08(6)
		O(6)^{iv}-K(1)-O(6)^{vii}	66.86(9)
		O(6)^{vi}-K(1)-O(6)^{vii}	116.32(7)
		O(6)^{vii}-K(1)-O(6)^{vii}	49.46(11)
		O(5)-K(1)-H(4)	84.3(16)
		O(6)^{iv}-K(1)-H(4)	90.06(8)
		O(6)^{vi}-K(1)-H(4)	90.06(9)
		O(6)^{vii}-K(1)-H(4)	98.0(14)
		O(6)^{vii}-K(1)-H(4)	98.0(14)
		O(2)-Co(1)-O(2)^{iii}	94.97(14)
		O(2)-Co(1)-O(6)	178.24(11)
		O(2)^{iii}-Co(1)-O(6)	86.78(12)
		O(2)-Co(1)-O(6)^{iii}	86.78(12)
		O(2)^{iii}-Co(1)-O(6)^{iii}	178.24(11)
		O(6)-Co(1)-O(6)^{iii}	91.46(18)
		O(2)-Co(1)-O(5)	88.45(12)
		O(2)^{iii}-Co(1)-O(5)	88.45(12)
		O(6)-Co(1)-O(5)	91.76(15)
		O(6)^{iii}-Co(1)-O(5)	91.76(15)
		O(2)-Co(1)-O(1)	92.33(11)
		O(2)^{iii}-Co(1)-O(1)	92.33(11)
		O(6)-Co(1)-O(1)	87.44(15)
		O(6)^{iii}-Co(1)-O(1)	87.44(15)
		O(5)-Co(1)-O(1)	178.85(18)

Symmetry transformations used to generate equivalent atoms:

(i) –x+1/2, -y+1, z-1/2; (ii) –x, y+1/2, -z+1 (iii) x,-y+1/2,z; (iv) -x,y,-z+1; (v) x, y, z-1; (vi) x, -y+1/2, z+1; (vii) x, y, z+1.

Table 3.C: Anisotropic displacement parameters ($Å^2$ x 10^3) for $K[Co(CH_4O_6P_2)_2(OH)_2(H_2O)_2]$.

	U11	U22	U33	U23	U13	U12
C(1)	13(2)	17(2)	10(2)	0	-2(2)	0
O(1)	44(2)	13(2)	17(2)	0	8(2)	0
O(2)	14(1)	13(1)	16(1)	-2(1)	-6(1)	2(1)
O(3)	15(1)	49(2)	19(1)	16(1)	1(1)	-2(1)
O(4)	31(1)	15(1)	15(1)	-2(1)	-6(1)	-5(1)
O(5)	21(2)	39(2)	47(3)	0	1(2)	0
O(6)	51(2)	22(1)	39(2)	-2(1)	-26(1)	-1(1)
P(1)	13(1)	15(1)	9(1)	1(1)	-2(1)	-3(1)
K(1)	28(1)	21(1)	30(1)	0	7(1)	0
Co(1)	13(1)	10(1)	10(1)	0	-4(1)	0

Table 4.C: Hydrogen coordinates (x 10^4) and isotropic displacement parameters ($Å^2$ x 10^3) for $K[Co(CH_4O_6P_2)_2(OH)_2(H_2O)_2]$.

	x	y	z	U(eq)
H(1)	1756	3291	1139	37
H(2)	3000(30)	4310(60)	3567(16)	28(13)
H(3)	2830(40)	2500	6910(60)	11(13)
H(4)	1810(50)	2500	7560(90)	34(19)
H(5)	-720(60)	1740(60)	4490(110)	30(30)
H(6)	-40(40)	1110(70)	800(30)	62(19)

Table 5.C: Hydrogen bonds for $K[Co(CH_4O_6P_2)_2(OH)_2(H_2O)_2]$.

D-H...A	d(D-H)	d(H...A)	d(D...A)	<(DHA)
O(1)-H(1)...O(3)^{i}	0.82	2.56	3.376(4)	172.9
O(1)-H(1)...O(4)^{i}	0.82	2.28	2.763(4)	118.6
O(3)-H(2)...O(4)^{i}	0.839(12)	1.723(19)	2.537(4)	163(5)
O5-H5…O4^{ii}	0.86(6)	2.31(8)	3.100(5)	153(8)

Symmetry transformations used to generate equivalent atoms:

(i) –x+1/2, -y+1, z-1/2; (ii) –x, y+1/2, -z+1 (iii) x,-y+1/2,z; (iv) -x,y,-z+1; (v) x, y, z-1; (vi) x, -y+1/2, z+1; (vii) x, y, z+1.

Table 6.C: Torsion angles (º) for $K[Co(CH_4O_6P_2)_2(OH)_2(H_2O)_2]$.

Torsion Angle (º)	
Co(1)-O(2)-P(1)-O(4)	-152.65(19)
Co(1)-O(2)-P(1)-O(3)	86.8(2)
Co(1)-O(2)-P(1)-C(1)	-31.0(3)
P(1)^{iii}-C(1)-P(1)-O(2)	39.3(3)
P(1)^{iii}-C(1)-P(1)-O(4)	162.7(2)
P(1)^{iii}-C(1)-P(1)-O(3)	-81.6(3)
Co(1)-O(5)-K(1)-O(6)^{iv}	-90.22(7)
Co(1)-O(5)-K(1)-O(6)^{vi}	90.22(7)
Co(1)-O(5)-K(1)-O(6)^{vii}	96.8(2)
Co(1)-O(5)-K(1)-O(6)^{vii}	-96.8(2)
P(1)-O(2)-Co(1)-O(2)^{iii}	16.9(3)
P(1)-O(2)-Co(1)-O(6)	-158(4)
P(1)-O(2)-Co(1)-O(6)^{iii}	-163.0(2)
P(1)-O(2)-Co(1)-O(5)	105.2(2)
P(1)-O(2)-Co(1)-O(1)	-75.7(2)
K(1)^{iv}-O(6)-Co(1)-O(2)	174(4)
K(1)^{v}-O(6)-Co(1)-O(2)	26(5)
K(1)^{v}-O(6)-Co(1)-O(2)^{iii}	-149.10(12)
K(1)^{iv}-O(6)-Co(1)-O(6)^{iii}	179.10(11)
K(1)^{v}-O(6)-Co(1)-O(6)^{iii}	30.7(2)
K(1)^{iv}-O(6)-Co(1)-O(5)	-89.1(2)
K(1)^{v}-O(6)-Co(1)-O(5)	122.56(14)
K(1)^{iv}-O(6)-Co(1)-O(1)	91.7(2)
K(1)^{v}-O(6)-Co(1)-O(1)	-56.62(13)
K(1)-O(5)-Co(1)-O(2)	-47.51(7)
K(1)-O(5)-Co(1)-O(2)^{iii}	47.51(7)
K(1)-O(5)-Co(1)-O(6)	134.24(9)
K(1)-O(5)-Co(1)-O(6)^{iii}	-134.24(9)
K(1)-O(5)-Co(1)-O(1)	180.000(4)

Symmetry transformations used to generate equivalent atoms:

(i) –x+1/2, -y+1, z-1/2; (ii) –x, y+1/2, -z+1 (iii) x,-y+1/2,z; (iv) -x,y,-z+1; (v) x, y, z-1; (vi) x, -y+1/2, z+1; (vii) x, y, z+1.

APPENDIX B

A. Data for $(NH_4)_2[Co(CH_4O_6P_2)_2(H_2O)_2]$

Table 1.A: Atomic coordinates ($x10^4$) and equivalent isotropic displacement parameters ($Å^2$ x 10^3) for $(NH_4)_2[Co(CH_4O_6P_2)_2(H_2O)_2]$. U(eq) is defined as one third of the trace of the orthogonalized U^{ij} tensor.

	x	y	z	U(eq)
C(1)	5579(4)	3958(4)	7336(4)	7(1)
N(1)	8607(4)	1905(4)	1802(4)	11(1)
O(1)	3251(3)	2146(3)	12322(3)	10(1)
O(2)	3231(3)	1617(3)	8788(3)	8(1)
O(3)	2171(3)	4231(3)	7028(3)	9(1)
O(4)	5476(3)	1357(3)	5238(3)	10(1)
O(5)	9736(3)	1641(3)	5450(3)	9(1)
O(6)	8576(3)	4110(3)	8124(3)	8(1)
O(7)	7476(3)	1228(3)	8847(3)	7(1)
P(1)	4024(1)	2666(1)	7129(1)	5(1)
P(2)	7967(1)	2625(1)	7450(1)	5(1)
Co(1)	5000	0	10000	6(1)

Table 2.A: Bond distances (Å) and angles (º) for $(NH_4)_2[Co(CH_4O_6P_2)_2(H_2O)_2]$.

Bond	Distance (Å)	Bond Angle	Angle(º)
C(1)-P(1)	1.795(4)	P(1)-C(1)-P(2)	116.9(2)
C(1)-P(2)	1.795(4)	P(1)-C(1)-H(3)	108.1
C(1)-H(3)	0.97	P(2)-C(1)-H(3)	108.1
C(1)-H(4)	0.97	P(1)-C(1)-H(4)	108.1
N(1)-H(6)	0.837(19)	P(2)-C(1)-H(4)	108.1
N(1)-H(7)	0.808(19)	H(3)-C(1)-H(4)	107.3
N(1)-H(8)	0.837(19)	H(6)-N(1)-H(7)	114(4)
N(1)-H(9)	0.813(19)	H(6)-N(1)-H(8)	101(4)
O(1)-Co(1)	2.103(2)	H(7)-N(1)-H(8)	112(4)
O(1)-H(1A)	0.832(19)	H(6)-N(1)-H(9)	106(4)
O(1)-H(1B)	0.847(19)	H(7)-N(1)-H(9)	118(4)
O(2)-P(1)	1.502(2)	H(8)-N(1)-H(9)	105(4)
O(2)-Co(1)	2.072(2)	Co(1)-O(1)-H(1A)	124(3)
O(3)-P(1)	1.547(2)	Co(1)-O(1)-H(1B)	121(3)

O(3)-H(2A)	0.82	H(1A)-O(1)-H(1B)	101(4)
O(4)-P(1)	1.536(2)	P(1)-O(2)-Co(1)	126.75(12)
O(4)-H(2B)	0.82	P(1)-O(3)-H(2A)	109.5
O(5)-P(2)	1.541(2)	P(1)-O(4)-H(2B)	109.5
O(5)-H(5A)	0.82	P(2)-O(5)-H(5A)	109.5
O(6)-P(2)	1.530(2)	P(2)-O(6)-H(5B)	109.5
O(6)-H(5B)	0.82	P(2)-O(7)-Co(1)	133.63(12)
O(7)-P(2)	1.516(2)	O(2)-P(1)-O(4)	112.63(12)
O(7)-Co(1)	2.136(2)	O(2)-P(1)-O(3)	112.43(11)
Co(1)-O(2)^{ix}	2.072(2)	O(4)-P(1)-O(3)	110.69(12)
Co(1)-O(1)^{ix}	2.103(2)	O(2)-P(1)-C(1)	111.78(12)
Co(1)-O(7)^{ix}	2.136(2)	O(4)-P(1)-C(1)	106.27(12)
		O(3)-P(1)-C(1)	102.42(13)
		O(7)-P(2)-O(6)	111.69(12)
		O(7)-P(2)-O(5)	111.80(12)
		O(6)-P(2)-O(5)	110.44(12)
		O(7)-P(2)-C(1)	109.67(12)
		O(6)-P(2)-C(1)	103.88(12)
		O(5)-P(2)-C(1)	109.04(13)
		O(2)^{ix}-Co(1)-O(2)	180.00(8)
		O(2)^{ix}-Co(1)-O(1)^{ix}	87.47(9)
		O(2)-Co(1)-O(1)^{ix}	92.53(9)
		O(2)^{ix}-Co(1)-O(1)	92.53(9)
		O(2)-Co(1)-O(1)	87.47(9)
		O(1)^{ix}-Co(1)-O(1)	180
		O(2)^{ix}-Co(1)-O(7)	84.77(9)
		O(2)-Co(1)-O(7)	95.23(9)
		O(1)^{ix}-Co(1)-O(7)	91.09(8)
		O(1)-Co(1)-O(7)	88.91(8)
		O(2)^{ix}-Co(1)-O(7)^{ix}	95.23(9)
		O(2)-Co(1)-O(7)^{ix}	84.77(9)
		O(1)^{ix}-Co(1)-O(7)^{ix}	88.91(8)
		O(1)-Co(1)-O(7)^{ix}	91.09(8)
		O(7)-Co(1)-O(7)^{ix}	180

Symmetry transformations used to generate equivalent atoms:

(ix) -x+1, -y, -z+2

Table 3.A: Anisotropic displacement parameters ($Å^2$ x 10^3) for $(NH_4)_2[Co(CH_4O_6P_2)_2(H_2O)_2]$.

	U11	U22	U33	U23	U13	U12
C(1)	7(1)	6(1)	7(1)	1(1)	-4(1)	-2(1)
N(1)	10(1)	10(1)	11(1)	1(1)	-5(1)	0(1)
O(1)	10(1)	7(1)	8(1)	1(1)	-1(1)	-3(1)
O(2)	7(1)	8(1)	9(1)	5(1)	-4(1)	-4(1)
O(3)	7(1)	7(1)	14(1)	5(1)	-7(1)	-3(1)
O(4)	11(1)	11(1)	7(1)	-1(1)	-2(1)	-7(1)
O(5)	8(1)	6(1)	8(1)	0(1)	0(1)	-3(1)
O(6)	5(1)	8(1)	11(1)	0(1)	-4(1)	-2(1)
O(7)	7(1)	8(1)	8(1)	3(1)	-3(1)	-4(1)
P(1)	5(1)	5(1)	6(1)	2(1)	-3(1)	-2(1)
P(2)	5(1)	5(1)	6(1)	2(1)	-2(1)	-2(1)
Co(1)	5(1)	5(1)	6(1)	2(1)	-2(1)	-2(1)

Table 4.A: Hydrogen coordinates (x 10^4) and isotropic displacement parameters ($Å^2$ x 10^3) for $(NH_4)_2[Co(CH_4O_6P_2)_2(H_2O)_2]$.

	x	y	z	U(eq)
H(3)	4660	4874	8467	8
H(4)	5988	4650	6261	8
H(2A)	1086	3935	7498	13
H(2B)	4900	621	5163	15
H(5A)	9682	597	5286	13
H(5B)	9887	3825	7590	12
H(1A)	2290(50)	2070(50)	13370(40)	18(10)
H(1B)	2710(70)	3270(30)	12200(60)	27(11)
H(6)	7780(60)	1730(70)	2880(40)	33(13)
H(7)	8250(60)	1810(60)	1010(50)	20(10)
H(8)	8540(60)	3000(30)	2030(50)	12(9)
H(9)	9810(40)	1250(50)	1580(60)	23(11)

Table 5.A: Hydrogen bonds for $(NH_4)_2[Co(CH_4O_6P_2)_2(H_2O)_2]$.

D-H...A	d(D-H)	d(H...A)	d(D...A)	<(DHA)
N(1)-H(8)...O(3)^{i}	0.837(19)	2.06(2)	2.891(4)	170(4)
O(1)-H(1B)...O(6)^{ii}	0.847(19)	1.98(2)	2.826(3)	179(5)
O(3)-H(2A)...O(6)^{iii}	0.82	1.66	2.436(3)	157.3
O(5)-H(5A)...O(5)^{iv}	0.82	1.66	2.464(4)	164.7
N(1)-H(9)...O(7)^{iv}	0.813(19)	2.18(2)	2.960(3)	161(4)
O(6)-H(5B)...O(3)^{v}	0.82	1.67	2.436(3)	153.5
O(1)-H(1A)...O(5)^{vi}	0.832(19)	1.98(2)	2.794(3)	165(4)
N(1)-H(7)...O(7)^{vii}	0.808(19)	2.16(2)	2.968(4)	173(4)
N(1)-H(9)...O(2)^{viii}	0.813(19)	2.60(4)	3.104(4)	122(4)

Symmetry transformations used to generate equivalent atoms:

(i) –x+1, -y+1, -z+1; (ii) –x+1, -y+1, -z+2; (iii) x-1, y, z; (iv) -x+2, -y, -z+1; (v) x+1, y, z; (vi) x-1, y, z+1; (vii) x, y, z-1; (viii) x+1, y, z-1; (ix) -x+1, -y, -z+2

Table 6.A: Torsion angles (º) for $(NH_4)_2[Co(CH_4O_6P_2)_2(H_2O)_2]$.

Torsion Angle (º)	
Co(1)-O(2)-P(1)-O(4)	73.74(17)
Co(1)-O(2)-P(1)-O(3)	-160.38(13)
Co(1)-O(2)-P(1)-C(1)	-45.83(18)
P(2)-C(1)-P(1)-O(2)	60.55(18)
P(2)-C(1)-P(1)-O(4)	-62.69(18)
P(2)-C(1)-P(1)-O(3)	-178.87(14)
Co(1)-O(7)-P(2)-O(6)	135.73(15)
Co(1)-O(7)-P(2)-O(5)	-99.94(17)
Co(1)-O(7)-P(2)-C(1)	21.1(2)
P(1)-C(1)-P(2)-O(7)	-46.39(19)
P(1)-C(1)-P(2)-O(6)	-165.90(14)
P(1)-C(1)-P(2)-O(5)	76.34(17)
P(1)-O(2)-Co(1)-O(2)^{ix}	-168(100)
P(1)-O(2)-Co(1)-O(1)^{ix}	-71.90(15)
P(1)-O(2)-Co(1)-O(1)	108.10(15)
P(1)-O(2)-Co(1)-O(7)	19.43(15)
P(1)-O(2)-Co(1)-O(7)^{ix}	-160.57(15)

P(2)-O(7)-Co(1)-O(2)^{ix}	173.71(17)
P(2)-O(7)-Co(1)-O(2)	-6.29(17)
P(2)-O(7)-Co(1)-O(1)^{ix}	86.35(17)
P(2)-O(7)-Co(1)-O(1)	-93.65(17)
P(2)-O(7)-Co(1)-O(7)^{ix}	-48(100)

Symmetry transformations used to generate equivalent atoms:

(ix) -x+1, -y, -z+2

B. Data for $Na_2[Co(CH_4O_6P_2)_2(H_2O)_2]\cdot 2H_2O$

Table 1.B: Atomic coordinates (x10^4) and equivalent isotropic displacement parameters (Å^2 x 10^3) for $Na_2[Co(CH_4O_6P_2)_2(H_2O)_2]\cdot 2H_2O$. U(eq) is defined as one third of the trace of the orthogonalized U^{ij} tensor.

	x	y	z	U(eq)
C(1)	3606(2)	4054(1)	-3732(2)	7(1)
O(1)	3341(2)	4557(1)	1941(1)	9(1)
O(2)	5268(2)	3512(1)	-864(1)	7(1)
O(3)	6121(2)	2548(1)	-3269(1)	8(1)
O(4)	2745(2)	2337(1)	-2143(1)	9(1)
O(5)	1754(2)	5864(1)	-3986(1)	9(1)
O(6)	-203(2)	4352(1)	-3131(1)	8(1)
O(7)	2361(2)	5162(1)	-1272(1)	8(1)
O(8)	207(2)	6743(1)	-261(2)	11(1)
Na(1)	661(1)	7422(1)	2272(1)	10(1)
P(1)	4377(1)	3063(1)	-2386(1)	5(1)
P(2)	1763(1)	4866(1)	-2955(1)	6(1)
Co(1)	5000	5000	0	5(1)

Table 2.B: Bond distances (Å) and angles (º) for $Na_2[Co(CH_4O_6P_2)_2(H_2O)_2]\cdot 2H_2O$.

Bond	Distance (Å)	Bond Angle	Angle(º)
C(1)-P(2)	1.7970(17)	P(2)-C(1)-P(1)	114.36(8)
C(1)-P(1)	1.8020(16)	P(2)-C(1)-H(3)	108.7
C(1)-H(3)	0.97	P(1)-C(1)-H(3)	108.7
C(1)-H(4)	0.97	P(2)-C(1)-H(4)	108.7
O(1)-Co(1)	2.0893(11)	P(1)-C(1)-H(4)	108.7
O(1)-H(1A)	0.853(17)	H(3)-C(1)-H(4)	107.6
O(1)-H(1B)	0.839(17)	Co(1)-O(1)-H(1A)	122.0(18)
O(2)-P(1)	1.5197(12)	Co(1)-O(1)-H(1B)	126(2)
O(2)-Co(1)	2.1145(12)	H(1A)-O(1)-H(1B)	109(3)
O(3)-P(1)	1.5777(13)	P(1)-O(2)-Co(1)	128.00(7)
O(3)-Na(1)^{ii}	2.3441(14)	P(1)-O(3)-Na(1)^{ii}	123.15(7)
O(3)-H(2)	0.836(18)	P(1)-O(3)-H(2)	112(2)
O(4)-P(1)	1.4967(12)	Na(1)^{ii}-O(3)-H(2)	125(2)
O(4)-Na(1)^{v}	2.3613(14)	P(1)-O(4)-Na(1)^{v}	130.62(7)
O(5)-P(2)	1.5814(13)	P(2)-O(5)-Na(1)^{viii}	120.43(6)
O(5)-Na(1)^{viii}	2.6248(14)	P(2)-O(5)-H(5)	112(2)
O(5)-H(5)	0.827(17)	Na(1)^{viii}-O(5)-H(5)	113(2)
O(6)-P(2)	1.5170(12)	P(2)-O(6)-Na(1)^{v}	121.17(7)
O(6)-Na(1)^{v}	2.4859(14)	P(2)-O(7)-Co(1)	131.38(7)
O(7)-P(2)	1.5074(12)	Na(1)-O(8)-Na(1)^{viii}	126.57(6)
O(7)-Co(1)	2.0904(12)	Na(1)-O(8)-H(6)	105(3)
O(8)-Na(1)	2.3146(14)	Na(1)^{viii}-O(8)-H(6)	109(3)
O(8)-Na(1)^{viii}	2.3673(14)	Na(1)-O(8)-H(7)	111.5(17)
O(8)-H(6)	0.833(19)	Na(1)^{viii}-O(8)-H(7)	100.1(16)
O(8)-H(7)	0.85(3)	H(6)-O(8)-H(7)	103(3)
Na(1)-O(3)^{ii}	2.3441(14)	O(8)-Na(1)-O(3)^{ii}	115.88(5)
Na(1)-O(4)^{v}	2.3613(14)	O(8)-Na(1)-O(4)^{v}	84.22(5)
Na(1)-O(8)^{ix}	2.3673(14)	O(3)^{ii}-Na(1)-O(4)^{v}	159.90(5)
Na(1)-O(6)^{v}	2.4859(14)	O(8)-Na(1)-O(8)^{ix}	163.89(7)
Na(1)-O(5)^{ix}	2.6248(14)	O(3)^{ii}-Na(1)-O(8)^{ix}	79.97(5)
Na(1)-Na(1)^{ix}	4.18213(17)	O(4)^{v}-Na(1)-O(8)^{ix}	79.94(5)
Na(1)-Na(1)^{viii}	4.18213(17)	O(8)-Na(1)-O(6)^{v}	83.05(5)
Na(1)-H(6)	2.65(3)	O(3)^{ii}-Na(1)-O(6)^{v}	92.18(5)
P(2)-O(7)^{i}	1.5074(12)	O(4)^{v}-Na(1)-O(6)^{v}	90.54(5)
Co(1)-O(1)^{ii}	2.0893(11)	O(8)^{ix}-Na(1)-O(6)^{v}	99.93(5)

Co(1)-O(7)^{ii}	2.0904(12)	O(8)-Na(1)-O(5)^{ix}	90.32(5)
Co(1)-O(7)^{i}	2.0904(12)	O(3)^{ii}-Na(1)-O(5)^{ix}	81.45(5)
Co(1)-O(2)^{ii}	2.1145(12)	O(4)^{v}-Na(1)-O(5)^{ix}	99.04(5)
		O(8)^{ix}-Na(1)-O(5)^{ix}	89.29(5)
		O(6)^{v}-Na(1)-O(5)^{ix}	167.77(5)
		O(8)-Na(1)-Na(1)^{ix}	158.30(5)
		O(3)^{ii}-Na(1)-Na(1)^{ix}	70.55(3)
		O(4)^{v}-Na(1)-Na(1)^{ix}	90.88(3)
		O(8)^{ix}-Na(1)-Na(1)^{ix}	26.39(3)
		O(6)^{v}-Na(1)-Na(1)^{ix}	75.85(3)
		O(5)^{ix}-Na(1)-Na(1)^{ix}	111.35(4)
		O(8)-Na(1)-Na(1)^{viii}	27.04(3)
		O(3)^{ii}-Na(1)-Na(1)^{viii}	109.36(3)
		O(4)^{v}-Na(1)-Na(1)^{viii}	88.36(3)
		O(8)^{ix}-Na(1)-Na(1)^{viii}	148.17(5)
		O(6)^{v}-Na(1)-Na(1)^{viii}	109.75(4)
		O(5)^{ix}-Na(1)-Na(1)^{viii}	63.28(3)
		Na(1)^{ix}-Na(1)-Na(1)^{viii}	174.35(4)
		O(8)-Na(1)-H(6)	17.7(6)
		O(3)^{ii}-Na(1)-H(6)	130.9(7)
		O(4)^{v}-Na(1)-H(6)	68.9(7)
		O(8)^{ix}-Na(1)-H(6)	148.3(6)
		O(6)^{v}-Na(1)-H(6)	75.0(8)
		O(5)^{ix}-Na(1)-H(6)	101.2(7)
		Na(1)^{ix}-Na(1)-H(6)	144.1(6)
		Na(1)^{viii}-Na(1)-H(6)	40.1(7)
		O(4)-P(1)-O(2)	115.28(7)
		O(4)-P(1)-O(3)	111.32(7)
		O(2)-P(1)-O(3)	105.44(7)
		O(4)-P(1)-C(1)	110.21(7)
		O(2)-P(1)-C(1)	110.01(7)
		O(3)-P(1)-C(1)	103.89(7)
		O(7)^{i}-P(2)-O(6)	115.47(7)
		O(7)-P(2)-O(6)	115.47(7)
		O(7)^{i}-P(2)-O(5)	106.64(7)
		O(7)-P(2)-O(5)	106.64(7)
		O(6)-P(2)-O(5)	109.48(7)
		O(7)^{i}-P(2)-C(1)	108.35(7)

		O(7)-P(2)-C(1)	108.35(7)
		O(6)-P(2)-C(1)	109.13(7)
		O(5)-P(2)-C(1)	107.48(7)
		$O(1)^{ii}$-Co(1)-O(1)	180
		$O(1)^{ii}$-Co(1)-$O(7)^{ii}$	86.62(5)
		O(1)-Co(1)-$O(7)^{ii}$	93.38(5)
		$O(1)^{ii}$-Co(1)-O(7)	93.38(5)
		O(1)-Co(1)-O(7)	86.62(5)
		$O(7)^{ii}$-Co(1)-O(7)	180
		$O(1)^{ii}$-Co(1)-$O(7)^{i}$	93.38(5)
		O(1)-Co(1)-$O(7)^{i}$	86.62(5)
		$O(7)^{ii}$-Co(1)-$O(7)^{i}$	180
		$O(1)^{ii}$-Co(1)-O(2)	86.84(5)
		O(1)-Co(1)-O(2)	93.16(5)
		$O(7)^{ii}$-Co(1)-O(2)	89.74(5)
		O(7)-Co(1)-O(2)	90.26(5)
		$O(7)^{i}$-Co(1)-O(2)	90.26(5)
		$O(1)^{ii}$-Co(1)-$O(2)^{ii}$	93.16(5)
		O(1)-Co(1)-$O(2)^{ii}$	86.84(5)
		$O(7)^{ii}$-Co(1)-$O(2)^{ii}$	90.26(5)
		O(7)-Co(1)-$O(2)^{ii}$	89.74(5)
		$O(7)^{i}$-Co(1)-$O(2)^{ii}$	89.74(5)
		O(2)-Co(1)-$O(2)^{ii}$	180.00(6)

Symmetry transformations used to generate equivalent atoms:

(i) x, y, z; (ii) –x+1, -y+1, -z; (iii) x, y, z-1; (iv) x, -y+1/2, z-1/2; (v) –x, -y+1, -z; (vi) x, -y+1/2, z+1/2; (vii) –x, -y+1, -z-1; (viii) x,-y+3/2,z-1/2; (ix) x,-y+3/2,z+1/2.

Table 3.B: Anisotropic displacement parameters ($Å^2$ x 10^3) for $Na_2[Co(CH_4O_6P_2)_2(H_2O)_2]\cdot 2H_2O$.

	U11	U22	U33	U23	U13	U12
C(1)	8(1)	7(1)	6(1)	0(1)	0(1)	0(1)
O(1)	10(1)	7(1)	10(1)	2(1)	4(1)	1(1)
O(2)	11(1)	6(1)	6(1)	-1(1)	-2(1)	1(1)
O(3)	7(1)	10(1)	8(1)	-3(1)	0(1)	2(1)
O(4)	7(1)	7(1)	11(1)	0(1)	0(1)	-1(1)
O(5)	12(1)	6(1)	8(1)	1(1)	-4(1)	0(1)

O(6)	7(1)	9(1)	8(1)	0(1)	-1(1)	-1(1)
O(7)	8(1)	10(1)	6(1)	-1(1)	-2(1)	2(1)
O(8)	9(1)	14(1)	11(1)	0(1)	1(1)	2(1)
Na(1)	8(1)	11(1)	10(1)	-1(1)	-1(1)	0(1)
P(1)	5(1)	5(1)	5(1)	-1(1)	0(1)	0(1)
P(2)	6(1)	6(1)	5(1)	0(1)	-1(1)	1(1)
Co(1)	5(1)	5(1)	4(1)	0(1)	-1(1)	0(1)

Table 4.B: Hydrogen coordinates (x 10^4) and isotropic displacement parameters (Å^2 x 10^3) for $Na_2[Co(CH_4O_6P_2)_2(H_2O)_2]\cdot 2H_2O$.

	x	y	z	U(eq)
H(3)	4731	4458	-3991	8
H(4)	3113	3752	-4718	8
H(1A)	2390(30)	4910(17)	2270(30)	23(7)
H(1B)	3240(40)	3968(15)	2290(30)	32(7)
H(2)	5760(50)	2270(20)	-4120(30)	44(9)
H(5)	1300(40)	5770(20)	-4900(20)	34(8)
H(6)	-910(30)	6500(30)	-260(50)	69(12)
H(7)	920(40)	6230(20)	-390(30)	17(6)

Table 5.B: Hydrogen bonds for $Na_2[Co(CH_4O_6P_2)_2(H_2O)_2]\cdot 2H_2O$.

D-H...A	d(D-H)	d(H...A)	d(D...A)	<(DHA)
O(8)-H(7)...O(7)^{i,v}	0.85(3)	1.89(3)	2.7162(18)	165(2)
C(1)-H(3)...O(1)^{ii,iii}	0.97	2.51	3.145(2)	123.2
C(1)-H(4)...O(4)^{iv}	0.97	2.5	3.435(2)	162.7
O(3)-H(2)...O(2)^{iv}	0.836(18)	1.811(19)	2.6390(16)	170(3)
O(1)-H(1A)...O(6)^{v}	0.853(17)	1.948(17)	2.7998(17)	176(3)
O(8)-H(6)...O(1)^{v}	0.833(19)	2.57(3)	3.2756(18)	143(3)
O(1)-H(1B)...O(4)^{vi}	0.839(17)	1.831(18)	2.6644(17)	172(3)
O(5)-H(5)...O(6)^{vii}	0.827(17)	1.801(18)	2.6262(16)	176(3)

Symmetry transformations used to generate equivalent atoms:

(i) x, y, z; (ii) –x+1, -y+1, -z; (iii) x, y, z-1; (iv) x, -y+1/2, z-1/2; (v) –x, -y+1, -z; (vi) x, -y+1/2, z+1/2; (vii) –x, -y+1, -z-1; (viii) x,-y+3/2,z-1/2; (ix) x,-y+3/2,z+1/2.

Table 6.B: Torsion angles (º) for $Na_2[Co(CH_4O_6P_2)_2(H_2O)_2]\cdot 2H_2O$.

Torsion Angle (º)	
$Na(1)^{viii}$-O(8)-Na(1)-$O(3)^{ii}$	-81.94(8)
$Na(1)^{viii}$-O(8)-Na(1)-$O(4)^{v}$	97.76(8)
$Na(1)^{viii}$-O(8)-Na(1)-$O(8)^{ix}$	87.2(2)
$Na(1)^{viii}$-O(8)-Na(1)-$O(6)^{v}$	-170.99(8)
$Na(1)^{viii}$-O(8)-Na(1)-$O(5)^{ix}$	-1.29(8)
$Na(1)^{viii}$-O(8)-Na(1)-$Na(1)^{ix}$	175.48(4)
$Na(1)^{v}$-O(4)-P(1)-O(2)	97.19(10)
$Na(1)^{v}$-O(4)-P(1)-O(3)	-142.78(8)
$Na(1)^{v}$-O(4)-P(1)-C(1)	-28.06(11)
Co(1)-O(2)-P(1)-O(4)	-108.15(9)
Co(1)-O(2)-P(1)-O(3)	128.65(8)
Co(1)-O(2)-P(1)-C(1)	17.20(11)
$Na(1)^{ii}$-O(3)-P(1)-O(4)	-126.76(8)
$Na(1)^{ii}$-O(3)-P(1)-O(2)	-1.07(10)
$Na(1)^{ii}$-O(3)-P(1)-C(1)	114.65(8)
P(2)-C(1)-P(1)-O(4)	66.49(10)
P(2)-C(1)-P(1)-O(2)	-61.71(11)
P(2)-C(1)-P(1)-O(3)	-174.16(8)
Co(1)-O(7)-P(2)-O(6)	134.80(9)
Co(1)-O(7)-P(2)-O(5)	-103.33(10)
Co(1)-O(7)-P(2)-C(1)	12.09(12)
$Na(1)^{v}$-O(6)-P(2)-$O(7)^{i}$	-74.18(9)
$Na(1)^{v}$-O(6)-P(2)-O(7)	-74.18(9)
$Na(1)^{v}$-O(6)-P(2)-O(5)	165.49(7)
$Na(1)^{v}$-O(6)-P(2)-C(1)	48.11(9)
$Na(1)^{viii}$-O(5)-P(2)-$O(7)^{i}$	-35.73(9)
$Na(1)^{viii}$-O(5)-P(2)-O(7)	-35.73(9)
$Na(1)^{viii}$-O(5)-P(2)-O(6)	89.85(8)
$Na(1)^{viii}$-O(5)-P(2)-C(1)	-151.74(7)
P(1)-C(1)-P(2)-$O(7)^{i}$	46.93(11)
P(1)-C(1)-P(2)-O(7)	46.93(11)
P(1)-C(1)-P(2)-O(6)	-79.55(10)
P(1)-C(1)-P(2)-O(5)	161.81(8)
P(2)-O(7)-Co(1)-$O(1)^{ii}$	43.02(10)
P(2)-O(7)-Co(1)-O(1)	-136.98(10)

P(2)-O(7)-Co(1)-O(7)^{ii}	-13(100)
P(2)-O(7)-Co(1)-O(2)	-43.83(10)
P(2)-O(7)-Co(1)-O(2)^{ii}	136.17(10)
P(1)-O(2)-Co(1)-O(1)^{ii}	-68.45(9)
P(1)-O(2)-Co(1)-O(1)	111.55(9)
P(1)-O(2)-Co(1)-O(7)^{ii}	-155.08(9)
P(1)-O(2)-Co(1)-O(7)	24.92(9)
P(1)-O(2)-Co(1)-O(7)^{i}	24.92(9)
P(1)-O(2)-Co(1)-O(2)^{ii}	35(100)

Symmetry transformations used to generate equivalent atoms:
(i) x, y, z; (ii) –x+1, -y+1, -z; (iii) x, y, z-1; (iv) x, -y+1/2, z-1/2; (v) –x, -y+1, -z; (vi) x, -y+1/2, z+1/2; (vii) –x, -y+1, -z-1; (viii) x,-y+3/2,z-1/2; (ix) x,-y+3/2,z+1/2.

C. Data for $Cs_2[Co(CH_4O_6P_2)_2(H_2O)_2]$

Table 1.C: Atomic coordinates (x10^4) and equivalent isotropic displacement parameters (Å^2 x 10^3) for $Cs_2[Co(CH_4O_6P_2)_2(H_2O)_2]$. U(eq) is defined as one third of the trace of the orthogonalized U^{ij} tensor.

	x	y	z	U(eq)
C(1)	2391(5)	858(5)	1117(5)	7(1)
O(1)	2881(4)	-565(4)	7205(4)	11(1)
O(2)	3853(4)	-1791(4)	3784(4)	8(1)
O(3)	665(4)	-2295(4)	3115(5)	8(1)
O(4)	3331(4)	-2604(4)	859(4)	8(1)
O(5)	1823(4)	4388(4)	1033(4)	11(1)
O(6)	107(4)	2058(4)	3619(4)	10(1)
O(7)	3538(4)	2426(4)	3621(4)	8(1)
P(1)	2638(1)	-1574(1)	2286(1)	5(1)
P(2)	1961(1)	2478(1)	2513(1)	5(1)
Co(1)	5000	0	5000	5(1)
Cs(1)	2846(1)	4549(1)	6929(1)	9(1)

Table 2.C: Bond distances (Å) and angles (º) for $Cs_2[Co(CH_4O_6P_2)_2(H_2O)_2]$.

Bond	Distance (Å)	Bond Angle	Angle(º)
C(1)-P(1)	1.797(4)	P(1)-C(1)-P(2)	116.7(2)
C(1)-P(2)	1.801(4)	P(1)-C(1)-Cs(1)^{v}	149.50(18)
C(1)-Cs(1)^{v}	3.619(4)	P(2)-C(1)-Cs(1)^{v}	93.21(15)
C(1)-H(3)	0.97	P(1)-C(1)-H(3)	108.1
C(1)-H(4)	0.97	P(2)-C(1)-H(3)	108.1
O(1)-Co(1)	2.125(3)	Cs(1)^{v}-C(1)-H(3)	64.4
O(1)-Cs(1)^{vi}	3.686(4)	P(1)-C(1)-H(4)	108.1
O(1)-H(1A)	0.87(2)	P(2)-C(1)-H(4)	108.1
O(1)-H(1B)	0.88(2)	Cs(1)^{v}-C(1)-H(4)	52.8
O(2)-P(1)	1.507(3)	H(3)-C(1)-H(4)	107.3
O(2)-Co(1)	2.079(3)	Co(1)-O(1)-Cs(1)^{vi}	89.84(9)
O(2)-Cs(1)^{vii}	3.163(3)	Co(1)-O(1)-H(1A)	129(4)
O(2)-Cs(1)^{vi}	3.173(3)	Cs(1)^{vi}-O(1)-H(1A)	84(4)
O(3)-P(1)	1.573(3)	Co(1)-O(1)-H(1B)	130(5)
O(3)-Cs(1)^{ii}	3.162(3)	Cs(1)^{vi}-O(1)-H(1B)	80(8)
O(3)-Cs(1)^{vi}	3.691(4)	H(1A)-O(1)-H(1B)	99(4)
O(3)-H(2)	0.64(6)	P(1)-O(2)-Co(1)	135.99(18)
O(4)-P(1)	1.516(3)	P(1)-O(2)-Cs(1)^{vii}	107.08(14)
O(4)-Cs(1)^{vii}	3.489(3)	Co(1)-O(2)-Cs(1)^{vii}	103.87(11)
O(5)-P(2)	1.568(3)	P(1)-O(2)-Cs(1)^{vi}	109.99(14)
O(5)-Cs(1)^{v}	3.118(4)	Co(1)-O(2)-Cs(1)^{vi}	106.15(12)
O(5)-Cs(1)^{viii}	3.716(4)	Cs(1)vii-O(2)-Cs(1)^{vi}	78.68(8)
O(5)-H(5)	0.85(2)	P(1)-O(3)-Cs(1)^{ii}	151.17(18)
O(6)-P(2)	1.516(3)	P(1)-O(3)-Cs(1)^{vi}	87.58(13)
O(6)-Cs(1)^{viii}	3.191(3)	Cs(1)ii-O(3)-Cs(1)^{vi}	101.33(9)
O(7)-P(2)	1.508(3)	P(1)-O(3)-H(2)	111(6)
O(7)-Co(1)	2.128(3)	Cs(1)^{ii}-O(3)-H(2)	98(6)
O(7)-Cs(1)	3.297(3)	Cs(1)^{vi}-O(3)-H(2)	61(6)
O(7)-Cs(1)^{ix}	3.492(3)	P(1)-O(4)-Cs(1)^{vii}	93.28(14)
P(1)-Cs(1)^{vii}	3.883(2)	P(2)-O(5)-Cs(1)^{v}	120.02(16)
P(1)-Cs(1)^{vi}	3.950(2)	P(2)-O(5)-Cs(1)^{viii}	91.85(13)
P(1)-H(2)	1.89(6)	Cs(1)^{v}-O(5)-Cs(1)^{viii}	124.39(9)
P(2)-Cs(1)^{viii}	4.080(2)	P(2)-O(5)-H(5)	115(10)
P(2)-Cs(1)^{v}	4.131(3)	Cs(1)^{v}-O(5)-H(5)	58(10)
P(2)-Cs(1)	4.200(2)	Cs(1)^{viii}-O(5)-H(5)	67(10)

Co(1)-O(2)^{vii}	2.079(3)	P(2)-O(6)-Cs(1)^{viii}	115.52(15)
Co(1)-O(1)^{vii}	2.125(3)	P(2)-O(7)-Co(1)	126.73(17)
Co(1)-O(7)^{vii}	2.128(3)	P(2)-O(7)-Cs(1)	116.87(15)
Co(1)-Cs(1)	4.181(2)	Co(1)-O(7)-Cs(1)	98.50(11)
Co(1)-Cs(1)^{vii}	4.181(2)	P(2)-O(7)-Cs(1)^{ix}	131.61(15)
Co(1)-Cs(1)^{vi}	4.249(2)	Co(1)-O(7)-Cs(1)^{ix}	95.14(10)
Co(1)-Cs(1)^{ix}	4.249(2)	Cs(1)-O(7)-Cs(1)^{ix}	72.47(6)
Cs(1)-O(5)^{iii}	3.118(4)	O(2)-P(1)-O(4)	114.87(17)
Cs(1)-O(3)^{ii}	3.162(3)	O(2)-P(1)-O(3)	109.96(18)
Cs(1)-O(2)^{vii}	3.163(3)	O(4)-P(1)-O(3)	107.50(17)
Cs(1)-O(2)^{x}	3.173(3)	O(2)-P(1)-C(1)	109.72(17)
Cs(1)-O(6)^{viii}	3.191(3)	O(4)-P(1)-C(1)	107.00(18)
Cs(1)-O(4)^{vii}	3.489(3)	O(3)-P(1)-C(1)	107.51(18)
Cs(1)-O(7)^{ix}	3.492(3)	O(2)-P(1)-Cs(1)^{vii}	51.14(12)
Cs(1)-C(1)^{iii}	3.619(4)	O(4)-P(1)-Cs(1)^{vii}	63.78(12)
Cs(1)-O(1)^{x}	3.686(4)	O(3)-P(1)-Cs(1)^{vii}	124.42(13)
Cs(1)-O(3)^{x}	3.691(4)	C(1)-P(1)-Cs(1)^{vii}	127.89(13)
Cs(1)-O(5)^{viii}	3.716(4)	O(2)-P(1)-Cs(1)^{vi}	49.01(11)
		O(4)-P(1)-Cs(1)^{vi}	103.61(13)
		O(3)-P(1)-Cs(1)^{vi}	68.98(12)
		C(1)-P(1)-Cs(1)^{vi}	148.59(13)
		Cs(1)^{vii}-P(1)-Cs(1)^{vi}	61.69(2)
		O(2)-P(1)-H(2)	94(2)
		O(4)-P(1)-H(2)	124.1(19)
		O(3)-P(1)-H(2)	18.4(19)
		C(1)-P(1)-H(2)	106.3(19)
		Cs(1)^{vii}-P(1)-H(2)	121.3(19)
		Cs(1)^{vi}-P(1)-H(2)	60.1(19)
		O(7)-P(2)-O(6)	114.84(18)
		O(7)-P(2)-O(5)	111.68(17)
		O(6)-P(2)-O(5)	109.48(17)
		O(7)-P(2)-C(1)	110.69(18)
		O(6)-P(2)-C(1)	107.96(17)
		O(5)-P(2)-C(1)	101.30(18)
		O(7)-P(2)-Cs(1)^{viii}	124.05(12)
		O(6)-P(2)-Cs(1)^{viii}	44.90(12)
		O(5)-P(2)-Cs(1)^{viii}	65.56(12)
		C(1)-P(2)-Cs(1)^{viii}	124.92(13)
		O(7)-P(2)-Cs(1)^{v}	118.56(12)
		O(6)-P(2)-Cs(1)^{v}	125.76(12)
		O(5)-P(2)-Cs(1)^{v}	40.80(12)
		C(1)-P(2)-Cs(1)^{v}	60.99(13)
		Cs(1)^{viii}-P(2)-Cs(1)^{v}	94.94(3)

		O(7)-P(2)-Cs(1)	44.45(11)
		O(6)-P(2)-Cs(1)	81.48(12)
		O(5)-P(2)-Cs(1)	98.82(13)
		C(1)-P(2)-Cs(1)	153.17(13)
		Cs(1)^{viii}-P(2)-Cs(1)	79.77(3)
		Cs(1)^{v}-P(2)-Cs(1)	133.88(4)
		O(2)-Co(1)-O(2)^{vii}	180
		O(2)-Co(1)-O(1)	90.70(12)
		O(2)^{vii}-Co(1)-O(1)	89.30(12)
		O(2)-Co(1)-O(1)^{vii}	89.30(12)
		O(2)^{vii}-Co(1)-O(1)^{vii}	90.70(12)
		O(1)-Co(1)-O(1)^{vii}	180
		O(2)-Co(1)-O(7)^{vii}	85.48(12)
		O(2)^{vii}-Co(1)-O(7)^{vii}	94.52(12)
		O(1)-Co(1)-O(7)^{vii}	88.56(12)
		O(1)^{vii}-Co(1)-O(7)^{vii}	91.44(12)
		O(2)-Co(1)-O(7)	94.52(12)
		O(2)^{vii}-Co(1)-O(7)	85.48(12)
		O(1)-Co(1)-O(7)	91.44(12)
		O(1)^{vii}-Co(1)-O(7)	88.56(12)
		O(7)^{vii}-Co(1)-O(7)	180
		O(2)-Co(1)-Cs(1)	132.73(9)
		O(2)^{vii}-Co(1)-Cs(1)	47.27(9)
		O(1)-Co(1)-Cs(1)	63.16(9)
		O(1)^{vii}-Co(1)-Cs(1)	116.84(9)
		O(7)^{vii}-Co(1)-Cs(1)	128.73(9)
		O(7)-Co(1)-Cs(1)	51.27(9)
		O(2)-Co(1)-Cs(1)^{vii}	47.27(9)
		O(2)^{vii}-Co(1)-Cs(1)^{vii}	132.73(9)
		O(1)-Co(1)-Cs(1)^{vii}	116.84(9)
		O(1)^{vii}-Co(1)-Cs(1)^{vii}	63.16(9)
		O(7)^{vii}-Co(1)-Cs(1)^{vii}	51.27(9)
		O(7)-Co(1)-Cs(1)^{vii}	128.73(9)
		Cs(1)-Co(1)-Cs(1)^{vii}	180.000(6)
		O(2)-Co(1)-Cs(1)^{vi}	45.82(8)
		O(2)^{vii}-Co(1)-Cs(1)^{vi}	134.18(8)
		O(1)-Co(1)-Cs(1)^{vi}	60.15(8)
		O(1)^{vii}-Co(1)-Cs(1)^{vi}	119.85(8)
		O(7)^{vii}-Co(1)-Cs(1)^{vi}	54.94(8)
		O(7)-Co(1)-Cs(1)^{vi}	125.06(8)
		Cs(1)-Co(1)-Cs(1)^{vi}	123.10(4)
		Cs(1)^{vii}-Co(1)-Cs(1)^{vi}	56.90(4)
		O(2)-Co(1)-Cs(1)^{ix}	134.18(9)
		O(2)^{vii}-Co(1)-Cs(1)^{ix}	45.82(8)

		O(1)-Co(1)-Cs(1)^{ix}	119.85(8)
		O(1)^{vii}-Co(1)-Cs(1)^{ix}	60.15(8)
		O(7)^{vii}-Co(1)-Cs(1)^{ix}	125.06(8)
		O(7)-Co(1)-Cs(1)^{ix}	54.94(8)
		Cs(1)-Co(1)-Cs(1)^{ix}	56.90(4)
		Cs(1)^{vii}-Co(1)-Cs(1)^{ix}	123.10(4)
		Cs(1)^{vi}-Co(1)-Cs(1)^{ix}	180.000(3)
		O(5)^{iii}-Cs(1)-O(3)^{ii}	91.45(8)
		O(5)^{iii}-Cs(1)-O(2)^{vii}	113.52(8)
		O(3)^{ii}-Cs(1)-O(2)^{vii}	103.32(9)
		O(5)^{iii}-Cs(1)-O(2)^{x}	125.58(8)
		O(3)^{ii}-Cs(1)-O(2)^{x}	120.32(8)
		O(2)^{vii}-Cs(1)-O(2)^{x}	101.32(8)
		O(5)^{iii}-Cs(1)-O(6)^{viii}	82.89(8)
		O(3)^{ii}-Cs(1)-O(6)^{viii}	81.37(9)
		O(2)^{vii}-Cs(1)-O(6)^{viii}	162.50(8)
		O(2)^{x}-Cs(1)-O(6)^{viii}	62.50(8)
		O(5)^{iii}-Cs(1)-O(7)	150.14(8)
		O(3)^{ii}-Cs(1)-O(7)	70.22(8)
		O(2)^{vii}-Cs(1)-O(7)	52.41(7)
		O(2)^{x}-Cs(1)-O(7)	84.28(9)
		O(6)^{viii}-Cs(1)-O(7)	115.83(8)
		O(5)^{iii}-Cs(1)-O(4)^{vii}	73.41(8)
		O(3)^{ii}-Cs(1)-O(4)^{vii}	124.22(8)
		O(2)^{vii}-Cs(1)-O(4)^{vii}	44.70(7)
		O(2)^{x}-Cs(1)-O(4)^{vii}	111.48(8)
		O(6)^{viii}-Cs(1)-O(4)^{vii}	144.64(7)
		O(7)-Cs(1)-O(4)^{vii}	97.08(8)
		O(5)^{iii}-Cs(1)-O(7)^{ix}	94.08(7)
		O(3)^{ii}-Cs(1)-O(7)^{ix}	170.70(8)
		O(2)^{vii}-Cs(1)-O(7)^{ix}	81.29(9)
		O(2)^{x}-Cs(1)-O(7)^{ix}	50.46(7)
		O(6)^{viii}-Cs(1)-O(7)^{ix}	91.89(9)
		O(7)-Cs(1)-O(7)^{ix}	107.53(6)
		O(4)^{vii}-Cs(1)-O(7)^{ix}	64.70(8)
		O(5)^{iii}-Cs(1)-C(1)^{iii}	44.81(9)
		O(3)^{ii}-Cs(1)-C(1)^{iii}	72.78(9)
		O(2)^{vii}-Cs(1)-C(1)^{iii}	78.49(9)
		O(2)^{x}-Cs(1)-C(1)^{iii}	166.10(8)
		O(6)^{viii}-Cs(1)-C(1)^{iii}	118.85(8)
		O(7)-Cs(1)-C(1)^{iii}	105.86(10)
		O(4)^{vii}-Cs(1)-C(1)^{iii}	58.61(8)
		O(7)^{ix}-Cs(1)-C(1)^{iii}	116.30(8)

		$O(5)^{iii}$-Cs(1)-$O(1)^{x}$	74.59(7)
		$O(3)^{ii}$-Cs(1)-$O(1)^{x}$	126.24(8)
		$O(2)^{vii}$-Cs(1)-$O(1)^{x}$	130.06(7)
		$O(2)^{x}$-Cs(1)-$O(1)^{x}$	51.04(8)
		$O(6)^{vii}$i-Cs(1)-$O(1)^{x}$	45.99(7)
		O(7)-Cs(1)-$O(1)^{x}$	135.25(7)
		$O(4)^{vii}$-Cs(1)-$O(1)^{x}$	101.43(7)
		$O(7)^{ix}$-Cs(1)-$O(1)^{x}$	48.79(7)
		$C(1)^{iii}$-Cs(1)-$O(1)^{x}$	118.60(9)
		$O(5)^{iii}$-Cs(1)-$O(3)^{x}$	125.44(8)
		$O(3)^{ii}$-Cs(1)-$O(3)^{x}$	78.67(9)
		$O(2)^{vii}$-Cs(1)-$O(3)^{x}$	121.00(8)
		$O(2)^{x}$-Cs(1)-$O(3)^{x}$	42.29(7)
		$O(6)^{viii}$-Cs(1)-$O(3)^{x}$	42.72(8)
		O(7)-Cs(1)-$O(3)^{x}$	75.22(9)
		$O(4)^{vii}$-Cs(1)-$O(3)^{x}$	152.48(6)
		$O(7)^{ix}$-Cs(1)-$O(3)^{x}$	92.02(7)
		$C(1)^{iii}$-Cs(1)-$O(3)^{x}$	148.79(8)
		$O(1)^{x}$-Cs(1)-$O(3)^{x}$	69.61(8)
		$O(5)^{iii}$-Cs(1)-$O(5)^{viii}$	55.61(9)
		$O(3)^{ii}$-Cs(1)-$O(5)^{viii}$	56.43(8)
		$O(2)^{vii}$-Cs(1)-$O(5)^{viii}$	153.13(7)
		$O(2)^{x}$-Cs(1)-$O(5)^{viii}$	104.40(7)
		$O(6)^{viii}$-Cs(1)-$O(5)^{viii}$	41.90(7)
		O(7)-Cs(1)-$O(5)^{viii}$	122.72(7)
		$O(4)^{vii}$-Cs(1)-$O(5)^{viii}$	128.45(8)
		$O(7)^{ix}$-Cs(1)-$O(5)^{viii}$	121.57(8)
		$C(1)^{iii}$-Cs(1)-$O(5)^{viii}$	78.40(8)
		$O(1)^{x}$-Cs(1)-$O(5)^{viii}$	73.88(6)
		$O(3)^{x}$-Cs(1)-$O(5)^{viii}$	75.43(8)

Symmetry transformations used to generate equivalent atoms:

(i) –x+1, -y, -z; (ii) –x, -y, -z+1; (iii) x, y, z+1; (iv) -x, -y+1, -z, (v) x, y, z-1; (vi) x, y-1, z; (vii) -x+1,-y,-z+1; (viii) -x,-y+1,-z+1; (ix) -x+1,-y+1,-z+1; (x) x,y+1,z.

Table 3.C: Anisotropic displacement parameters ($Å^2$ x 10^3) for $Cs_2[Co(CH_4O_6P_2)_2(H_2O)_2]$.

	U11	U22	U33	U23	U13	U12
C(1)	8(2)	6(2)	5(2)	0(1)	-1(1)	-1(1)
O(1)	9(1)	15(2)	8(1)	-2(1)	0(1)	-3(1)

O(2)	9(1)	7(1)	9(1)	-2(1)	-3(1)	-1(1)
O(3)	7(1)	11(1)	7(2)	-4(1)	1(1)	-4(1)
O(4)	10(1)	7(1)	9(1)	-4(1)	1(1)	-1(1)
O(5)	16(1)	6(1)	9(1)	0(1)	-6(1)	-1(1)
O(6)	7(1)	13(1)	9(1)	-4(1)	1(1)	-2(1)
O(7)	9(1)	6(1)	10(1)	-2(1)	-3(1)	0(1)
P(1)	6(1)	5(1)	6(1)	-1(1)	-1(1)	-1(1)
P(2)	6(1)	6(1)	5(1)	-1(1)	-1(1)	-1(1)
Co(1)	5(1)	6(1)	6(1)	-2(1)	-1(1)	0(1)
Cs(1)	10(1)	9(1)	8(1)	-1(1)	0(1)	1(1)

Table 4.C: Hydrogen coordinates (x 10^4) and isotropic displacement parameters ($Å^2$ x 10^3) for $Cs_2[Co(CH_4O_6P_2)_2(H_2O)_2]$.

	x	y	z	U(eq)
H(3)	1390	995	369	8
H(4)	3504	1218	304	8
H(1A)	2970(80)	-1080(80)	8350(30)	27(16)
H(1B)	1690(40)	-680(150)	7210(110)	110(40)
H(2)	470(90)	-2180(90)	3910(90)	16(17)
H(5)	1000(150)	4500(200)	320(160)	160(60)

Table 5.C: Hydrogen bonds for $Cs_2[Co(CH_4O_6P_2)_2(H_2O)_2]$.

D-H...A	d(D-H)	d(H...A)	d(D...A)	<(DHA)
C(1)-H(4)...O(4)^{i}	0.97	2.56	3.481(5)	159
O(1)-H(1B)...O(6)^{ii}	0.88(2)	1.97(7)	2.725(4)	142(10)
O(3)-H(2)...O(6)^{ii}	0.64(6)	1.91(6)	2.549(5)	175(7)
O(1)-H(1A)...O(4)^{iii}	0.87(2)	1.99(2)	2.856(5)	171(6)
O(5)-H(5)...O(5)^{iv}	0.85(2)	2.44(6)	3.232(6)	156(13)

Symmetry transformations used to generate equivalent atoms:

(i) –x+1, -y, -z; (ii) –x, -y, -z+1; (iii) x, y, z+1; (iv) -x, -y+1, -z.

Table 6.C: Torsion angles (º) for $Cs_2[Co(CH_4O_6P_2)_2(H_2O)_2]$.

Torsion Angle (º)	
Co(1)-O(2)-P(1)-O(4)	130.0(2)
Cs(1)^{vii}-O(2)-P(1)-O(4)	-2.74(19)
Cs(1)^{vi}-O(2)-P(1)-O(4)	-86.61(18)
Co(1)-O(2)-P(1)-O(3)	-108.6(3)
Cs(1)^{vii}-O(2)-P(1)-O(3)	118.66(16)
Cs(1)^{vi}-O(2)-P(1)-O(3)	34.79(19)
Co(1)-O(2)-P(1)-C(1)	9.5(3)
Cs(1)^{vii}-O(2)-P(1)-C(1)	-123.30(16)
Cs(1)^{vi}-O(2)-P(1)-C(1)	152.83(15)
Co(1)-O(2)-P(1)-Cs(1)^{vii}	132.8(3)
Cs(1)^{vi}-O(2)-P(1)-Cs(1)^{vii}	-83.87(13)
Co(1)-O(2)-P(1)-Cs(1)^{vi}	-143.4(3)
Cs(1)^{vii}-O(2)-P(1)-Cs(1)^{vi}	83.87(13)
Cs(1)^{vii}-O(4)-P(1)-O(2)	2.38(16)
Cs(1)^{vii}-O(4)-P(1)-O(3)	-120.35(14)
Cs(1)^{vii}-O(4)-P(1)-C(1)	124.42(14)
Cs(1)^{vii}-O(4)-P(1)-Cs(1)^{vi}	-48.45(8)
Cs(1)^{ii}-O(3)-P(1)-O(2)	-136.8(3)
Cs(1)^{vi}-O(3)-P(1)-O(2)	-27.47(15)
Cs(1)^{ii}-O(3)-P(1)-O(4)	-11.1(4)
Cs(1)^{vi}-O(3)-P(1)-O(4)	98.23(15)
Cs(1)^{ii}-O(3)-P(1)-C(1)	103.8(4)
Cs(1)^{vi}-O(3)-P(1)-C(1)	-146.88(14)
Cs(1)^{ii}-O(3)-P(1)-Cs(1)^{vii}	-80.9(4)
Cs(1)^{vi}-O(3)-P(1)-Cs(1)^{vii}	28.45(13)
Cs(1)^{ii}-O(3)-P(1)-Cs(1)^{vi}	-109.3(3)
P(2)-C(1)-P(1)-O(2)	-44.5(3)
Cs(1)^{v}-C(1)-P(1)-O(2)	123.2(3)
P(2)-C(1)-P(1)-O(4)	-169.7(2)
Cs(1)^{v}-C(1)-P(1)-O(4)	-2.0(4)
P(2)-C(1)-P(1)-O(3)	75.0(3)
Cs(1)^{v}-C(1)-P(1)-O(3)	-117.2(3)
P(2)-C(1)-P(1)-Cs(1)^{vii}	-100.1(2)
Cs(1)^{v}-C(1)-P(1)-Cs(1)^{vii}	67.7(4)
P(2)-C(1)-P(1)-Cs(1)^{vi}	-3.1(4)

$Cs(1)^{v}$-C(1)-P(1)-$Cs(1)^{vi}$	164.63(15)
Co(1)-O(7)-P(2)-O(6)	80.6(2)
Cs(1)-O(7)-P(2)-O(6)	-45.2(2)
$Cs(1)^{ix}$-O(7)-P(2)-O(6)	-135.08(18)
Co(1)-O(7)-P(2)-O(5)	-153.97(19)
Cs(1)-O(7)-P(2)-O(5)	80.23(19)
$Cs(1)^{ix}$-O(7)-P(2)-O(5)	-9.7(3)
Co(1)-O(7)-P(2)-C(1)	-41.9(3)
Cs(1)-O(7)-P(2)-C(1)	-167.72(15)
$Cs(1)^{ix}$-O(7)-P(2)-C(1)	102.4(2)
Co(1)-O(7)-P(2)-$Cs(1)^{viii}$	131.62(15)
Cs(1)-O(7)-P(2)-$Cs(1)^{viii}$	5.83(19)
$Cs(1)^{ix}$-O(7)-P(2)-$Cs(1)^{viii}$	-84.1(2)
Co(1)-O(7)-P(2)-$Cs(1)^{v}$	-109.30(17)
Cs(1)-O(7)-P(2)-$Cs(1)^{v}$	124.90(10)
$Cs(1)^{ix}$-O(7)-P(2)-$Cs(1)^{v}$	35.0(2)
Co(1)-O(7)-P(2)-Cs(1)	125.8(3)
$Cs(1)^{ix}$-O(7)-P(2)-Cs(1)	-89.9(2)
$Cs(1)^{viii}$-O(6)-P(2)-O(7)	114.18(17)
$Cs(1)^{viii}$-O(6)-P(2)-O(5)	-12.4(2)
$Cs(1)^{viii}$-O(6)-P(2)-C(1)	-121.82(17)
$Cs(1)^{viii}$-O(6)-P(2)-$Cs(1)^{v}$	-55.07(18)
$Cs(1)^{viii}$-O(6)-P(2)-Cs(1)	84.03(12)
$Cs(1)^{v}$-O(5)-P(2)-O(7)	109.07(18)
$Cs(1)^{viii}$-O(5)-P(2)-O(7)	-118.76(14)
$Cs(1)^{v}$-O(5)-P(2)-O(6)	-122.61(17)
$Cs(1)^{viii}$-O(5)-P(2)-O(6)	9.56(16)
$Cs(1)^{v}$-O(5)-P(2)-C(1)	-8.8(2)
$Cs(1)^{viii}$-O(5)-P(2)-C(1)	123.39(14)
$Cs(1)^{v}$-O(5)-P(2)-$Cs(1)^{viii}$	-132.17(17)
$Cs(1)^{viii}$-O(5)-P(2)-$Cs(1)^{v}$	132.17(17)
$Cs(1)^{v}$-O(5)-P(2)-Cs(1)	153.37(12)
$Cs(1)^{viii}$-O(5)-P(2)-Cs(1)	-74.46(7)
P(1)-C(1)-P(2)-O(7)	61.8(3)
$Cs(1)^{v}$-C(1)-P(2)-O(7)	-112.02(14)
P(1)-C(1)-P(2)-O(6)	-64.7(3)
$Cs(1)^{v}$-C(1)-P(2)-O(6)	121.51(14)
P(1)-C(1)-P(2)-O(5)	-179.6(2)
$Cs(1)^{v}$-C(1)-P(2)-O(5)	6.54(15)
P(1)-C(1)-P(2)-$Cs(1)^{viii}$	-111.68(19)
$Cs(1)^{v}$-C(1)-P(2)-$Cs(1)^{viii}$	74.51(13)
P(1)-C(1)-P(2)-$Cs(1)^{v}$	173.8(3)
P(1)-C(1)-P(2)-Cs(1)	42.5(4)

Cs(1)^{v}-C(1)-P(2)-Cs(1)	-131.3(2)
P(1)-O(2)-Co(1)-O(2)^{vii}	26(100)
Cs(1)^{vii}-O(2)-Co(1)-O(2)^{vii}	159(100)
Cs(1)^{vi}-O(2)-Co(1)-O(2)^{vii}	-119(100)
P(1)-O(2)-Co(1)-O(1)	99.2(3)
Cs(1)^{vii}-O(2)-Co(1)-O(1)	-127.11(11)
Cs(1)^{vi}-O(2)-Co(1)-O(1)	-45.10(11)
P(1)-O(2)-Co(1)-O(1)^{vii}	-80.8(3)
Cs(1)^{vii}-O(2)-Co(1)-O(1)^{vii}	52.89(11)
Cs(1)^{vi}-O(2)-Co(1)-O(1)^{vii}	134.90(11)
P(1)-O(2)-Co(1)-O(7)^{vii}	-172.3(3)
Cs(1)^{vii}-O(2)-Co(1)-O(7)^{vii}	-38.61(10)
Cs(1)^{vi}-O(2)-Co(1)-O(7)^{vii}	43.40(11)
P(1)-O(2)-Co(1)-O(7)	7.7(3)
Cs(1)^{vii}-O(2)-Co(1)-O(7)	141.39(10)
Cs(1)^{vi}-O(2)-Co(1)-O(7)	-136.60(11)
P(1)-O(2)-Co(1)-Cs(1)	46.3(3)
Cs(1)^{vii}-O(2)-Co(1)-Cs(1)	180
Cs(1)^{vi}-O(2)-Co(1)-Cs(1)	-97.99(10)
P(1)-O(2)-Co(1)-Cs(1)^{vii}	-133.7(3)
Cs(1)^{vi}-O(2)-Co(1)-Cs(1)^{vii}	82.01(10)
P(1)-O(2)-Co(1)-Cs(1)^{vi}	144.3(3)
Cs(1)^{vii}-O(2)-Co(1)-Cs(1)^{vi}	-82.01(10)
P(1)-O(2)-Co(1)-Cs(1)^{ix}	-35.7(3)
Cs(1)^{vii}-O(2)-Co(1)-Cs(1)^{ix}	97.99(10)
Cs(1)^{vi}-O(2)-Co(1)-Cs(1)^{ix}	180
Cs(1)^{vi}-O(1)-Co(1)-O(2)	35.85(9)
Cs(1)^{vi}-O(1)-Co(1)-O(2)^{vii}	-144.15(9)
Cs(1)^{vi}-O(1)-Co(1)-O(1)^{vii}	-114(100)
Cs(1)^{vi}-O(1)-Co(1)-O(7)^{vii}	-49.60(9)
Cs(1)^{vi}-O(1)-Co(1)-O(7)	130.40(9)
Cs(1)^{vi}-O(1)-Co(1)-Cs(1)	174.82(9)
Cs(1)^{vi}-O(1)-Co(1)-Cs(1)^{vii}	-5.18(9)
Cs(1)^{vi}-O(1)-Co(1)-Cs(1)^{ix}	180
P(2)-O(7)-Co(1)-O(2)	11.0(2)
Cs(1)-O(7)-Co(1)-O(2)	144.01(10)
Cs(1)^{ix}-O(7)-Co(1)-O(2)	-142.99(10)
P(2)-O(7)-Co(1)-O(2)^{vii}	-169.0(2)
Cs(1)-O(7)-Co(1)-O(2)^{vii}	-35.99(10)
Cs(1)^{ix}-O(7)-Co(1)-O(2)^{vii}	37.01(10)
P(2)-O(7)-Co(1)-O(1)	-79.8(2)
Cs(1)-O(7)-Co(1)-O(1)	53.19(10)
Cs(1)^{ix}-O(7)-Co(1)-O(1)	126.19(10)
P(2)-O(7)-Co(1)-O(1)^{vii}	100.2(2)

Cs(1)-O(7)-Co(1)-O(1)^{vii}	-126.81(10)
Cs(1)^{ix}-O(7)-Co(1)-O(1)^{vii}	-53.81(10)
P(2)-O(7)-Co(1)-O(7)^{vii}	-145(100)
Cs(1)-O(7)-Co(1)-O(7)^{vii}	-12(100)
Cs(1)^{ix}-O(7)-Co(1)-O(7)^{vii}	61(100)
P(2)-O(7)-Co(1)-Cs(1)	-133.0(2)
Cs(1)^{ix}-O(7)-Co(1)-Cs(1)	73.00(7)
P(2)-O(7)-Co(1)-Cs(1)^{vii}	47.0(2)
Cs(1)-O(7)-Co(1)-Cs(1)^{vii}	180
Cs(1)^{ix}-O(7)-Co(1)-Cs(1)^{vii}	-107.00(7)
P(2)-O(7)-Co(1)-Cs(1)^{vi}	-26.0(2)
Cs(1)-O(7)-Co(1)-Cs(1)^{vi}	107.00(7)
Cs(1)^{ix}-O(7)-Co(1)-Cs(1)^{vi}	180
P(2)-O(7)-Co(1)-Cs(1)^{ix}	154.0(2)
Cs(1)-O(7)-Co(1)-Cs(1)^{ix}	-73.00(7)
P(2)-O(7)-Cs(1)-O(5)^{iii}	97.2(2)
Co(1)-O(7)-Cs(1)-O(5)^{iii}	-41.7(2)
Cs(1)^{ix}-O(7)-Cs(1)-O(5)^{iii}	-134.44(13)
P(2)-O(7)-Cs(1)-O(3)^{ii}	42.11(15)
Co(1)-O(7)-Cs(1)-O(3)^{ii}	-96.80(12)
Cs(1)^{ix}-O(7)-Cs(1)-O(3)^{ii}	170.47(8)
P(2)-O(7)-Cs(1)-O(2)^{vii}	168.0(2)
Co(1)-O(7)-Cs(1)-O(2)^{vii}	29.07(8)
Cs(1)^{ix}-O(7)-Cs(1)-O(2)^{vii}	-63.67(9)
P(2)-O(7)-Cs(1)-O(2)^{x}	-83.00(16)
Co(1)-O(7)-Cs(1)-O(2)^{x}	138.10(10)
Cs(1)^{ix}-O(7)-Cs(1)-O(2)^{x}	45.36(6)
P(2)-O(7)-Cs(1)-O(6)^{viii}	-27.33(18)
Co(1)-O(7)-Cs(1)-O(6)^{viii}	-166.24(8)
Cs(1)^{ix}-O(7)-Cs(1)-O(6)^{viii}	101.03(8)
P(2)-O(7)-Cs(1)-O(4)^{vii}	166.00(15)
Co(1)-O(7)-Cs(1)-O(4)^{vii}	27.09(10)
Cs(1)^{ix}-O(7)-Cs(1)-O(4)^{vii}	-65.64(7)
P(2)-O(7)-Cs(1)-O(7)^{ix}	-128.36(18)
Co(1)-O(7)-Cs(1)-O(7)^{ix}	92.73(10)
P(2)-O(7)-Cs(1)-C(1)^{iii}	106.69(16)
Co(1)-O(7)-Cs(1)-C(1)^{iii}	-32.22(12)
Cs(1)^{ix}-O(7)-Cs(1)-C(1)^{iii}	-124.95(7)
P(2)-O(7)-Cs(1)-O(1)^{x}	-79.87(18)
Co(1)-O(7)-Cs(1)-O(1)^{x}	141.22(9)
Cs(1)^{ix}-O(7)-Cs(1)-O(1)^{x}	48.49(10)
P(2)-O(7)-Cs(1)-O(3)^{x}	-40.94(15)
Co(1)-O(7)-Cs(1)-O(3)^{x}	-179.85(11)

Cs(1)^{ix}-O(7)-Cs(1)-O(3)^{x}	87.42(7)
P(2)-O(7)-Cs(1)-O(5)^{viii}	20.46(19)
Co(1)-O(7)-Cs(1)-O(5)^{viii}	-118.45(9)
Cs(1)^{ix}-O(7)-Cs(1)-O(5)^{viii}	148.82(6)

Symmetry transformations used to generate equivalent atoms:

(i) –x+1, -y, -z; (ii) –x, -y, -z+1; (iii) x, y, z+1; (iv) -x, -y+1, -z, (v) x, y, z-1; (vi) x, y-1, z;

(vii) -x+1,-y,-z+1; (viii) -x,-y+1,-z+1; (ix) -x+1,-y+1,-z+1; (x) x,y+1,z.